Molecular insights into the function of the *DISC* locus

Jennifer E. Chubb

PhD
The University of Edinburgh
2007

Declaration

I declare that this thesis has been comprised by myself, comprises my own work, except where otherwise stated and has not been submitted for any other degree or professional qualification.

Acknowledgments

Throughout my PhD I have worked within the chromosome 1 group. I can only hope that my time spent as a PhD student has been as productive as the group in general (2 weddings and 3 babies in 2 years!). I never expected things to change so much in what now seems like such a short time but I can honestly say that change has engulfed us all, not least me. You have helped me to grow not only as a scientist but also as a person and I will take away many fond memories of you all.

I would especially like to thank Kirsty Millar and David Porteous, my supervisors, for their continuous help and support. I am indebted to many members of the medical genetics section for their help and support throughout my PhD. I would like to give a special thank you to Sheila Christie, Shaun Mackie and Fumiaki Ogawa for their help with RNA extractions, PDE4 assays and centrosome isolation procedures; Ben Pickard and Heather Davidson for the use of their microscopes; Judith Mitchell for her help with 2D protein analysis and Simon Cooper for his help with artwork.

Outside the section I would like to thank Professor Tetsu Akiyama for providing the αDISC1 antibody and Dr. Wei Cui for providing the human embryonic stem cell RNA samples.

Of course, a lot more than technical support is needed to stay the course of a PhD and I know that for me it would not have been possible without my friends. I have been blessed with a long list of friends, every one of which has contributed a small bit to this PhD by helping to keep me sane. I would like to give a special mention to my fellow PhD and gym buddies, Vicky, Lorna and Andrea, without whom it would not have been so much fun.

Lastly, but most importantly, I want to thank my parents, my family and John. I would like to dedicate this PhD thesis to my parents as it is the product of their love, support and encouragement. To John, I can only dedicate what is left, me! I love you all and couldn't have done it without you.

One lesson I have learnt from my PhD is that time really does fly by and we should make the most of every minute!

"Dance like nobody's watching; love like you've never been hurt. Sing like nobody's listening; live like it's heaven on earth." (Mark Twain)

Abstract

Disrupted-In-Schizophrenia 1 (*DISC1*) and *Disrupted-In-Schizophrenia 2* (*DISC2*) have been identified as novel candidate genes for psychiatric illness through analysis of a t(1;11)(q42.1;q14.3) translocation which segregates with schizophrenia and other major psychiatric illness in a large Scottish family. The *DISC* locus at 1q42 has been independently implicated in psychiatric illness in multiple populations. *DISC1* encodes a novel protein with the potential to interact with many cellular proteins and is likely to act as a molecular scaffold with wide ranging cellular functions. *DISC2* is a putative non-coding RNA gene located antisense to *DISC1* and may play a role in regulation of *DISC1* expression.

This PhD thesis investigates the molecular basis of disease pathogenesis in the t(1;11) family as a result of disruption of *DISC1* and *DISC2*, providing evidence for reduced expression of *DISC1* within translocation carriers. This refutes previous conjecture of the existence of an abnormal truncated DISC1 protein resulting from the translocation. These data support a disease model of DISC1 haploinsufficiency as the direct cause of illness in this family, which is further investigated using RNA interference technology. DISC1 knock-down demonstrates that DISC1 may function in multiple diverse cellular pathways with implications for cAMP signal transduction, cell cycle progression and apoptosis.

The complex biology of the DISC1 protein is highlighted by the demonstration of isoform specific sub-cellular localisation which may result in isoform specific protein-protein interactions. Furthermore DISC1 is shown to be dynamically regulated during neuronal differentiation of embryonic stem cells.

The *DISC2* gene has been successfully extended to its likely 5' end and novel splicing has been uncovered. This data provides a platform on which to take forward the functional characterisation of *DISC2* including the current hypothesis that it functions as an antisense regulator of *DISC1*.

Table of contents

Chapter 2 - Materials and Methods

Chapter 3 – Defining the disease mechanism operating within the t(1;11) family

Chapter 5 – Optimising RNA interference to knock down DISC1

Chapter 6 – RNA interference for the DISC1 gene

List of figures

List of tables

Abbreviations

2D	Two dimensions
2N	Diploid
4N	Tetraploid
°C	Degrees Celsius
-ve	Negative
+ve	Positive
µl	Microlitre
µg	Microgram
µm	Micron
µM	Micromolar
µCi	Microcuries
α	alpha
aa	Amino acid
Air	Antisense Igf2R
AKAP	A kinase anchor protein
AMP	Adenosine monophosphase (5'-adenylic acid)
ATP	Adenosine 5'-triphosphate
β	beta
BAC	Bacterial artificial chromosome
BLAST	Basic Local Alignment search tool
bp	Base pair
BrdU	5'-bromo-2'-deoxyuridine
BSA	Bovine serum albumin
cAMP	3'-5'-cyclic adenosine monophosphate
cDNA	Complimentary deoxyribonucleic acid
CG-NAP	Centrosome and golgi localised PKN associated protein
cm	centimetre
CO_2	Carbon Dioxide
COMT	Catechol-O-Methyl transferase

CREB	cAMP response element binding protein
DA	Dopamine
DAAO	D-aminoacid Oxidase
DAQ	Dopamine quinone
DCX	Doublecortin
dH_2O	Distilled water
DISC1	Disrupted in schizophrenia 1
DISC2	Disrupted in schizophrenia 2
DNA	Deoxyribonucleic acid
DNAse	Deoxyribonuclease
dNTP	Deoxyribonucleotide triphosphate
dsRNA	Double stranded RNA
DSM	American diagnostic and statistical manual
DTNBP1	Dystrobrevin Binding Protein 1
DTT	Dithiothreitol
Dyn IC	Dynein intermediate chain
EDTA	Ethylenediaminetetraacetic acid
EMBL	European Molecular Biology Laboratory
ERP	Event related potential
EST	Expressed Sequence Tag
FACS	Fluorescence Activated Cell Sorting
FEZ	Fasciculation and elongation
FISH	Fluorescent in-situ hybridisation
FITC	Fluorescein isothiocyanate
fMRI	Functional Magnetic Resonance Imaging
γ	gamma
g	Gram
G6PD	Glucose-6-phosphase dehydrogenase
GABA	Gamma-aminobutyric acid
GAD	Glutamate Decarboxylase
GAPDH	Glyceraldehyde-6-phosphate dehydrogenase
GCP	Glutamate Carboxypeptidase

GFP	Green fluorescent protein
GRM	Metabotropic glutamate receptor
HEK293	Human Embryonic Kidney 293
hnRNA	Heterogeneous nuclear ribonucleic acid
hPFK	Human Phosphofructokinase
HPLC	High Performance Liquid Chromatography
Hr	Hour
HRP	Horseradish peroxidase
ICD	International Classification of Diseases
IEF	Isoelectric focusing
IF	Immunofluorescence
IQ	Intelligence quotient
kb	Kilobase
kDa	Kilo Dalton
KLHL1	Kelch-like 1
λ	lambda
L	Litre
LIS1	Lissencephaly 1
LMP	low melting point
LOD	Logarithm of odds
M	Molar
ml	Millilitre
mm	Millimetre
mM	Millimolar
mg	Milligram
mins	Minutes
mRNA	Messenger ribonucleic acid
mtDNA	Mitochondrial DNA (refers to the mitochondrial genome)
MTOC	Microtubule organising centre
N	Any nucleotide
NA	Not applicable
NAA	N-acetylaspartate

NAAG	N-acetylaspartylglutamate
nACh	Nicotinic acetylcholine receptor
NAT	Natural antisense transcript
ncRNA	Non-coding ribonucleic acid
ng	Nanogram
nm	Nanometre
nM	Nanomolar
NMDA	N-methyl-D-aspartic acid
NRG1	Neuregulin 1
nud	Nuclear distribution
NUDEL	Nuclear Distribution E - like
OD	Optical density
ORF	Open reading frame
PACT	Pericentrin-AKAP450 Centrosomal Targeting
PAGE	Polyacrylamide Gel Electrophoresis
PBS	Phosphate buffered saline
PBST	Phosphate buffered saline with Tween
PCP	Phencyclidine
PCR	Polymerase Chain Reaction
PDE	Phosphodiesterase
Py	Pyrimidine (T or C nucleotide)
PFA	Paraformaldehyde
pI	Isoelectric point
PI	Propidium Iodide
PKA	Protein Kinase A
PPI	Prepulse Inhibition
PRODH	Proline Dehydrogenase
PSD	Postsynaptic density
PVDF	Polyvinylidene fluoride
RACE	Rapid Amplification of cDNA ends
rcf (g)	relative centrifugal force
RGS4	Regulator of G-protein signalling 4

RIPA	Radioimmunoprecipiatation Assay
RNA	Ribonucleic acid
RNAse	Ribonuclease
RNAi	RNA Interference
Rpm	Revolutions per minute
rRNA	Ribosomal RNA
RT	Room temperature
RT-PCR	Reverse Transcriptase PCR
SDS	Sodium Dodecyl Sulphate
shRNA	Short hairpin ribonucleic acid
siRNA	Short interfering ribonucleic acid
SNP	Single nucleotide polymorphism
TAE	Tris Acetate Electrophoresis
TBS	Tris buffered saline
TBST	Tris buffered saline with Tween
TRAX	Translin associated factor X
tRNA	Transfer RNA
UCSC	University of San Diego supercomputer
UK	United Kingdom
UoE	University of Edinburgh
UPD	Ubiquitin proteosome degradation
UTR	Untranslated region
UV	Ultraviolet
V	Volts
VCFS	Velocardiofacial syndrome
WT	Wild-type
Xist	X-(inactive) specific transcript

Chapter 1

Introduction

1.1 Schizophrenia – History, phenotype and phenomenology

1.1.1 What is schizophrenia?

"At first it was as if parts of my brain "awoke" which had been dormant, and I became interested in a wide assortment of people, events, places and ideas which normally would make no impression on me... The walk of a stranger on the street could be a "sign" to me which I must interpret. Every face in the windows of a passing streetcar would be engraved on my mind, all of them concentrating on me and trying to pass me some sort of message." (Norma McDonald, 1960)

Schizophrenia is a complex and debilitating mental illness. The term schizophrenia, meaning split mind, was coined by Eugen Bleuler in the early 20th century. This term has replaced dementia praecox, the original classification of functional psychosis by Emil Kraepelin in the late 19th century (*Frith and Johnstone, 2003*). These functional psychoses were so called as they had no apparent structural basis, although Kraepelin believed it to be only a matter of time before an underlying neuropathology would be uncovered. Even today however, psychiatrists and researchers alike are still searching for the underlying biological basis of schizophrenia.

Unlike many medical conditions schizophrenia is not an illness you have but rather an illness 'you are' and which affects all aspects of one's personality. Schizophrenic patients are aware of their difference and are tormented and frightened by the symptoms of the illness, which can be either positive (abnormally present) or negative (abnormally absent). The psychotic (or positive) symptoms of the illness are most easily treated using antipsychotic medication albeit still with a high number of non-responders to medication. These symptoms include hallucinations, delusions and possible physical aggression in response to these. Hallucinations are false perceptions and many schizophrenia sufferers experience both visual and auditory hallucinations. Patients often report hearing voices which command the patient to carry out disturbing actions.

"Those voices commanded me to do, and made me believe a number of false and terrible things... I refused to obey these voices on several occasions, when by obeying them I was afraid of taking away the life of my attendants..." (John Perceval, 1838)

Visual hallucinations are also common and distressing for schizophrenia sufferers. In one case a 19 year old woman reported watching in the mirror as her face changed into that of a rabbit with ears and whiskers (*Case 240, Frith and Johnstone 2003*). Further to this, patients also hold false beliefs (delusions), often of a persecutory nature believing that they are being pursued, that people are controlling their thoughts or putting thoughts into their heads. It is not surprising that patients experience anxiety and fury and can respond aggressively to these symptoms. Many of these psychotic symptoms are treatable using anti-psychotic medication; however the emotional (or negative) symptoms of this illness are not as easily treated. These negative symptoms include social withdrawal, lack of emotional responsiveness, apathy and general hopelessness (*'Schizophrenia is there an answer?' National Institute of Mental Health, 1972*).

'...they do not bear the same affection towards their parents and relatives; they become unfeeling to kindness, and careless of reproof...As their apathy increases, they are negligent of their dress and inattentive to personal cleanliness..' (John Haslam, 1809)

These symptoms are just as distressing for patients as the vivid hallucinations and torturous delusions and this is represented by an increase in the rates of self-harming and suicide amongst schizophrenia sufferers (*Frith and Johnstone, 2003*).

"I felt all this tumult of madness-all this stark, lonely living which is worse than death-and the pain, futility and hopelessness of it all-and the endlessness, the eternity."(Lara Jefferson, 1964)

"My fate when I reflect upon it is the most horrible one can conceive of. I cannot picture anything more frightful than for a well-endowed cultivated human being to live through his own gradual deterioration fully aware of it all the time" (statement of an 18 year old boy quoted by Sir Aubrey Lewis in 1967)

In addition to psychotic and emotional symptoms patients often exhibit cognitive impairments and movement disorders (*Hall et al. 2005*). Cognitive impairments in

schizophrenia often exist prior to the onset of psychotic or emotional symptoms and may be an underlying hallmark of the illness. It is obvious that schizophrenia is a phenotypically complex illness and not every patient will exhibit the same spectrum or severity of symptoms. Diagnosis of schizophrenia is a difficult task and standardised diagnostic criteria have therefore been employed to ensure conformity. The most widely used are the Diagnostic and Statistical Manual (DSM-IV) of the American Psychiatric Association and the World Health Organisation International Classification of Disease (ICD-10) (*Frith and Johnstone 2003*).

Although subtle brain abnormalities have been reported in the brains of schizophrenic individuals there are currently no diagnostic pathological markers for schizophrenia. Recently however, with the development of new imaging technologies there has been much research invested in this area. Researchers are attempting to identify endophenotypes that may give insights into to the pathogenesis of illness or serve as physiological markers of illness.

Although the symptoms described in this section are clearly severe it must be remembered that schizophrenia is a spectrum disorder with the nature and severity of symptoms differing between individuals. One interesting question is whether it is possible to extend this spectrum into the normal population? Most people at some time in their lives experience periods of extreme stress or anxiety or may even experience mild psychotic episodes, but without receiving a diagnosis of psychiatric illness. Therefore those who do receive a psychiatric diagnosis may represent the extreme end of a normal spectrum of behavioural, cognitive and emotional function.

1.1.2 Structural and cognitive abnormalities in schizophrenia

The human brain consists of the brainstem, the cerebellum and the cerebral cortex (divided into two hemispheres). Each cerebral hemisphere contains four lobes of disparate function. The parietal lobe performs essential roles in touch, spatial awareness and attention; the occipital lobe is the main visual centre of the brain; the temporal lobe (which contains the hippocampus and the amygdala) is important for language, emotion, hearing, object recognition and memory; finally the frontal lobe is responsible for problem solving, planning and decision making. The brain also

contains four fluid filled ventricles, two of which are called lateral ventricles (one in each cerebral hemisphere), a third ventricle which lies between the cerebral hemispheres and a fourth ventricle between the cerebellum and the brain stem (*Frith and Johnstone 2003*). Figures 1.1 depicts these key brain regions in a simplified format. Image A in this figure represents a structural MRI scan of my brain with all the visible brain structures labelled. Sub-groups of these structures are represented in the simplified diagrams B, C and D. Malfunction of some of these brain structures has been implicated in schizophrenia and will be discussed below.

Although there is no defining neuropathology for schizophrenia there have been numerous reports of subtle abnormalities of brain structure and function in schizophrenic individuals. Reductions in brain volume and weight have been reported in addition to enlargement of the ventricles (*Harrison and Weinberger, 2005, Harrison 1999, Wright et al. 2000*). Structural abnormalities have mainly been associated with hippocampal, frontal and temporal lobe structures in addition to the thalamus and some whiter matter (axons and dendrites) defects (*Hall et al. 2005, Harrison and Weinberger, 2005*). Histologically there is evidence for impairments in neuronal migration, survival and connectivity during brain development which stems from observations of aberrantly located and clustered neurons and reductions in certain neuronal populations (*Harrison and Weinberger, 2005*).

Impaired brain function is likely to be related to cognitive defects observed in schizophrenic individuals. One process reportedly impaired in schizophrenia is executive function, which is the ability to apply strategy to perform or solve a given task (*Frith and Johnstone, 2003*). Executive function is the responsibility of the frontal lobe and indeed prefrontal cortex dysfunction seems to be a consistent abnormality present in schizophrenic individuals (*Winterer and Weinberger 2004*). Schizophrenic patients also perform poorly on memory recognition tests, which has been shown to be associated with smaller hippocampal volume and abnormal hippocampal activation within the temporal lobe region (*Weiss et al. 2004, Heckers 2001*).

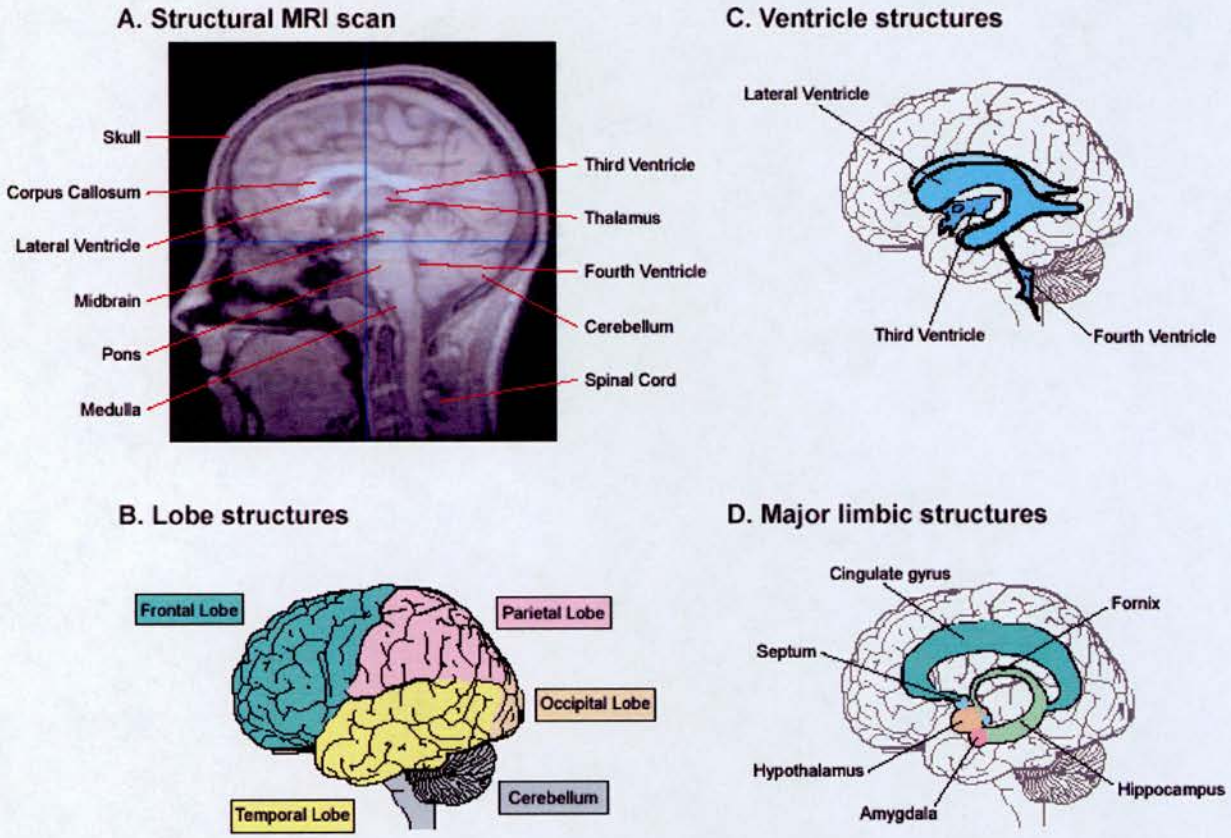

Figure 1.1. Structural features of the human brain. Image **(A)** represents a structural MRI scan with all visible structures labelled. Diagrams B, C and D represent sub-groups of key brain structures. The human brain consists of four lobe structures and the cerebellum **(B).** There are four fluid filled ventricles located deep within the human brain **(C)**. The major limbic structures of the brain deal with cognition and emotion, some of which have been implicated in schizophrenia **(D).** The brain outline for these figures was adapted from www.brainconnection.com.

Defects in electrical activity reflecting abnormal attention and working memory are consistently reported in schizophrenic individuals. The P300 event related potential is an electrophysiological measurement of brain activity associated with a specific stimulus or response and is representative of cortical processing (*Patel and Azzam, 2005, Linden 2005*). Reduced amplitude and increased latency of the P300 is a regular finding amongst schizophrenics. Family studies have reported deficits in P300 ERP in schizophrenics and their unaffected relatives compared to normal controls (*Davenport et al. 2006, Bharath et al 2000*). Studies involving schizophrenics, unaffected siblings and unrelated controls have also reported differences in various sub-components of this P300 ERP between siblings (affected and unaffected) and controls although the specific brain regions contributing to the P300 deficit seen in schizophrenia are still debatable (*Winterer et al. 2003, Turetsky et al. 2000*). The fact that P300 abnormalities are detected in healthy siblings of schizophrenic patients indicates that although reduced P300 amplitude may be a genetically controlled trait marker of schizophrenia, indicating underlying defects in cortical function, it is not a definite indicator of illness.

The P300 ERP is just one of many electrophysiological measures that have been studied in schizophrenia. Many other electroencephalography (EEG) recordings have demonstrated aberrant cortical activation and a general deterioration in connectivity and functional organisation of the schizophrenic brain (*Hajos 2006*). In addition to the attention deficits associated with reduced P300, defects in neuronal-network oscillations and diminished information processing (auditory-gating deficits, mismatch negativity deficits) have also been reported (*Hajos 2006*). Understanding the relationship between neuronal-network oscillations and attention/information processing will be crucial to understanding the biological basis of schizophrenia.

It is important to note than many structural and functional defects associated with schizophrenia precede the onset of symptoms and are also present in unaffected relatives suggesting that these are underlying developmental defects most likely resulting from genetic predisposition to schizophrenia. In addition neuropathological abnormalities do not correlate well with severity or duration of illness and

schizophrenia does not appear to follow a progressive or degenerative course providing further support for a neurodevelopmental basis to schizophrenia (*Harrison 1999*). However a recent study of childhood early-onset schizophrenia suggests that there may be a progressive loss of grey matter in the parietal and frontal cortices during early adolescence, which eventually extends to the temporal cortex following puberty and the onset of clinical symptoms (*Thompson et al. 2001*).

1.1.3 Neurochemical abnormalities of schizophrenia

The ability of natural and synthetic drugs to re-produce schizophrenia like symptoms in normal individuals has resulted in a number of neurochemical theories. Current thinking supports a neurodevelopmental basis for schizophrenia that results in secondary signalling abnormalities. It is still unknown which of the major neurochemical signalling pathways is responsible for producing the spectrum of symptoms associated with schizophrenia; however there is a growing belief that multiple interacting pathways are disrupted.

For many years the prevailing hypothesis has been that a disruption in dopamine signalling in the brain produces the psychosis associated with schizophrenia. This is not surprising considering the ability of dopamine agonists such as amphetamines to produce schizophrenia-like psychotic symptoms in normal individuals and the fact that all typical antipsychotic drugs alleviate psychosis by antagonising the dopamine system. Dopamine is thought to mediate reward prediction and motivational salience, a process whereby neutral events and representations become attention-grabbing and capture thought and behaviour (*Berridge and Robinson 1998, Kapur 2004*). This has parallels with the heightened perceptual experiences of schizophrenic individuals making dopamine an attractive schizophrenia candidate signalling pathway. However, upregulation of dopamine within the brains of schizophrenic individuals has not yet been demonstrated (*Frith and Johnstone 2003*). Furthermore, not all patients respond to dopamine blockade suggesting there are other signaling elements to consider.

Recent studies of dopamine signalling suggest that it is important for maintaining the balance of glutamate (excitatory) and GABA (gamma-aminobutyric acid, inhibitory) neurotransmission in the prefrontal cortex (*Winterer and Weinberger 2004*). To upset this balance may result in over-alertness and unstable attention potentially manifesting as hallucinations. This failure to focus prefrontal activity may result in cognitive deficits such as have been reported for schizophrenia (*Winterer and Weinberger 2004*).

Glutamate signalling has also been implicated in the generation of schizophrenia-like psychosis. Phencyclidine (PCP) acts on glutamine receptors and produces many schizophrenic like symptoms including delusions, hallucinations, incoherence, paranoia and catatonia. Similarly ketamine, an NMDA (glutamate) receptor antagonist, can produce schizophrenic-like hallucinations and delusions (*Frith and Johnstone 2003*). This has resulted in an NMDA hypofunction hypothesis for schizophrenia. There is strong genetic evidence implicating the glutamate signalling pathway in schizophrenia (*Collier and Li 2003*). Neuregulin 1 is a strong schizophrenia candidate gene which is involved in regulating the expression and kinetics of NMDA glutamate receptors and also impacts on inhibitory neurotransmission via GABA signalling (*Moghaddam 2003*, *Harrison and Weinberger 2005*).

It is clear with both the glutamate and the dopamine hypotheses that neither pathway alone can account for all the complex symptoms associated with schizophrenia. Furthermore, extensive cross-talk between the major signalling pathways of the brain implies that abnormalities in one signalling pathway will undoubtedly have wider implications for neurochemical signalling. It is therefore important to identify the genetic factors that underlie the abnormal development of the schizophrenic brain, and hence where these signalling defects are born, if the pathological mechanism of schizophrenia is to be understood.

1.1.4 Mitochondrial dysfunction in schizophrenia

The mitochondrion is an important organelle whose main role is to meet the energy demands of the cell in the form of adenosine triphosphate (ATP) produced by the process of oxidative phosphorylation. However, the mitochondrion is also important in the biogenesis of other important cellular components such as amino acids and nucleotides and plays an important role in programmed cell death (*Attardi and Schatz 1988, Green and Reed 1998*). The mitochondrion is particularly important for brain function due to the high energy demands of this organ. The human brain uses approximately 20% of the body's energy which is staggering considering that the brain accounts for only 2% of total body weight (*Drubach 2000*). 75% of the brain's energy is consumed by signalling processes related to information processing (*Attwell and Gibb 2005*).

Each mitochondrion contains its own genome of approximately 16.5kb which contains 37 genes encoding its own transcription, translation and protein synthesis systems (*Schon 2000*). The mitochondrial genome is responsible for producing polypeptide components of the oxidative phosphorylation system required for ATP production. Unlike the nuclear genome the mitochondrial genome does not undergo recombination and lacks efficient repair mechanisms to eradicate accumulating mutations which results in many mitochondrial diseases, mostly associated with the brain (*Wallace 1999, Schon 2000*). Many proteins required for the normal functioning of the mitochondria are encoded within the nuclear genome. Mutations in nuclear genes may therefore also affect mitochondria biogenesis (*Schon 2000*).

Mitochondrial dysfunction is a process implicated in Parkinson's disease where it is thought that inappropriately sequestered dopamine may result in oxidative stress leading to cell damage and neurodegeneration (*Gluck and Zeevalk 2004*). Dopamine is a cytotoxic molecule and has been shown to inhibit respiration of isolated brain mitochondria and actively induce damage along with other mitochondrial toxins (*Boada et al 2000, Moy et al. 2000*). Under normal physiological conditions dopamine is sequestered in vesicles which eliminates the cytotoxicity; however under conditions where dopamine levels are increased (e.g. amphetamine challenge)

dopamine derivatives are up-regulated within the cytosol where they may exert toxic effects (*Mosharov et al. 2003*). Dopamine has been shown to reduce ATP production in cultured human neuroblastoma cells which is thought to result from inhibition of mitochondrial respiration via mitochondrial Complex I, a complex which has been shown to be altered in the prefrontal cortex of schizophrenic brains (*Ben-Shachar et al. 2004, Karry et al. 2004*). Inhibition of ATP production occurs at dopamine concentrations which are non-toxic to neuroblastoma cell viability (*Ben-Shachar et al. 2004*). This is an interesting finding as it suggests that dopamine may cause mitochondrial dysfunction without overt cellular toxicity such that mitochondrial dysfunction and cellular degeneration are not inextricably linked. Furthermore Complex I deficiency, which may be a factor in schizophrenia, is a common cause of mitochondrial encephalomyopathy and presents as severe brain dysfunction (*Schon 2000*).

Microarray studies have been carried out looking at metabolic gene expression in schizophrenia. These microarray studies are complicated by factors such as brain pH which have been shown to affect mitochondrial gene expression (*Li et al. 2004*). Despite this, changes in mitochondrial gene expression in schizophrenia are still observed even when brain pH is accounted for (*Iwamoto et al. 2005*). These genes tend to be down-regulated and are involved in many aspects of mitochondrial function including respiration, transcription, membrane function and transport to name a few. One additional caveat is that medication used to treat the symptoms of psychiatric illness can cause mitochondrial toxicity (*Iwamoto et al. 2005*). Indeed analysis of mitochondrial gene expression in bipolar disorder suggests that many of these changes in expression can be accounted for by medication although some changes are still evident in medication-free patients (*Iwamoto et al. 2005*). It is likely that the effects of medication on post-mortem gene expression in schizophrenia would be similar to those reported for bipolar disorder. Therefore, although there is evidence for changes in the expression of mitochondrial related genes in schizophrenia, confounding factors make conclusions hard to come by and much more work is required to uncover the mechanism of mitochondrial dysfunction in schizophrenia.

In addition to global changes in gene expression, specific mitochondrial DNA (mtDNA) sequence variants have been associated with schizophrenia. *Marchbanks et al. 2003* have identified a sequence variation in the mtDNA that was significantly more common in schizophrenics that control subjects. This specific variant resulted in a non-conservative amino acid substitution in the ND4 subunit of NADH-ubiquinone reductase (also known as Complex I) and was associated with increased oxidative stress in schizophrenia (*Marchbanks et al. 2003*). Further mtDNA variants have been identified in mother-parent offspring pairs showing maternal transmission of schizophrenia. Five substitutions were identified all of which were absent in 95 control subjects. Three of these variants were non-conservative such that they may affect the structure or function of cytochrome c oxidase, ATP synthase and NADH-ubiquinone oxidoreductase (*Martorell et al. 2006*).

Although the precise nature of mitochondrial dysfunction in schizophrenia in not known, studies of gene expression, oxidative phosphorylation and mtDNA sequence variation all point to a mitochondrial dysfunction phenotype that is associated with schizophrenia. Further pathological studies have reported abnormalities in the number and morphology of mitochondria within schizophrenic brains (*Ben-Shachar 2002*). It is unclear how these defects are caused and whether they are the cause or result of illness; however many diseases of the mitochondria affect the brain and present with variable and complex phenotypes comparable to schizophrenia.

1.2 The molecular genetic basis of schizophrenia

1.2.1 Heritability and Heterogeneity

Schizophrenia is a complex genetic illness with a lifetime risk of approximately 1% within the general population. Schizophrenia is highly heritable with rates of inheritance increasing with the degree of relatedness to an individual. There is an approximate 10 fold increase in risk to individuals with a first degree relative affected by schizophrenia (*Owen and O'Donovan 2002*). For example, the relative risk of developing schizophrenia for an individual with an affected sibling is 9%, the

risk for dizygotic twins ranges from 0-28% and for monozygotic twins the risk is between 41% and 65%. Schizophrenia is a highly heritable disorder, with heritability representing a measure of the amount of phenotypic variance that can be attributed to genetic effects (*Cardno and McGuffin, 2002*). The risk values for schizophrenia correlate to an estimated heritability of 80-85% (*Owen and O'Donovan 2002*). Furthermore adoption studies provide supportive evidence that this increased risk is due to an increase in the number of shared genes and not due to shared environmental factors (*Owen and O'Donovan 2002*).

If schizophrenia was purely a genetic illness the concordance rate for MZ twins would be expected to be 100%, rather the concordance rate is ~50% suggesting that a component of the risk for developing schizophrenia must come from other factors, presumably environmental and epigenetic. A myriad of environmental factors have been associated with schizophrenia including exposure to infectious agents, season of birth, adverse or stressful life events, nutrition and substance abuse (*Frith and Johnstone 2003*). Epigenetic modification of DNA is also becoming a popular theory in the field of schizophrenia. Epigenetic changes are alterations to the functional state of the DNA which can alter gene expression. These changes can also be modified by the environment and hormonal state of the body such that the effects of the epigenetic modification may change during a person's lifetime (*Petronis 2004*). There is no experimental data to substantiate the theory of an epigenetic basis to schizophrenia but it is entirely probable that environmental and epigenetic as well as stochastic cellular events will impact upon predisposing genetic alterations ultimately leading to the pathogenesis of schizophrenia.

1.2.2 Finding genes in a gene-pool – linkage and association

Schizophrenia exhibits a complex non-mendelian pattern of inheritance and is likely to be an oligogenic or polygenic disorder, or even a mixture of both. Numerous linkage and association studies have been carried out with the hope of identifying positional or functional candidate genes. Unfortunately, both association and linkage studies encounter interpretation problems, as positive results are generally ambiguous and difficult to replicate, as would be expected with a complex illness.

Despite this, there have recently been several convincing reports of replicated linkage and association which identify potential genetic susceptibility loci on several chromosomes. Some exciting candidate genes which are emerging from these studies are discussed in the subsequent section.

1.2.2.1 The schizophrenia candidates

DTNBP1

The *Dystrobrevin-Binding Protein 1* (*Dysbindin, DTNBP1*) gene is located on chromosome 6p22.3. Originally identified by *Straub* and colleagues in 2002, *dysbindin* is an interesting candidate gene for schizophrenia as it is known to be expressed in the axon terminals of adult mouse brains and may be important for normal synaptic function (*Benson et. al. 2001, Harrison & Owen 2003)*. Although extensively replicated in a number of populations, the haplotypes and alleles associated with schizophrenia have been very different between the studies (*Harrison and Weinberger 2005*). No causative allele has been identified although some single nucleotide polymorphisms (SNPs) have been associated with intermediate cognitive phenotypes, including IQ, episodic and working memory (*Harrison and Weinberger 2005*).

Dysbindin is associated with the dystrophin-associated protein complex present within the postsynaptic density (PSD) (*Benson et al. 2001*). Here it is thought to function in trafficking and tethering of neurotransmitter receptors and other proteins (*Harrison and Weinberger 2005*). Dysbindin mRNA (post-mortem *in*-situ) and protein (immunohistochemistry in post-mortem brains) is decreased in brains of some schizophrenic individuals (*Weickert et al. 2004, Talbot et al 2004*). Furthermore, over-expression or suppression of *dysbindin* expression has been shown to impact on pre-synaptic protein expression and glutamate release by cortical neurons in culture (*Numakawa et al. 2004*). Therefore alterations in dysbindin expression or function may have implications for glutamate signalling defects in schizophrenia.

NRG1

Neuregulin 1 (NRG1) is located on chromosome 8p. *NRG1* was initially identified as a schizophrenia candidate gene by a genome wide scan and fine mapping study in an Icelandic population (*Stefansson et al. 2002*). A highly significant association to a 7 marker haplotype within the 5' region of the gene was reported (*Stefansson et al. 2002)*. Albeit with some allelic heterogeneity, this association has been replicated in 2 UK populations, 4 Chinese populations and 1 Irish population (*Harrison and Weinberger 2005)*. A recent meta-analysis of case-control association studies of the *NRG1* gene has also reported significant associations of markers within this 5' haplotype in Caucasian and Asian populations (*Li et al. 2006*).

No functional variant in the *NRG1* gene has been identified for schizophrenia; however it is likely that associated variants may affect gene expression or splicing. There is evidence for an imbalance in the type of *NRG1* isoforms (by qRT-PCR) present in postmortem brains of schizophrenics with the type I isoform being up-regulated in cases versus control brains (*Law et al. 2006*, *Hashimoto et al. 2004, Harrison and Weinberger 2005*). Furthermore altered expression of *NRG1* isoforms have been reportedly associated with disease-associated polymorphisms from the original 5' haplotype identified by *Stefansson et al. 2002* (*Law et al. 2006*). In addition, a variant in the promoter region of the *NRG1* gene, which has been associated with higher expression levels of *NRG1* type IV, has been further associated with decreased cortical activation, decreased premorbid IQ and increased psychotic symptoms in schizophrenia (*Hall et al. 2006, Law et al. 2006*).

NRG1 has a multiplicity of functions all of which may be important in the aetiology of schizophrenia, including acting as a glial growth factor and also playing a role in neuronal migration and myelination and modulation of NMDA receptor signalling (*Collier & Li 2003, Michailov et al. 2004, Gu et al. 2005*). NRG1 also has a role in inducing expression of nicotinic acetylcholine receptors (*Yang et al. 2005, Liu et al. 2001*). Nicotine has been found to improve sensory gating deficits in schizophrenic patients and their relatives and α7 nACh agonists improve amphetamine induced sensory gating in rats (*Hajos 2006*). In this respect it is interesting that a high

proportion of individuals with schizophrenia smoke and that a worldwide meta-analysis has indicated a positive association between smoking and schizophrenia (*de Leon and Diaz 2005*). Smoking may be a form of self-medication for schizophrenia sufferers.

COMT and PRODH

Two further genes of interest have been identified from chromosomal region 22q11, *Catechol-O-Methyl Transferase (COMT)* and *Proline Dehydrogenase (PRODH).* Both of these genes are present within the region of chromosome 22 that is deleted in patients with velocardiofacial syndrome. VCFS patients present with learning abnormalities and schizophrenia-like psychosis among other symptoms (*Murphy 2002*). *COMT* has a direct role in the metabolism of dopamine and other catechols and is expressed abundantly in neurons of the hippocampus and prefrontal cortex suggesting it is an ideal candidate gene for schizophrenia (*Harrison and Weinberger 2005*).

Unlike many of the other schizophrenia candidate genes the *COMT* gene shows association of a functional SNP with schizophrenia. The nature of this SNP is such that it alters the enzymatic activity of the protein with functional consequences for the metabolism of dopamine (*Collier and Li 2003, Harrison and Weinberger 2005*). This SNP replaces a high activity valine allele at position 158 with a low activity methionine allele (val158met) (*Lotta et al. 1995, Lachman et al. 1996*). Clear association of either allele with schizophrenia has not been demonstrated due a high number of negative studies; however the higher activity COMT-valine allele has shown association with poorer prefrontal cortical function (*Harrison and Weinberger 2005*). This would seem counterintuitive considering the original dopamine hypothesis predicts higher dopamine levels as the cause of illness but perhaps COMT has a more important role in cognitive impairments associated with schizophrenia rather than the psychotic aspects. Other non-functional alleles within the *COMT* gene have also been implicated in schizophrenia although they are not well replicated and contradictory studies of mRNA and protein levels of COMT in the brains of schizophrenics only complicates the picture further (*Harrison and Weinberger*

2005). Although the genetic association of the *COMT* gene with schizophrenia is complex the function of this gene and the functional implications of the associated SNPs suggest that COMT is indeed an important mediator of dopamine signalling in the brain with significant implications for schizophrenia. It is postulated that there is an 'optimum' level of dopamine signalling in the brain and current thinking suggests that the COMT Val/Met polymorphism may have a positive or negative effect in a given individual, depending on their intrinsic levels of dopamine signalling. This intrinsic dopamine signalling level ('set-point') is likely to be determined by additional genetic factors and the effect of the Val/Met COMT polymorphism will vary between individuals depending on whether they lie above or below the 'optimum' dopamine signalling level.

Proline dehydrogenase (*PRODH2*) is contained within the same 22q11 region deleted in VCFS as the *COMT* gene. Although statistical association for this gene is weak *PRODH* knockout mice show prepulse inhibition (PPI) deficits and decreases in glutamate and GABA in selected brain regions (*Gogos et al. 1999, Harrison and Weinberger 2005*).

Other candidate genes

G72 is a novel primate gene located within chromosomal region 13q22-34 and was initially reported as a candidate gene for schizophrenia due to its association with schizophrenia in French-Canadian and Russian populations (*Chumakov et. al. 2002*). G72 is of unknown function but has a predicted interaction with D-aminoacid Oxidase (DAAO), an activator of the NMDA receptor. Association has been confirmed three times for *G72* and the original SNP identified by *Chumakov et al.* has been shown to be associated with some cognitive and physiological impairments seen in schizophrenia (*Harrison and Weinberger 2005*).

The *RGS4* (Regulator of G-protein signalling 4) gene located on chromosome 1q21-22 is involved in neuronal differentiation and has been implicated in schizophrenia by microarray (*Mirnics et al. 2001b*) and weakly by association (*Harrison and Weinberger 2005*).

GRM3 is a type II metabotropic glutamate receptor which has shown association with schizophrenia in German, Japanese, and American populations (*Harrison and Weinberger 2005*). Extended analyses have provided evidence of association for an intron 2 variant with characteristic cognitive impairments of schizophrenia (*Egan et al. 2004*).

Glutamate decarboxylase (GAD67) is a synthesising enzyme for GABA, the neurotransmitter of inhibitory interneurons. This synthesising enzyme is reportedly reduced in a specific subset of GABA containing neurons in the prefrontal cortex of schizophrenics (*Hashimoto et al. 2003*).

Other groups of genes implicated in the schizophrenia disease process by studies of gene expression include genes involved in the regulation of presynaptic function, oligodendrocyte/myelin-related genes and metabolic enzymes (*Mirnics et al. 2000, Mirnics 2001a, Katsel et al. 2005, Vawter et al. 2004*). In addition, expression of genes involved in protein turnover, cytoskeletal dynamics, mitochondrial oxidative energy metabolism, neurite outgrowth and synaptic plasticity has been reportedly reduced in laser-captured dentate granule neurons of the hippocampus (*Altar et al. 2005*).

Genetic studies have clearly identified many candidate genes for schizophrenia. Many of these candidates highlight processes that may be involved in pathogenesis of illness but the founding genetic defect is still not clear. It seems more likely that this is a genetically heterogeneous illness and that there is no one founding mutation but rather a mixed bag of genes, each contributing to the risk for developing schizophrenia. Furthermore, although these studies may highlight important genes and pathways, the disease mechanism remains enigmatic. With the exception of *COMT* and *NRG1* functional variants within theses genes remain to be identified. Therefore further research is needed to elucidate the mechanism of action of potential candidates.

One candidate schizophrenia gene, which is the main subject of this thesis, is *DISC1*. Unlike the previously discussed genes *DISC1* was identified using a cytogenetics approach. Cytogenetics uses labelled chromosomal probes to identify chromosomal abnormalities such as deletions, duplications, inversions or translocations by fluorescent in-situ hybridisation (FISH). Cytogenetics is a very powerful tool when tackling complex diseases because it has the power to identify rare mutations with major effect. Furthermore these studies can pinpoint the exact genes that are disrupted. Cytogenetic studies are generally confined to a few pedigrees and results may not represent the cause of illness in the general population, especially with such a complex illness as schizophrenia. Nevertheless, isolation of single gene defects is extremely helpful in understanding the pathogenesis of illness. This appears to be the case for the *DISC1* gene, originally identified in one pedigree, but with additional research has now come to be one of the most promising schizophrenia candidate genes to date. Subsequent sections discuss the identification of *DISC1* and our current understanding of its potential role in the biology of schizophrenia.

1.3 The t(1;11) translocation

1.3.1. The t(1;11) family

The t(1;11) family is so named as a result of an inherited balanced translocation between chromosomes 1 and 11 (*St.Clair et al. 1990*). It is a large Scottish pedigree which was first identified in 1970 (*Jacobs et al. 1970*) and has been under investigation for more than 30 years. Within this family the t(1;11)(q42.1,q14.3) balanced chromosomal translocation segregates with major psychiatric illness including schizophrenia, bipolar disorder and major depression (*Blackwood et al. 2001*). Figure 1.3 adapted from *Blackwood et al. 2001*, shows family members whose carrier status has been determined and their associated psychiatric diagnoses. It is noted that some family members without the translocation present with minor psychiatric diagnoses such as alcoholism and minor depression; however all severe psychiatric illness is restricted to carriers of the translocation.

Linkage studies on this family produced a highly significant LOD score of 7.1 when cases of schizophrenia, bipolar disorder or recurrent major depression were all considered as affected. Linkage analysis with the most severe psychiatric diagnosis of schizophrenia also produced a significant LOD score of 3.6 (*Blackwood et al. 2001*). In linkage analysis LOD stands for the $\log_{10}$ of the odds score for linkage. In the case of the t(1;11) family the odds score for linkage is a measure of the likelihood that major psychiatric illness and the t(1;11) translocation will segregate by chance as opposed to being linked. A LOD score of 3 equates to 1:1000 (10^3) odds against the linkage between the clinical phenotype and the translocation occurring by chance. Therefore in this family a LOD score of 7.1 equates to >1:10,000,000 odds against observing the linkage between major psychiatric diagnosis and the t(1;11) translocation by chance, implying that inheritance of this translocation is causal (*Pericak-Vance 1998*).

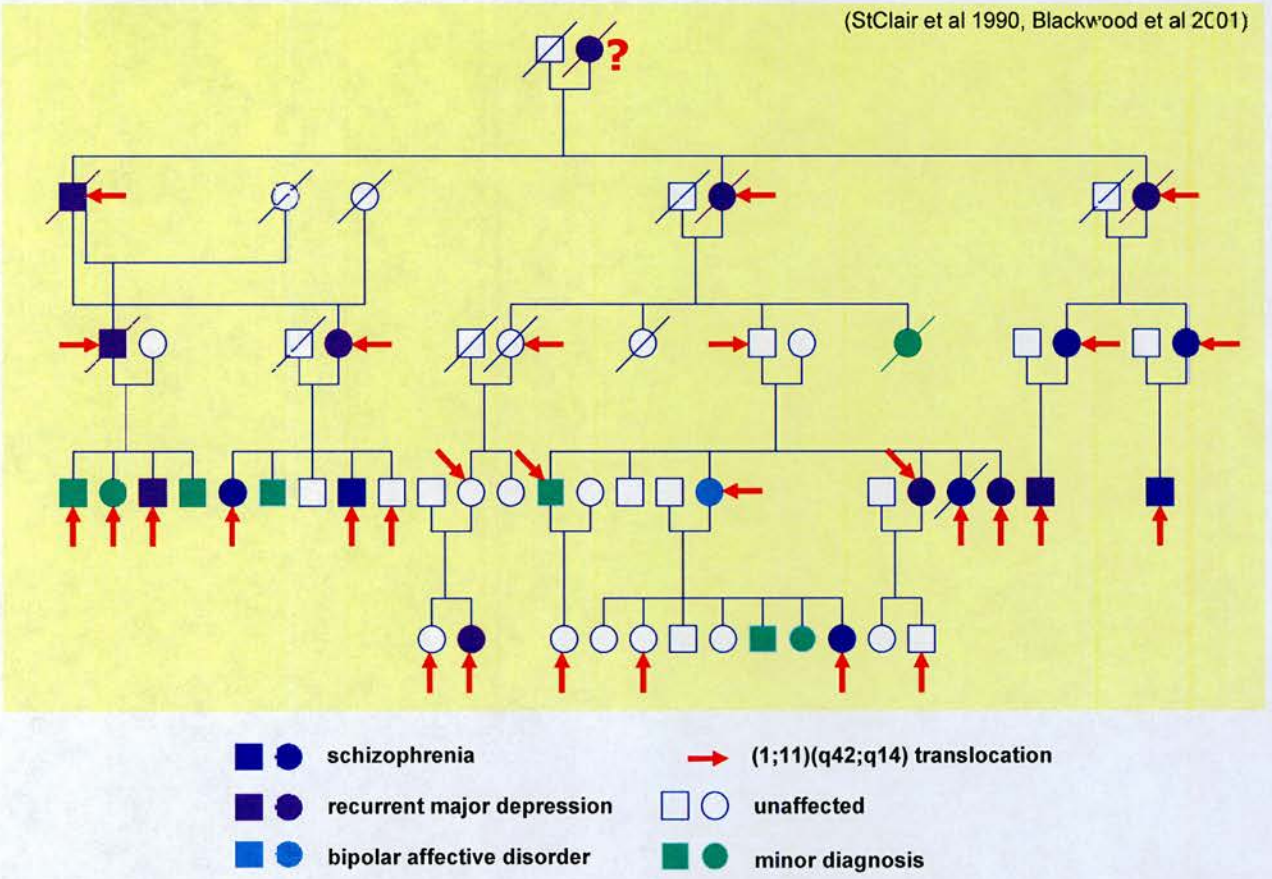

Figure 1.3. This figure depicts the t(1;11) family, a large Scottish kindred with a very high incidence of psychiatric illness. Within this family a balanced translocation between chromosomes 1 and 11 segregates with schizophrenia, bipolar and related affected disorders.

All family members have an IQ within the normal range as determined by the National Adult Reading Test. Furthermore, the translocation does not appear to associate with either neurological or developmental abnormalities. Interestingly however, the translocation does associate with reduced amplitude of the auditory P300 Event Related Potential (ERP) in both affected and unaffected translocation carriers (*Blackwood et al 2001*). The P300 ERP is an electrophysiological measurement using electroencephalography (EEG). It is a measurement of brain activity associated with a specific stimulus or response and is representative of cortical processing (*Patel and Azzam 2005, Linden 2005*). Normal P300 ERPs typically appear 300 to 400ms post stimulus and range in amplitude from 5 to 20 μV. For t(1;11) family members with a normal karyotype the latency and amplitude of the P300 ERP were within the normal range with mean values of at 338.3ms and 12.1μV respectively. In contrast family members possessing the translocation recorded P300 ERPs with increased latency averaging 366.2ms and significantly reduced amplitude with a mean value of 6.8μV (*Blackwood et al. 2001*). These values were similarly reduced in unaffected and affected individuals, therefore the reduction in P300 amplitude observed in this family appears to be a marker of schizophrenia susceptibility conferred by the t(1;11) translocation. Reduced P300 amplitudes reflect abnormal neural functions in carriers of the t(1;11) translocation. As discussed previously these defects in electrical brain activity are likely to represent abnormal attention and working memory deficits in these family members.

1.3.2. Candidate genes within the t(1;11) breakpoint regions

The translocation breakpoints on chromosome 1 and 11 have been studied in detail. No major sequence rearrangements are found at the breakpoint on the derived 11 chromosome and there are no genes disrupted in this region (*Millar et al. 2000*). However with position effects of translocations ranging as far as 1.3Mb from the breakpoint it is possible that the chromosome 11 breakpoint may alter expression of the surrounding genes (*Velagaleti et al. 2005*). Indeed three genes lie in close proximity to the breakpoint on chromosome 11, the metabotropic glutamate receptor *GRM5*, *NAALADase II* and *Tyrosinase* (*Semple et al. 2001, Devon et al. 1997, Petit*

et al. 1999). As discussed below, these genes have been previously implicated in schizophrenia.

GRM5 (mGluR5) is a modulator of NMDA signalling and maps to 11q14 >850kb centromeric to the chromosome 11 breakpoint (*Devon and Porteous 1997*). Due to its role in NMDA signalling mGluR5 is a good biological candidate gene for schizophrenia. mGluR5 knockout mice show deficits in pre-pulse inhibition (PPI), a deficit that is also induced by NMDA antagonists and often reported in schizophrenic patients (*Kinney et al. 2003*). It has been suggested that enhancement of mGluR5 activity may produce anti-psychotic effects in rodents and mGluR5 antagonists have been shown to impair long term potentiation and induce working memory deficits, two other characteristic features of schizophrenia (*Pietraszek et al. 2006*).

There is limited genetic evidence to support the involvement of mGluR5 in schizophrenia. A Case-control association of microsatellite markers within the *mGluR5* gene revealed significant association between a novel intragenic marker and schizophrenia ($p = 0.046$) (*Devon et al. 2001*). No other such associations have been reported for *mGluR5*. Despite being a good biological candidate gene the mechanism by which mGluR5 interacts with NMDA receptor signalling to either alleviate or exacerbate psychotic symptoms is not well understood and impaired mGluR5 function alone is not sufficient to induce these symptoms. Furthermore, strong statistical evidence for *mGluR5* as a candidate schizophrenia gene is lacking.

NAALADase II is more commonly known as glutamate carboxypeptidase II (GCP II). It is a membrane-bound metallopeptidase responsible for cleavage of N-acetylaspartylglutamate (NAAG) to N-acetylaspartate (NAA) and glutamate (*Robinson et al. 1987, Slusher et al. 1990*). NAAG is the most abundant neuropeptide in the human brain and has been linked immunocytochemically to glutamatergic pyramidal neurons of the hippocampus and cerebral cortex. (*Neale et al. 2000, Passani et al. 1997*). Post-mortem studies report alterations in GCP II mRNA and enzymatic activity in the hippocampus and prefrontal cortex of schizophrenic brains (*Tsai et al. 1995, Ghose et al. 2004*). Studies of the involvement

of *GCP II* in schizophrenia are limited and there is currently no genetic evidence to support *GCP II* as a general candidate schizophrenia gene.

Tyrosinase maps 1.2Mb centromeric to the 11q14.3 breakpoint (*Petit et al. 1999*). It is an interesting candidate gene for schizophrenia due to its role in the metabolism of catecholamines. In the brain tyrosinase acts as a melanin synthesising enzyme which has been shown to have protective effects against dopamine induced neurotoxicity. It exerts its protective effect by oxidising dopamine (DA) and dopamine quinones (DAQ) to produce stable melanin (*Miyazaki et al. 2006*). This is a potentially important step in regulating intracellular DA levels as DA is a cytotoxic molecule that auto-oxidizes to form DAQ and reactive oxygen species contributing to cellular oxidative stress. DAQ are highly toxic as they bind and inactivate molecules crucial for the function of DA neurons including the DA transporter and tyrosine hydroxylase, the rate-limiting enzyme in the production of catecholamine neurotransmitters (*Whitehead et al. 2001, Kuhn et al. 1999*). Furthermore, inhibition of tyrosinase increases DA-induced cell death (*Higashi et al. 2000*) and tyrosinase null mice are more vulnerable to metamphetamine induced neurotoxicity (*Miyazaki et al. 2006*).

Although chromosome 11q harbours possible schizophrenia candidate genes in order for them to be involved in pathogenesis of schizophrenia in the t(1;11) family long range position effects of up to 1.2Mb would have to occur as none of the above genes are in the immediate vicinity of the breakpoint. Although extensive studies have not been carried out there is no evidence that expression of these genes is altered by the t(1;11) translocation segregating in this family.

On chromosome 1q42.1 however the translocation directly disrupts two novel genes which have been named *Disrupted-In-Schizophrenia 1* and *2* (*Millar et al. 2000*). *DISC1* was identified from mRNA sequence overlapping the derived chromosome 1 breakpoint (accession number AB007926). This novel gene was found to be 6913nt in length (accession no. AF222980) and encodes a novel protein of 854 amino acids (*Millar et al. 2000*). The second gene, *DISC2,* was identified from expressed

sequence tags surrounding the chromosome 1 breakpoint region (accession no. AF222981). This gene is expressed in the reverse orientation to *DISC1* and is likely to represent a natural anti-sense non-coding RNA gene (*Millar et al. 2000*). The full extent of this gene remains to be characterised.

Just 5'of *DISC1* lies the gene *TRAX* which although not directly disrupted may be altered by position effects as a result of the translocation. However protein expression studies demonstrate that this is unlikely to be the case as TRAX protein expression remains the same in translocation and non-translocation cell lines from this family (*Millar et al. 2005b*).

The t(1;11) family represents a rare resource for identifying candidate genes for psychiatric illness as the translocation itself appears to be the direct cause of illness. Furthermore the translocation pinpoints the region of interest and suggests that disruption of the novel genes, *DISC1* and *DISC2*, is the primary event leading to illness in later life. These genes are discussed in detail in introductory sections 1.4-1.5 and 1.6 respectively.

1.4 The *DISC1* gene

1.4.1 Independent genetic evidence implicates DISC1 in psychiatric illness

The 1q region of chromosome 1 has been implicated in susceptibility to psychiatric illness in a number of genetic studies (*Brzustowicz et al. 2000, Gurling et al. 2001 Macgregor et al. 2004, Curtis et al. 2003, Hamshere et al. 2005*).

The first independent genetic evidence directly implicating the *DISC1* gene as a schizophrenia susceptibility gene came from a genome wide screen of an internal Finnish isolate (*Hovatta et al. 1999*). This isolate had a particularly enriched risk for developing schizophrenia with a lifetime prevalence of 3.2% compared to 1.1% in the general Finnish population (*Hovatta et al. 1999*). The most significant region identified in this study was chromosomal region 1q.32.2-q41 producing a pairwise

LOD score of 3.82 when schizophrenia and schizoaffective disorder were considered affected (*Hovatta et al. 1999*). Fine-mapping of this region in a second large population-based study of the Finnish population identified positive linkage to an intragenic marker of *DISC1* (*Ekelund et al. 2001*). This intragenic *DISC1* marker is in close proximity to the t(1;11) breakpoint region residing within intron 9 of the *DISC1* gene. These original findings have since been replicated in a further independent Finnish population (*Ekelund et al. 2004*).

An additional association study of the Finnish population implicates undertransmission of a haplotype of *DISC1* spanning intron 1 to exon 2 in susceptibility to schizophrenia in females only (*Hennah et al. 2003*). Under-transmission of this haplotype has been confirmed in an independent study of a North American population with schizoaffective disorder patients (*Hodgkinson et al. 2004*). *Hodgkinson et al.* provided further evidence for association of additional *DISC1* markers with susceptibility to schizophrenia, schizoaffective and bipolar disorder, including a nonsynonymous Leucine to Phenylalanine amino-acid substitution at position 607 (*Hodgkinson et al. 2004*). The functional consequences of this polymorphism are unknown but magnetic resonance imaging suggests the Phe allele may be associated with reduced grey matter volume and increased psychotic symptoms (*Malhotra et al. 2006*).

Hwu et al. also reported linkage of another chromosome 1q marker, D1S251, with schizophrenia, schizoaffective and additional psychotic disorders in a Taiwanese population (*Hwu et al. 2003*). This marker lies upstream of *DISC1* between the *DISC1* and *TRAX* genes. The *TRAX/DISC1* region has been further implicated in both bipolar and schizophrenia in the Scottish population (*Thomson et al. 2005b*). This study provides evidence that the *DISC1* gene is a susceptibility factor for psychiatric illness in the general Scottish population and not just in the t(1;11) family.

Interestingly the idea that *DISC1* may contribute to risk for psychiatric illness in a sex-dependent manner as originally suggested by the Finnish group (*Hennah et al.*

2003) is supported by other studies demonstrating sex-dependent associations between *DISC1* and schizophrenia in a Han-Chinese population and *DISC1* and bipolar disorder in the Scottish population (*Chen et al. 2006, Thomson et al. 2005b*).

Recently a study of a North American family with schizophrenia and schizoaffective disorder reported an association between a frame-shift mutation within the *DISC1* gene and these psychiatric diagnoses (*Sachs et al. 2005*). The frame-shift mutation did not however unequivocally segregate with illness and it now appears that a study of schizophrenia in a UK and Irish population has identified this same mutation in control subjects but not in schizophrenic subjects (*Green et al. 2006*). This questions the relevance of this mutation in the development of psychiatric illness.

In summary positive linkage and associations between the 1q region of chromosome 1 and the *DISC1* gene itself have been reported with respect to schizophrenia, schizoaffective and bipolar disorder in multiple populations including, British, Irish, North America, Finnish, Han-Chinese, Icelandic and Taiwanese.

Of course in spite of these positive findings there are also a number of negative findings which do not support these linkage and association data (*Levinson et al. 2002, Kockelkorn et al. 2004, Zhang et al. 2005, Wilson-Annan et al. 1997, Devon et al. 2001)*. Two of these studies within the Scottish population use only 2 microsatellite markers and 5 SNPs respectively to determine an association between *DISC1* and psychiatric illness (*Wilson-Annan et al. 1997, Devon et al. 2001*). Considering the small number of markers tested it is likely that these studies did not possess the power to detect associations that may have been present. The more recent association study on the Scottish population by *Thomson et al.* first constructed a linkage disequilibrium map of the *DISC1* region such that informative markers could be chosen to cover the entire gene region and this study did find positive associations for the *DISC1* gene and psychiatric illness (*Thompson et al. 2005b*).

Two of the other studies which reported negative findings with respect to association of *DISC1* and schizophrenia came from the Japanese population (*Kockelkorn et al.*

2004, Zhang et al. 2005). It is possible that *DISC1* is not a major genetic risk factor for schizophrenia within the Japanese population despite the positive findings in many additional populations. Of interest however, one recent study within the Japanese population has reported significant associations for *DISC1* with major depression (*Hashimoto et al. 2006*). Whilst this study also reported association with schizophrenia the association was weak ($p = 0.0496$); however upon analysis of gender effects a stronger association was determined between *DISC1* and male schizophrenic subjects, albeit for a different SNP.

As schizophrenia is a complex illness with multiple interacting genetic factors it is unlikely that the same genetic risk variants will be present in all populations. It is likely that this genetic heterogeneity is accountable for failure to replicate linkage to the 1q42 region in a large study of affected sib pairs (*Levinson et al. 2002, Macgregor et al. 2002*).

Although the genetic evidence implicating *DISC1* in psychiatric illness is now considered to be strong these studies have implicated various regions along the length of the *DISC1* gene; these are depicted in figure 1.4.A. With the exception of the t(1;11) translocation these studies have yet to identify a disease causing variant that affects the function of *DISC1*. Although these variants are not deemed to be disease causing, some have been associated with measures of cognitive performance in affected individuals and therefore are likely to be markers for underlying functional variants in the *DISC1* gene. Alternatively they may represent synonymous disease causing variants similar to the *NRG1* polymorphisms that alter expression of various *NRG1* isoforms (*Law et al. 2006*).

A non-conservative SNP (Ser704Cys) within the *DISC1* gene has recently been associated with schizophrenia in a population of schizophrenic patients of American-European ancestry (*Callicott et al. 2005*). This SNP results in substitution of a serine allele with a cysteine within exon 11 of the *DISC1* gene. The serine allele of this SNP was seen to be overtransmitted in schizophrenic patients compared to controls. Furthermore this serine variant was associated with reduced grey matter volume

within the left hippocampal formation in healthy individuals in addition to abnormal hippocampal activation (using fMRI) during tests of cognitive function (*Callicott et al. 2005*). The serine allele was also associated with minor cognitive abnormalities and reduced levels of N-acetylaspartate (NAA) within the left hippocampal formation of schizophrenic individuals (*Callicott et al. 2005*). The impact of the Ser704Cys substitution on DISC1 function is unknown and again may merely be a marker of an underlying causative variant within the *DISC1* gene. What is very interesting about this particular study is that they examine the effects of the *DISC1* variant in healthy subjects and provide evidence that variation in *DISC1* may alter brain structure and function in otherwise healthy individuals.

This same Ser704Cys allelic variation has recently been studied within the Scottish population with respect to normal cognitive ageing in healthy individuals. Cognitive function was assessed in a cohort of individuals at the ages of 11 and 79. This study found that there was no direct effect of *DISC1* genotype on cognitive function at age 11 although by age 79 there was sex-dependent *DISC1* genotype effect on cognitive function with females homozygous for the Cys allele performing relatively poorer than males of the same genotype (*Thomson et al. 2005a*). Again this study highlights the importance of *DISC1* in cognitive function in healthy individuals; however this study reports that the Cys allele is associated with cognitive deficits rather than the Ser allele from the *Callicott* study. This Ser704Cys SNP has also been associated with severity of delusions within schizophrenic patients (*DeRosse et al. 2006*).

The previously reported HEP3 haplotype originally associated with schizophrenia in the Finnish population (*Hennah et al. 2003*) has also been associated with impaired visual attention and working memory in a subset of individuals used in the initial association study. In fact this haplotype proved more significantly associated with these cognitive traits than schizophrenia and again some deficits were also seen in unaffected individuals, further supporting DISC1s role in cognitive function (*Hennah et al. 2005*).

Additional associations of the HEP1 haplotype and a rare haplotype derived from the HEP2/HEP3 haplotypes (from the *Hennah et al. 2003* study), have further been

reported with reduced grey matter density and impairments in long-term and spatial memory in a twin based study of the Finnish population (*Cannon et al. 2005*).

A recent study has further confirmed the association between *DISC1* and schizophrenia in a second Taiwanese population and also demonstrated sustained attention deficits within affected individuals form this population (*Liu et al. 2006*).

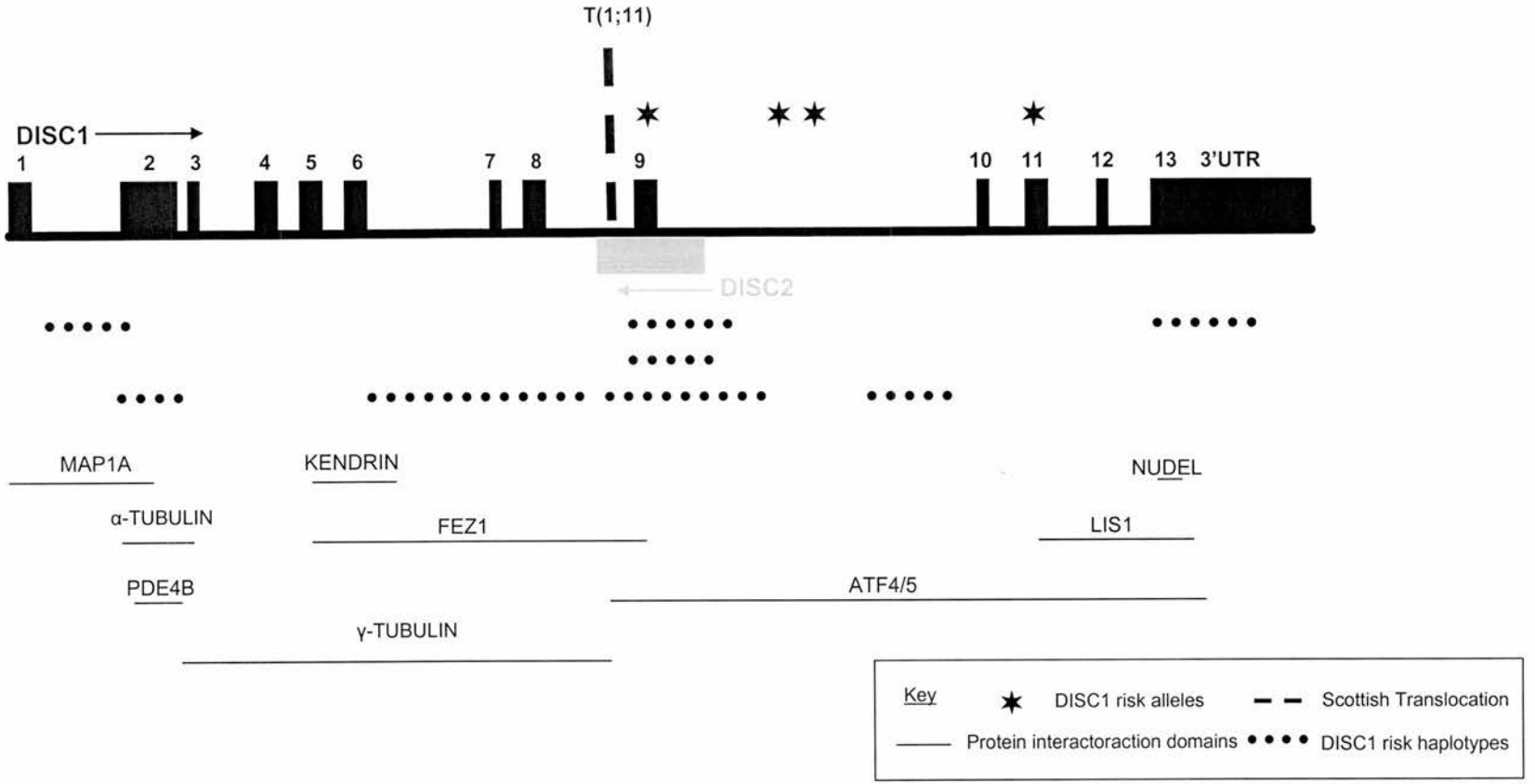

Figure 1.4.A. This figure depicts the genomic structure of the *DISC1* and *DISC2* genes. DISC1 protein interaction domains and genetic evidence implicating the *DISC1* gene in psychiatric illness are shown as indicated by the key. Genetic evidence spans the full length of the *DISC1* gene and also overlaps the *DISC2* gene, a putative non-coding RNA gene, which is yet to be fully characterised. Thus these data implicate both *DISC1* and *DISC2* in psychiatric illness. It is apparent also that genetic risk alleles and haplotypes overlap many of the DISC1 protein interaction domains and thus could affect the functionality of the protein. Further information on these genetic data can be found in the following references; *Ekelund et al. 2001, Ekelund et al. 2004, Hennah et al. 2003, Hennah et al. 2005, Cannon et al. 2005, Hodgkinson et al. 2004, Blackwood et al. 2001.*

1.4.2 DISC1 gene structure and evolution

The *DISC1* gene spans ~400kb of genomic DNA and consists of 13 exons producing a full length transcript of approximately 7.5kb in length (*Millar et al. 2000*). Comparative genomics reveals conservation of *DISC1* genomic sequence in mouse (*Mus musculus*), zebrafish (*Danio rerio*) and pufferfish (*Fugu rubripes*) and RT-PCR confirms the presence of *DISC1* cDNA sequences (*Taylor et al. 2003*). The genomic structure of mammalian *DISC1* differs from pufferfish and zebrafish, which lack exon 9a of mammalian *DISC1* and possess an additional exon 11a that appears to have been lost in mammalian *DISC1* homologues. Intron 12 of human *DISC1* is of the rare AT/AC type and is conserved between human, mouse and pufferfish (*Millar et al. 2001, Taylor et al. 2003, Ma et al. 2002*).

Mammalian *DISC1* produces 4 alternative splice isoforms denoted Long (L, full length, exons 1-13, EMBL:Af222950), Long variant (Lv, excludes distal 66 nucleotides of exon 11, EMBL:AB007926), Short (S isoform, uses an alternative 3'UTR in intron 9 (exon 9a) EMBL:AJ06177) and Extremely short (Es isoform, terminates transcription two intronic codons after exon 3 EMBL: AJ506178) (*Taylor et al. 2003*).

DISC1 also shows intergenic splicing with its neighbouring gene *TRAX* (translin-associated factor X). This splicing event produces novel fusion transcripts, although translation of these transcripts is yet to be documented (*Millar et al. 2000*). The *TRAX* gene produces a 33kDa protein that binds to Translin (*Aoki et al. 1997*). Translin is an RNA binding protein with potential involvement in dendritic mRNA translation, an important process necessary for synaptic plasticity (*Muramatsu et al. 1998, Pfeiffer and Huber 2006*).

The full length *DISC1* transcript is translated into a protein of 854 amino acids that is predicted to consist of a globular N-terminal region and a C-terminal region (*Millar et al. 2000*). The N-terminal region contains a nuclear localisation signal (*Taylor et al. 2003*) and the C-terminal region contains conserved leucine zipper and coiled-coil motifs likely to be required for DISC1 protein-protein interactions (*Millar et al.*

2001, Millar et al. 2000). The mouse ortholog, *Disc1*, also contains this nuclear localisation signal, leucine zippers and coiled coil domains suggesting they are of functional importance (*Ma et al. 2002*). The protein structure of *DISC1* is such that it possesses the ability to bind a multiplicity of protein interactors and therefore is a likely molecular scaffold protein.

The t(1;11) translocation disrupts the *DISC1* gene within intron 8 resulting in the 3' end translocating to chromosome 11. If the disrupted *DISC1* allele on chromosome 1 was transcribed it may produce a truncated transcript that hypothetically could produce a C-terminally truncated protein lacking many of the coiled coil domains necessary for DISC1 protein interactions.

1.4.3 DISC1 gene expression in mammals

1.4.3.1 *DISC1* expression in brain

Initial Northern blotting experiments revealed that *DISC1* mRNA is expressed in many adult human tissues (heart, brain, placenta, kidney and pancreas). *DISC1* appears to be most highly expressed in human heart and brain with *DISC1* transcripts detected in multiple brain regions (*Millar et al. 2000*). In recent years much work has been carried out to define more clearly the regions of *DISC1* expression using the mouse, rat and monkey as more accessible systems. These studies aimed to investigate the role of *DISC1* in brain function and development and with schizophrenia being increasingly thought of as a neurodevelopmental disorder these studies are necessary to sustain this current thinking.

Northern blotting of adult mouse tissues detects *Disc1* expression in heart, brain, kidney and testis (*Ma et al. 2002*). In concordance with human data, the highest expression level was detected in heart tissues. Northern blotting in rat also reveals heart to be the highest expressing tissue (*Ma et al. 2002*). *In situ* hybridisation of adult mouse brain tissue demonstrated high *Disc1* expression in the dentate gyrus of the hippocampus in addition to low expression in many additional tissues including the cerebellum, cerebral cortex, ammon's horn and olfactory bulbs. Very low

expression was also detected within the paraventricular and arcuate nuclei of the hypothalamus and amygdala (*Ma et al. 2002*). A further study of rodent *Disc1* demonstrated expression within hippocampal, cortical, cerebellar and olfactory neurons of rat brains (*Miyoshi et al. 2003*).

Subsequent *in situ* studies for *DISC1* in brains of adult African Green Monkeys also revealed widespread expression including the lateral septum and dentate gyrus of the hippocampus and lower expression within the cerebral cortex, amygdala, cerebellum, paraventricular hypothalamus and the interpenduncular and subthalamic nuclei (*Austin et al. 2003*).

Thus, the most consistent observation common to rodent and primates is prominent expression in the dentate gyrus. This is an interesting finding considering the neurodevelopmental abnormalities of the hippocampus implicated in schizophrenia. The cerebral cortex and the cerebellum also express *DISC1* in these three species whilst other regions of expression differ. Although this may be due to differences in experimental methods, including the library used to isolate the *DISC1* probe and the isoforms of *DISC1* detected by each probe it is also possible that *DISC1* performs distinct functions in rodent brains to that of the primate brain.

Attempts to determine a developmental expression profile for *Disc1* have shown that *Disc1* is expressed in the hippocampus throughout mouse brain development from embryonic day 14 to postnatal day 21. *Disc1* appears to be expressed more prominently in ammon's horn at birth but this expression diminishes during postnatal stages in favour of increased expression in the dentate gyrus. *Disc1* expression is seen in cortical neurons and interneurons at the time of neuronal birth and migration (*Austin et al. 2004*). The finding that *Disc1* is expressed throughout brain development is further supported by expression studies of the DISC1 protein in the developing mouse brain (*Schurov et al. 2004*). This study demonstrated DISC1 expression in similar limbic brain regions to the mRNA studies. DISC1 expressing cells were neuronal in nature, both excitatory and inhibitory. Furthermore, a 100kDa DISC1 isoform demonstrated dynamic expression during mouse brain development

with most prominent expression at embryonic day 13.5 and postnatal day 35, which correspond to periods of active neurogenesis and puberty respectively (*Schurov et al. 2004*).

DISC1 is well placed for a role in schizophrenia considering its widespread expression in the brain and prominent expression in the hippocampus and other limbic brain regions. Hippocampal function has been implicated in schizophrenia and hippocampal lesions in rodents and primates can lead to neuropsychological defects including cognitive, locomotor and behavioural abnormalities similar to those reported in schizophrenia (*Bachevalier et al. 1999, Swerdlow et al. 2001, Lipska 2004, Marquis et al. 2006*).

Although the expression of *DISC1* in the brain is most intriguing due to the nature of illness caused by disruption by the translocation (i.e. severe psychiatric illness), *DISC1* has also been seen to be highly expressed in heart tissue from human, mouse and rat, and therefore may play additional important functions in other locations.

1.4.3.2 Sub-cellular DISC1 expression in cultured cells

Using cell culture techniques, exogenous and endogenous DISC1 protein expression has been studied in detail in many mammalian cell types, including primary cells and established cell lines. DISC1 has a very varied expression pattern occupying many sub-cellular locations including the cytoplasm, cytoskeleton, nucleus, mitochondria and centrosome (*Ozeki et al. 2003, Morris et al. 2003, Miyoshi et al. 2004, Brandon et al. 2004, James et al. 2004, Brandon et al. 2005, Kamiya et al. 2005, Ogawa et al. 2005, Millar et al. 2005a*). These sites of DISC1 expression are depicted in figure 1.4.B and will be discussed in more detail in relation to the function of DISC1 in subsequent sections.

Similar to studies of DISC1 expression in brain tissues a number of these studies using cell lines have demonstrated changes in DISC1 expression which are related to neuronal differentiation. DISC1 expression is seen to be augmented in differentiating

rodent neuronal (PC12) cells and coincides with movement of the DISC1 protein from cytoplasmic puncta into neurite-like processes (*Ozeki et al. 2003*). A similar change is DISC1 distribution has been reported using a human neuroblastoma cell line (SH-SY5Y) (*James et al. 2004*). Furthermore, in cultured rat hippocampal neurons DISC1 expression has been localised in growth cones (*Miyoshi et al. 2003*).

Studies of DISC1 interacting proteins should give insights into the many potential functions of DISC1 within each sub-cellular compartment and hopefully will enable us to understand the role of DISC1 in the mammalian brain and how it may contribute to the pathogenesis of psychiatric illness.

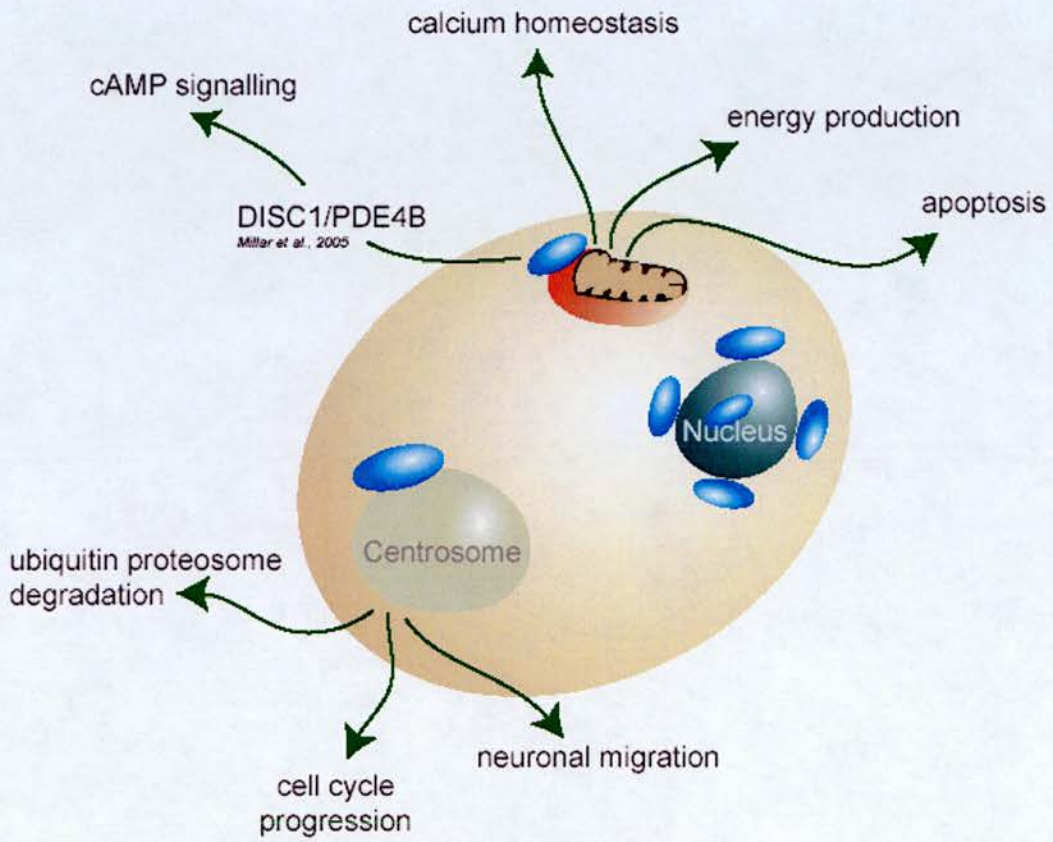

Figure 1.4.B. DISC1 has been shown to be expressed in multiple sub-cellular locations within mammalian cells. These locations which are depicted here include the mitochondrion, the nucleus, the centrosome and the cytoplasm (in particular the perinuclear region).

1.5 DISC1 function and protein interactions

1.5.1 DISC1 yeast two-hybrid studies

To date, seven yeast two-hybrid screens have been carried out with the aim of identifying DISC1 interacting proteins (*Millar et al. 2003, Morris et al. 2003, Miyoshi et al. 2003, Ozeki et al. 2003, Miyoshi 2004, Brandon et al. 2004, Camargo et al. 2006*). The yeast two-hybrid study by *Millar et al.* uncovered 21 potential interactors by screening human (adult and foetal) brain libraries. The proteins identified were from multiple sub-cellular compartments including the cytosol, centrosome, golgi, nucleus, cell membrane and the mitochondria. Seven of the clones identified in this screen produced very strong interactions with DISC1. Of these seven proteins, two are centrosomal proteins (NUDE and NUDEL (NudE-like), one protein localises to both the centrosome and the golgi (AKAP9), one additional golgi protein (GM130) was also amongst the strong interactors and three further cytosolic/nuclear proteins were identified (ATF4, GRIPAPI, ARHGEF11). If these proteins represent true DISC1 interactors then DISC1 is clearly a multi-functional protein.

Additional yeast two-hybrid studies also identified ATF4 and NUDEL as potential DISC1 interactors (*Morris et al. 2003, Ozeki et al. 2003, Brandon et al. 2004*). These studies suggest that DISC1 may play important roles in transcriptional regulation within the nucleus/cytosol through interactions with ATF4, and also at the centrosome via interactions with NUDEL. Two additional yeast two-hybrid studies again using human brain cDNA libraries identified a further centrosomal protein kendrin/pericentrin-B (*Miyoshi et al. 2004)* and FEZ1 (fasciculation and elongation protein zeta-1), a protein involved in axonal outgrowth and fasciculation (*Miyoshi et al. 2003).*

Most recently a study of the DISC1 interactome has been published (*Camargo et al. 2006*). This study utilised a yeast two-hybrid system to identify and categorise DISC1 interactors into functional networks. This study strongly supports the multi-functionality of the DISC1 protein, with DISC1 protein:protein interactions

postulated to pay a role in many biological processes including biogenesis and organisation of the cytoskeleton, mRNA and protein synthesis, cell cycle and cell division and intracellular transport and signalling. The majority of interactions presented within this interactome however are yet to be confirmed experimentally.

1.5.2 DISC1 at the centrosome

The centrosome represents the microtubule organising centre (MTOC) of mammalian cells, a highly complex organelle that functions to nucleate and organise microtubules. Published literature suggests that more than 100 regulatory proteins localise to the centrosome, creating a hub of activity and a control centre for multiple diverse cellular functions (*Doxsey et al. 2005*). Coiled coil domains, as seen in DISC1, are common to many of the regulatory proteins that localise to centrosomes.

The centrosome has a key role in cell cycle progression and neuronal migration both of which will be discussed in more detail in the following sections. In addition, the centrosome acts as a centre of proteolytic activity with components of the ubiquitin-proteosome degradation pathway (UPD pathway) concentrated here. This pathway is important for mediating many cellular processes including cellular differentiation, stress response, neurotransmission and apoptosis (*Badano et al. 2005*). Furthermore the centrosomal UPD pathway has been implicated in Parkinson's disease (*Nussbaum and Ellis 2003, Badano et al. 2005*).

1.5.2.1 The centrosome in cell cycle progression

Centrosomes have a critical role in cell cycle progression and mitosis. The mammalian cell cycle consists of four stages, G_1, S phase, G_2 and M phase, in addition to a G_0 stage in which cells remain quiescent. M phase is the stage at which cells undergo mitosis. Mitosis itself has 7 progressive stages, Interphase, Prophase, Prometaphase, Metaphase, Anaphase, Telophase and Cytokinesis. During interphase the DNA replicates and centrioles are duplicated; this replicated DNA and the associated proteins condense to form visible chromosomes during prophase; the microtubule cytoskeleton disassembles leaving free building blocks of tubulin to

generate the mitotic spindle which forms during prometaphase; once the mitotic spindle is formed sister chromatids attach via associated protein bundles which form the kinetochore; these chromosome are then aligned at the centre of the cell during metaphase to form the metaphase plate; once the chromosomes are in the correct alignment anaphase commences, during which the spindle fibres of the mitotic spindle shorten and the sister chromatids become separated; this process continues into telophase, the point at which the chromatids arrive at opposite poles of the mitotic spindle ready for cytokinesis; an actin ring then contracts in the region of the metaphase plate producing two daughter cells which re-organise a new microtubule cytoskeleton before beginning the whole process again (*Sullivan 2006 http://www.cellsalive.com/mitosis.html*).

The cell cycle is an intricate process into which multiple checkpoints are incorporated. These checkpoints monitor the cells size and environment as well as DNA replication and alignment of chromosomes during metaphase. Cells that evade checkpoint controls are harmful to the organism as they may accumulate mutations due to errors during DNA replication or produce chromosomal abnormalities due to misalignment of chromosomes. A comprehensive review of the cell cycle and its regulation is beyond the scope of this introduction, but some salient features will be mentioned.

Accumulation of many regulatory proteins at the centrosome has been documented to be important for cell cycle progression; some of these are known regulators of the cell cycle whereas others have a less well defined role. These regulatory proteins and protein complexes include Cdk1-cycB, Aurora-A kinase, Polo kinase, Pericentrin B/Kendrin, AKAP450-PKA, γ-tubulin and Pericentrin-γTuRC (*Prigozhina et al. 2004, Kramer et al. 2004, Zimmerman et al. 2004, Hirota et al. 2003, Keryer et al. 2003, Marumoto et al. 2003, Gillingham and Munro 2000, Lee et al. 1998*). These proteins have importance not least for entry into mitosis from G_2 but also for the transition between G_1 to S phase, cytokinesis and mitotic exit (*Doxsey et al. 2005*). Consistent with these data, removal of whole centrosomes by microsurgery results in mitotic defects (*Hinchcliffe et al. 2001, Khodjakov and Rieder 2001*). Centrosomes

may also play a role in responding to genotoxic stress by inducing mitotic catastrophe, a process whereby mitotic division of aberrant cells fails providing a mechanism of eliminating these cells from the normal cycling population (*Doxsey et al. 2005*).

1.5.2.2 The centrosome in nuclear migration and nucleokinesis

Neuronal migration occurs as a stepwise process. In the first instance the migrating neurons extend a leading process (neurite) in response to chemoattractants or chemorepellants. This is then followed by translocation of the centrosome into the leading process, followed by the nucleus and retraction of the trailing process (*Tsai and Gleeson 2005*). It is postulated that the centrosome plays a role in determining the direction of migration and in nuclear translocation into the leading process, which is termed nucleokinesis (*Badano et al. 2005*). Some of the key players in this process are components of a conserved nuclear migration pathway, including LIS1, NUDEL and Cytoplasmic Dynein.

Nudel (*NudE-like or Ndel1*) is the mammalian homologue of the *Aspergillus nidulans nudE* gene. *NudE* is known to interact with *nudF,* which is homologous to mammalian *Lis1* (*Xiang et al. 1995, Efimov and Morris 2000*). The *nudF* and *nudE* genes were so named as they were initially identified as nuclear distribution mutants (nud mutants). The *nudF* and *nudE* genes are important components of the nuclear migration pathway in *A. nidulans*. *A. nidulans* is a multinucleate filamentous fungi and this nuclear migration pathway is essential for nuclei to migrate towards the hyphal tip of the growing fungal colony (*Morris 2000*). Cytoplasmic dynein is another important component of this nuclear migration pathway as it was also identified as a nud mutant, *nudA,* in *A. nidulans* (*Morris 2000*). Mammalian homologues LIS1 and NUDEL also interact with cytoplasmic dynein and recently there has been much research aiming to elucidate the individual functions and the mechanism of interaction of these proteins (*Niethammer et al. 2000, Sasaki et al. 2000*).

One current model of nuclear migration proposes that the nucleus is attached to the microtubule network via LIS1 at the centrosome and a microtubule stabilising protein DCX at the nucleus. The ability of NUDEL and Dynein to bind LIS1 then provides a means for dynein, a molecular motor protein involved in retrograde movement along microtubules, to move the nucleus towards the centrosome, located in the leading process of the migrating neuron (*Badano et al. 2005*). This model proposes that NUDEL, LIS1 and Dynein interactions link the nucleus, centrosome and microtubule network making nucleokinesis possible. Research in this area is now providing evidence in support of such a model some of which is outlined below.

LIS1 is known to play an important role in neuronal migration in mammals as mutations in the *Lis1* gene result in lissencephaly, a developmental brain disorder resulting in smooth cerebral surface and disorganisation of cortical layers due to an arrest in neuronal migration (*Reiner et al. 1993, Dobyns et al. 1993, Lo Nigro et al. 1997*). LIS1 and NUDEL are highly co-expressed during neuronal development and a direct interaction between these two proteins has been observed by yeast two-hybrid screening and co-immunoprecipitation (*Niethammer et al. 2000, Sasaki et al. 2000*). The NUDEL/LIS1 interaction may be particularly important in neuronal migration as point mutations in the *Lis1* gene which affect its interaction with NUDEL have been found in human patients with lissencephaly (*Lo Nigro et al. 1997, Sasaki et al. 2000*). As nuclear migration is an important feature of neuronal migration the roles of NUDEL and LIS1 in this process may explain the neuronal migration defects seen in lissencephaly.

Microtubule dynamics are also an important feature of neuronal migration as nuclear translocation requires a close association of the nucleus with the microtubule organising centre (MTOC or centrosome) (*Morris 2000, Tsai and Gleeson. 2005*). NUDEL and LIS1 have been localised to the centrosome in developing neurons and therefore it is plausible that they may play a role in the nucleokinesis aspect of neuronal migration (*Niethammer et al. 2000, Sasaki et al. 2000).*

Cytoplasmic dynein is a multi-subunit protein complex consisting of heavy, intermediate and light chains. Both LIS1 and NUDEL can bind directly to cytoplasmic dynein heavy chain (*Sasaki et al. 2000*). Cytoplasmic dynein heavy chain also possesses an intrinsic ATPase activity and homo-dimers of LIS1 have been shown to regulate this ATPase activity of cytoplasmic dynein (*Smith et al. 2000, Mesngon et al. 2006*). Furthermore, NUDEL is required to facilitate this interaction between LIS1 and cytoplasmic dynein and in budding yeast it has been demonstrated that this NUDEL/LIS1 interaction is necessary to target dynein to microtubule ends (*Shu et al. 2004, Li et al. 2005*).

To examine the effects of disrupting this conserved nuclear migration pathway *Shu et al.* performed RNA interference to reduce expression of all three components. Migrating neurons that have been treated using RNAi to silence any of the three components of this nuclear migration pathway (NUDEL, LIS1 or Dynein) produce neuronal migratory defects (*Shu et al. 2004*). Furthermore, in the subset of RNAi treated neurons that have not migrated correctly there is a reported increase in the distance between the nucleus and the centrosome. This suggests that translocation of the nucleus into the leading process of the migrating neuron may be affected (*Shu et al. 2004*). Indeed these neurons are seen to complete the first stage of migration correctly by extending an outgrowing neurite, but the distance that the nucleus travels is much shorter than in control neurons (*Shu et al. 2004*). It appears to be the case that neurons cannot migrate successfully unless this nuclear migration pathway is fully functional as all three components are necessary in order for neurons to migrate and position correctly. Although *Shu et al.* did not report changes in neuroblast proliferation, reductions in LIS1 have previously been shown to result in increased programmed cell death and decreased neuroblast proliferation (*Gambello et al. 2003*). Therefore it is possible that some neuronal migratory defects may also result from a decrease in the numbers of viable neurons.

1.5.2.3 DISC1 interacts with components of a conserved nuclear migration pathway and plays a role in neuronal migration

Yeast two-hybrid studies identified NUDEL as a robust DISC1 interacting protein. This NUDEL-DISC1 interaction has been confirmed by co-immunoprecipitation and immunofluorescence experiments (*Brandon et al. 2004, Kamiya et al. 2005*). DISC1 has been found to co-exist with NUDEL as part of a neurodevelopmentally regulated macromolecular complex in mouse brain lysates (*Brandon et al. 2004)*. DISC1 has also been shown to bind LIS1, suggesting the existence of a DISC1/NUDEL/LIS1 multi-subunit complex (*Brandon et al. 2004*). NUDEL and LIS1 are established evolutionarily conserved interactors but this new data proposing DISC1 as a third component of this macromolecular complex gives exciting clues as to the potential functions of DISC1.

LIS1 has dose-dependent effects on neuronal migration and haploinsufficiency of the *Lis1* gene is sufficient to perturb neuronal migration and give rise to lissencephaly (*Reiner et al. 1993, Lo Nigro et al. 1997, Gambello et al. 2003*). It is conceivable that if DISC1 functions in the same pathway as LIS1, that haploinsufficiency for full length DISC1 as seen in the t(1;11) family may also produce defects in nuclear translocation and hence neuronal migration. This is an attractive hypothesis as schizophrenia is considered to be a disorder of mis-connectivity resulting from aberrant neuronal migration (*Harrison and Weinberger 2005*).

A recent study by *Kamiya et al. 2005* has demonstrated that in addition to NUDEL and LIS1, DISC1 also co-immunoprecipitates with γ-tubulin, Dynactin ($p150^{glued}$) and Dynein intermediate chain (Dyn IC) providing further evidence that it may play a role in the nuclear migration pathway. However this data is contradictory to data published previously. *Brandon et al. 2004* showed that DISC1 and LIS1 indeed interact either in a direct manner or indirectly via DISC1 binding to NUDEL; however this study reported that DISC1 does not immunoprecipitate γ-tubulin or any other Dynein related proteins.

Despite this contradictory data, which may be due to methodological differences, it is interesting that DISC1 may function as part of the conserved LIS1/NUDEL/Dynein nuclear migration pathway. *Kamiya et al 2005.* performed RNA interference experiments to reduce *DISC1* levels in the developing mouse brain, similar to the *Lis1/Nudel/Dynein* RNAi experiments by *Shu et al. 2004*. These experiments aimed to address the role of DISC1 in neuronal migration. *Kamiya et al. 2005* delivered *DISC1* shRNA into developing mouse brains by *in utero* electroporation at embryonic day 14. They found that reducing *DISC1* levels resulted in a severe neuronal migration defect by postnatal day 2, with neuronal migration 'virtually inhibited' following RNAi for *DISC1*. Furthermore examination of the orientation of neurons that did migrate, at postnatal day 14, showed that these neurons were malpositioned and had reduced dendritic outgrowth. Similar to the *Shu et al. 2004* study *Kamiya et al. 2005* also measured the distance between the nucleus and centrosome in migrating neurons which had received *DISC1* shRNA and found that the distance between the nucleus and the centrosome was significantly increased relative to control neurons at embryonic day 18.5. Intriguingly *Kamiya et al. 2005* demonstrate similar neuronal migration defects in mice transfected in utero with a hypothetical 'mutant' C-terminally truncated DISC1 protein that could theoretically be produced by the t(1;11) translocation.

Extended analyses demonstrate that this 'mutant' DISC1 protein disrupts the β-tubulin microtubule network, fails to immunoprecipitate LIS1, NUDEL or Dynein and causes re-distribution of these proteins from the centrosome. The authors suggest that interaction between the full length (wild-type) DISC1 and the 'mutant' DISC1 via a self-association domain results in less available full length DISC1, due to mislocalisation. The authors imply that the 'mutant' DISC1 acts in a dominant-negative manner; however mislocalisation of DISC1 by 'mutant' DISC1 would also mimic a haploinsufficient phenotype as less DISC1 is available for protein interactions (*Porteous and Millar, 2006*). Although the specific mechanism is debatable this 'mutant' DISC1 protein is postulated to affect the ability of full length DISC1 to interact with LIS1, NUDEL and Dynein in the correct sub-cellular location and hence results in inhibition of neuronal migration. These neuronal migratory

defects during embryonic brain development are proposed by *Kamiya et al. 2005* to explain the high incidence of psychiatric illness in the t(1;11) family.

Although the experimental design of this study is impressive, certain aspects of the study are not clear. The authors describe the use of a 'strong suppressor' of DISC1 (referred to as RNAi #1). The authors use co-transfection of exogenous DISC1 and shRNA constructs to determine the levels of protein knockdown by western blotting. Refer to figure 1.5.A (*Figure 5 (a) Kamiya et al 2005*). From this exogenous DISC1 knockdown (upper panel) they infer that RNAi #1 has 'strong suppression' of DISC1, although the same cannot be said for the levels of endogenous knockdown seen in the bottom panel of this figure. This study does not state which antibody has been used to detect DISC1. Previously this group has produced DISC1 N-terminal and C-terminal antibodies which detect both 100kDa DISC1 and 75kDa DISC1 in PC12 cells (*Ozeki et al. 2003*). *Ozeki et al.* state that differentiating PC12 cells have augmented DISC1 expression in comparison to undifferentiated cells, with both 100kDa and 75kDa isoforms detectable. In this study *Kamiya et al. 2005* are examining DISC1 knockdown in differentiating PC12 cells however it is not clear whether the 75kDa isoform of DISC1 is detected or indeed knocked down as the only the 100kDa DISC1 band is shown by western blotting.

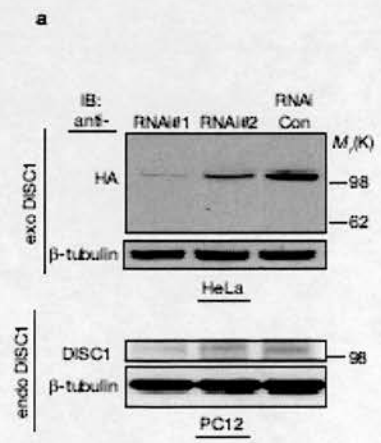

Figure 1.5.A. (*Figure 5 (a) from Kamiya et al. 2005*). In this diagram the upper panel shows DISC1 knockdown induced by co-transfection of exogenous DISC1 and *DISC1* shRNA constructs. The lower panel shows DISC1 RNAi induced knockdown of the endogenous protein.

These levels of DISC1 knockdown would not be sufficient to analyse RNAi phenotypes at a cell population level; however *Kamiya et al. 2005* have managed to show endogenous DISC1 knockdown on an individual cell basis by immunofluorescent staining in PC12 cells. See figure 1.5.B (*Kamiya et al. 2005 supplementary figure S2 (a)*)

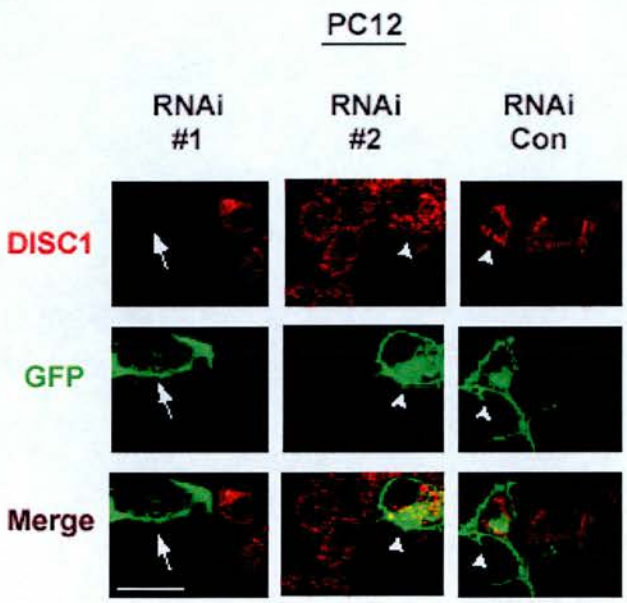

Figure 1.5.B. (*Figure S2 (a) from Kamiya et al. 2005*). This figure depicts knockdown of DISC1 by immunofluorescence following RNAi. The 'strong suppressor' #1 does indeed result in reduced DISC1 protein levels in transfected cells.

The *in utero* electroporation experiments of DISC1 shRNA into developing mouse brains demonstrated that the strong suppressor RNAi #1 inhibited almost all neuronal migration and construct RNAi #2 produced a weaker inhibition. In addition the distance between the nucleus and the centrosome in transfected neurons, that had managed to migrate, was significantly increased in comparison to control neurons. Surprisingly however the distance was generally greater in migrating neurons that received the RNAi #2 'weak' construct than in those that had received the RNAi #1 'strong' construct.

To summarise the study, *Kamiya et al. 2005* has shown that RNAi for *DISC1* produces migratory defects similar to that of over-expressing 'mutant' DISC1 (see also *Ozeki et al. 2003*). Extended analysis of the over-expression of 'mutant' DISC1 shows disruption of the microtubule network and perturbations in the accumulation of NUDEL and LIS1 at the centrosome. The suggestion from the RNAi work is that this neuronal migration defect is a secondary effect resulting from defects in nucleokinesis. The authors draw parallels between the phenotypes obtained using RNAi and that of over-expression of 'mutant' DISC1 and *Kamiya et al. 2005* place a lot of emphasis on the adverse effects of the 'mutant' DISC1 protein on the LIS1/NUDEL/Dynein pathway. However, production of this truncated protein has never been demonstrated in individuals possessing the t(1;11) translocation. This should not detract from the RNAi work, which clearly has exciting implications for the role of DISC1 in neuronal migration. The RNAi generated neuronal migration phenotypes reported in this paper are exciting as DISC1 haploinsufficiency is the potential disease mechanism operating within the t(1;11) family.

To date, *Kamiya et al. 2005* are alone in their observations of endogenous DISC1 at the centrosome. Over-expression studies have however demonstrated the existence of DISC1 at the centrosome (*Morris et al. 2003, Miyoshi et al. 2004, Millar et al. 2005a*). Clearly additional work needs to be carried out to characterise the multiple potential sub-cellular locations of endogenous DISC1.

1.5.3 DISC1 at the mitochondria

In addition to the centrosome another prominent site of DISC1 expressions appears to be the mitochondrion (*James et. al. 2004)*. Mitochondrial dysfunction has been implicated in schizophrenia (*Ben-Shachar, 2000*). Key functions of the mitochondrion such as oxidative phosphorylation and calcium homeostasis are important for synaptic plasticity and the role of the mitochondrion in apoptosis is essential for normal brain development (*Ben-Shachar, 2002)*. Apoptosis is important to limit and mould cortical connectivity in the developing brain affecting neural precursor cells, immature neurons and synapse-bearing neurons (*Morilak et al. 2000, Roth and D'Sa, 2001*). In particular apoptosis related to the mitochondrial apoptosome appears to be important and mitochondria isolated from immature neural precursors are more sensitive to apoptosis induction than those of mature neurons (*Roth and D'Sa, 2001, Polster et al 2003*).

DISC1 has been shown to interact by yeast two-hybrid assay with mitofilin (IMMT), a protein present within the inner mitochondrial membrane (*Millar et. al. 2003*). The function of IMMT is currently unknown and lends no clues to the potential role of DISC1 in the mitochondrion. Further evidence shows that mitochondrially located DISC1 is resistant to trypsin digestion which is consistent with DISC1 being located within the mitochondrion or within the mitochondrial membrane (*James et al. 2004*). Currently there are two clues to functions that DISC1 may perform at the mitochondria. Firstly, over-expression of DISC1 results in a mitochondrial ring phenotype suggesting that DISC1 may be involved in mitochondrial fission and fusion (*Millar et al. 2005a*). Secondly, recent data demonstrating an interaction between 71kDa DISC1 and Phosphodiesterase type 4B suggests that DISC1 may be involved in cAMP signalling at the mitochondria (*Millar et al. 2005b*). Considering the implications of mitochondrial dysfunction in schizophrenia, it will be of great interest to further examine the role of DISC1 at the mitochondria.

1.5.4 *DISC1; A molecular bridge linking components of the cAMP signalling pathway?*

1.5.4.1 Compartmentalisation of cAMP signalling

Cyclic AMP (cAMP) is a signalling molecule which transduces the primary signals of hormones and neurotransmitters interacting with their cognate membrane bound receptors. Cyclic AMP is synthesised by adenylate cyclases and is coupled to receptor signalling at the membrane. Membrane bound signals are transduced via cAMP to activate Protein kinase A (PKA), which subsequently phosphorylates downstream target genes, thus eliciting a signal transduction cascade. Following this signalling cascade cAMP is degraded to 5'AMP by locally expressed phosphodiesterases thus re-setting baseline cAMP signals within the cell (*Beavo and Brunton 2002, Houslay and Adams 2003*). Sub-cellular targeting of PKA and other regulatory proteins to specific sites of action is an essential feature of the cAMP signalling cascade. Protein kinase A is trafficked and anchored at specific sub-cellular locations by molecular scaffold proteins called A-Kinase Anchor Proteins (AKAPs) (*Feliciello et al. 2001*). There are numerous AKAP proteins each with the ability to bind PKA but which localise to independent sub-cellular locations thus providing a mechanism to compartmentalise cAMP signalling (*Colledge and Scott 1999, Diviani and Scott 2001*).

Cyclic AMP signalling has implications for psychiatric illness and related brain disorders as it plays an important role in learning and memory. The phosphodiesterase responsible for degrading cAMP was first identified by genetic screening for learning and memory defects in Drosophila (*Dudai et al. 1976, Chen et al. 1986*). As aforementioned, cAMP potentiates signals by activating PKA; PKA acts by phosphorylating CREB, a transcription factor that then goes on to elicit transcription of downstream genes. Genes transcribed by CREB have been implicated in long term potentiation and CREB mutant mice produce deficits in LTP, learning and memory (*Bauman et al. 2004*).

1.5.4.2 DISC1 interacts with components of the cAMP signalling pathway

A yeast two-hybrid study for DISC1 originally identified *AKAP9* as a putative interacting protein (*Millar et al. 2003*). *AKAP9* is a multiply spliced gene which encodes multiple protein isoforms (*Keryer et al. 1993, Lin et al. 1998, Schmidt et al. 1999, Takahashi et al. 1999*). The largest isoform produced from this gene, AKAP450, is located predominantly at the centrosome; however its protein alias CG-NAP (Centrosome- and golgi-localised PKN-associated protein) is so named because it has been documented to exist at the centrosome and golgi apparatus (*Witczak et al. 1999*, *Takahashi et al. 1999*). AKAP450/CG-NAP is reported to localise to the centrosome in interphase cells, at the mitotic spindle poles in metaphase cells and additionally at the cell midbody during telophase and cytokinesis (*Takahashi et al. 1999*). AKAP450/CG-NAP will subsequently be referred to as AKAP450.

The dynamic localisation of AKAP450 at the centrosome during mitosis suggests that it may play a role in cell cycle progression. Indeed it has been demonstrated that perturbation of AKAP450s role at the centrosome produces defects in the cell division cycle (*Keryer et al. 2003*). The centrosomal targeting domain of AKAP450, the PACT domain, has been localised to the C-terminus of the protein (*Gillingham and Munro, 2000*). By exogenously expressing the PACT domain of AKAP450 *Keryer et al. 2003* demonstrated displacement of endogenous AKAP450 and PKA type II from the centrosome. This manifested as defects in centriole duplication and a block in cell cycle progression (*Keryer et al. 2003*). Core components of the centrioles and centrosome, were not found to be affected in this study in the same manner as PKA type II suggesting that cAMP signalling at the centrosome is important for cell cycle progression.

Recently a member of the type 4 phosphodiesterase gene family, PDE4D3, has been shown to be phosphorylated by PKA type II and to co-localise and interact with AKAP450 at the centrosome (*McCahill et al. 2005*). Type 4 phosphodiesterases specifically inactivate cellular cAMP helping to maintain intracellular cAMP

gradients (*Houslay and Adams, 2003*). This particular AKAP/PKA/PDE complex may be of particular importance at the centrosome and in cell cycle progression.

Furthermore PDE4D3 has recently been shown to bind DISC1 using a co-transfection followed by immunoprecipitation approach (*Millar et al. 2005b*) and AKAP450 has previously been identified as a putative DISC1 interactor by yeast two-hybrid screening (*Millar et al. 2003*). AKAP450 is known to bind PKA type II and localise it to the centrosome (*Keryer et al.* 2003) and has also been shown to bind PDE4D3 at the centrosome (*McCahill et al. 2005*). This suggests a potential AKAP mediated mechanism for regulating the interaction between PDE4D3 and PKA type II at the centrosome, with DISC1 potentially playing a role in this process.

DISC1 has a documented role in binding to type 4 phosphodiesterases but the only interaction studied in detail is that of DISC1 and PDE4B1 at the mitochondrion (*Millar et al. 2005b*). The proposed interaction between DISC1 and PDE4B1 is one whereby DISC1 binds and renders PDE4B1 inactive until such time as PDE4B1 becomes phosphorylated and undergoes a conformational change resulting in release of DISC1. This proposed mechanism would maintain PDE4B1 in an inactive state, thus blocking hydrolysis of cAMP, until such time as PKA, perhaps delivered by a mitochondrial AKAP, can release the inhibition of DISC1 upon PDE4B, resulting in hydrolysis of cAMP. These protein interactions create an auto-regulatory loop for maintaining intracellular gradients of cAMP at the mitochondrion. These processes are common throughout the cell and specific combinations of PKA, PDEs, AKAPs and potentially DISC1, present in specific sub-cellular compartments, may function to regulate local cAMP gradients.

Therefore as DISC1/PDE4B1 is to the mitochondrion, so DISC1/PDE4D3 may be to the centrosome. But the question remains as to whether DISC1, or specific isoforms of DISC1, are expressed in such a compartmentalised manner?

There is support for DISC1 interaction with additional centrosomal proteins from work by *Miyoshi et al.* who identified the protein kendrin (also known as Pericentrin-B) as a putative DISC1 interactor by yeast two-hybrid screening (*Miyoshi et al.*

2004). The DISC1/Kendrin interaction was confirmed in cultured cells by immunoprecipitation and immunofluorescent co-localisation. Furthermore this interaction was deemed necessary to localise DISC1 at the centrosome (*Miyoshi et al.* 2004). Kendrin is a large centrosomal protein which exhibits restrictive localisation to the poles of the mitotic spindle during mitosis (*Flory et al. 2000*). Kendrin co-localises with Pericentrin and γ-tubulin at the poles of the mitotic spindle and is postulated to play a role in microtubule nucleation during spindle formation (*Flory et al. 2000*).

Interestingly kendrin has been shown to interact with AKAP450 *in vivo* and to form complexes with AKAP450, γ-tubulin and one of the γTuRC proteins, necessary to nucleate microtubules during mitotic spindle formation (*Takahashi et al. 2002*). It was also reported that disrupting this complex formation inhibited microtubule nucleation from isolated centrosomes suggesting that AKAP450 and kendrin may provide a mechanism for anchoring γTuRC to the centrosome (*Takahashi et al. 2002*). The fact that DISC1 may form complexes with either or all of these proteins indirectly implicates DISC1 in cAMP signalling and mitosis.

Although DISC1 has been shown to co-localise to the centrosome when over-expressed (*Morris et al. 2003, Miyoshi et al. 2004, Millar et al. 2005a*), only one of three studies of endogenous DISC1 have localised DISC1 to the centrosome, whilst the other studies place DISC1 predominantly at the mitochondria (*Brandon et al. 2004, James et al. 2004, Kamiya et al. 2005*). Therefore the potential for DISC1 interactions at the centrosome is tantalising but further demonstration of endogenous DISC1 at the centrosome is needed to substantiate the current speculations.

1.6 The *DISC2* gene

1.6.1 DISC2; Gene structure, evolution and expression

With *DISC1* emerging as an important candidate gene involved in the aetiology of schizophrenia it will be imperative to understand how *DISC1* is regulated within the cell. One gene, which could be of paramount importance in regulation of *DISC1,* is *DISC2*. *DISC2* is also disrupted by the t(1;11) translocation and as such may also have important implications for schizophrenia. *DISC2* is located on the opposite strand to *DISC1* and is transcribed in a distal to proximal orientation thus representing a natural antisense transcript partially overlapping *DISC1* (*Millar et al. 2000*).

To date 15kb of *DISC2* sequence has been published (AF222981, *Millar et al. 2000*). This sequence encompasses one large exon, with the 3' end residing within intron 8 of the *DISC1* gene; the 5' end of this gene remains uncharacterised (*Millar et al 2000, Taylor et al. 2003*) and is hypothesised to lie within intron 9 of *DISC1*. This is a very large intron of approximately 150kb in length in humans. Furthermore, the large size of this intron appears to be conserved across species with mouse *Disc1* intron 9 being approximately 51kb (*Ma et al. 2002*). This suggests that intron 9 sequence is functionally important in some manner, possibly because it harbours the *DISC2* gene; however no species conservation has been detected for *DISC2* (*Taylor et al. 2003*).

Detailed analysis of the known *DISC2* sequence has identified the longest open reading frame as 57 codons in length, with the context of the putative start codon unlikely to initiate translation (*Taylor 2001, PhD Thesis*). Therefore *DISC2* is presumed to be a non-coding RNA gene. Expression of this gene has been reported in human heart where it appears to produce multiple splice isoforms (*Millar et al. 2000*)

1.6.2 Genetic evidence supporting DISC2 as a schizophrenia candidate gene

Although the genetic evidence for *DISC1* is strong with many positive linkage and associations across the length of the gene, these studies do not rule out *DISC2* as a candidate gene. In fact none of these genetic studies can discriminate between *DISC1* and *DISC2* in terms of positive linkage and association because at best linkage studies define only a region of interest, and association studies identify markers that are in linkage disequilibrium with the causative mutation and not necessarily the actual disease casing variant. Furthermore many of these positive studies report markers that are within the *DISC2* gene region (*Hennah et al. 2003, Hodgkinson et al. 2004, Ekelund et al. 2001, Ekelund et al. 2004, Cannon et al. 2005*). Therefore *DISC2* represents an important schizophrenia candidate gene in its own right. See figure 1.4.A which depicts these linkage and association data within the *DISC1* gene.

It is difficult to hypothesise how disruption of the *DISC2* gene is relevant to psychiatric illness as the gene is not fully characterised. One possibility however is that as a non-coding RNA gene *DISC2* functions to regulate the expression of its cognate sense partner *DISC1*. This and other functional possibilities are discussed in the following sections.

1.6.3 Non-coding RNA molecules and antisense gene regulation

The central dogma states that DNA gives rise to RNA which gives rise to protein. However we now know that this is not necessarily the case and that not all RNA gives rise to protein, nor does RNA need to code for protein to possess functionality. It has become apparent in recent years that non-coding RNA molecules, many of which are produced from antisense transcripts, are more widespread within the human genome than initially thought. Indeed non-coding RNA molecules are some of the most important regulatory molecules in the cell and are absolutely required for normal transcription and translation. Since the completion of the human genome project it has become evident that an organism's complexity cannot alone be attributed to the number of protein-coding genes it possesses (*International Human*

Genome sequencing Consortium, 2004). Paradoxically it appears that the more complex the organism, the less of its genome actually codes for protein (*Szymanski and Barciszewski 2002)*. For example 86% of the genome of *Escherichia Coli* codes for protein whereas only 29% of the genome of *Arabidopsis Thaliana* codes for protein and perhaps even more strikingly, only 1.4% of the human genome codes for protein (*Szymanski and Barciszewski, 2002*). There must therefore be something other than proteins contributing to the complexity of the eukaryotic genome. This complexity is potentially derived from the multitude of non-coding RNAs present within the human transcriptome. Non-coding RNAs make up approximately 50-75% of the eukaryotic transcriptome (*Szymanski and Barciszewski 2002*). These non-coding RNAs include familiar housekeeping RNA molecules involved in the translation of genetic information, RNA editing, RNA processing and other ribonucleoprotein particles (*Eddy 2001*, *Szymanski and Barciszewski, 2006*). Other non-coding RNAs are considered regulatory RNAs and perform various important functions including X-chromosome inactivation (*Xist* RNA), X-dosage compensation (*roX1/roX2* in drosophila) and genetic imprinting (*H19*, *Air*) (*Eddy 1999, Szymanski and Barciszewski 2006*). Normal gene expression would not be possible without these regulatory RNA molecules.

A sub-group of putative regulatory RNA molecules that are becoming increasingly interesting are natural antisense transcripts (NATs), of which *DISC2* is one. Naturally occurring antisense RNAs have been well documented in prokaryotes where they are important in carrying out a multiplicity of functions including regulation of transcription and replication (*Inouye, 1988*). To date *in-silico* approaches have identified more than 2500 human NATs with 1600 of these analysed and predicted to be true (*Yelin et. al. 2003*). Many important genes are known to have associated NATs; these include genes involved in regulation of development, cell-cycle, apoptosis and translation (*Vanhee-Brossollet & Vaquero, 1998*).

There are a variety of ways in which antisense RNA molecules can regulate their cognate sense mRNA. They may regulate the expression of sense mRNAs at the

level of transcription via competition for regulatory factors, or through physically hindering the progress of transcription, either topologically or by being transcribed themselves (*Munroe and Zhu, 2006*). They may also regulate sense gene expression post-transcriptionally by binding and blocking regulatory binding sites in the sense mRNA. This can potentially regulate any step in RNA processing including translation, polyadenylation, splicing, transport or even degradation (*Munroe and Zhu, 2006*).

Moreover sense:antisense dsRNAs can also result in activation of cellular siRNA-related pathways. The consequences of this can be two-fold. Firstly dsRNA duplexes may be subject to RNA editing, which can result in a change in coding potential, nuclear retention or cytoplasmic degradation (*Kumar and Carmichael, 1998*). The second mechanism for dealing with dsRNA is that of RNA interference. This is a mechanism whereby dsRNA duplexes are chopped up to produce short interfering RNAs which target homologous mRNA sequences for degradation and can also function to recruit chromatin remodelling factors to the endogenous gene region, thus silencing transcription (*Hannon, 2002*). Although this is a possible mechanism for controlling sense gene expression, and chemical siRNAs are routinely used to experimentally reduce gene expression, natural antisense transcripts have not yet been shown to produce siRNAs via dsRNA formation with their cognate sense mRNA (*Munroe and Zhu, 2006*).

The mechanisms of antisense mediated gene regulation discussed so far involve antisense:sense binding within the nucleus; however antisense gene regulation may also occur *in-trans*, i.e. in the cytoplasm. The mechanics of this are currently unknown although they may be similar to that of microRNAs, which regulate the translation of messenger RNAs in the cytoplasm (*Bartel 2004*).

To date the importance of non-coding RNA genes has been underestimated and they have been overlooked in favour of protein coding genes; however antisense transcription within the human genome is a very worthy topic for further research as many natural antisense transcripts have been implicated in the pathogenesis of

disease. Of particular interest in relation to psychiatric illness is their implication in neurological disorders.

Several non-coding RNAs have recently been implicated in neurological diseases. *Nemes et. al. 2000* reported a triplet repeat expansion in the human *cis*-antisense RNA SCA8 that causes spinocerebellar ataxia, a neurodegenerative disorder involving the purkinje neurons of the cerebellum. The SCA8 antisense RNA is thought also to control the sense gene *KLHL1*; however a mechanism for this is yet to be described *(Nemes et. al. 2000)*. Angelman and Prader-Willi syndrome are neurobehavioural disorders largely caused by deletions/mutations within the 15q11-15q13 chromosomal region but have also been associated with defects in imprinting, regulation or expression of non-coding RNA molecules at this chromosomal locus (*Costa, 2005*). Furthermore decreased expression of another small non-coding RNA molecule, BC200 has been associated with Alzheimer's disease (*Costa, 2005*).

Considering the large repertoire of currently known non-coding RNA molecules and the fact the there are likely to be many more to come, we are beginning to appreciate the complex nature of the human genome. It appears that proteins are no longer the centre of the cellular universe as originally thought....

"Biologists should not deceive themselves with the thought that some new class of molecules, of comparable importance to proteins, remains to be discovered. This seems highly unlikely." Francis Crick 1958

....Rather it now appears that RNA itself possesses multifunctionality which is required to orchestrate a diversity of molecular interactions within eukaryotic cells. Figure 1.6 taken from *Costa 2005* depicts this scenario where RNA represents the central hub integrating complex cellular networks. Considering the obvious importance of 'non-coding' RNA molecules, it is an exciting possibility that *DISC2* functions as a non-coding RNA molecule. The fact that it is antisense to *DISC1* opens up the possibility that it may act as a riboregulator of *DISC1*, and therefore it is plausible that disruption of *DISC2* might have a role in the pathological mechanism of schizophrenia by dysregulation of *DISC1*. It may also be the case however that

DISC2 functions independently of *DISC1* and that its function may be independently important in the pathology of schizophrenia.

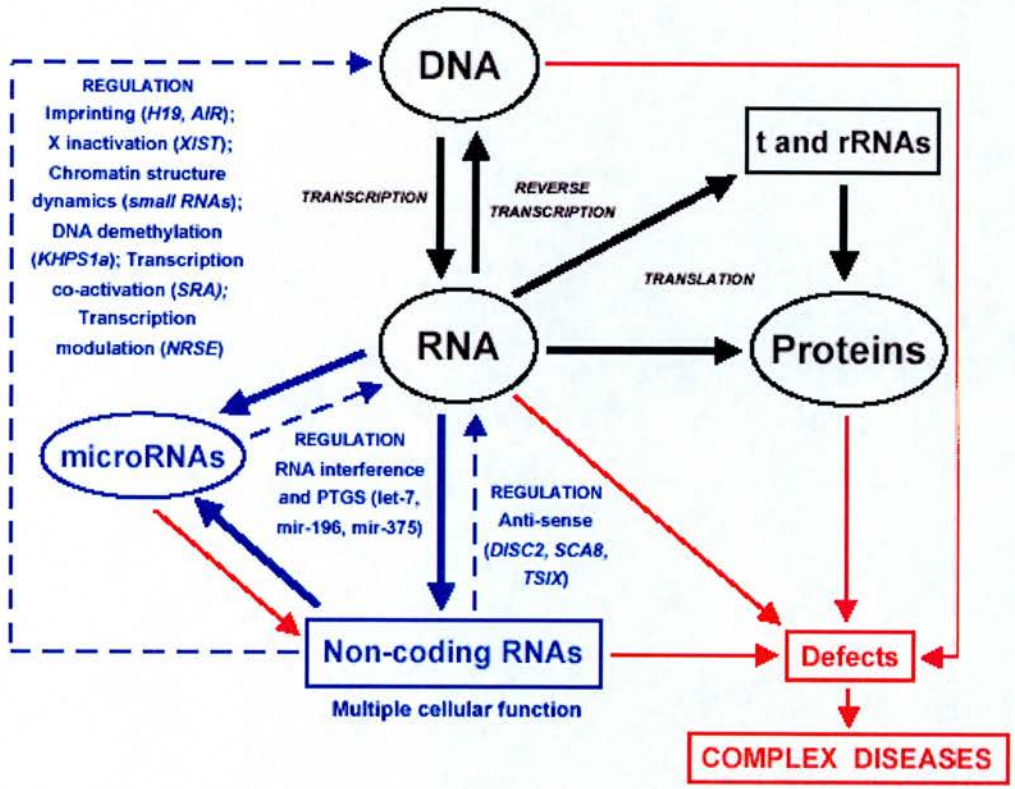

Figure 1.6. This figure taken from *Costa 2005* depicts a new 'molecular pipeline' whereby RNA acts as a centre of molecular network integration. This figure depicts the multifunctionality of RNA and further proposes *DISC2* as an important antisense regulatory gene.

1.7 PhD Aims

The aims of this PhD were fourfold;

- To elucidate the disease mechanism operating within the t(1;11) family.

This has been a topic of much controversy in recent years. I aim to uncover the disease mechanism by examining whether the t(1;11) results in production of an abnormal DISC1 protein with aberrant cellular functions or whether the translocation affects gene transcription such that overall levels of *DISC1* are reduced.

- To clarify sites of DISC1 sub-cellular localisation.

Many studies have examined the sites of DISC1 protein expression within mammalian cells. These studies have produced conflicting results; however it is becoming apparent that DISC1 occupies multiple sub-cellular locations. I aim to explore this in more depth and examine if this localisation is isoform specific.

- To examine cellular phenotypes resulting from *DISC1* RNA interference.

The biological functions of DISC1 are not well understood; however considering that it has multiple interacting protein partners these functions are likely to be wide ranging. I aim to utilise RNA interference to elucidate further the functions of the DISC1 protein.

- To further characterise the *DISC2* gene.

DISC2 has been overlooked to date in favour of *DISC1* which is promising to be a very exciting candidate gene for psychiatric illness. However considering the genetic evidence and the nature of *DISC2* as a non-coding RNA gene, it remains a worthy gene deserving of further exploration. As a start I aim to characterise the gene structure further by identifying the 5' end of *DISC2* and hopefully shed some light on the effects of the t(1;11) on this gene.

Benjamin Franklin once said that one should *"either write something worth reading or do something worth writing*". I hope that in the context of these experiments and this thesis, I have accomplished both.

Chapter 2

Materials and Methods

2.1 Preface

This chapter details the experimental procedures used throughout this PhD thesis. Additional details concerning solutions and reagents can be found in Appendix II. Protocols were developed from *Sambrook et al. 1989* unless otherwise specified.

2.2. Mammalian cell culture

2.2.1 Cell lines and growth conditions

All mammalian cells were classified as containment level 1 and were manipulated using Envair Bio2+ Class II Safety Cabinets. Cells were grown under humid conditions (37°C, 5% Carbon Dioxide) in the appropriate growth medium. T.25, T.75 and T.175 tissue culture flasks with filter caps were used to maintain cell cultures (CellStar®, Greiner Bio-One). Details of cell lines and growth conditions can be found in table 2.2.A at the end of this section.

2.2.1.1 Feeding and passage of adherent cells

Cell medium was replenished every 3-4 days as required. Cells were passaged at 70-90% confluency. To do this, growth medium was aspirated using a sterile glass pipette and cells were washed in D-PBS (GIBCO®) to remove any remaining serum. Cells were incubated with a 1:1 solution of versene plus trypsin (GIBCO) at 37°C to lift them from the flask surface. The versene:trypsin solution was inactivated by adding an equal volume of growth medium containing 10% fetal bovine serum serum. Cells were centrifuged gently at 1000rpm for 5 minutes (CR312 Jouan centrifuge) at room temperature and then re-seeded into new medium. Cells were re-seeded at 1 in 10 to 1 in 50 dilutions.

2.2.1.2 Feeding and passage of suspension cells

Lymphoblastoid cell lines derived from the t(1;11) family members were grown in suspension in upright T.75 tissue culture flasks. Cells were maintained by feeding every 3-4 days (25-50ml medium). It is recommended that lymphoblastoid cell cultures be maintained at a density of 3-9 x 10^4 cells per ml (www.ecacc.org.uk). If the cells were to be used for protein or RNA extraction the media was replenished daily for 3-4 days prior to harvesting. Healthy lymphoblastoid cells grow in floating aggregates which settle at the bottom of the tissue culture flask. To replenish medium or passage cells the flasks were removed from the incubator into the tissue culture hood with minimum agitation to avoid disrupting the cell aggregates. The medium was removed using a sterile glass pipette. The medium was then either replenished or to split the cells an appropriate volume of cells was removed and placed into a new flask of fresh medium. Once in fresh medium cells were agitated to dissociate clumps and promote growth.

2.2.1.3 Preparation and recovery of cell stocks

To prepare frozen cell stocks an appropriate amount of cells (4-9 x10^6-lymphoblastoid cells or 1–2 x 10^6-adherent cells) were centrifuged for 5 minutes at 1000rpm. Cell pellets were resuspended in 1ml of cell freezing medium (Appendix II) and placed in a CryoTube™ (NUNC™). Cells were frozen slowly using a Cryo 1°C freezing container (NALGENE). The freezing chamber is filled with 100% ethanol or propan-2-ol and the CryoTube is placed in the holder provided. This was stored at -70°C overnight. Using this container the cells are frozen slowly at a rate of -1 °C /minute. The cells can then be placed for long term storage in liquid nitrogen.

Frozen cells were recovered by thawing quickly at 37°C and placing into a T.25 tissue culture flask with 5mls of growth medium. Cells were incubated overnight at 37°C, 5% CO_2 to recover and adhere. Following this, cells were given fresh medium and grown as normal.

2.2.2 Haemocytometer counting to determine cell number

The haemocytometer (improved Neubar) was prepared by cleaning with 70% ethanol. A coverslip was placed over the haemocytometer chamber. Cells were trypsinised as normal and resuspended in fresh growth medium. Confluent cell suspensions were diluted 1 in 10 for counting. Each chamber of the haemocytometer was filled by capillary action using a pasteur pipette to place a drop of the cell suspension at the chambers edge. A minimum of four 1mm squares (divided into 16 smaller squares) were counted and the average cell number was calculated. This represents the number of cells x 10^4/ml.

2.2.3 Chemical transfection of mammalian cell lines

2.2.3.1 Transfection of adherent cells using Lipofectamine™ 2000

Cells were transfected in 6 or 12 well COSTAR® flat bottom plates. Cells were pre-plated 24-48 hours prior to transfection. If cells were to be used for immunofluorescence they were pre-plated onto 16mm glass coverslips into 12-well plates (typically $1x10^5$ cells per well). For RNA and Protein applications cells were transfected at approximately 70-80% confluency.

Lipofectamine2000™ transfection conditions		
	12-well plate	6-well plate
LF2000 reagent	1-6µl	3-12µl
Short Interfering RNA	10-50 nM	10-50nM
AND / OR		
DNA	0.4µg	4-5µg
Final plating volume	1ml	2ml

To perform the transfection, LF2000 (Invitrogen), siRNA (Ambion®, Table 2.2.B) or DNA were diluted in Opti-MEM® 1 reduced serum medium (GIBCO) according to the manufacturers instructions. Transfection complexes were added dropwise to the cells and normal growth medium was added to make up the final volume.

2.2.3.2 Transfection of adherent cells using siPORT-Amine

siPORT™ *Amine* (Ambion) is a polyamine reagent that was used specifically for transfection of HEK293 cells. 24 hours prior to transfection, cells were plated in 6 or 12-well plates at a density of 1-2x10^5 per well respectively. Cells were plated onto 16mm glass coverslips in 12-well plates for immunofluorescence purposes.

siPORT™ *Amine* transfection conditions		
Reagent	12-well plate	6-well plate
siPORT™ *Amine*	4µl	8-10µl
Short Interfering RNA	10-100nM	10-100nM
AND / OR		
DNA	0.4µg	NA
Final plating volume	1ml	2ml

DNA, siRNA and siPORT™ were diluted in Opti-MEM 1 according to the manufacturers instructions. The complexes were added dropwise to the cells and normal growth medium was added to make up the final reaction volume.

2.2.3.3 Reverse transfection of adherent cells using siPORT-Amine

Reverse transfection involves transfecting cells in suspension before plating. The conditions for transfection are the same as those in section 2.2.3.2, however complexes are added to the empty wells of the tissue culture plate and then an appropriate number of cells are overlaid in normal growth medium. This method is advantageous in that no pre-plating of cells is required. Furthermore there is a greater cell surface area available for transfection as the cells are in suspension. Cell suspensions should not be prepared more than 1hr in advance of plating and should be kept at 37°C at all times.

Table 2.2.A Mammalian cell lines and growth conditions					
Commercially available cell lines					
Cell line	**Origin**	**Cell type**	**Growth Medium**	**Growth Type**	**Received from**
HEK293	Human	Embryonic kidney	DMEM[1] /10% FBS[2]	Adherent	Ian Simpson; Genes & Development group, UOE[3]
SH-SY5Y	Human	Brain, neuroblastoma	DMEM /10%FBS	Adherent	Organon Laboratories NV / ECACC[4]
U373 MG	Human	Brain, glioblastoma	DMEM /10% FBS	Adherent	Helen Bell; Dept of Clinical Neurosciences, UOE
COS7	Monkey	Kidney, Fibroblast	DMEM /10% FBS	Adherent	ECCAC
T(1;11) Family Cell lines					
Lymphoblastoid KK	Human	Blood, lymphocytes	RPMI 1640[5] /10% FBS	Suspension	Medical Genetics, UOE

[1]Dulbecco's Modified Eagle Media (GIBCO®) (media contains L-glutamine, pyruvate and Glucose) [2]Fetal Bovine Serum (GIBCO®)

[3]University of Edinburgh [4]The European Collection of Cell Cultures [5]RPMI Media 1640 (with L-glutamine, GICBO®)

Table 2.2.B Silencer pre-designed siRNA sequences (5' to 3' read direction)	
siRNA identifier	siRNA sequence (DISC1 target region)
DISC1 siRNA #1	GGAUGUUUGUGCUGGAAGCtt (exon 6)
DISC1 siRNA #2	GGAUUUGAGAAUAGUUUCAtt (exon 13)
DISC1 siRNA #3	GGAAAAGCAGCAGCUACAGtt (exon 5)
DISC1 siRNA #4	CGAUAUUGAAACCCAACUAtt (exon 8)
DISC1 siRNA #5	GCGUGACAUGCAUUCUUUAtt (exon 2)
Negative control siRNA #1	21bp scrambled sequence with no homology to human sequences

2.3 Preparation of nucleic acids

These following techniques were used to isolate DNA for use in PCR (polymerase chain reaction) and mammalian cell transfection. RNA preparations were used for cDNA synthesis and RT-PCR (reverse transcriptase PCR).

2.3.1 DNA isolation from mammalian cells

Total DNA was isolated from human cultured cells using the DNeasy® Tissue kit (QIAGEN). A maximum of $5x10^6$ cells were used. In brief, cells were lysed using proteinase K; ethanol was added to the lysate, which was then applied to a spin column with a specialised silica-gel membrane that binds the DNA. Contaminants were removed by washing the column and the DNA was then eluted. DNA was eluted twice using 2 x 200µl volumes of AE buffer provided. For a detailed protocol refer to instruction manual QIAGEN #69504. Isolated DNA was stored temporarily at 4°C or at -20°C for long term storage.

2.3.2 Quantification of DNA

2.3.2.1 Quantification of DNA using a spectrophotometer

DNA concentration was determined by measuring the absorbance of the sample at 260nm. This reading (OD_{260}) was then used to calculate the concentration of the DNA sample. DNA was diluted 1:100 and 100µl of dilute DNA was placed in a quartz cuvette with a 10mm path length. The absorbance was measured using the GeneQuant spectrophotometer and the following calculation was used to determine the DNA concentration. Conversion factors are listed in section 2.3.7.1.

- OD_{260} x conversion factor x dilution factor = concentration µg/ml

2.3.2.2 Quantification of DNA by agarose gel electrophoresis

To quantify DNA by gel electrophoresis 1µl of DNA sample (1µl DNA + 8µl H_20 + 1µl 10X Orange G loading buffer) was run alongside 500ng of λHindIII (10µl @ 50ng/µl, Invitrogen) molecular weight marker. The DNA concentration was deduced

by comparing the band intensity of the unknown DNA sample to band intensity of the λHindIII marker.

2.3.3 Extraction of total RNA from mammalian cells

Total RNA was isolated using the RNeasy® Mini kit (QIAGEN #74104) according to the manufacturer's instructions. In brief, mammalian cell cultures were harvested and centrifuged at 1000 rpm for 5 minutes ($\leq 1x10^7$ cells). Cell pellets were lysed by vortexing in an appropriate volume of lysis buffer and homogenised using a 20-guage needle. 70% ethanol was added to the lysate and this was applied to an RNeasy mini column. The RNA binds to a silica-gel membrane in the mini column. The membrane was then washed to remove contaminants before elution of RNA in nuclease free water. All procedures were performed at room temperature. These RNA preparations were subject to DNase treatment to remove any contaminating DNA.

2.3.4 Isolation of mRNA from mammalian cells

To isolate mRNA from cultured mammalian cells the Poly(A)Pure™ mRNA purification kit was used (Ambion). This kit is ideal for procedures where unspliced or partially spliced RNA is problematic. This kit specifically isolates polyadenylated RNA by hybridisation to Oligo(dT) cellulose. This kit requires high cell numbers in comparison to kits that isolate total RNA. A minimum of $5x10^6$ cells and a maximum of 200×10^6 cells were used for each mRNA isolation. The procedure briefly entails, cell lysis, lysate dilution, incubation with Oligo(dT) cellulose to bind polyA RNA, washing to remove non-specifically bound ribosomal RNA and other contaminants followed by elution of the polyA RNA. For a detailed protocol refer to instruction manual Ambion #1915.

2.3.5 RNA storage and stabilisation

If cell pellets were not used immediately for isolation of RNA they were either frozen on dry ice and stored at -70°C or alternatively, the cells were stored in

RNA*later*® stabilisation reagent (Ambion). To store cells in RNA*later* cells were centrifuged for 5 minutes at 1000rpm. These pellets were washed and resuspended in 100µl of phosphate buffered saline (PBS). 5 to 10 volumes of RNA*later* stabilisation reagent was then added to the cell suspension. These cells were stored at 4°C for up to 4 weeks or placed at -70°C for long term storage. For a detailed protocol refer to the manufacturer's instructions (Ambion #7020).

2.3.6 DNase treatment of RNA

These procedures were used to remove genomic DNA contamination that may exist in RNA isolated from mammalian cells.

2.3.6.1 DNase I treatment and phenol/chloroform extraction of RNA

RNA was incubated with DNase I to remove genomic DNA and the RNA was then recovered by phenol/chloroform extraction and overnight precipitation in isopropanol. This procedure was performed as follows.

DNAse treatment

1µg RNA
1µl DNase I (Roche,10 U/µl)
1µl RNase Inhibitors (Roche, 40 U/µl)
X µl sterile water
50 µl reaction volume - 37°C for 30 minutes

Phenol/Chloroform extraction

- Add 50µl Phenol + 50µl Chloroform to reaction mixture, vortex well and centrifuge at 13,000rpm for 2 minutes (This step separates the aqueous layer containing the nucleic acids from the insoluble protein layer).
- Remove the aqueous (top) layer; to this add 50µl chloroform, vortex and centrifuge as before.
- Keep aqueous layer.

RNA precipitation To the aqueous layer from the phenol/chloroform extraction add,

1/10th volume Ammonium Acetate

2.5 volumes 100% ethanol

2µl glycogen

- Precipitate RNA overnight at -20°C.
- Recover RNA by centrifugation ≥ 12,000rpm for 20 minutes.

This procedure is time consuming and requires the use of harmful substances. Therefore a safer and quicker method using the TURBO DNA-*free*™ kit was subsequently used (Ambion #1907).

2.3.6.2 TURBO DNase treatment of RNA

TURBO DNase has a higher affinity for DNA than DNase I with 350% greater catalytic activity. TURBO DNase is incubated with RNA in an optimised reaction buffer for 30 minutes at 37°C. The DNase is then removed using a DNase inactivation reagent, which also remove divalent cations from the RNA sample. The DNase inactivation reagent requires a 2 minutes incubation step followed by a 1.5 minute centrifugation step. The RNA supernatant is then recovered. For a detailed protocol refer to instruction manual (Ambion #1907).

2.3.7 Quantification of RNA

2.3.7.1 Quantification of RNA using a spectrophotometer

To determine RNA concentration, extracted RNA was diluted 1:50 to 1:100 in RNAse free water. 100µl of each dilution was placed in a quartz cuvette with a 10mm path length. The absorbance at 260nm (OD260) of each RNA dilution was determined by spectrophotometry using the GeneQuant RNA/DNA calculator (Pharmacia). The following conversion factors were used to determined RNA or DNA concentration.

An OD260 unit of 1 equates to the following nucleic acid concentration	
Double stranded DNA	50µg/ml
Single stranded RNA	40µg/ml
Single stranded DNA	35µg/ml
Single Stranded oligo	20µg/ml

*Values taken from Bioreference.net

The following calculation was used to determine RNA concentration; OD260 x 40 x dilution factor = RNA concentration in µg/ml

2.3.7.2 Quantification of RNA using the Agilent 2100 Bioanalyser

The Agilent Bioanalyser was used to determine the quality and purity of extracted RNA. To analyse samples the Agilent RNA 6000 Nano kit was used. 1µl of neat RNA is sufficient to determine concentration and quality of extracted RNA. For details refer to the Agilent user manuals at www.chem.agilent.com.

2.3.8 Preparation of complementary DNA (cDNA)

This method was used to make cDNA for use as a template in non-quantitative and real-time PCR techniques. cDNA was made by reverse-transcription of mammalian RNA using the 1st Strand cDNA Synthesis Kit for RT-PCR (AMV) (Roche). This method produces single stranded RNA using AMV reverse transcriptase. A typical cDNA synthesis reaction is shown below.

cDNA Synthesis Reaction		
Volume	Reagent	Final concentration
2µl	10X Reaction Buffer	1X
4µl	25mM Magnesium Chloride	5mM
2µl	10mM dNTPs	1mM
2µl	Random Primers $p(dN)_6$	3.2µg

1µl	RNase Inhibitor	50 units
0.8µl	AMV Reverse transcriptase	20 units
X µl	Total RNA, or PolyA RNA	≤ 1µg total RNA 100ng PolyA RNA
X µl	Sterile Water	
Final Reaction Volume = 20µl		

A master mix containing the appropriate reagents was prepared, mixed and centrifuged before aliquoting into 0.5ml RNase free thin walled tubes. The reactions were then cycled on a thermal cycler (Peltier PTC-225) as shown below.

Thermal cycling of cDNA synthesis reactions		
25°C	10 minutes	Primer Annealing
42°C	60 minutes	Reverse Transcription
99°C	5 minutes	AMV Inactivation
4°C	5 minutes	
Store at -20°C		

For all cDNA reactions a negative control reaction was prepared alongside which contained RNA but no reverse transcriptase enzyme. This was to ensure no DNA contamination exists in the RNA preparations that may interfere with downstream PCR applications. Negative controls containing distilled water plus reverse transcriptase were also prepared to ensure all reagents were free of contamination.

To ascertain if the cDNA synthesis was successful all samples were assayed for amplification of *Glyceraldehyde-6-phosphate Dehydrogenase* (*GAPDH*) by PCR. PCR products were analysed by agarose gel electrophoresis.

2.3.9 DNA isolation from agarose gels

This gel extraction method was used to isolate PCR products for the purposes of cloning or sequencing. PCR products were extracted from low melting point (LMP)

agarose gels using the QIAquick Gel Extraction kit (Qiagen, #28704) according to the manufacturers' instructions. In brief gel slices containing the desired PCR product are dissolved at 50°C in an appropriate buffer. An appropriate volume of isopropanol is added and the mixture is then applied to a spin column where the DNA binds to a silica membrane. After impurities are washed away (e.g. salt and agarose) the DNA is eluted and ready for use.

2.4 Amplification of nucleic acids

2.4.1 Non-quantitative Polymerase Chain Reaction (PCR)

Gene expression was measured non-quantitatively using a Thermo-Start® DNA polymerase (Abgene®, cat # AB-0908/a). This enzyme is thermostable and requires a high temperature activation step to begin the reaction, thus increasing the stringency of the PCR reaction and eliminating non-specific priming. Details of the PCR reaction mix and thermal profile of the reaction are given below.

Recipe for a single PCR reaction mixture	
2µl	10X Thermo-Start reaction buffer
1.2µl	25mM Magnesium Chloride
0.5µl	10mM dNTPs (SIGMA)
0.1µl	Thermo-Start DNA polymerase
75-100ng	Forward Primer
75-100ng	Reverse Primer
~1µl Template DNA	Template amount depends on source and concentration
Add distilled water to a make the final reaction volume 20µl	

Thermal Profile of a typical PCR		
95 °C	15 minutes	Enzyme activation step, 1 cycle
Followed by 36 cycles		

94 °C	20 seconds	DNA denaturation step
Tm °C	30 seconds	Annealing Temperature of Primers
72 °C	30-60 seconds	Extension step for 500bp-1Kb product
Followed by		
72 °C	10 minutes	Final extension
4 °C Hold		

If annealing temperatures of primers were not closely matched a touchdown program was used for amplification. A typical touchdown PCR thermal profile is given below.

Thermal Profile of a touchdown PCR		
95 °C	15 minutes	Enzyme activation step, 1 cycle
Followed by 6 cycles		
94 °C	20 seconds	DNA denaturation step
70 °C	30 seconds	Highest annealing temperature -2 °C per cycle
Followed by 29 cycles		
94 °C	20 seconds	DNA denaturation
60 °C	30seconds	Lowest annealing temperature
72 °C	30-60 seconds	Extension step for 500bp-1Kb product
Followed by		
72 °C	10 minutes	Final extension
4 °C Hold		

Details of primers including sequences and annealing temperatures are listed in table 2.4 at the end of this section. PCRs were performed using a Peltier Thermal Cycler (PTC-225, MJ Research).

2.4.2 Allele-Specific PCR

Allele-specific PCR was carried out for *DISC2* SNP rs1535530. Forward and reverse primers were designed with the 3' base representing the polymorphic nucleotide as shown below.

SNP rs1535530 surrounding sequence		ttccattc**A/G**gtttgcca
G Allele primers	J3 Forward	tattagcaaacacaggttgagacag
	J10 Reverse	caggtgccttggcaaac**C**
A Allele primers	J3 Forward	tattagcaaacacaggttgagacag
	J11 Reverse	caggtgccttggcaaac**T**

Allelic specificity of the primers was optimised by a gradient PCR program the details of which are shown below.

Thermal Profile of a Gradient PCR		
95 °C	15 minutes	Enzyme activation step, 1 cycle
Followed by 36 cycles		
94 °C	20 seconds	DNA denaturation step
62 °C to 72 °C	30 seconds	Temperature varies across the PCR block. Each sample anneals at a different temperature and the optimum annealing temperature can be determined.
72 °C	30-60 seconds	Extension step for 500bp-1Kb product
Followed by		
72 °C	10 minutes	Final extension
4 °C Hold		

Allele-specific PCR was carried out by nested PCR. Initially primers were used to amplify the region containing the SNP and this product was used as the template for the allele-specific PCR. ThermoStart DNA polymerase was used to carry out this

PCR reaction. All primer sequences and conditions are listed in table 2.4. PCRs were performed on a Peltier gradient thermal cycler (PTC-225, MJ Research).

2.4.3 Quantitative Real-Time PCR

Gene expression was measured quantitatively with SYBR® Green Real-Time PCR using the MyiQ™ Single-Colour Real-Time PCR Detection System (Bio-Rad laboratories Ltd. Cat# 170-9740). This technique calculates relative gene expression compared to a control by measuring fluorescence of a SYBR® Green dye which is incorporated into the DNA during amplification.

PCR master mix (iQ™ SYBR® Green Supermix cat# 170-8882) was obtained from Bio-Rad Laboratories, Ltd. Real-time PCR Primer sequences are listed in table 2.4. *Glyceraldehyde-3-phosphate Dehydrogenase* (*GAPDH*), *Glucose-6-phosphate dehydrogenase* (*G6PD*) and *Human Phosphofructokinase* (*hPFKm*) reference genes were amplified to facilitate normalisation. Details of the PCR reaction mix and thermal profile are listed below.

Recipe for a single qRT-PCR reaction mixture	
7.5µl	2X iQ™ SYBR Green Supermix
75-100ng	Forward and Reverse Primers
3µl Template	Single stranded cDNA, 1:3 dilution
dH_2O to final volume of 15µl	

Thermal Profile of a typical RT-PCR reaction		
95 °C	3 minutes	1 cycle
Followed by 40 cycles		
95 °C	10 seconds	DNA denaturation
66 °C	30 seconds	Primer annealing
72 °C	45 seconds	Extension
Followed by melt curve analysis		
55 °C	10 seconds	+0.5 °C per cycle for 80 cycles

Melt curve analysis was carried out to ensure primer specificity. All samples were tested a minimum of three times. Each primer set had an internal standard curve to determine primer efficiencies'. Dilutions of pooled cDNAs were used as standards. Each curve consisted of four dilutions, Neat, 1:10, 1:100 and 1:1000. Relative gene expression levels were determined using the MyiQ™ Real-Time PCR detection system optical software system version 1.0 (Bio-Rad Laboratories, Ltd.).

2.4.4 Rapid Amplification of cDNA Ends (RACE)

This technique was used to isolate the 5' end of the novel *DISC2* gene. The FirstChoice™ RNA-Ligase-Mediated (RLM) RACE kit (Ambion) was used. This particular protocol uses a cDNA library that has been enriched for mRNAs containing true 5' ends. Gene specific primers for *DISC2* were generated (see table 2.4) and used to amplify a human heart RACE ready cDNA library according to the manufacturer's protocol. SUPER TAQ *plus* (HT Biotechnology) and Thermostart Taq (Abgene) were tested with this protocol. Both enzymes generated products. I routinely used Thermostart Taq as this enzyme is compatible with PCR cloning of RACE products if necessary. For these experiments however PCR direct sequencing was chosen as the optimum method for sequencing products. To do this RACE products were excised from a low melting point gel and purified and sequenced as previously described.

Table 2.4 PCR Primers		
Primer Name	**Sequence**	**Annealing Tm**
DISC2 nested PCR primers (see chapter 8)		
DISC2 forward J5 (outer)	AAAATGCTCAAGACCTTGCC	62°C
DISC2 reverse J6 (outer)	CTGTTGGTGTTGAGTTCCAGG	67°C
DISC2 forward J3 (inner)	TATTAGCAAACACAGGTTGAGACAG	67°C
DISC2 reverse J4 (inner)	AAAAAGCTGGGAAGTGTTAAAGAAG	65°C
DISC2 Allele-specific primers (SNP rs1535530, see chapter 8)		
DISC2 forward J3	TATTAGCAAACACAGGTTGAGACAG	66°C
G allele reverse J10	CAGGTGCCTTGGCAAACC	
A allele reverse J11	CAGGTGCCTTGGCAAACT	
DISC2 intron 9 primers (See chapter 8)		
Primer pair 1 forward J25	TGACCCAGCCTCAGGTATTC	TD 70-60°C
Primer pair 1 reverse J26	CAGAGAAGGGGCAGTTGAAG	
Primer pair 2 forward J27	AAAAGGCATAAATGAAAGGGC	TD 70-60°C
Primer pair 2 reverse J28	GAAAGGGAGGAGGTGAGGAG	
Primer pair 3 forward J29	CGCAGCCACATAAAGAAATG	TD 70-60°C
Primer pair 3 reverse J30	CTTCCCCTATTCTGCTTCCC	
Primer pair 4 forward J31	GCGAATAGCCAGGTTTGAAG	TD 70-60°C
Primer pair 4 reverse J32	TGAGTGTGCAAGACAGGAGG	
Primer pair 5 forward J33	CAGAGCCGCAGAGAAGAGAC	TD 70-60°C
Primer pair 5 reverse J34	GTGCTTTCAGAGATCAGGGG	
Primer pair 6 forward J35	CTAGCTGATGCAGGAGGAGG	TD 70-60°C
Primer pair 6 reverse J36	TTTTGGACAGGCTGATTTCC	
Other DISC2 primers (see chapter 8)		
DISC2 intron8-intron9 forward J56	TAAGGAGAGCAATATTTTTCCAGG	66°C
DISC2 intron8-intron9 reverse J57	ATTAGCAAACACAGGTTGAGACAG	
DISC2 RACE Primers (see chapter 8)		
RACE outer J26	CAGAGAAGGGGCAGTTGAAG	60°C
RACE inner J26	CCTAATTCTTGGCACAGTCTCA	
DISC1 Primers (see chapter 3)... continues onto next page		
Exon 2 forward J14	GAACGTGGAGAAGCAGAAGG	66°C
Exon 2 reverse J15	CAGAGAACTGGAGGAGCCAG	
Exon 4-6 forward J43	AGCCTGCACTTTCAACTTCC	66°C

Exon 4-6 reverse J44	AGTTGCTGCTCTTGCTCCTC	
Exon 9 forward J37	AGAGAGAGAAGGGCTGGAGG	66°C
Exon 9 reverse J38	GTCTCCTGGTGCTCCACTTC	
Exon 11-12 forward J39	CAGGGGAAGCCTGTCTGTAG	66°C
Exon 11-12 reverse J40	TGGATTGCTGTGTGAAGTTG	
Intron 10-11 forward J54	ACAGAATCTTAGCTAATCACCATGC	66°C
Intron 10-11 reverse J55	TCTGGTCTCTCTAATTTCACATTCC	
Reference Genes		
GAPDH forward	GGGAGCCAAAAGGGTCATCA	66°C
GAPDH reverse	GTGGCAGTGATGGCATGGAC	
hPFK(m)A forward	AGAGCGTTTCGATGATGCTT	66°C
hPFK(m)B reverse	GTGTTCCTCCCAGTCGTCAT	
G6PD A forward	ATCTTGGTGTACACGGCCTC	66°C
G6PD B reverse	CAACCACATCTCCTCCCTGT	

All primers were designed using Primer 3 software (SDSC Biology Workbench)

2.5 Agarose gel electrophoresis

Stock solutions for this section are detailed in Appendix II. Standard agarose gels of 1-1.5% were used to separate fragments of size 0.2-0.5 kb and 0.8-1% gels were used to resolve fragments of size 0.5kb or greater. Gels were prepared and run using 1X Tris-Acetate buffer. Samples were loaded using 10X Orange buffer (Appendix II). Electrophoresis was carried out using Hybaid Electro-4 gel tanks. Voltage applied (usually 80-100V) creates an electric current causing the DNA to migrate through the agarose from the cathode (-ve) to the anode (+ve) due to the negatively charged phosphate backbone of the DNA.

DNA was stained with Ethidium Bromide (0.5µg/ml molten agarose, SIGMA) or SYBR Safe™ (1µl/100ml molten agarose, Invitrogen™ #SS33102). Fragments were visualised using a UV transilluminator (Thistle Scientific) with the aid of a uvidoc (Uvitec, DOC-CF08.XD). The molecular weight of each fragment was determined by comparing its mobility to a 1Kb DNA ladder (Invitrogen) or a λHindIII (Invitrogen, Appendix II) marker for larger fragments of up to 23Kb in size.

DNA fragments were also run on low melting point (LMP) agarose gels to allow for recovery of the DNA after electrophoresis. LMP agarose gels were prepared using 1X TAE and usually run at 80V.

2.6 Sequencing of DNA

DNA templates for sequencing consisted mainly of PCR products. All DNA for sequencing was checked by agarose gel electrophoresis before sequencing was carried out. In some cases (e.g. multiple PCR products in the same reaction) the DNA was gel extracted before use in sequencing procedures.

2.6.1 Preparation of sequencing templates

Sequencing templates were prepared by one of three methods; the gel extraction method has been previously described; the other two methods, drop dialysis and ExoSAP-IT treatment, are described below.

2.6.1.1 Drop dialysis of DNA

DNA derived from extraction or PCR procedures may contain excess salts or detergents which can inhibit sequencing reactions. Problematic sequencing can usually be resolved by removing these inhibitors using a microdialysis procedure. To dialyse DNA 0.025µm MF-Millipore™ membrane filters were used (MLLIPORE). The 25mm membranes were placed floating on a petri-dish of distilled water (shiny surface upwards). After allowing the membrane to wet for about 5 minutes a small volume of DNA was then pipetted onto the membrane and left for 1hour. The DNA is removed with a pipette and ready for use. This method is adapted from *Silhavy et al. 1984.*

2.6.1.2 ExoSAP-IT treatment of DNA

ExoSAP-IT™ (GE Healthcare) contains exonuclease I and alkaline shrimp phosphatase which effectively removes all excess primers and dNTPs before sequencing. 5µl of PCR product was incubated with 1µl of ExoSAP-IT™ on a thermal cycler for 30 minutes at 37°C followed by 30 minutes at 80°C.

2.6.2 PCR direct sequencing

Sequencing reactions were carried out in 10µl volumes using BigDye® Terminator Ready Reaction Mix v3.1 as detailed below.

BigDye v3.1 Sequencing Reaction	
1µl	2.5X Ready Reaction Mix (final concentration 0.25X)
1.5µl	5X sequencing buffer (final concentration 0.75X)
1.5 – 10ng	PCR product (usually ~1µl of treated PCR reaction)
25ng	Forward and Reverse sequencing primers
dH_2O to make final volume 10µl	

Sequencing reactions were performed using a Peltier PTC-225 thermal cycler. The thermal profile of the sequencing reaction is detailed below.

Thermal Profile of BD v3.1 sequencing reaction	
96°C	1 minute, 1 cycle
Followed by 25 cycles	
96°C	10 seconds
60°C	5 seconds
60°C	4 minutes
4°C Hold	

2.6.3 Ethanol/EDTA precipitation of sequencing reactions

After sequencing, DNA was precipitated by adding 2.5µl of 125mM EDTA and 30µl 100% Ethanol. This was mixed and incubated at room temperature for 15 minutes followed by centrifugation at 13,000rpm for 20 minutes. All ethanol was removed and a further 30µl of 70% ethanol was added. This was centrifuged at 4°C for 5 minutes and again all ethanol was removed. After air-drying samples were stored at -20°C until they were analysed. Samples were analysed using Applied Biosystems 3730 DNA Analyser and sequences examined using the CONSED (*Gordon et al. 1998*) or Chromas (version 1.45, *McCarthy C. 1996*) analysis software.

2.7 Analysis of protein expression

2.7.1 Protein lysate preparation from cultured mammalian cells

To prepare lysates, cultured cells were harvested as previously described. Cells were pelleted at 4°C, at 1000-2000rpm for 5minutes and pellets were washed once in PBS. Pellets were resuspended in an appropriate amount of RIPA buffer with complete protease inhibitors (Roche, Appendix II). Typically, pellets recovered from 12 or 6 well plates were resuspended in 30-50µl of RIPA buffer and pellets from 10cm dishes were resuspended in 100-500µl RIPA buffer depending on cell density at time of harvest. Pellets were resuspended by pipetting followed by sonication in ice for 5-10 seconds at (2 microns, peak-to-peak) using an MSC Sonicator. Lysates were stored at -70°C until use.

2.7.2 Determining protein concentration

The Bio-Rad Protein Assay (Bio-Rad Laboratories) was used to determine the concentration of protein lysates. The manufacturers' protocol was modified to perform reactions in 1.5ml eppendorfs. 25µl of a 1:10 dilution of each protein sample was made in distilled water (2.5µl lysate + 22.5µl water). 6 protein standards were prepared in a 25µl volume as shown below.

Concentration	µl of protein standard	Distilled water
Standard 1 = 0.2 mg/ml	2.5	22.5
Standard 2 = 0.4 mg/ml	5	20
Standard 3 = 0.6 mg/ml	7.5	17.5
Standard 4 = 0.8 mg/ml	10	15
Standard 5 = 1.0 mg/ml	12.5	12.5
Standard 6 = 1.5 mg/ml	18.25	6.75

For the protein assay 125µl of Bio-Rad Reagent A was added to each sample and standard followed by 1ml of Bio-Rad Reagent B. The reactions were allowed to develop for 15-30 minutes in darkness and the absorbance of each was measured at 750nm in plastic cuvettes (1cm path length, Fisherbrand). A standard curve was created using Microsoft Excel by plotting concentration (x-axis) Vs absorbance (y-axis) of each standard. Unknown concentrations were deduced from this using the equation of the line.

2.7.3 One dimension SDS-Polyacrylamide gel electrophoresis

2.7.3.1 Gel preparation

SDS-PAGE resolving gels of 8-15% polyacrylamide were prepared using 30% Acrylamide/Bis solution (Bio-Rad Laboratories). 25% Ammonium persulfate solution (Sigma) and TEMED (Sigma) were used to catalyze polymerisation. High porosity stacking gels of 4% polyacrylamide were used for loading samples. Gels were cast 1mm thick using the Mini-PROTEAN 3 electrophoresis system casting

module (Bio-Rad Laboratories). Gel preparation methods were adapted from Molecular Cloning, *Sambrook et al.* 1989.

2.7.3.2 SDS-PAGE sample preparation

Protein lysates were prepared for electrophoresis using Laemmli sample buffer (Appendix II) containing detergent (20% Sodium Dodecyl Sulphate solution). DTT (Dithiothreitol) was used as a reducing agent in protein sample preparation. Typically, 10-30µg of protein lysate was prepared in 15-30µl volume. A typical lysate preparation is shown below.

20µg	protein lysate
10 µl	2x Laemmli PSB
2 µl	1M DTT

Distilled water to final volume of 20 µl

Samples were heated at 70-100°C for 5 minutes to dissociate polypeptide subunits before loading on SDS-Polyacrylamide gels. Samples were either run on homemade polyacrylamide gels or pre-cast gradient polyacrylamide gels.

2.7.3.3 Bio-Rad Acrylamide/Bis gel electrophoresis

Protein electrophoresis was carried out using the discontinuous Tris-Glycine Buffer system (10X Tris/Glycine buffer, Bio-Rad Laboratories). The Mini-PROTEAN 3 gel tank system (Bio-Rad laboratories) was used for electrophoresis. After boiling, protein samples were loaded into the wells of the stacking gel and run at 50 volts (V) (Bio-Rad PowerPac3000) until the protein samples had passed through the resolving gel interface. The voltage was then increased to 100-150V. 15µl of protein standard was loaded alongside samples to determine polypeptide sizes. The two protein standards used for the purposes of these experiments were the Precision Plus Protein™ standard (Bio-Rad Laboratories) and SeeBlue™ plus2 pre-stained standard (Invitrogen).

2.7.3.4 Pre-cast gradient gel electrophoresis

Electrophoresis was carried out using NuPAGE® Novex Tris-Acetate 3-8% gradient gels (Invitrogen). This method was used to achieve good resolution of the three DISC1 protein isoforms of between 75 and 71kDa in size. Pre-cast gels were run using the XCell *Sure*Lock™ gel tank (Invitrogen). 500mls of NuPAGE Tris-Acetate SDS running buffer (Invitrogen) was used to fill the upper and lower chambers and protein samples were loaded. The samples were run at 150V for approximately 1-1.5hrs. Current was applied using the Bio-Rad PowerPac300. Typically, the SeeBlue™ Plus2 pre-stained standard was run alongside samples to allow size determination.

2.7.4 Two dimension SDS-Polyacrylamide gel electrophoresis

Two-dimension (2D) gel electrophoresis separates proteins based on their isoelectric point (pI) in the first dimension and on their size in the second dimension. This system allows clear resolution of proteins very close in size which may not be resolved using one-dimensional electrophoresis.

For the purposes of these experiments 2D gels were run using the ZOOM® IPGRunner™ System (Invitrogen). Approximately 100µg of lysate was mixed with rehydration buffer (RB) to a final volume of 155µl. This lysate mixture was loaded into a channel of the IPGRunner cassette and a ZOOM strip was slotted into each channel with the sample (acidic end (+) of the strip is inserted first). ZOOM strips are thin strips of polyacrylamide gel containing an immobilised pH gradient (IPG strips). These strips allow for isoelectric focusing (IEF) of protein samples. Isoelectric focusing separates proteins depending on their pI.

Once all the samples were loaded the cassette was sealed and incubated on the bench overnight. This procedure serves to solubilise and denature the proteins and also to rehydrate the IPG strips before IEF. The strips used in these experiments contained a wide non-linear pH gradient ranging from pH 3-10. IEF was performed using a PowerEase®500 power pack (Invitrogen) for 4 hours at 500V (0.5 Watts per strip,

1mAmp per strip). Following focusing the IPG strips can be stored at -70°C until ready for second dimension SDS-PAGE.

Immediately prior to SDS-PAGE the IPG strips were equilibrated in NuPAGE® LDS sample buffer (Invitrogen). The strips were equilibrated for 15 minutes in LDS buffer containing NuPAGE sample reducing agent (Invitrogen) followed by 15 minutes in LDS buffer containing an alkylating solution (ProteoPrep™ iodoacetamide, Sigma). The IPG strips were then inserted into NuPAGE Novex 4-12% Bis-Tris ZOOM gels (Invitrogen). One IPG strip was inserted into the well of each ZOOM gel and the well was sealed using 400µl of 0.5% agarose solution (made in 1X MES running buffer, Invitrogen). SDS-PAGE was performed at 200V for 50 minutes in 1X MES buffer (using the PowerEase®500 power pack). Once completed the gels were analysed by western blotting.

2.7.5 Fixing/Staining SDS-polyacrylamide gels

These methods were used to fix and stain proteins after electrophoresis. This was done to determine equal protein loadings as confirmation of successful protein concentration determination and also to determine successful transfer of proteins after western blotting.

2.7.5.1 GelCode® Blue staining

After electrophoresis the gels were rinsed 3 times for 15 minutes each in distilled water followed by 1 hour incubation at room temperature with the protein stain reagent. Gels were then de-stained in water which removes excess stain and enhances the protein staining.

2.7.5.2 Coomassie Brilliant Blue staining

Polyacrylamide gels were incubated in coomassie protein stain (Appendix II) for 30 minutes followed by multiple de-stain washes in Methanol:Acetic Acid (Appendix II).

2.7.6 Drying SDS-polyacrylamide Gels

Polyacrylamide gels can be stored long term after drying. To dry gels they were placed face down on 1 sheet of saran wrap (Dow chemical company). One piece of wet Whatman 3MM was placed on top of the gel followed by one piece of dry 3MM. The gel is place saran side up in a vacuum pump and dried for approximately 1 hour. It is crucial that the vacuum is not released with the first 30 minutes of drying.

2.7.7 Western Blotting

2.7.7.1 Immobilising proteins on PVDF membrane – Wet transfer

This system was used to transfer proteins from pre-cast Tris-Acetate gels and 2D Bis-Tris ZOOM gels onto 0.2µm PVDF membranes (Invitrolon™ PVDF). The membrane was prepared by soaking briefly in 100% methanol followed by 5-15 minutes equilibration in NuPAGE transfer buffer. The gel was sandwiched with the PVDF membrane and two pieces of 3MM filter paper, according to the manufacturers' instructions. This sandwich was placed in the XCell II™ blot module (Invitrogen) within the XCell *Sure*Lock gel tank. The blot module was filled with NuPAGE transfer buffer and the outer chamber of the tank was filled with water. A current of 30V was applied for 1 hour using the Bio-Rad PowerPac300.

2.7.7.2 Immobilising proteins on PVDF membrane – Semi-Dry transfer

This system was used to transfer proteins from homemade polyacrylamide gels onto Hybond-P PVDF membranes optimised for protein transfer (Amersham Biosciences). After electrophoresis gels were equilibrated three times for 10 minutes in semi-dry transfer buffer (Appendix II). The membrane was prepared by soaking in 100% methanol, followed by 15 minutes equilibration in transfer buffer. The gel was placed on top of four pieces of Whatman 3MM filter paper soaked in transfer buffer, the PVDF membrane was placed over the gel and then four more pieces of soaked 3MM filter paper were used to complete the sandwich. Transfer was carried out at 20V for 1.5 hours using the TRANS-BLOT® semi-dry transfer cell (Bio-Rad Laboratories) and the Bio-Rad PowerPac300.

2.7.7.3 PonceauS staining membranes

Ponceau's stain (Appendix II) was used to determine successful protein transfer onto PVDF membranes. After transfer, membranes were rinsed in distilled water followed by 5 minutes incubation in PoncauS. Membranes were de-stained in distilled water.

2.7.8 Immunoblotting; Detection of immobilised proteins

Once proteins were immobilised on membranes antibodies were used to detect specific proteins of interest. Membranes were typically incubated at 4°C overnight in blocking buffer (PBST or TBST, see Appendix II). Antibodies were diluted appropriately in PBST/TBST and incubated with membranes overnight at 4°C or for 1 hour at RT. Membranes were washed in PBST/TBST (1 x 15minutes, 3 x 5 minutes) and incubated with Horseradish Peroxidase (HRP) conjugated secondary antibodies for 20-30 minutes at RT. Following a second wash stage bound antibodies were detected by chemiluminescence using ECL plus Western Blotting detection reagents (Amersham Biosciences). Details of suggested immunoblotting and detection protocols can be found in user manual RPN2132. For specific antibody conditions see table 2.7.

2.7.9 Immunofluorescence (IF); Visualisation of proteins in fixed cells

Immunofluorescence was used to visualise sub-cellular localisation of proteins in fixed mammalian cells. Cells were plated on 16mm glass coverslips to enable microscopic analysis and fixed in 100% methanol or 4% Paraformaldehyde (PFA, Appendix II) for 10 minutes at room temperature (RT). Cells fixed in PFA require a further permeabilisation step which was performed using 0.5% Triton-X 100 (in PBS) for 15 minutes at RT. Cells were incubated in antibody blocking buffer for a minimum of 15 minutes at RT (Appendix II). For blocking and all subsequent incubation steps a damp paper towel was placed over the wells inside the plate to create a humid chamber.

After blocking cells were incubated with primary antibody (150-200µl, in a 12 well plate) for 1 hour at RT followed by 3 x 5 minute washes in PBS/BSA (0.02% solution, Appendix II). Alexa Fluor conjugated secondary antibodies were used to visualise proteins by fluorescent microscopy. Secondary antibodies were diluted appropriately in PBS/BSA and incubated for 1 hour at RT. Washes were repeated as for the primary incubation and coverslips were mounted face down in Mowiol/DAPI (Appendix II). For antibody details see table 2.7.

Table 2.7 Antibodies

Primary Antibodies				Working dilution[1]	
Antibody	**Species[&]**	**Raised In**	**Source**	**IB***	**IF***
AKAP450	Human	Mouse	BD Transduction Laboratories	NA	1-200
α-tubulin	Human	Mouse	Sigma	1-60,000	1-3000
β-actin	Human	Mouse	Sigma	1-60,000	NA
β-tubulin	Human	Rabbit	Abcam	NA	1-250
γ-tubulin	Human	Mouse	Sigma	1-5000, O/N	1-3000
Cytochrome C	Human	Rabbit	Clontech	1-2,000	1-100
DISC1 R47-8	Human N-Term	Rabbit	In house	1-500	NA
DISC1 R47-15	Human N-Term	Rabbit	In house	1-500	NA
DISC1 R47-14	Human N-Term	Rabbit	In house	NA	1-100
DISC1 R47-16	Human N-Term	Rabbit	In house	NA	1-100
αDISC1	Human C-Term	Rabbit	T.Akiyama[2]	1-2000, O/N	1-400, 2hrs
FLAG	M2 Monoclonal	Mouse	Sigma	1-1000	1-3000
GM130	Human	Mouse	BD Transduction Laboratories	NA	1-1500
MTCO2	Human	Mouse	Abcam	NA	1-1000
Myosin	Human	Rabbit	Sigma	1-1000	NA

Continues overleaf

Secondary Antibodies		Working Dilution	
HRP conjugated antibodies	**Source**	**IB***	**IF***
Swine anti-Rabbit	DakoCytomation	1-3000, 20mins	NA
Rabbit anti-Mouse	DakoCytomation	1-80,000, 30mins	NA
Alexa Fluor conjugated antibodies	**Source**	**IB***	**IF***
Goat anti-Rabbit 488	Molecular Probes	NA	1-500
Goat anti-mouse 488	Molecular Probes	NA	1-500
Goat anti-Rabbit 594	Molecular Probes	NA	1-800
Goat anti-Mouse 594	Molecular Probes	NA	1-800

[&]Denotes which species were detected using the antibody not the cross reactivity of the antibody

*IB = Immunoblotting IF = Immunofluorescence

[1] All antibodies were incubated for 1hour at RT at the appropriate working dilution unless otherwise specified.

[2] Tetsu Akiyama, Institute of Molecular and Cellular Biosciences, University of Tokyo, Japan.

2.8 FACS analysis (Fluorescence Activated Cell Sorting)

2.8.1 Analysis of cell proliferation using 5'-bromo-2'-deoxyuridine

5-bromo-2'-deoxyuridine (BrdU) incorporation was used as a measure of cell proliferation. BrdU is a thymidine analogue that becomes incorporated into replicating DNA. Cells replicate their DNA during S phase of the cell cycle; these cells can be selectively labelled by pulsing cells with BrdU for short periods of time. BrdU incorporation was detected by a fluorescein conjugated monoclonal anti-BrdU antibody using the In Situ Cell Proliferation Kit, FLUOS (Roche). In brief cells were incubated with 10μM BrdU in normal growth medium for 35-45 minutes. Cells were then harvested, fixed (Appendix II) and resuspended to yield a singe cell suspension. The cellular DNA is then denatured, non-specific binding sites are blocked and the fluorescein conjugated monoclonal anti-BrdU antibody is applied. Cells are then washed to remove unbound antibody and resuspended for FACS analysis. The amount and intensity of fluorescein (bound antibody) was determined by flow cytometry using a BD FACSCalibur by exciting the sample at 488nm. The percentage of fluroescein positive cells in a BrdU-treated cell population relative to an untreated population is a direct reflection of the number of dividing cells. This was quantified using the CellQuest™ software. For detailed experimental protocols refer to user manual 1-810-740, version 3 (Roche).

2.8.2 Analysis of DNA content to determine cell cycle profile

This assay is based on the principle that cells contain different amounts of DNA depending on their stage of the cell cycle. Cells which have entered mitosis and are within the G1 phase will be diploid (2N) as they have not yet replicated their DNA. After replication (S phase) the cells will be have twice as much DNA (4N) before dividing to produce two diploid daughter cells. During S phase cells will have an intermediate DNA content to that of G1 or G2 phase cells. By determining the cellular DNA content it is possible to calculate the cell cycle profile of a cell population.

This technique used propidium iodide (PI, Sigma) incorporation as a measure of total cellular DNA. In brief cells are harvested by trypsinisation and resuspended in 50µl of a hypotonic citrate buffer (Appendix II) which causes the cell membrane to become permeable to PI. To this 225µl of trypsin solution A are added and the cells are incubated at room temperature for 10 minutes (Appendix II). Following this 162µl of trypsin inhibitor/RNAse A solution B is added and cells are incubated for 10 minutes at room temperature (Appendix II). RNAse A incubation is necessary to remove dsRNA which would also be stained using PI. Finally 125µl of PI solution C (Appendix II) is added and the cells are incubated on ice for 10 minutes. References: *Vindelov et al. 1983 A-D.*

Cells were assessed using a Coulter® EPICS® XL™ flow cytometer (Beckman Coulter). The FL3 detector was used to examine PI staining and hence the DNA content of each cell. DNA histogram plots of FL3 staining were created using the EXPO32™ ADC cytometer software. These histograms were exported to the MultiCycle DNA Analysis software programme (Phoenix Flow Systems, USA, www.phnxflow.com) to calculate more accurately the percentage of cells within each phase of the cell cycle.

2.8.3 Apoptosis assay

Apoptotic cell death was measured in cultured mammalian cells using the Annexin V-FITC Apoptosis detection kit I (BD Pharmingen™ #556547). This kit takes advantage of the fact that apoptotic cells translocate the membrane phospholipid phosphatidylserine (PS) to the outer leaflet of the cell membrane whilst undergoing programmed cell death. Annexin is a protein capable of binding PS and hence capable of identifying apoptotic cells. This kit uses Annexin V in conjunction with propidium iodide (PI) a vital dye that stains DNA in a similar manner to ethidium bromide. Early apoptotic cells exclude PI whereas necrotic cells and late stage apoptotic cells take up PI thus enabling the identification of three distinct cell populations, early apoptotic, late apoptotic and necrotic (or dead) cells.

To measure apoptosis in a cell population cell culture medium was removed and spun down to recover any detached cells. The remaining cells were trypsinised and pooled with any cells collected from the culture medium. Cells were then washed and resuspended at approximately $1x10^6$cells/ml in binding buffer (provided). 100µl of this cell suspension was used for each apoptosis assay and to this 5µl each of Annexin V-FITC and PI were added. The cells were vortexed gently and incubated at room temperature in the dark for 15 minutes. 400µl of binding buffer was added to each test and this was analysed using a Coulter EPICS XL flow cytometer. The FL1 channel was used to detect cells which have bound Annexin V and the FL3 channel to detect cells that have incorporated PI. Dot plots of FL1 (X axis) versus FL3 (Y axis) were generated using the EXPO32 ADC software. Quadrant statistics were used to determine the proportion of green, red and double labelled cells.

2.9 PDE4 activity assay

Protein lysates were prepared by resuspending cells in 3T3 lysis buffer (Appendix II) and lysing on a rotary wheel for 1 hour at 4°C. Lysates were cleared by ultracentrifugation at 30,000 x g (rcf) for 30 minutes (Beckman optima ultracentrifuge, TLA100.3 fixed angle rotor). The appropriate concentration of lysate (as determined by a standard activity curve) is added to PDE Tris buffer (Appendix II) with and without 20µM of a PDE4 inhibitor rolipram (Sigma) to make a final reaction volume of 50µl. A negative control containing Tris buffer only should be included. 50µl of 2µM H^3-cAMP substrate is added to each reaction (Appendix II). Samples are incubated at 30°C for 30 minutes to allow the PDE4s to hydrolyse the H^3-cAMP substrate to produce 5'AMP, followed by boiling for 2 minutes to stop the reaction. Samples are cooled for 15 minutes on ice, before adding 25µl snake venom to each reaction (Sigma, Appendix II). Incubation with snake venom for 10 minutes at 30°C de-phosphorylates the H^3-5'AMP product (thus removing its negative charge). A dowex ion resin is then used to remove the negatively charged H^3-cAMP substrate remaining in the reaction (400µl of Dowex Slurry per sample, see Appendix II). This is incubated for 15 minutes on ice, mixing frequently before

centrifuging at 13,000rpm for 3 minutes to spin down the resin and bound H^3-cAMP. 150µl of supernatant was added to 1ml of Ecoscint Scintillation fluid and counted using a scintillation counter (tritium channel). 50µl of the H^3-cAMP substrate is counted to determine total ^3H counts added to the reaction. PDE4 activity can be determined by removing the rolipram insensitive (not PDE4) activity from the total activity. For these experiments total counts (or activity) were graphed as % of control activity.

2.10 Centrosome isolation from SH-SY5Y cells

Centrosomes were isolated from mammalian cells using a modified version of the technique published by *Moudjou and Bornens, 1998*. Some reagents and solutions are detailed in Appendix II where indicated, others can be obtained from the original reference. In brief cells were treated with 1µg/ml Cytochalasin D and 0.2µM Nocodazole for 1 hour prior to centrosome isolation (Appendix II). Cells were trypsinised and pellets washed with TBS Buffer. Cells were recovered and washed again using TBS 1/10-8% Sucrose buffer. Cells were recovered and resuspended in TBS 1/10-8% Sucrose and lysis buffer (Appendix II) was added. Lysate was filtered through a cell strainer and incubated at 4°C for 30 minutes with HEPES and DNase at final concentrations of 10mM and 1µg/ml respectively.

Lysates were applied to a discontinuous sucrose gradient and ultracentrifuged at 40,000 x g (15,300 rpm) for 1 hour in a Sorvall Ultra Pro 80 (swinging bucket rotor TH-641) in 14x89mm Beckman centrifuge tubes. Centrosomes settled between 65% and 50% sucrose using this procedure and were removed using a syringe. This centrosomal lysate was diluted with four volumes of 20% sucrose and centrifuged at 43,000 rpm for 30 minutes using a Beckman Optima Ultracentrifuge (TLA 100.3 fixed angle rotor) in 13x51mm Beckman centrifuge tubes. Centrosome pellets were resuspended using 40mM Tris pH 8.0 with 0.3% SDS and stored at -70°C. The procedure is depicted in figure 2.10.

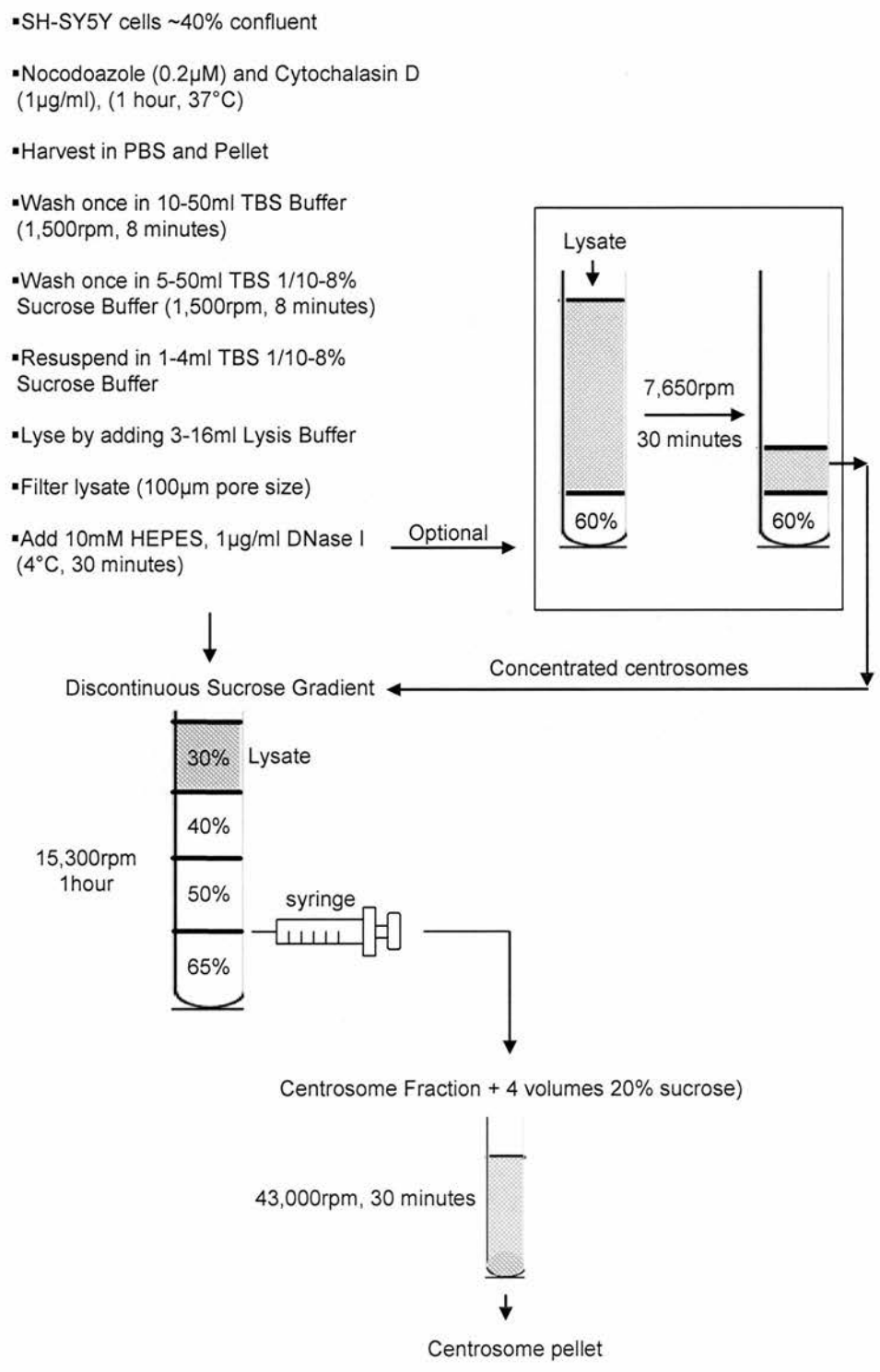

Diagram 2.10. This Diagram depicts the centrosome isolation process using SH-SY5Y cells.

2.11 Bioinformatics

2.11.1 Single Nucleotide Polymorphism (SNP) selection

The NCBI dbSNP database and the USCS genome browser were used to identify SNPs in *DISC1* and *DISC2*.

2.11.2 Bioinformatics programs

www.ucsc.edu	UCSC Genome Bioinformatics
www.ncbi.nlm.nih.gov www.ncbi.nlm.nih.gov/SNP/ www.ncbi.nlm.nih.gob/BLAST/	National Centre for Biotechnology Information dbSNP BLAST
www.ensembl.org	Ensembl
www.biologyworkbench.com	San Diego Supercomputer Centre Biology Workbench
www.hgmp.mrc.ac.uk www.softberry.com	Promoter predictions (Grail, Genscan, FPROM and TSSG)
www.gene-regulation.com	BIOBASE Biological Databases (TRANSFAC®)
www.genomatix.de	Genomatix (MatInspector)

Chapter 3

Defining the disease mechanism operating in the t(1;11) family

3.1 Preface

Schizophrenia is a complex disease with multiple genetic factors contributing to disease aetiology in the general population. The t(1;11) family is unique because a balanced translocation co-segregates through four generations with major psychiatric illness. We can infer that a gene of major effect has been disrupted which directly confers susceptibility to illness. This overcomes a huge hurdle in the genetics of complex diseases as the region of interest is immediately apparent because it is marked by the translocation. It is still necessary however to elucidate the consequences of the translocation and the mechanism of disease pathogenesis.

There are two genes disrupted by the translocation. The priority candidate gene in this family is *DISC1*, a novel protein coding gene, which is expressed in regions of the brain implicated in psychiatric illness. There are two disease mechanisms that could potentially leads to pathogenesis of illness in this family via disruption of *DISC1*. The first mechanism assumes production of aberrant DISC1 truncated or fusion proteins. Such putative proteins might arise by one or more of the following processes. A C-terminally truncated DISC1 protein might be produced from the derived chromosome 1. Such a truncated protein would lack much of the coiled-coil forming potential of wild type (WT) DISC1 and would lose the ability to interact with many DISC1 protein partners. Alternatively the derived chromosome 11 might lead to the production of an N-terminally truncated DISC1 isoform. Such a protein would be predicted to retain some of the functional capacity of WT DISC1, but without the N terminal region which is needed for correct sub-cellular localisation of DISC1 (*Millar et al. 2005a*). Finally, the possibility of fusion proteins resulting from juxtaposition of chromosome 1 and chromosome 11 sequences cannot be ruled out. The downstream consequences any of these scenarios would be that either truncated/fusion DISC1 fails to perform its correct cellular functions and/or may

acquire abnormal properties with detrimental cellular effects. In order for a truncated/abnormal protein to be produced it is necessary that transcription occurs on the derived 1 and 11 chromosomes and that this sequence then becomes translated. To date there have been no studies investigating this in t(1;11) family members.

The second disease mechanism which may operate within the t(1;11) family is one of haploinsufficiency. Haploinsufficiency occurs when a 50% reduction in gene product (i.e. disruption of one allele) is sufficient to cause a disease phenotype. Family members possessing the t(1;11) translocation have only one intact copy of the *DISC1* gene. Haploinsufficiency would explain the co-segregation with illness if there was no productive expression from the derived chromosome 1 allele. There is evidence to support this from protein expression studies in a limited number of translocation carriers. This data suggests that there is a reduction in the levels of DISC1 protein in translocation carriers versus those with a normal karyotype (*Millar et al. 2005b*). It is unknown whether this is as a result of ablated transcription from the derived *DISC1* allele or a cellular surveillance mechanism which degrades aberrant *DISC1* transcripts. It is important to note that the two disease mechanisms mentioned here are not necessarily mutually exclusive because it is possible that an abnormal protein may also affect the function of the full length protein. *Kamiya* et al. have recently reported that DISC1 can dimerise via a self-association domain (*Kamiya et al. 2005*). Furthermore in vitro over-expression of the hypothetical C-terminally truncated DISC1 isoform results in disruption of the normal localisation of full length DISC1, which is postulated to occur via this self-association mechanism (*Kamiya et al. 2005*).

This chapter presents data from an extensive study of lymphoblastoid cell lines derived from t(1;11) family members, which express the *DISC1* gene. This study analyses *DISC1* transcription from the normal and derived alleles and examines the expression of *DISC1* at both the mRNA and protein level. It further investigates the presence of C-terminally or N-Terminally truncated DISC1 isoforms and whether these are likely to contribute to disease pathogenesis in this family.

3.2 *DISC1* transcripts are produced from the derived chromosome 1

3.2.1 DISC1 SNP selection and genotyping

DISC1 protein expression in lymphoblastoid cell lines from t(1;11) family members has been previously analysed and no aberrant DISC1 isoforms detected (*Millar et al. 2005b*). The effects of the t(1;11) translocation on transcription of this gene has yet to be investigated. In order to assess transcription from the derived *DISC1* allele it is necessary to distinguish it from the full length, wild-type allele. To do so exonic single nucleotide polymorphisms were identified and genotyped in genomic DNA isolated from t(1;11) lymphoblastoid cell lines. A panel of cell lines possessing both normal and translocation karyotypes were analysed. Genotypes were determined by amplifying the region using PCR and subsequent sequencing across the SNP.

SNP rs2492367 located in exon 6 of the *DISC1* gene was found to be homozygous in all individuals and therefore not useful for discriminating the *DISC1* alleles. A translocation carrier heterozygous for SNP rs3738401 located in *DISC1* exon 2 was however available for analysis. Using SNP rs3738401, the A allele is present in all carriers whereas some non-carriers possess a GG homozygous genotype. This infers that the A allele of SNP rs3738401 represents the translocated *DISC1* allele and the G allele represents the wild-type *DISC1* allele. As this translocation is inherited and recombination is repressed in this region of chromosome 1 we can be confident in this SNPs ability to discriminate between the alleles. Figure 3.2.A depicts the inheritance of the translocation and thus how it is possible to discriminate the alleles using this SNP.

Table 3.2. T(1;11) exonic *DISC1* SNP genotyping data				
T(1;11) Cell line status	**Forward**	**Reverse**	**Forward**	**Reverse**
	Genomic rs2492637 exon 6		**cDNA rs2492637**	
N	CC	CC	ND	ND
T	CC	CC	ND	ND
T	CC	CC	ND	ND
				ND = Not determined
	Genomic rs3738401 exon 2		**cDNA rs3738401 exon 2**	
N	GG	GG	GG	GG
T	AG	AG	AG	AG

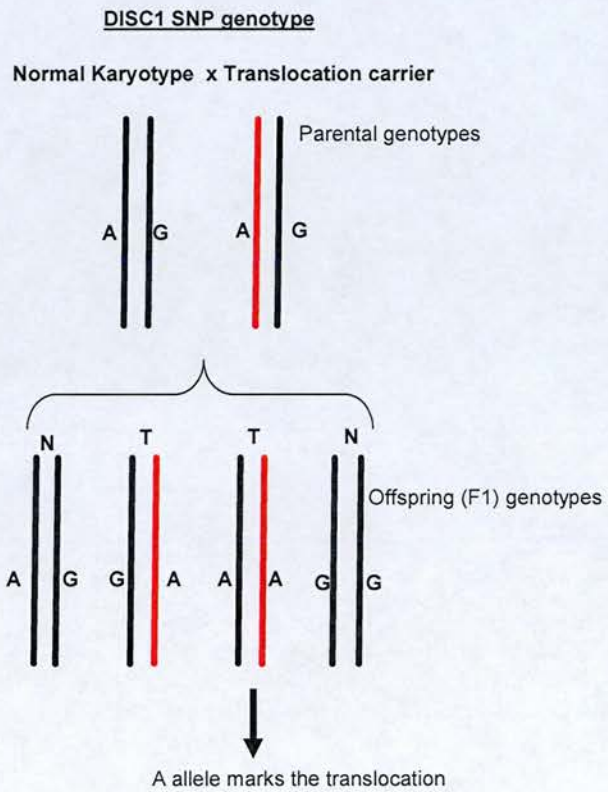

Figure 3.2.A. Genotyping data for *DISC1* exonic SNPs are shown in table 3.2. Below is a cartoon depicting inheritance of the translocation. The chromosome carrying the translocation is marked in red. Although the parental genotypes do not distinguish the allele marking the translocation the presence of an AA translocation carrier and a GG non-carrier in the F1 generation indicates that the A allele of *DISC1* marks the translocation chromosome.

3.2.2 Analysis of DISC1 transcripts

To assess whether transcription occurs from the derived *DISC1* allele, cDNA was prepared using mRNA isolated from t(1;11) lymphoblastoid cell lines that were heterozygous for SNP rs3738401. The region surrounding this SNP was amplified by PCR and sequenced in the same manner as for genomic DNA. If mRNAs are transcribed from both alleles A and G, both alleles should be detected when sequenced. Products were sequenced in both forward and reverse orientations for normal and translocation carrying cell lines. Figure 3.2.B shows sequencing chromatograms obtained from these cell lines. Cell line 74 possesses a normal karyotype (N) and is homozygous GG for SNP rs3738401. Cell line 94 possesses the translocation (T) and is heterozygous AG for rs3738401. It is clear that whilst only the normal G allele is detected from cell line 74 (N), cell line 94 (T) produces transcripts from both alleles as indicated by the presence of both A and G peaks (indicated by N) at the position of the SNP. This method of sequencing is indicative of abnormal transcripts being produced from the derived *DISC1* allele, however it is not a quantitative assay so does not have the ability to inform on the relative abundance of each transcript. Quantitative Real-Time PCR (qRT-PCR) was therefore carried out on patient lymphoblastoid cell lines in order to determine whether *DISC1* levels are affected by the translocation.

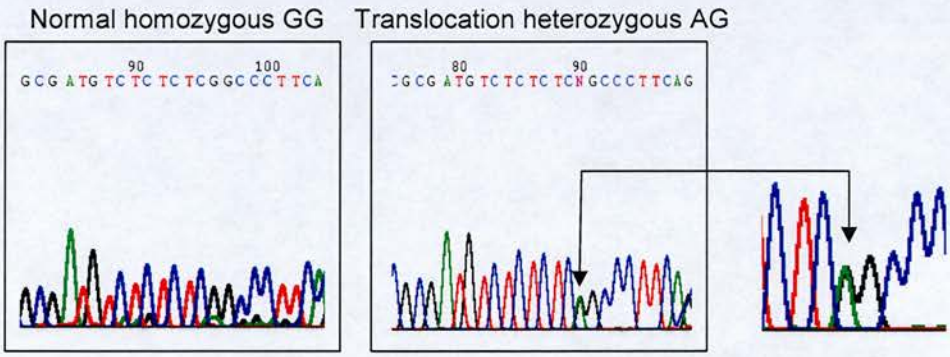

Figure 3.2.B. This figure shows sequencing chromatograms for *DISC1* exon 2 SNP rs3738401. The normal cell line (74) is homozygous GG for SNP rs3738401 and as such only the G allele is detected. However, it is clear that both alleles produce a transcript in the translocation carrying cell line (94) as both A and G SNP alleles are clearly visible in the chromatogram. This region containing the SNP is blow up on the right as indicated by the arrows. This data is published in *Millar et al. 2005b*.

3.3 Real-Time PCR reports a reduction in *DISC1* transcription in cell lines possessing the t(1;11) translocation

3.3.1 DISC1 primer design

Quantitative Real-Time PCR (qRT-PCR) was carried out to determine the relative transcript abundance in translocation carriers compared to normal karyotype controls. Primer pairs for *DISC1* qRT-PCR were designed within exon 2, spanning exons 4-6, within exon 9 and spanning exons 11-12. Figure 3.3.A outlines the location of these primers and the specific transcripts targeted by each pair. In brief, primers from exon 2 and exons 4-6 were used to amplify *DISC1* sequence proximal to the breakpoint region. These will detect transcription from the non-translocated *DISC1* allele and also any C-terminally truncated or fusion transcripts produced from the derived *DISC1* allele on the derived 1 chromosome. Primers within exon 9 and exons 11-12 will amplify sequences distal to the translocation breakpoint, which includes transcripts from the non-translocated *DISC1* allele and any N-terminally truncated or fusion transcripts from the derived 11 chromosome.

3.3.2 SYBR green Real-Time PCR design and optimisation

SYBR green Real-Time PCR uses DNA binding dye chemistry during PCR amplification to quantify the relative transcript abundance. SBYR green is a non-sequence specific intercalating agent similar to ethidium bromide which emits a strong fluorescent signal when it becomes incorporated into double stranded DNA (*Morrison et al. 1998*). Incorporation of SYBR green during PCR can be used as a measure of the amount of transcript being amplified. PCR primers designed for non-quantitative standard PCR techniques are compatible with this type of qRT-PCR unlike Taqman technology (Applied Biosystems) which requires specific probes. The disadvantage of SYBR green qRT-PCR is that optimisation of primers is required on each template that is to be amplified. This is due to the fact that each primer pair will amplify DNA with different efficiencies. Primer pairs are described as being 100% efficient if amplification is exponential. However, few primers will truly amplify all templates in every cycle. To calculate individual primer pair efficiencies, standard

curves were constructed using a 4 point dilution curve (1 in 10 dilution series). The cDNA used to construct standard curves was a pooled cDNA sample consisting of translocation carriers and normal karyotype cDNA. Ideally primers should be at least 90% efficient and replicate samples should have a correlation coefficient greater than 0.99.

Another area of concern when using DNA binding dyes such as SYBR green is that these dyes can bind to non-specific amplicons in addition to primer dimers and these will also emit fluorescent signals. It is necessary to ensure that this non-specific fluorescence is not confused for a specific signal. To control for this, melt curve (a.k.a. dissociation curve) analysis was carried out after each amplification. If the products are specific they should have the same melting temperature and this can be seen using melt curve analysis. An example of a melt curve plot is shown in figure 3.3.B. Primer dimers, contaminating DNA and non-specific products are easily detectable if they exist. PCR products were also routinely checked by agarose gel electrophoresis to ensure specificity of the reactions.

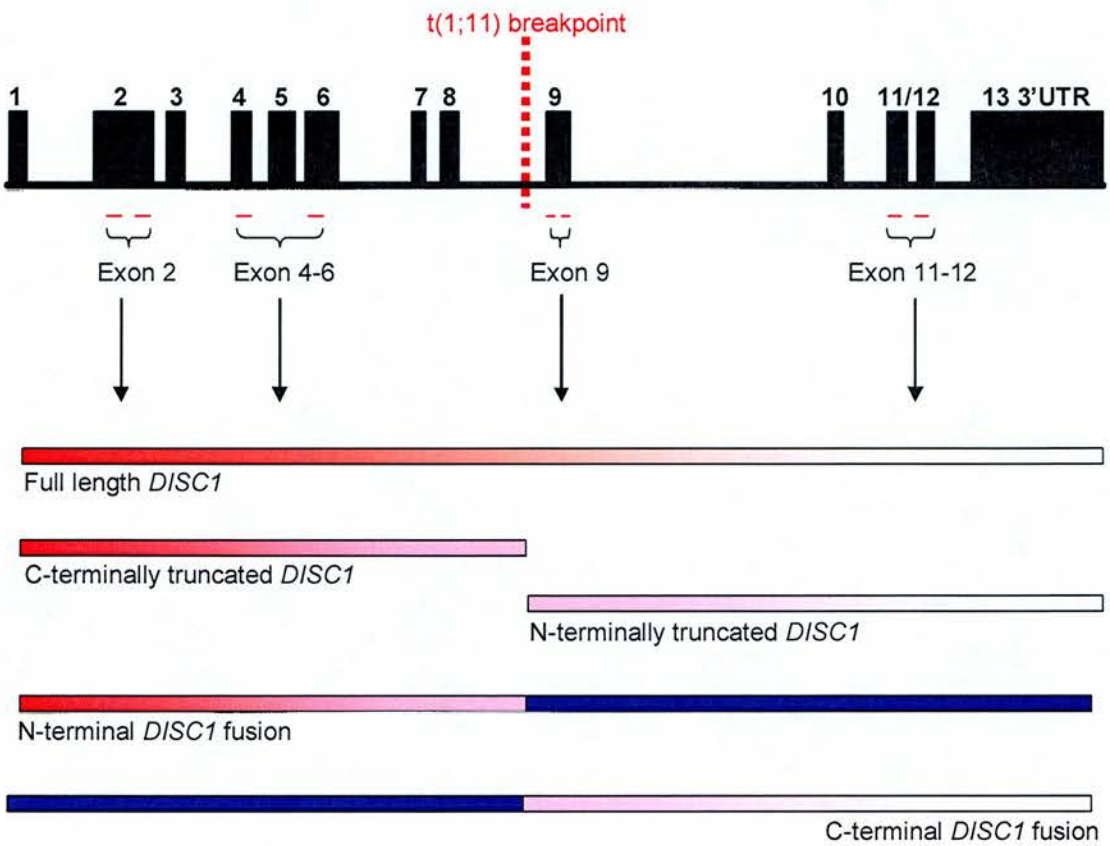

Figure 3.3.A. This diagram shows the location of *DISC1* primers used for quantitative Real-Time PCR to determine the relative expression of transcripts in t(1;11) cell lines with and without the translocation.

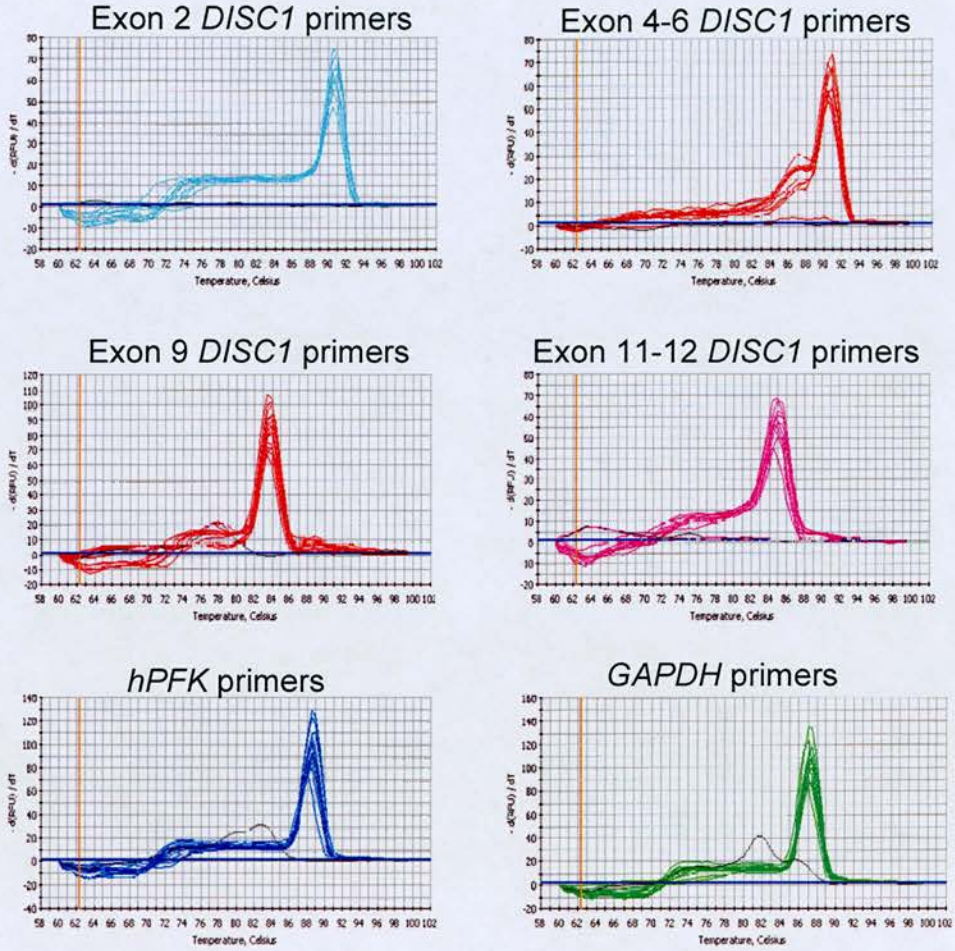

Figure 3.3.B. Melt curve plots of qRT-PCR primers are shown. Negative controls are indicated in black and experimental samples are represented using coloured lines. Specificity of primers is determined by analysing the peaks of the melt curve, which will be identical for specific products. Peak height is an indication of relative transcript abundance and does not correlate to specificity however non-specific products generally produce lower peak heights.

3.3.3 Relative quantification of DISC1 mRNA levels in t(1;11) lymphoblastoid cell lines

RNA was extracted from lymphoblastoid cell lines, DNase treated and complementary DNA (cDNA) synthesised under sterile conditions. All cDNAs were tested for contaminating genomic DNA before use in qRT-PCR applications (see chapter 2). A panel of cell lines derived from t(1;11) translocation carriers and their karyotypically normal relatives were examined for their relative levels of *DISC1* transcripts. At least two independent RNA samples were used to make cDNA. *DISC1* levels were determined both proximal and distal to the translocation using two sets of primers in each case. Two housekeeping genes were used to normalise cDNA levels between preparations, *Glyceraldehyde-3-phosphate dehydrogenase* (GAPDH) and *Human Phosphofructokinase* (hPFKm). Relative levels of *DISC1* were calculated using the Gene Expression Macro™ (Bio-Rad Laboratories Ltd.). Algorithms are derived from *Vandesompele et al.* 2002 and also from the geNorm website. This macro performs calculations similarly to the delta-delta CT method modified to incorporate differences in primer efficiencies using the Pfaffl equation (*Livak and Schmittgen, 2001, Pfaffl et al.* 2001). The methodology is outlined in box 3.3.C.

Using SYBR green qRT-PCR, *DISC1* is seen to be dramatically reduced in translocation carriers compared to karyotypically normal cell lines (Figure 3.3.D I-III). This reduction is apparent using primers located in exon 2, exon 4-6 and exon 11-12. The differences in expression between translocation carriers and normal karyotype controls are significantly different for primers located in exon 2 (**$p<0.01$) and for primers spanning exon 4-6 (**$p<0.01$) of the *DISC1* gene. P values were calculated by a two-tailed t-test using mean expression values for each cell line. Statistical analysis was performed using the Prism software (GraphPad Software, Inc.).

Box 3.3.C. Methodology for calculating relative gene expression values

After Real-Time PCR amplification each product amplified is assigned a cycle threshold value. This represents the PCR cycle number at which a particular sample crosses a defined threshold level. The cycle threshold value is inversely correlated to transcript abundance (i.e. high abundance transcripts will have a lower cycle threshold than low abundance transcripts). This value is termed a Ct value and is used to calculate the relative abundance of each transcript as detailed below.

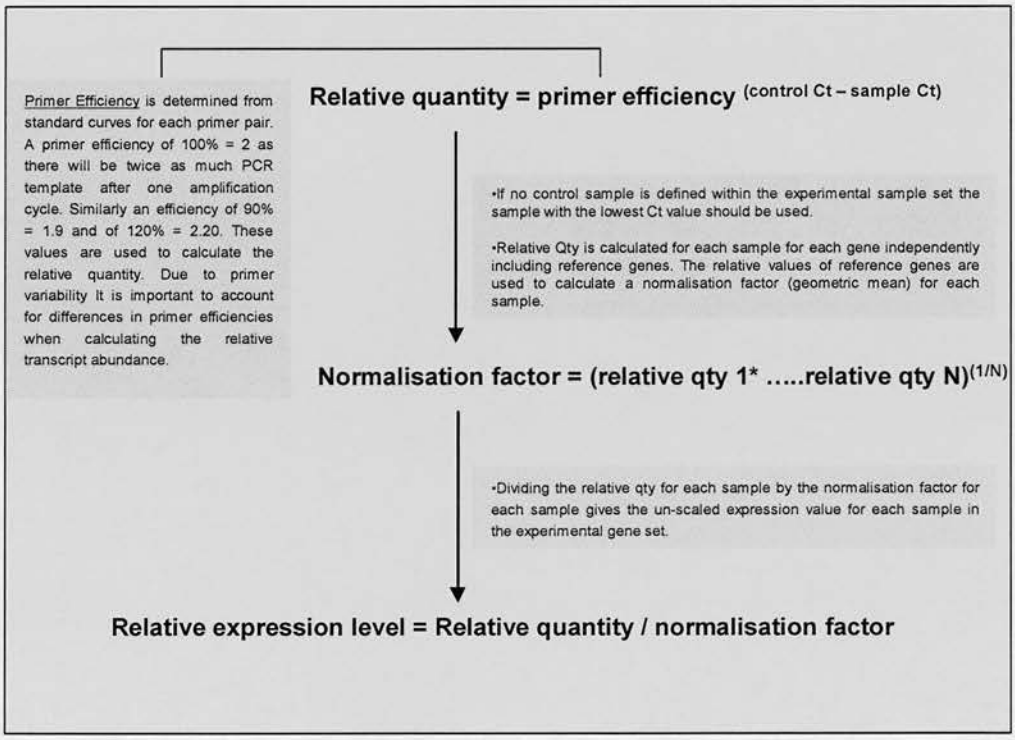

The relative *DISC1* expression values were not as well correlated for primers spanning exon 11-12. These primers are located close to the 3'UTR of *DISC1* and there was difficulty amplifying the 3' end of the gene. These primers were therefore more difficult to optimise than primers located more N-terminally and required more cDNA template per reaction. However running end-point qRT-PCR products on agarose gels revealed that *DISC1* transcripts are less abundant in translocation carriers than normal karyotype controls, which is in agreement with primers located proximal to the translocation breakpoint (Figure 3.3.D (III)).

In contrast, primers designed within exon 9 of *DISC1* (i.e. distal to the breakpoint) appeared to indicate an up-regulation of transcription in some t(1;11) cell lines carrying the translocation suggesting the possibility of transcription from the derived chromosome 11 (Figure 3.3.E). This data was not significant ($p>0.05$, two-tailed t test) due a significant difference in the variance of each data set. On examining the breakpoint region of chromosome 11 using the UCSC genome browser however three novel expressed sequence tags (ESTs) were found. Two of these ESTs overlap the breakpoint region and are in the correct orientation to elicit transcription of derived *DISC1* sequences (Figure 3.4.A (I)). Albeit, this result is not supported by primers spanning exon 11-12, which are also distal to the breakpoint. It is unlikely therefore that this transcript, if real, extends as far as translocated 3'UTR sequence of *DISC1*. For this reason the possibility of a stable N-terminally truncated *DISC1* transcript or protein in t(1;11) cell lines is highly unlikely but remains to be investigated.

There is one other possibility which could account for this apparent transcriptional up-regulation immediately distal to the breakpoint region. The primers within exon 9 of *DISC1* are also within the known *DISC2* sequence, which overlaps *DISC1* in the reverse orientation, therefore these primers could be detecting transcription of *DISC2* sequence from the derived chromosome 11. Although this has not been formally tested future work will incorporate experiments to analyse this.

In summary, *DISC1* levels in t(1;11) cell lines possessing the translocation are dramatically reduced in comparison to cell lines possessing a normal karyotype. This is supported by qRT-PCR data using two primer pairs proximal to the translocation breakpoint and one primer pair distal to the breakpoint. However, one primer set, located distally in exon 9 of *DISC1*, shows apparent up-regulation of *DISC1* sequences in some translocation carriers compared to controls. This could be explained by *DISC1* transcription initiated from the derived 11 chromosome which terminates before the derived *DISC1* 3'UTR, but perhaps more likely reflects transcription of the anti-sense gene *DISC2* from the derived chromosome 11.

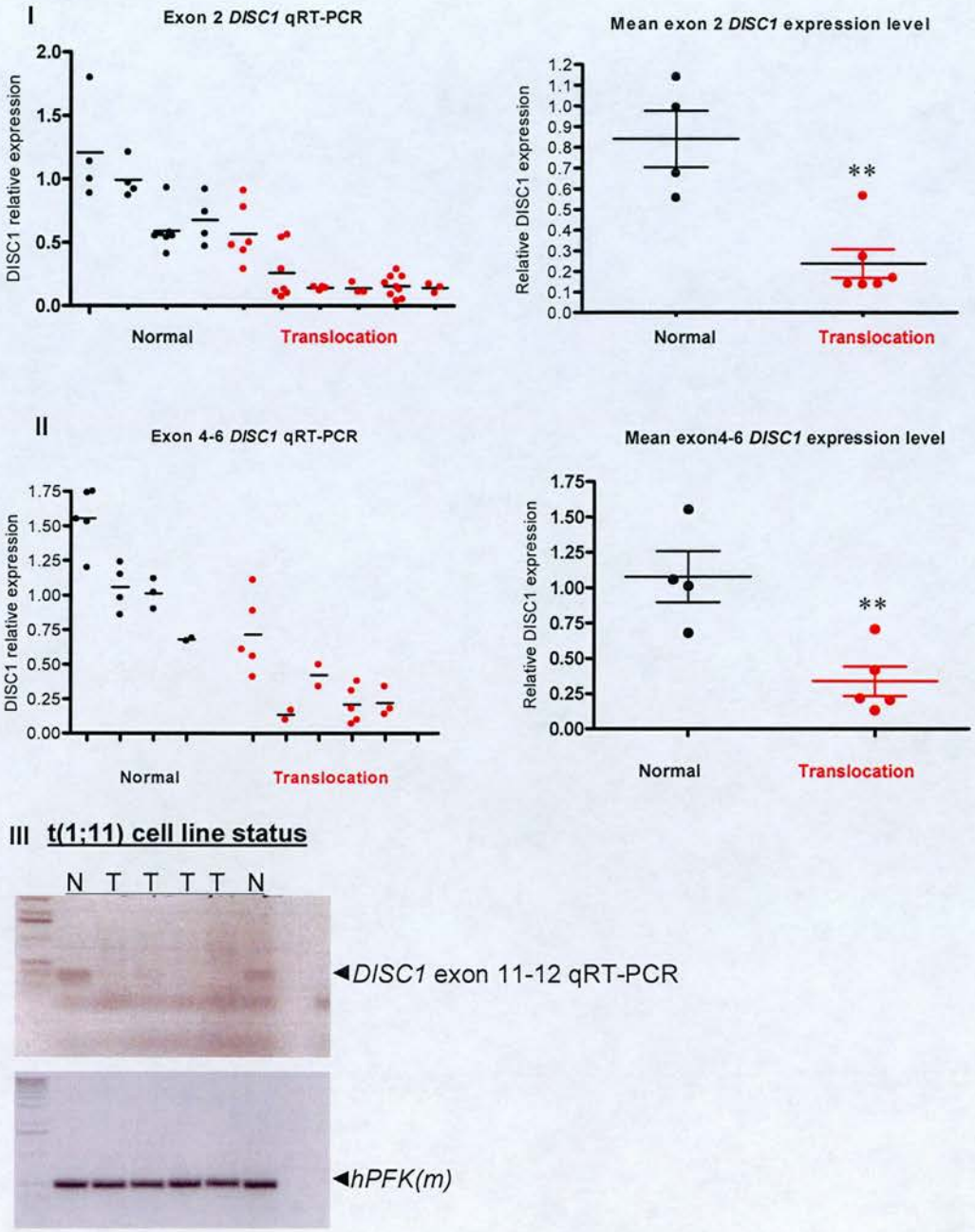

Figure 3.3.D. This figure shows quantitative Real Time PCR *DISC1* expression data from t(1;11) cell lines. *DISC1* expression levels are compared between translocation carriers (red) and normal karyotype controls (black). Primer proximal to the t(1;11) breakpoint show a reduction in *DISC1* expression levels (I and II). Scatter plots in the left panel indicate individual cell lines with replicate values for each and graphs in the right panel show the group mean and SEM for translocation and control cell lines. This reduction in *DISC1* expression reaches significance as determined by a two-tailed t-test, **p<0.01 (GraphPad Prism). Primers spanning exon 11-12, distal to the t(1;11) breakpoint, also support this data showing a reduction in *DISC1* expression in translocation carriers as seen by agarose gel electrophoresis following qRT-PCR (III).

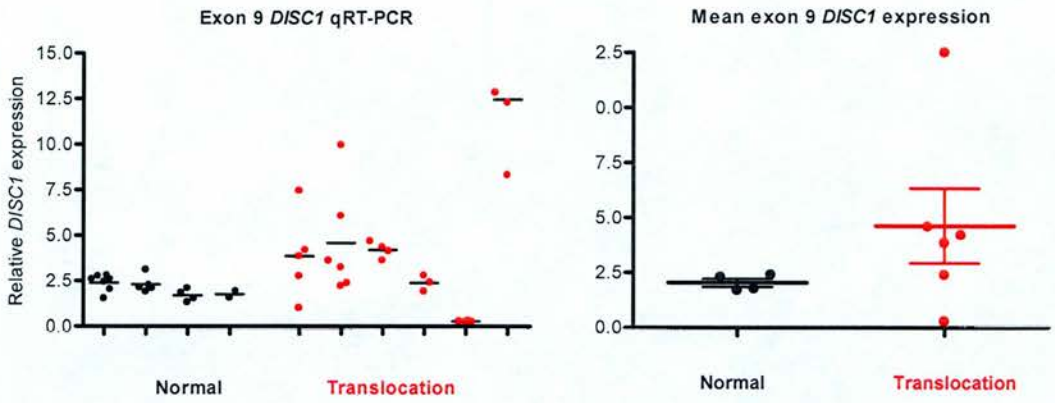

Figure 3.3.E. This figure shows *DISC1* qRT-PCR data using SYBR green Real-Time PCR. *DISC1* expression was compared between t(1;11) cell lines possessing the translocation and normal karyotype controls. Exon 9 *DISC1* primers are located distal to the translocation breakpoint. The scatter plot on the left shows the individual cell lines with replicate values for each and the scatter plot on the right shows the group mean and SEM for translocation and control cell lines. This data indicates up-regulation of *DISC1* expression in some translocation carrying cell lines suggesting there may be possible transcription of *DISC1* sequences on the derived 11 chromosome. This data is not significant due to the high variance of expression within the translocation data set.

3.4 The derived chromosome 11 is unlikely to support *DISC1* transcription and translation

In light of the apparent up-regulation of transcription distal to the breakpoint it is necessary to examine the chromosome 11 breakpoint region in detail. The three novel ESTs found in this region are all orientated towards the centromere and thus have the potential to elicit transcription of derived *DISC1* sequences (Figure 3.4.A (I)). If *DISC1* sequence is transcribed in this region it could hypothetically produce an N-terminally truncated DISC1 protein isoform provided it is in frame with the existing EST sequence.

Conceptual translation studies were carried out *in silico* on juxtaposed *DISC1*-chromosome 11 EST sequences using the SIXFRAME translation programme (SDSC Biology Workbench). This programme translates nucleic acid sequences to produce six translations. The programme produces three forward translation frames beginning in the first frame with the first nucleotide of the start codon and then beginning with the second and then third nucleotide in the subsequent frames. Similarly it produces three translations using the reverse sequence. These sequences can then be exported for further analysis using protein analysis software.

Using this programme, *DISC1*-chromosome 11 EST fusion sequences produced an open reading frame of 268 amino acids in length when *DISC1* was fused to EST CK000409 (Figure 3.4.A (II)). This open reading frame possesses the final two coiled coil domains of DISC1. This region of the protein has been reported to be responsible for interactions with NUDEL and LIS1 (*Ozeki et al.* 2003, *Morris et al.* 2003, *Brandon et al.* 2004). If translated, this could result in a DISC1 protein missing the N-terminal region, but potentially possessing the ability to bind to NUDEL and LIS1.

DISC1 is a multi-compartmentalised protein. The N-terminal globular domain directs sub-cellular localisation to the nucleus, mitochondria and cytoplasm (*Ozeki et al.* 2003, *Millar et al.* 2005a). If this hypothetical N-terminally truncated sequence were

translated, an abnormal protein possessing some of the functional capacity of WT DISC1 without its ability to localise correctly could be produced.

However, this scenario is considered unlikely for the following reasons. The penultimate coiled coil domain of DISC1 is encoded by exon 9, for which qRT-PCR data suggested an up-regulation in translocation cell lines, but the last coiled coil domain of DISC1 is encoded by exons 11 and 12 and qRT-PCR in this region does not support the theory of *DISC1* transcription from chromosome 11. Therefore if *DISC1* sequences are transcribed from chromosome 11 they are unlikely to extend as far as exon 11-12 before terminating. Therefore the translocated *DISC1* sequence is not likely to be in frame with these ESTs. Nonetheless it is still desirable to demonstrate the absence of such a truncated protein by examining DISC1 protein lysates from normal and translocation carrying t(1;11) cell lines.

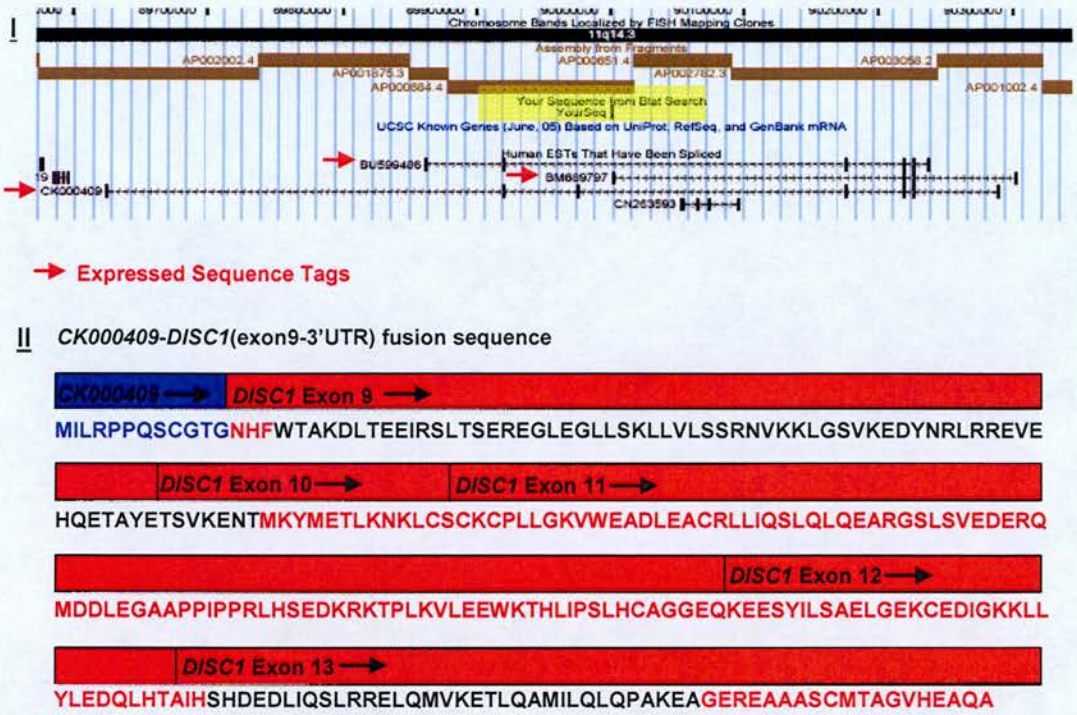

Figure 3.4.A. Examination of the breakpoint region on chromosome 11 revealed three novel EST sequences correctly orientated to elicit transcription of derived *DISC1* sequence **(I)**. Translation studies using SIXFRAME suggest there is a possibility of a 268 amino acid open reading frame (ORF) derived from fused sequences of CK000409 and *DISC1*. If translated this ORF would possess two of DISC1's coiled coil interaction domains **(II)**. CK000409 sequence is shown in dark blue, DISC1 sequence is shown in red, with the coiled coil domains marked in black.

3.5 There are no detectable truncated *DISC1* isoforms in cell lines possessing the t(1;11) translocation

3.5.1 One Dimension SDS-PAGE does not detect abnormal DISC1 protein isoforms

The existing DISC1 expression data from t(1;11) family members has focused solely on the hypothetical C-terminally truncated DISC1 isoform for the valid reason that over-expression of C-terminally truncated DISC1 constructs have been shown to have detrimental effects on neurite outgrowth and neuronal migration (*Ozeki et al.* 2003, *Kamiya et al.* 2005). Current data reports a reduction in DISC1 protein levels in translocation carriers compared to non-translocation cell lines (*Millar et al. 2005b*). One-dimension SDS-Polyacrylamide gel electrophoresis (SDS-PAGE) using an antibody designed to the N-terminus of DISC1 (R47, see Figure 3.5.A) reports a reduction in the three alternatively spliced DISC1 isoforms of approximately 71-80kDa in size. Furthermore, studies of a natural polymorphism in mouse *Disc1* resulting in a premature stop codon in exon 7 resulting in a truncated *Disc1* allele demonstrated that although *Disc1*transcript abundance is not altered the predicted C-terminally truncated protein is not detected suggesting instability of this protein (*Koike et al.* 2006). One caveat to this study is that an uncharacterised *Disc1* antibody was used and therefore further evidence is needed to substantiate these findings.

Therefore current data does not support the existence of a human C-terminally truncated DISC1 isoform in t(1;11) family members. The predicted molecular weight of this truncated protein is approximately 75kDa. The signal may therefore be masked by wild-type DISC1 isoforms. Moreover the *Millar et al 2005b.* study has not addressed the question of an N-terminally truncated DISC1 protein that may be produced from the derived chromosome 11 or the existence of potential t(1;11) fusion proteins. Consequently more evidence is needed to support the current hypothesis of haploinsufficiency within the t(1;11) family.

To further address this issue one (1D) and two (2D) dimension SDS-PAGE was performed on lysates from t(1;11) lymphoblastoid cell lines using N-terminal and C-terminal DISC1 antibodies to determine the presence or absence of aberrant DISC1 protein isoforms.

Lysates from normal and translocation carrying cell lines were initially analysed by 1D western blotting using a C-terminal DISC1 antibody (*Ogawa et al. 2005*). This antibody detects full length DISC1 and the long variant DISC1 isoform at approximately 93-100kDa (Figure 3.5.A). As this antibody is designed to the C-terminus it should detect any abnormal DISC1 isoforms produced from the derived 11 chromosome. Using this antibody there were no detectable N-terminally truncated DISC1 isoforms in t(1;11) translocation carriers (Figure 3.5.B).

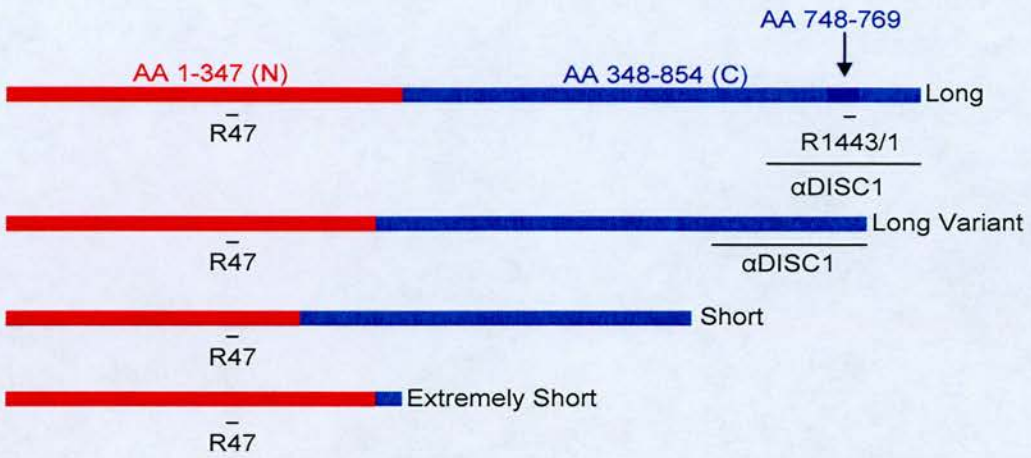

Figure 3.5.A. This figures shows the locations of antibodies used to analyse t(1;11) lysates by one and two dimension SDS-PAGE followed by western blotting.

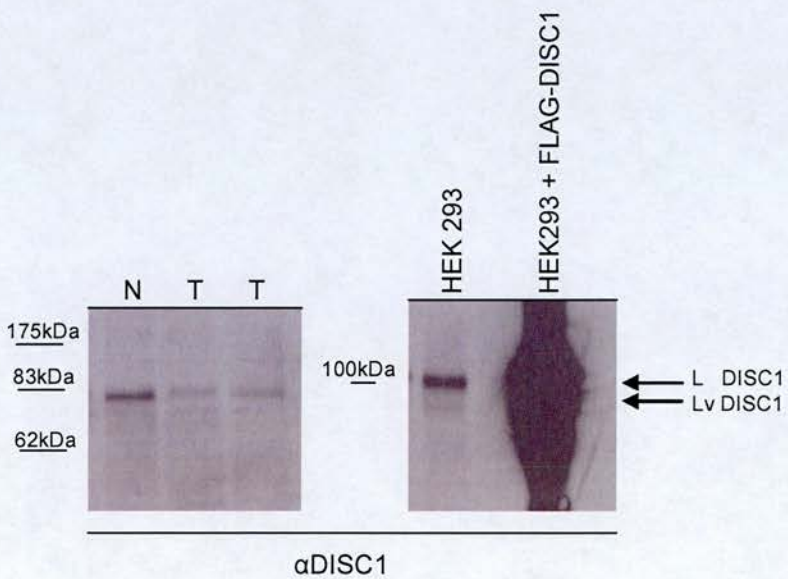

Figure 3.5.B. This figure shows lysates from t(1;11) cell lines probed using DISC1 C-terminal antibody αDISC1. N = Non-translocation/Normal cell lines, T = Translocation carrying cell lines. There are no N-terminally truncated isoforms detected by one dimension SDS-PAGE. Antibody specificity is indicated in the right panel by probing endogenous DISC1 and FLAG-tagged DISC1 over-expressed in HEK293 cells.

3.5.2 Two Dimension SDS-PAGE does not detect abnormal DISC1 protein isoforms

Analysis of DISC1 protein isoforms was further examined using a two-dimension SDS-PAGE system (2D-PAGE). This system will address the presence of a C-terminally truncated DISC1 isoform or DISC1 fusion proteins possessing the C-terminal region in t(1;11) cell lines. While the C-terminally truncated isoform may be too similar in size to wild-type DISC1 isoforms to be resolved by one-dimension SDS-PAGE, two-dimension SDS-PAGE resolves proteins based on their isoelectric point and size, therefore it has the power to resolve proteins with similar molecular weights.

Lymphoblastoid lysates from t(1;11) family members were analysed by western blotting using N-terminal and C-terminal DISC1 antibodies R47 (original antibody used by *Millar et al. 2005b*) and αDISC1 respectively. Figure 3.5.C presents the results of 2D western blots using these antibodies. R47 detects three specific protein spots by 2D western blotting. Two spots are approximately 75kDa in size and are likely to correspond to DISC1 short isoforms. One protein spot is approximately 39kDa in size which could possibly represent the extremely short DISC1 isoform (*James et al. 2004*). C-terminal αDISC1 detects one additional protein spot at approximately 100kDa; this is likely to represent the Long or Long Variant DISC1 isoform. There is no difference in DISC1 isoforms present in t(1;11) cell lines possessing the translocation and those possessing a normal karyotype.

In summary the N-terminal DISC1 antibody R47 does not detect a C-terminally truncated DISC1 isoform by 1D or 2D SDS-PAGE in lymphoblastoid cell lines possessing the t(1;11) translocation. 1D analysis using the αDISC1 C-terminal antibody corroborates this data. Subsequent 2D SDS-PAGE using αDISC1 shows similar DISC1 isoforms are present in translocation cell lines as in those possessing a normal karyotype. There is no evidence therefore for the existence of DISC1 truncated isoforms as a result of the t(1;11) translocation.

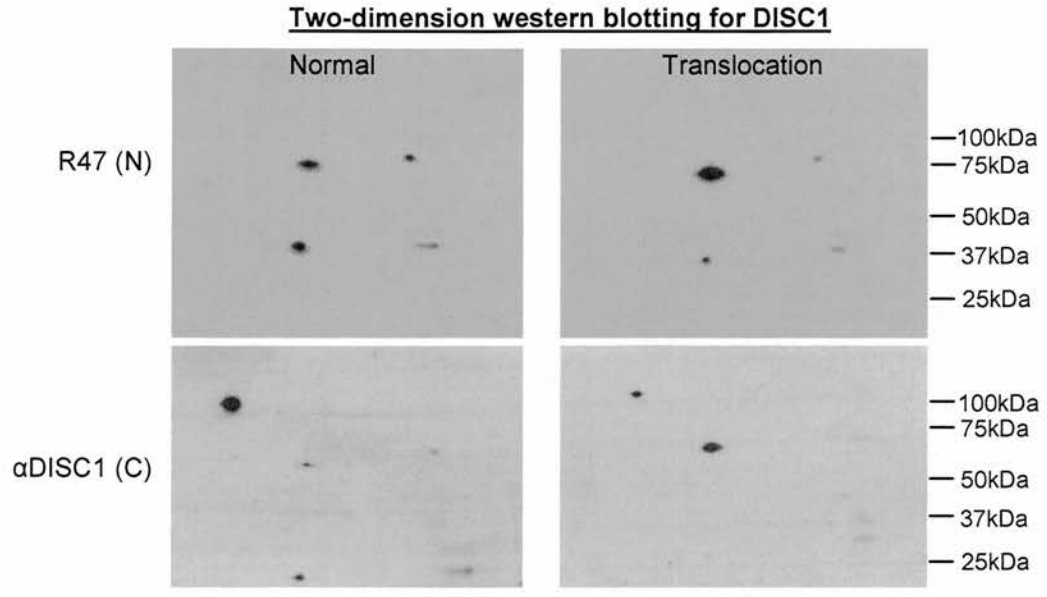

Figure 3.5.C. T(1;11) lysates were probed using N-terminal DISC1 antibody R47 and C-terminal antibody αDISC1. No N-terminally or C-terminally truncated DISC1 isoforms are detected by two dimension SDS-PAGE. Antibody R47 detects three spots, two of ~75kDa in size, likely to represent DISC1 short (S) isoforms, and one of ~39kDa which possibly represents the extremely short (Es) DISC1 isoform. αDISC1 detects an additional spot of ~100kDa, likely to represent either L or Lv DISC1. With the exception of one of the 75kDa isoforms all isoforms appear to be expressed at reduced levels in translocation carrying cell lines.

3.6 Discussion

The data presented in this chapter aims to shed light on the mechanism of disease pathogenesis in carriers of the t(1;11) translocation. The main competing hypotheses for disease pathogenesis in this family are one of haploinsufficiency for DISC1 versus the production of an abnormal truncated DISC1 protein with detrimental effects on the cell. When cDNAs designed to express the hypothetical truncated DISC1 protein are over-expressed many adverse effects at the level of neuronal migration and neurite outgrowth have been seen (*Kamiya et al. 2005, Ozeki et al. 2003*). As a result of this work this C-terminal DISC1 truncation has been termed in some cases the 'disease mutant form of DISC1' (*Ozeki et al* 2003). While there is no disputing the phenotypic consequences, it must be remembered that there has been no human truncated DISC1 isoform detected in the translocation carriers from the t(1;11) family. Therefore as far as human disease pathogenesis is concerned the involvement of a C-terminal truncated DISC1 isoform is purely speculative. Until direct evidence for this protein is observed this protein remains hypothetical. It is also noted that evidence for a reduction is DISC1 protein synthesis in t(1;11) translocation carriers has been reported and therefore the only direct evidence to come from the t(1;11) family supports a haploinsufficiency disease model (*Millar et al. 2005b*). This evidence is however limited and alone cannot rule out the presence of abnormal truncated/fusion proteins.

In order to address these issues an extensive study of *DISC1* expression was undertaken using lymphoblastoid cell lines derived from t(1;11) family members. This data reports transcription from the derived *DISC1* allele on chromosome 1. This transcription however is unlikely to produce a stable transcript as overall *DISC1* mRNA levels are significantly reduced in translocation carriers compared to normal karyotype controls (a subset of this data is published in *Millar et al. 2005b*). This data suggests that transcripts produced from the derived *DISC1* allele are likely to be subject to cellular surveillance mechanisms and subsequently degraded.

Primers located distal to the breakpoint spanning exons 11-12 corroborate this data however one primer pair located distally, within exon 9, shows conversely that some

t(1;11) translocation carriers possess more transcripts than normal cell lines. Although further evidence is needed to support this up-regulation, this could potentially be due to either amplification of *DISC2* sequences (which also overlaps this region of *DISC1* in anti-sense orientation) or *DISC1* transcription from the derived allele on chromosome 11. It is considered likely that this up-regulation is a result of transcription of *DISC2* from the derived chromosome 11 for the following reasons.

Examination of the chromosome 11 breakpoint region revealed novel ESTs with the potential to drive transcription of *DISC1*. However, as the second set of distal *DISC1* primers (exon11-12) showed a reduction in *DISC1* levels in t(1;11) carriers, this transcription does not extend to the translocated 3' *DISC1* sequence. This suggests that the translocated sequence may be out of frame with chromosome 11 juxtaposed sequence, consequently producing a premature stop codon. Furthermore, it is highly unlikely, that even if this transcript does exist, that this sequence would produce a stable protein. To this end the absence of truncated/fusion DISC1 isoforms has been confirmed by 1D and 2D SDS-PAGE which detects no abnormal DISC1 protein isoforms within translocation carrier cell lines. In conclusion the data presented in this chapter supports a disease model of haploinsufficiency for DISC1 as the most likely cause of illness in carriers of the t(1;11) translocation. This haploinsufficiency is most probably a result of cellular surveillance mechanisms which degrade abnormal *DISC1* transcripts.

However, the *DISC2* gene is also disrupted by this translocation, and stable transcripts may be produced from the derived *DISC2* allele. As the function of the *DISC2* gene is currently unknown we can only speculate as to what consequences disruption of this gene may have. *DISC2* represents a putative non-coding RNA gene antisense to *DISC1* which may have a role in regulating *DISC1* expression. It is important therefore to understand the consequences of the t(1;11) translocation on *DISC2* gene expression in addition to studying *DISC1*. Gene expression analysis of *DISC2* in t(1;11) family members has been carried out and the data are presented in chapter 8.

Chapter 4

Isoform specific enrichment of DISC1 at the centrosome

4.1 Preface

Functional studies of the DISC1 protein suggest that it occupies multiple sub-cellular locations and interacts with multiple protein partners. DISC1 has been reported to localise to the nucleus, cytoplasm, mitochondria and centrosome (Table 4.1.A). This chapter aims to shed some light on the multiple locations of the DISC1 protein by examining isoform specific protein expression in mammalian cells, focusing on DISC1 at the centrosome.

DISC1 has been shown to bind various centrosomal proteins including NUDEL, LIS1 and Kendrin/PericentrinB (see introductory section) therefore studies demonstrating DISC1 occupation at the centrosome are not surprising. Three studies using exogenous over-expressed tagged DISC1 have shown co-localisation to the centrosome (*Morris et al. 2003, Miyoshi et al. 2004, and Millar et al. 2005a*). All three studies utilise γ-tubulin as a marker of centrosome position. Taken together these studies have shown that SH-SY5Y (human neuroblastoma) cells, COS7 (African green monkey) cells and HeLa (human epithelial) cells exhibit DISC1 immunoreactivity at the centrosome.

It is possible that over-expressing DISC1 at high levels may alter the sub-cellular distribution profile. Furthermore, using bulky tags such as GFP to label the protein may hamper localisation to the correct sub-cellular compartment. For these reasons studies of the endogenous protein are important to substantiate these findings. Two studies examining endogenous DISC1 sub-cellular distribution refute the findings of these over-expressing studies. *Brandon et al. 2004* reported that although endogenous DISC1 does interact with the centrosomal proteins LIS1 and NUDEL, it does not localise to the centrosome. This was demonstrated by non overlapping immunoreactivities of endogenous DISC1 and γ-tubulin in SH-SY5Y cells. *James et*

al. 2004 also support this finding that endogenous DISC1 and γ-tubulin do not co-localise.

There is however one recent study which does support endogenous DISC1 localisation at the centrosome. *Kamiya et al. 2005* reported endogenous DISC1 to be co-localised with γ-tubulin and an additional centrosomal protein LIS1 in COS7 cells and mouse cortical neurons.

One complication with these studies of endogenous DISC1 is that all three studies utilised different antibodies to detect the protein. *James et al. 2004* used two DISC1 antibodies, one designed to the N-terminus of DISC1, R47, and a C-terminal antibody R1443/1. These antibodies are known to detect distinct DISC1 isoforms (*James et al. 2004*). Brandon *et al. 2004* used a C-terminal DISC1 antibody (D26). The R47 N-terminal antibody detects all DISC1 isoforms, R1443/1 detects major DISC1 isoforms of 100kDa and 75kDa whereas antibody and D26 detects a 95kDa DISC1 isoform (*James et al. 2004, Brandon et al. 2004*). Sub-cellular localisation studies have shown that the N-terminal antibody, R47, detects DISC1 at the mitochondria in SH-SY5Y (*James et al. 2004*). The C-terminal antibody R1443/1 detects DISC1 at the mitochondria and additionally within the cytoplasm in SH-SY5Y cells whereas the C-terminal antibody D26 detects DISC1 mainly in the perinuclear region in this same cell type (*James et al. 2004, Brandon et al. 2004*). Furthermore DISC1 R47 has been shown to co-localise with specific mitochondrial markers (*James et al. 2004, Brandon et al.* 2005) whereas R1443/1 and D26 detect additional DISC1 isoforms associated with cytoskeletal markers (*James et al. 2004, Brandon et al. 2004*). It is likely to be the case that the R47, D26 and R1443/1 antibodies are detecting isoform specific localisation of DISC1 to different sub-cellular compartments. It is clear from these experiments that the sub-cellular distribution pattern of DISC1 is complex; however none of these antibodies detect DISC1 at the centrosome.

In the *Kamiya et al.* study, which did report DISC1 localisation at the centrosome, the authors have not specified which antibody has been used to detect DISC1 so we cannot be sure which DISC1 isoforms this antibody is detecting.

Acquisition of a new C-terminal antibody (αDISC1, see table 2.7) has enabled me to address this issue of DISC1 sub-cellular localisation further. These experiments utilise immunofluorescent techniques in combination with sub-cellular fractionation to address the issue of isoform specific localisation of DISC1 at the centrosome.

Table 4.1 DISC1 sub-cellular localisation in mammalian cells

Study	Antibody / Tag	Cell Model	Source DISC1	DISC1 Sub-cellular Localisation
Ozeki et al. 2003	N-terminal / C-terminal	Hela*	Endogenous	Mitochondria (unpublished observation)
		PC12* undifferentiated		Cytoplasm (cell body)
Miyoshi et al. 2003	C-terminal	SK-N-SH*	Endogenous	Cytosol (perinuclear)
Morris et al. 2003	FLAG tag	NT2N*	Exogenous	Cytoplasm Centrosome
	GFP tag	SH-SY5Y*		
Miyoshi et al. 2004	GFP tag	SH-SY5Y	Exogenous	Cytosol (perinuclear) Centrosome
		Hela		
Brandon et al. 2004	C-terminal D26 and D27	SH-SY5Y	Endogenous	Cytoplasm (perinuclear)
		Mouse Cortical Neuron		
James et al. 2004	R47 N-terminal	U373 MG*	Endogenous	Mitochondria
		SH-SY5Y		
James et al. 2004	R1443/1 C-terminal	U373 MG	Endogenous	Mitochondria, Cytoplasm and Nucleus
		SH-SY5Y		

Continues onto next page

Study	Antibody / Tag	Cell Model	Source DISC1	DISC1 Sub-cellular Localisation
Brandon et al. 2005	N-terminal R47	SH-SH5Y	Endogenous	Mitochondria
	GFP	Hela	Exogenous	Cytoplasm
Kamiya et al. 2005	Not Available	COS 7*	Endogenous	Centrosome
		Rodent cortical Neurons		
Ogawa et al. 2005	FLAG	SH-SY5Y	Exogenous	Cytoplasm
	C-terminal αDISC1	SH-SY5Y	Endogenous	Cell body, neurites and nucleus
Millar et al. 2005	V5 tag	COS7	Exogenous	Cytoplasm, nucleus, mitochondria and centrosome
J. Chubb Unpublished	R47 N-terminal	SH-SY5Y	Endogenous	Mitochondrial and centrosomal
J. Chubb Unpublished	αDISC1 C-terminal	HEK293 SH-SY5Y COS7	Endogenous	Centrosomal and cytoplasmic punctate

*SK-N-SH - Human Neuroblastoma / NT2N - Human neurons / SH-SY5Y - Human neuroblastoma / U373 - Human Glioblastoma / Hela = Human epithelial / PC12 – Rat Neuronal / COS 7 – African green monkey fibroblasts

Table 4.1.A This table summarises the current data on DISC1 sub-cellular localisation. The key beneath the table details the cell types used in each study.

4.2 Endogenous *DISC1* localises to the centrosome

4.2.1 *DISC1 Long and Long variant isoforms occupy cytoplasmic and centrosomal locations*

The C-terminal αDISC1 antibody exhibits a different affinity for DISC1 than either of the current in house antibodies R47 and R1443/1. *Ogawa et al.* showed that αDISC1 detects a DISC1 doublet at 100kDa and a single band at 80kDa by immunoblotting in SH-SY5Y cells (*Ogawa et al. 2005*). In my hands this antibody robustly detected the doublet at 100kDa and occasionally the 80kDa band. This doublet most likely represents the full length (L) and long variant (Lv) DISC1 isoforms. Although this antibody detects the two long DISC1 isoforms, as does the N-terminal R47 antibody, it does not detect the DISC1 triplet at ~75kDa that the R47 N-terminal antibody detects. It will be interesting therefore to compare the sub-cellular profiles of the isoforms detected using these two antibodies. This will allow us to determine if all DISC1 isoforms localise to similar sub-cellular compartments or if the longer isoforms exhibit different sub-cellular patterns to the shorter DISC1 isoforms.

HEK293 and SH-SY5Y cells were processed by immunofluorescence for DISC1 using αDISC1 and R47. In agreement with the differences in isoform specificity seen by immunoblotting, these antibodies detected DISC1 immunoreactivity at distinct sub-cellular locations. R47 detected DISC1 at the mitochondria as reported previously (*James et al. 2004)*. The C-terminal αDISC1 antibody however exhibited a very different pattern of localisation. This antibody did not exhibit a mitochondrial pattern of localisation but rather a punctate cytoplasmic distribution and a dense spot in the perinuclear region. On initial observation this perinuclear spot looked likely to correspond to either the golgi apparatus or the centrosome (Figure 4.2.A).

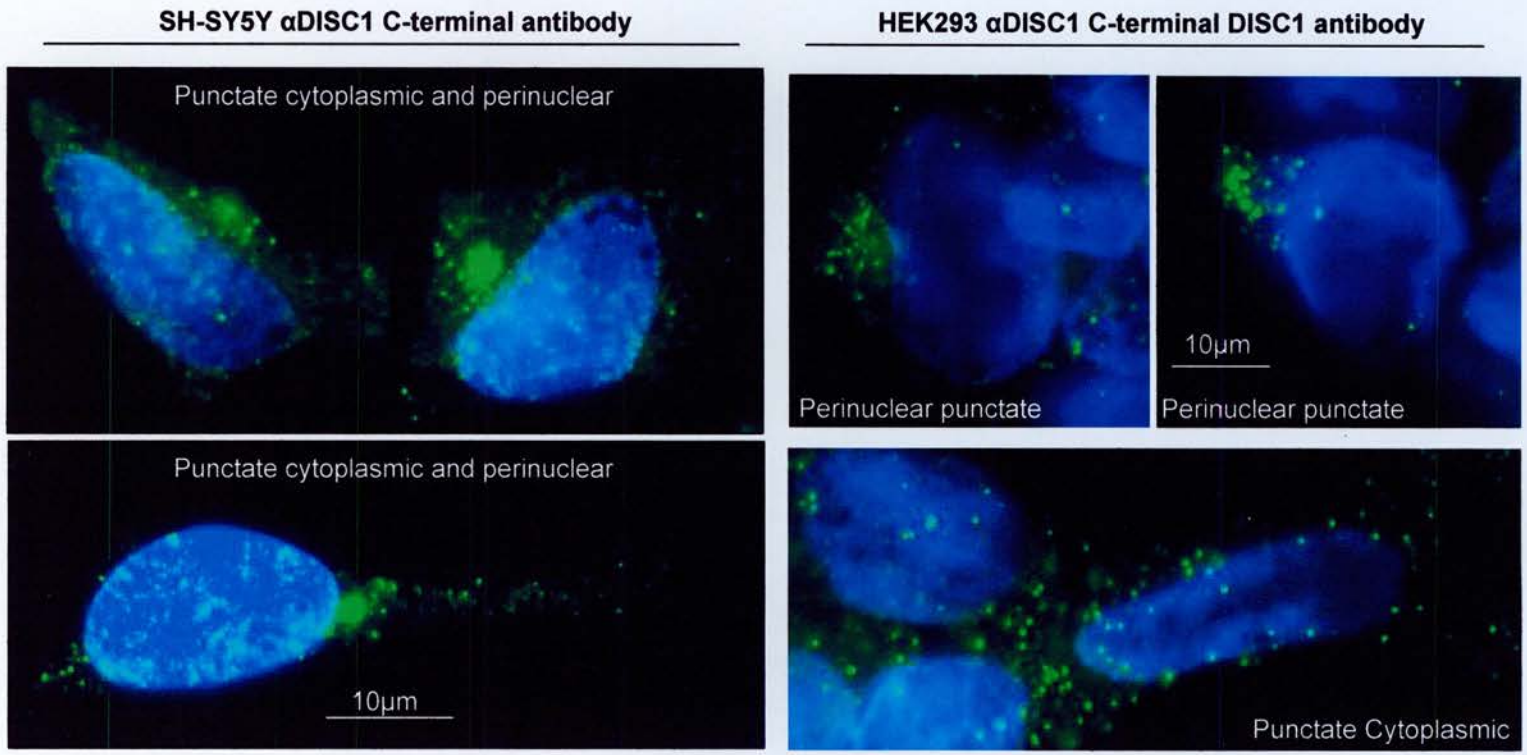

Figure 4.2.A. SH-SY5Y and HEK293 cells were processed by immunofluorescence using the αDISC1 C-terminal antibody (green). The left panel shows DISC1 sub-cellular distribution in SH-SY5Y cells. This antibody assumes a cytoplasmic punctate distribution with a dense perinuclear spot. HEK293 cells shown in the right panel also exhibit a punctate cytoplasmic distribution and some clear perinuclear staining. Images were taken at 100X magnification. Nuclei were DAPI stained (blue).

To examine this localisation further sub-cellular markers were employed. Mitochondrial marker cytochrome oxidase subunit II (MTCO2), Golgi matrix protein (GM130) and centrosome marker γ-tubulin were tested for co-localisation with DISC1. αDISC1 immunoreactivity was found to overlap with γ-tubulin in both SH-SY5Y and HEK293 cells, suggesting that this C-terminal antibody detects a centrosomal DISC1 isoform (Figure 4.2.B and Figure 4.2.C). In dividing SH-SY5Y cells αDISC1 assumes a clear centrosomal location at the poles of the mitotic spindle (Figure 4.2.C, lower panel). The DISC1 isoforms detected using the αDISC1 antibody are distinct from the major DISC1 isoforms detected using the DISC1 antibody R47 as they do not co-localise with the mitochondrial cytochrome oxidase subunit II (Figure 4.2.D, upper panel). DISC1 isoforms detected using the R47 antibody mainly co-localise with the mitochondria (Figure 4.2.D, lower panel); however a small amount of DISC1 detected using this antibody occupies a centrosomal location (Figure 4.2.E).

The golgi matrix protein, GM130, has previously been identified as a putative DISC1 interactor by yeast two-hybrid analysis (*Millar et al. 2003)*. GM130 showed no co-localisation with either R47 or αDISC1 (Figure 4.2.F (αDISC1/GM130), R47 data not shown).

Therefore, of the markers tested, the only sub-cellular marker seen to co-localise with C-terminal DISC1 antibody αDISC1 is the centrosomal marker γ-tubulin. To confirm this result an additional centrosomal marker was chosen. I decided to examine αDISC1 co-localisation with the centrosomal protein AKAP450 (also known as CG-NAP, AKAP350 or Yotiao) in SH-SY5Y cells. AKAP450 was chosen as it was identified previously as a putative DISC1 interactor by yeast two-hybrid analysis (*Millar et al. 2003*). Figure 4.2.G (A-D) demonstrates the presence of AKAP450 at the centrosome in SH-SY5Y cells. AKAP450 is known by many alternative names, including CG-NAP. It was named CG-NAP (Centrosome and Golgi PKN associated protein) because it can be associated with both the centrosome and golgi apparatus (*Takahashi et al. 1999*). Figure 4.2.H presents additional images of AKAP450 alongside images of GM130 in SH-SY5Y cells. AKAP450 and GM130

have distinct sub-cellular distribution patterns in this cell type. AKAP450 is localised at the poles of the mitotic spindle in dividing cells consistent with a centrosomal location. Furthermore AKAP450 is seen to co-localise with an additional centrosomal protein, Ninein, in SH-SY5Y cells (Figure 4.2.G (E-H)).

When SH-SY5Y cells were processed by immunofluorescence AKAP450 and αDISC1 immunoreactivity showed strong co-localisation at the centrosome further confirming the presence of DISC1 at the centrosome (Figure 4.2.I). Some additional co-localisation is seen within the cytoplasm as indicated by arrows in figure 4.2.I (image H). It is intriguing that these two proteins may interact in additional locations other than the centrosome. AKAP450 is an A Kinase Anchor Protein which functions to traffic Protein Kinase A (PKA) to the centrosome (*Keryer et al. 2003*). It is possible therefore that DISC1 interacts with this complex before or after it assumes its centrosomal location.

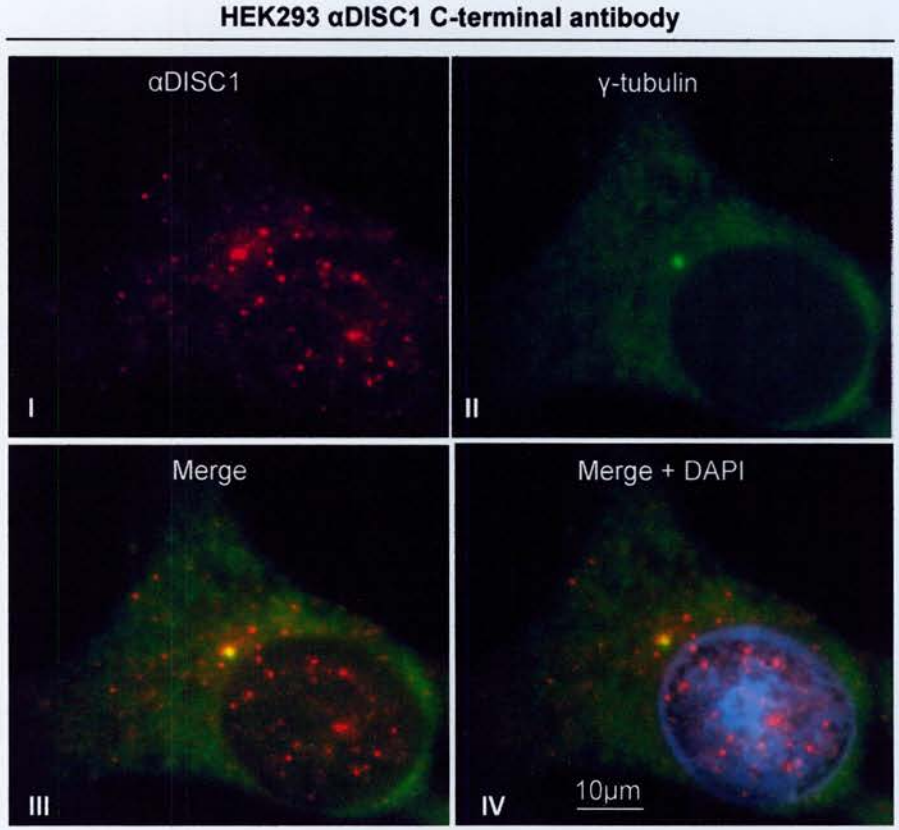

Figure 4.2.B. DISC1 species detected using the C-terminal antibody αDISC1 (red) co-localise with the centrosomal marker γ-tubulin (green) in HEK293 cells as shown in images **I-IV**. All images were taken at 100X magnification. The nucleus is visualised using DAPI (blue).

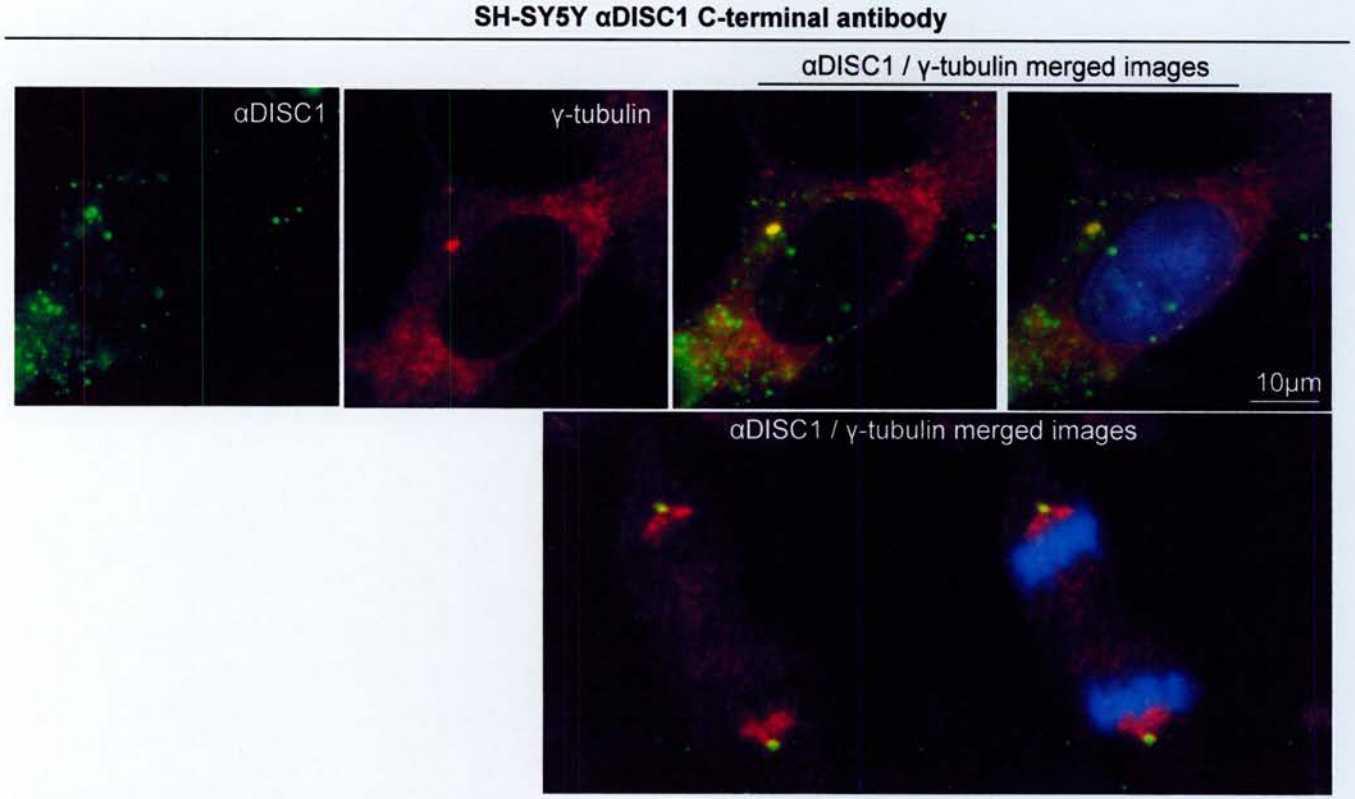

Figure 4.2.C. αDISC1 C-terminal antibody detects DISC1 isoforms (green) at the centrosome as seen by overlapping immunoreactivity with the centrosomal marker γ-tubulin (red). This overlap is seen in non-dividing (top panel) and dividing cells (bottom panel). In dividing cells DISC1 and γ-tubulin co-localise at the poles of the mitotic spindle. Images were taken at 100X magnification. Nuclei are visualised using DAPI (blue).

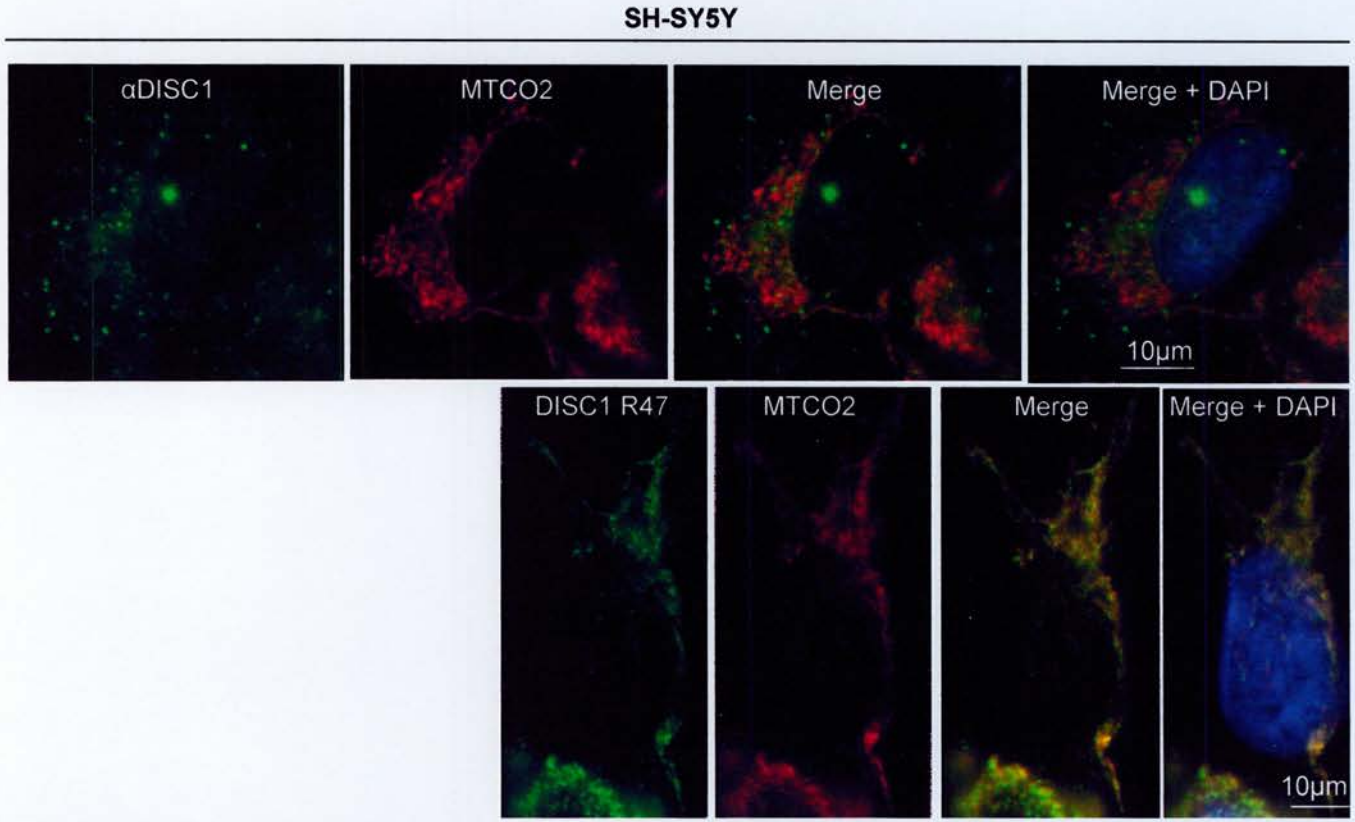

Figure 4.2.D. The αDISC1 C-terminal antibody (green) does not co-localise with the mitochondria (red) in SH-SY5Y cells as seen by non-overlapping immunoreactivity with mitochondrial cytochrome oxidase subunit II (MTCO2) (Top panel). In contrast the N-terminal R47 DISC1 antibody (green) does co-localise with MTCO2 (red) as has been previously described (*James et al 2004* and bottom panel of images). Images were taken at 100X magnification. Nuclei are visualised using DAPI (blue).

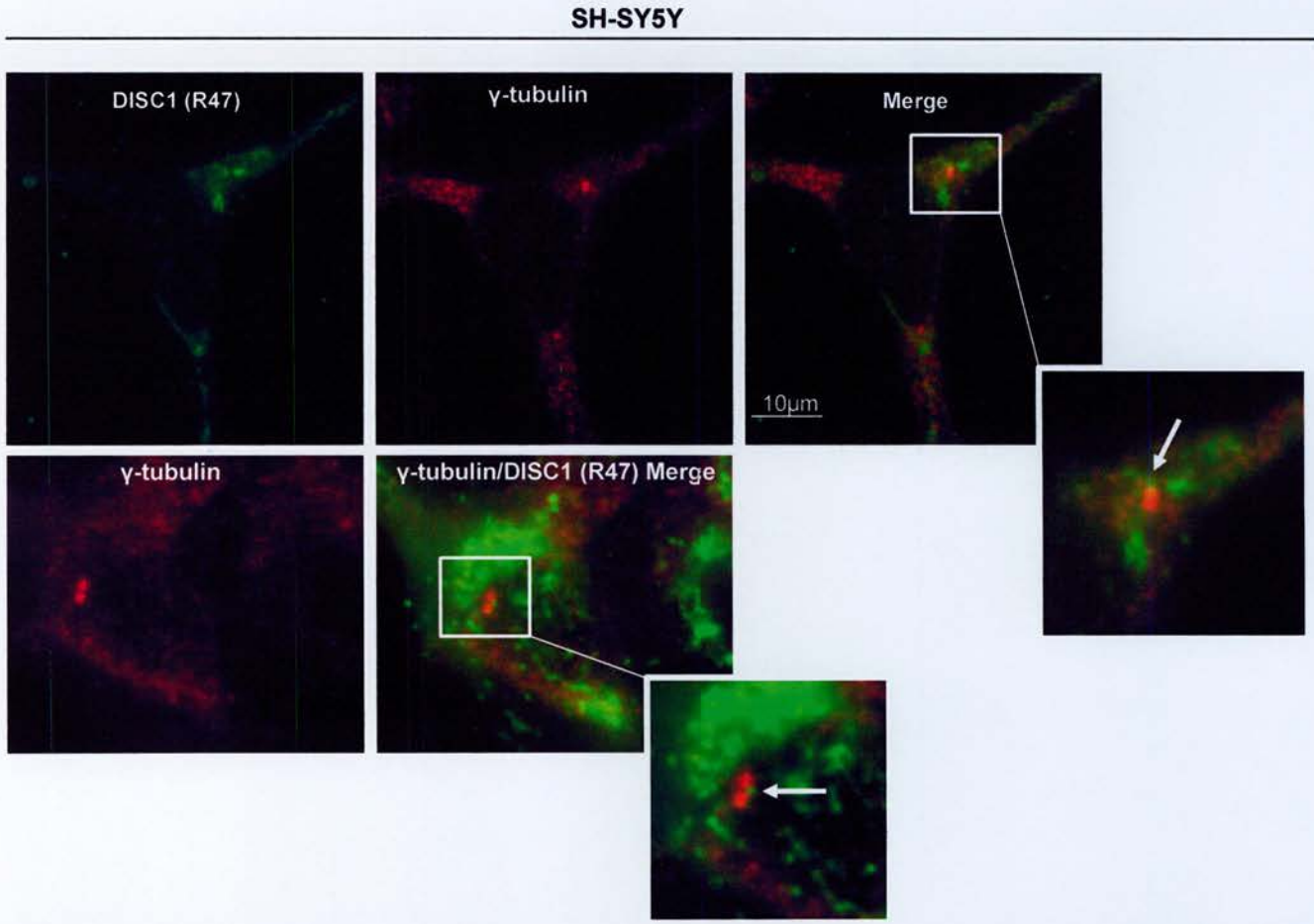

Figure 4.2.E. DISC1 R47 antibody (green) detects some DISC1 immunoreactivity at the centrosome (seen using γ-tubulin in red) as depicted here in SH-SY5Y cells. DISC1 centrosomal staining is indicated within the boxed regions which have been increased in size to ease visualisation and is further indicated by the position of the white arrows. Images were taken at 100X magnification.

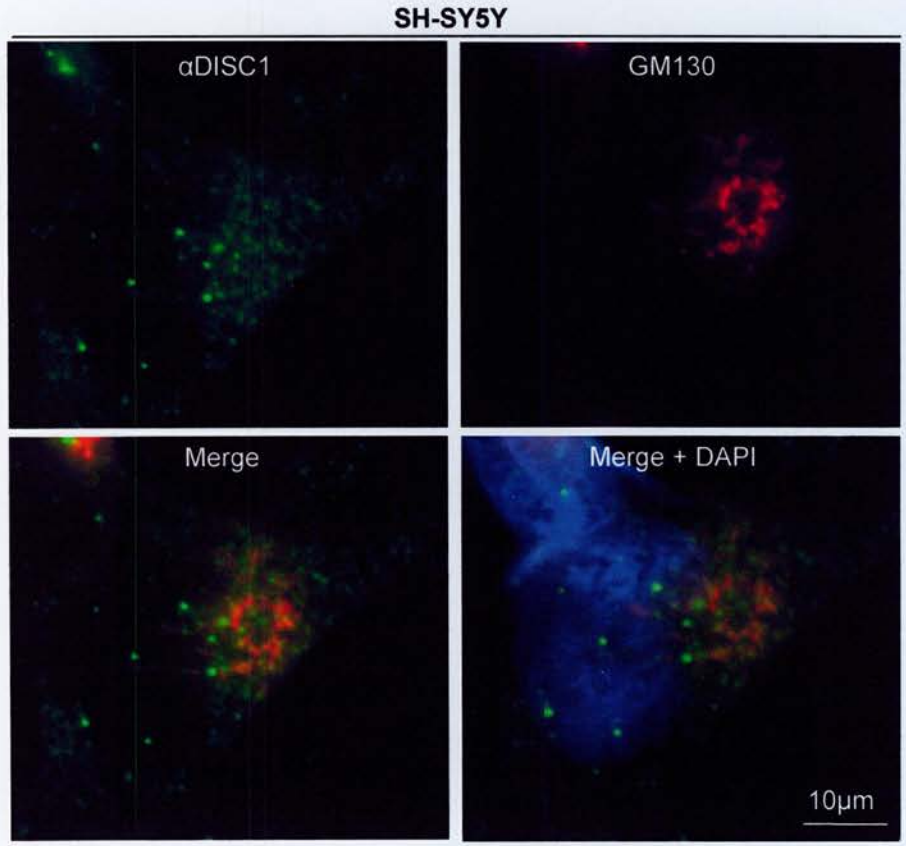

Figure 4.2.F. αDISC1 C-terminal antibody immunoreactivity (green) does not overlap with the golgi matrix protein GM130 (red) in SH-SY5Y cells. Images were taken at 100X magnification. The nucleus is visualised using DAPI (blue).

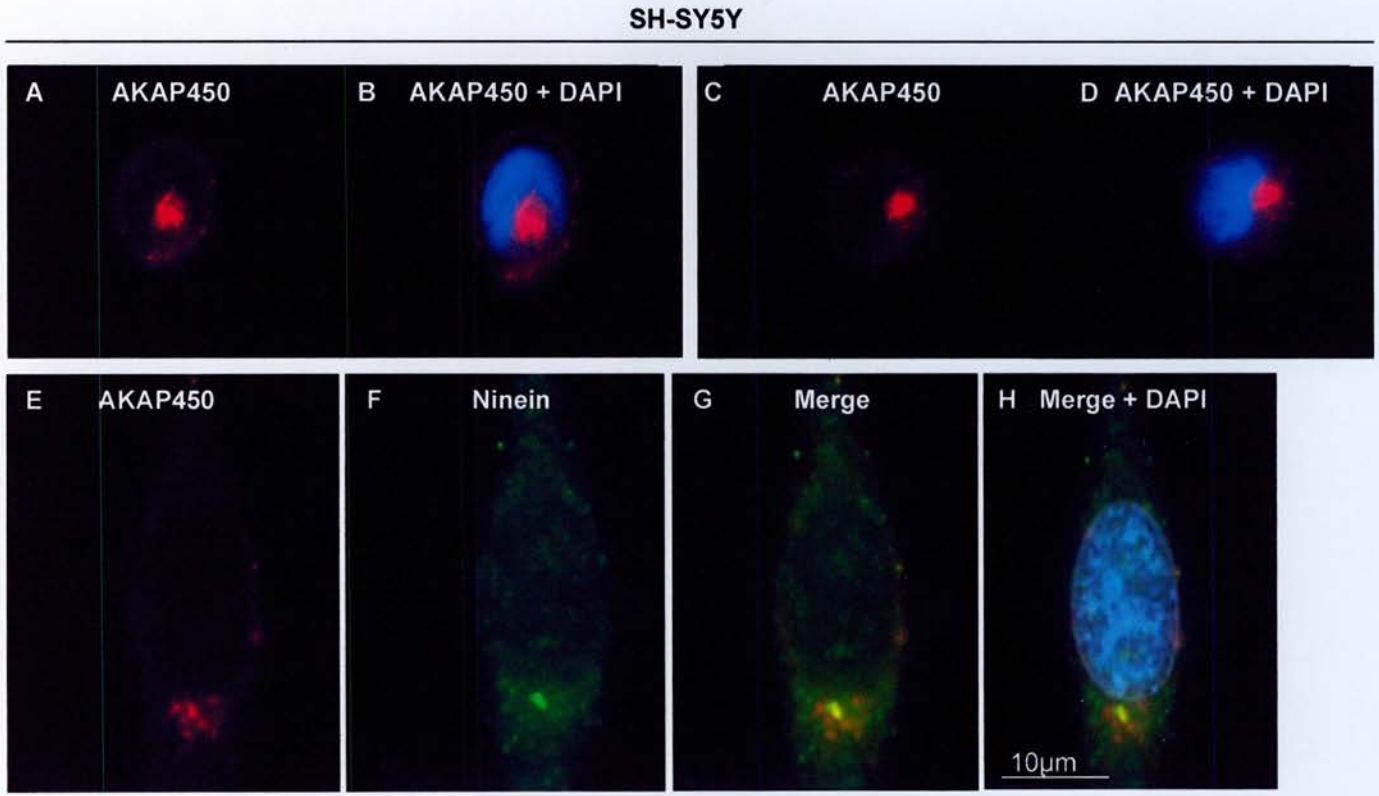

Figure 4.2.G. This figure depicts the centrosomal location of the AKAP450 protein (red) in SH-SY5Y cells. Images A-D indicate the centrosomal position of AKAP450 which is further confirmed by co-localisation with an additional centrosomal protein, Ninein (green), in images E-H. Images were taken at 100X magnification. Nuclei are visualised with DAPI (blue).

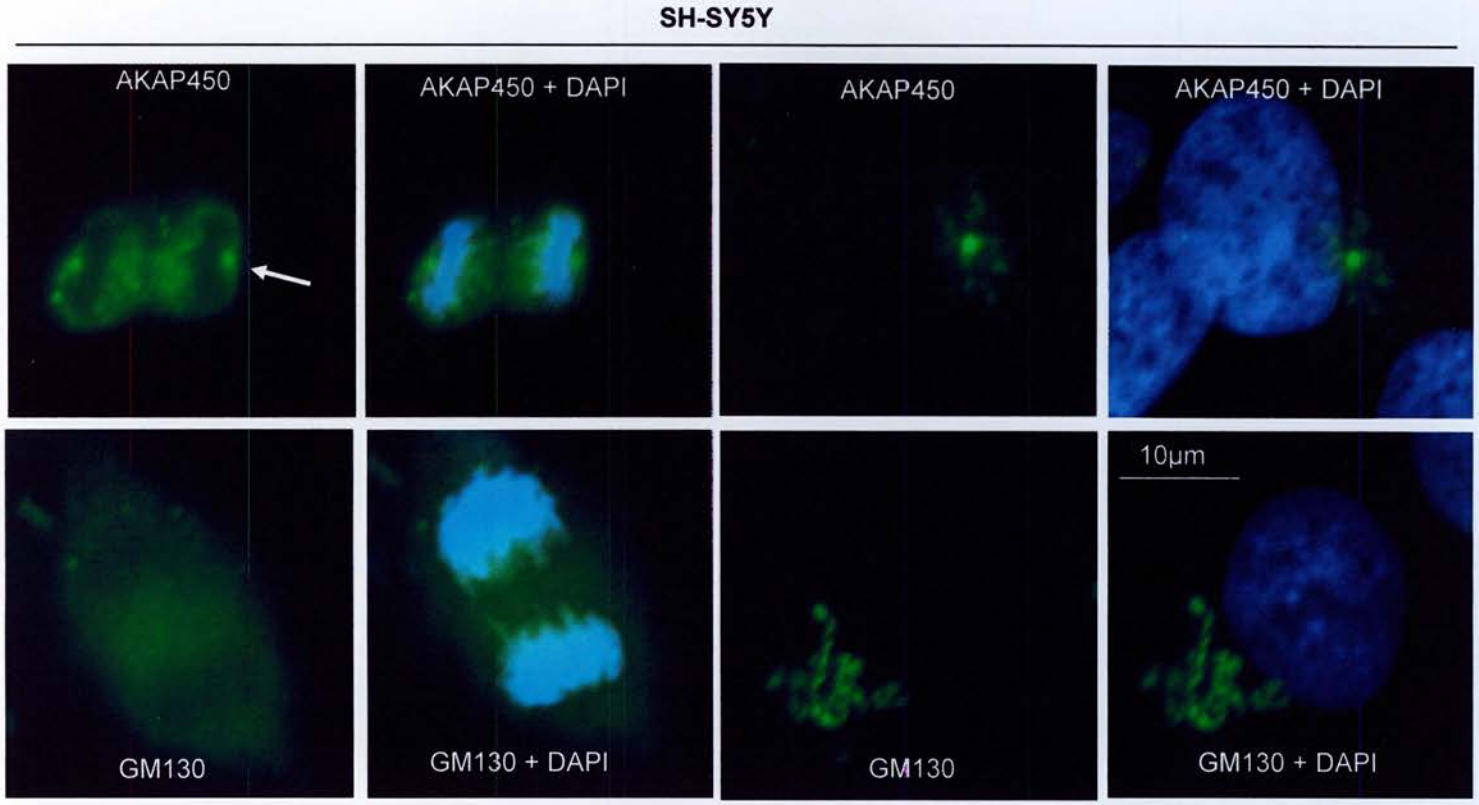

Figure 4.2.H. AKAP450 (upper panel) and GM130 (lower panel) exhibit different patterns of immunoreactivity in SH-SY5Y cells. AKAP450 is found as a dense perinuclear spot (indicated by the white arrow) which is duplicated and detected at a location corresponding to the spindle poles in dividing cells. This is in contrast to the pattern of the golgi matrix protein GM130 which does not assume a centrosomal location. Nuclei are visualised with DAPI (blue).

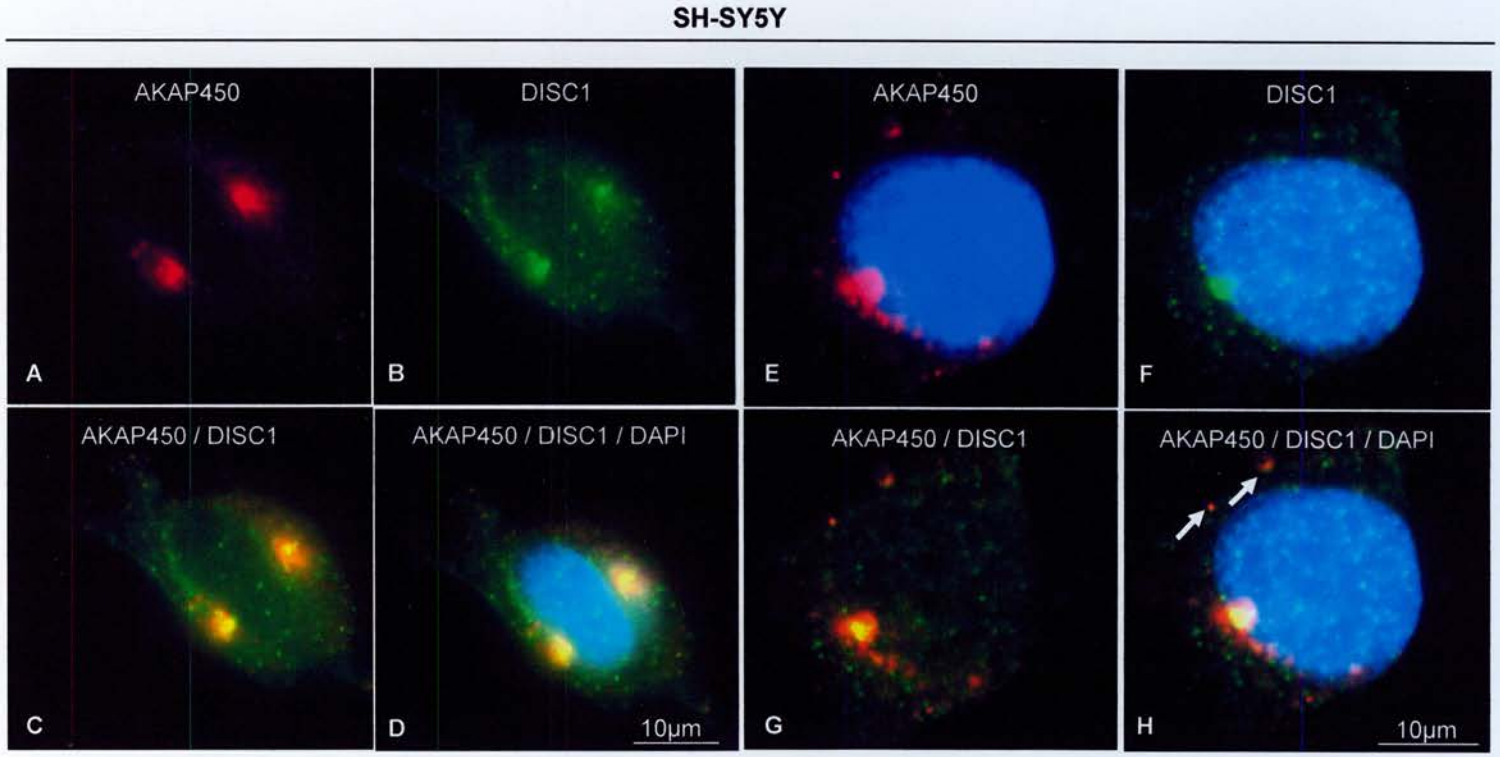

Figure 4.2.I. αDISC1 immunoreactivity (green) overlaps with AKAP450 (red) at the centrosome in SH-SY5Y cells (A-D). Some cytoplasmic co-localisation is also evident as indicated by the arrows in the merged image (E-H). Nuclei are visualised with DAPI (blue).

The data obtained from these immunofluorescence microscopy experiments suggest that the DISC1 isoforms detected by the N-terminal R47 antibody are predominantly mitochondrially located, which is in agreement with previously published data (*James et al. 2004, Brandon et al. 2005*). However these experiments also show a small amount of R47 immunoreactivity at the centrosome, which has not been shown before. This centrosomal pattern is hard to detect due to the abundance of mitochondrial DISC1 staining which possibly explains why this has not been reported previously. The pattern of αDISC1 localisation is in contrast to this; the longer DISC1 isoforms are detected within the cytoplasm and strongly at the centrosome. Due to its multiple interaction partners DISC1 is considered likely to be a molecular scaffold protein. These data support this and suggest that DISC1 may perform isoform specific interactions in specific sub-cellular compartments. Subsequent experiments have attempted to confirm (and define) the existence of centrosomal DISC1 isoforms by sub-cellular fractionation.

4.3 The Long DISC1 isoform is abundant in fractions of isolated centrosomes

Sub-cellular fractionation protocols to recover P1 (nuclear) and P2 (mitochondria enriched) fractions are well established in the laboratory. Isolation of centrosomes required a new technique and was modified from *Moudjou and Bornens, 1998.* Protocol details can be found in chapter 2 and the isolation process is depicted in diagram 2.10.

4.3.1 Enrichment of 100kDa DISC1 in fractions of isolated centrosomes

4.3.1.1 The isolated centrosome fraction is distinct in protein composition from total cell lysate and P2 fractions

Centrosomal lysates were processed alongside SH-SY5Y total cell lysate and a mitochondrion enriched (P2) lysate by SDS-PAGE. These lysates were subsequently

analysed by western blotting to examine the proteins present in each fraction. Gamma tubulin was initially used as a marker of centrosomal identity and the mitochondrial protein cytochrome C was used to demonstrate mitochondrion enrichment of the P2 fraction. Figure 4.3.A shows western blotting for γ-tubulin in all three fractions. This figure demonstrates that γ-tubulin is present in the total cell lysate, P2 and centrosomal lysate. Although γ-tubulin is an important centrosomal component and a reliable marker of centrosomal position using fluorescence microscopy, it does exhibit a wide cellular distribution pattern. It has been reported that at least 80% of total cellular γ-tubulin is present in the cytosol (*Moudjou et al. 1996*) therefore it is not surprising that γ-tubulin is present in the total cell lysate and the P2 fraction in addition to the centrosomal fraction. This is also consistent with the immunofluorescence data presented here, which demonstrates γ-tubulin at the centrosome and additionally in a diffuse pattern within the cytoplasm (for examples see figures 4.2.A and 4.2.B). Furthermore, it is likely that only a small proportion of the γ-tubulin pool associated with the centrosome is examined in this centrosome fraction. In these experiments γ-tubulin was solubilised from centrosome fractions using 40mM Tris pH 8.0 with 0.3% SDS. Subsequent reading suggests that more stringent buffers may be required to release γ-tubulin from the centrosome (*Moudjou et al. 1996*). Using the current conditions it is likely that less than 60% of γ-tubulin associated with the centrosome has been released. The difficulties encountered solubilising γ-tubulin should not affect our ability to examine DISC1 associated with the centrosome as DISC1 is likely to be more loosely associated with the centrosome than γ-tubulin. DISC1 constructs that lack the ability to localise at the centrosome do not affect γ-tubulin itself, the core component of the centrosome, suggesting that DISC1 does not function to keep γ-tubulin at the centrosome and is likely to have a looser association with the centrosome (*Kamiya et al. 2005*).

The centrosomal fraction was further demonstrated to be distinct from total and P2 lysates using the mitochondrial marker cytochrome C. Using this antibody cytochrome C is detected in the total cell lysate and enriched in the P2 fraction but there is no cytochrome C present in the centrosome fraction as expected (Figure 4.3.B).

It can be concluded from these western blotting experiments that the centrosome fractionation procedure has produced a fraction distinct from total cell lysate and mitochondrial enriched fractions that contains the centrosomal protein γ-tubulin. It would be desirable to confirm the success of the fractionation procedure with another centrosomal protein; however none of the additional centrosomal antibodies tested were suitable for immunoblotting.

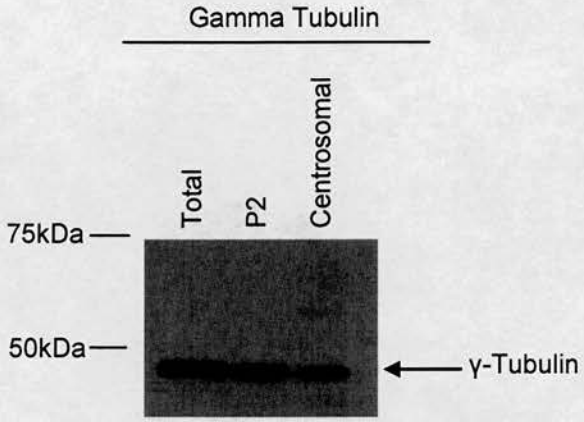

Figure 4.3.A SDS-PAGE followed by western blotting demonstrates the presence of γ-tubulin in all three SH-SY5Y fractions.

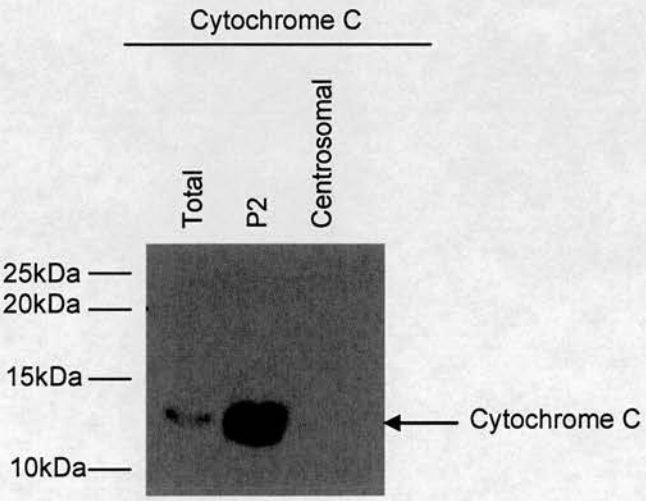

Figure 4.3.B. Cytochrome C is present within total and P2 fractions from SH-SY5Y cells but not within the centrosome fraction.

4.3.1.2 A 100kDa DISC1 isoform is enriched at the centrosome

SH-SY5Y total cell lysate, P2 lysate and centrosomal lysates were processed by SDS-PAGE followed by immunoblotting for DISC1. Using the DISC1 N-terminal antibody R47 it was shown that distinct DISC1 isoforms are enriched in the P2 and centrosome fractions. The 71kDa DISC1 isoform was seen to be enriched within the mitochondrial P2 fraction as previously published (*James et al. 2004* and figure 4.3.C). In concordance with the immunofluorescence data a DISC1 isoform of approximately 100kDa in size is enriched within the centrosome fraction (Figure 4.3.C). This is consistent with the presence of either the L or Lv DISC1 isoform at the centrosome.

Surprisingly, 75kDa and 80kDa DISC1 isoforms were also detected within the centrosome fraction (Figure 4.3.C). Previously, sub-cellular fractionation has localised these DISC1 isoforms to the post-mitochondrial supernatant which contains cytosolic and membranous cellular components (*James et al. 2004*). It is intriguing that these isoforms also appear to be enriched at the centrosome and that DISC1 may have a more prominent presence at the centrosome than previously thought.

Using the C-terminal αDISC1 antibody a DISC1 doublet comprising the L and Lv isoforms is present within the total cell lysate and the P2 fraction (Figure 4.3.D). As the P2 fraction is not a pure mitochondrial fraction these isoforms in the P2 lysate are likely to represent cytoplasmic DISC1 forms as this antibody does not detect mitochondrial DISC1 isoforms by immunofluorescence. Using this antibody a 100kDa DISC1 isoform is indeed present within the centrosome fraction however only one band of the DISC1 doublet is detected (Figure 4.3.D). Unfortunately the same enrichment of DISC1 is not seen using this antibody as with the N-terminal R47 antibody, however as only one of the DISC1 long isoforms appears to be present at the centrosome the DISC1 pool is already reduced within the centrosome fraction. The presence of only one band within the centrosome fraction indicates that either the L or Lv DISC1 isoform is present at the centrosome, while both are located in the cytoplasm. It is difficult to determine which of these DISC1 isoforms is present at the centrosome as this isoform appears to have a slight band shift in the centrosomal

fraction. This could be due to a modification of this isoform at the centrosome or more simply this could be due to use of a different buffer to solubilise the centrosomal pellet causing the isoforms to migrate at a slightly altered molecular weight. Due its size it is most likely that this isoform represents the L DISC1 isoform.

In summary, analysis of total, P2 and centrosomal lysates from SH-SY5Y cells demonstrated that the 71kDa DISC1 isoform is present in the mitochondrial enriched fraction as previously published. These new data demonstrate the absence of this isoform and preferential enrichment of DISC1 100kDa, 75kDa and 80kDa isoforms within the centrosome fraction. This is consistent with the immunofluorescence data showing DISC1 localisation at the centrosome with both the αDISC1 and R47 DISC1 antibodies.

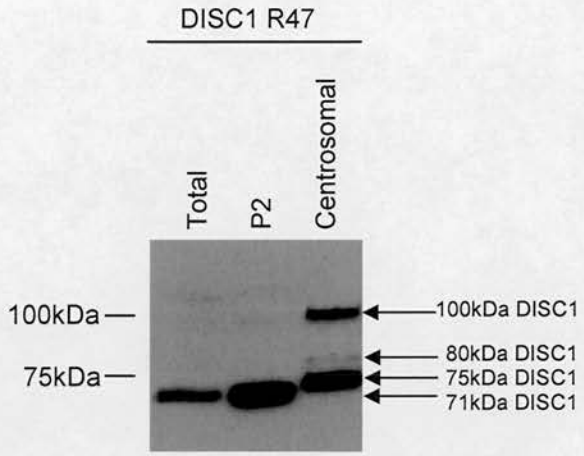

Figure 4.3.C. 20µg of each lysate was processed by SDS-PAGE followed by immunoblotting for DISC1. Using DISC1 N-terminal antibody R47 an enrichment of 100kDa DISC1 is seen within the centrosome fraction of SH-SY5Y cells. 75kDa and 80kDa DISC1 isoforms are also detected within this fraction.

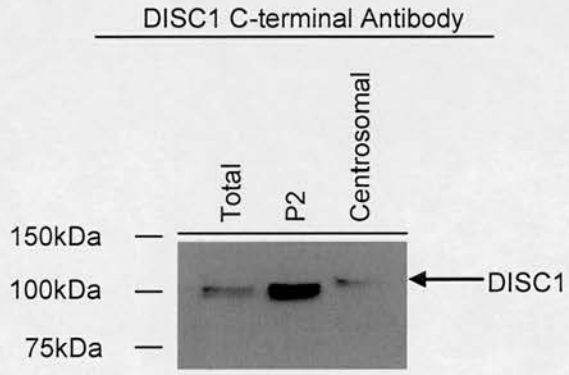

Figure 4.3.D. 25µg of each lysate was processed by SDS-PAGE followed by immunoblotting for DISC1. The αDISC1 C-terminal antibody detects a DISC1 doublet at 100kDa in total and P2 lysates, representing the Long and Long variant DISC1 isoforms. In contrast, only one DISC1 isoform is detected in the centrosome fraction indicating that either the L or Lv isoform is present at the centrosome but not both. Due to the size it is most likely that this isoform represents the DISC1 L isoform.

4.4 DISC1 is localised to the poles of the mitotic spindle throughout the cell cycle

As DISC1 assumes a centrosomal location and the centrosome is an important organelle for progress through mitosis I was interested to examine the localisation of DISC1 throughout mitosis in mammalian cells. I utilised COS 7 African Green Monkey cells and performed immunofluorescent staining for α-tubulin (to locate the mitotic spindle) and DISC1. In non-dividing (interphase) cells, αDISC1 immunoreactivity co-localised with α-tubulin at the site of microtubule nucleation which is equivalent to the position of the centrosome (Figure 4.4.A (A-D)). DISC1 was present as one or quite often two bright centrosomal puncta (Figure 4.4.A (E-J)). These paired puncta are likely to correspond to the two centrioles which comprise each mammalian centrosome. Interestingly DISC1 exhibits asymmetric staining at the centrioles with one centriole staining more prominently than the other (Figures 4.4.A (E-J)).

DISC1 was found to localise to the poles of the mitotic spindle throughout cell division (Figures 4.4.B). Figure 4.4.B, images A-D, represent a cell in prophase which has just duplicated its centrosome, which can be seen migrating towards the opposite side of the cell. Images E-H of this figure show a late stage prophase cell where this replicated centrosome has assumed its position at the opposite pole of the cell and the mitotic spindle is beginning to form. Images I-L show the condensed chromosomes aligning on the pro-metaphase spindle and migrating towards the metaphase plate.

Figure 4.4.C shows the later mitotic stages of metaphase and anaphase during which DISC1 is still localised to the poles of the mitotic spindle. Figure 4.4.D depicts cells approaching the completion of mitosis (telophase). The chromosomes have migrated to opposite ends of the spindle and the cells are beginning to separate into two daughter cells. DISC1 remains localised to the mitotic spindle poles even at these late stages.

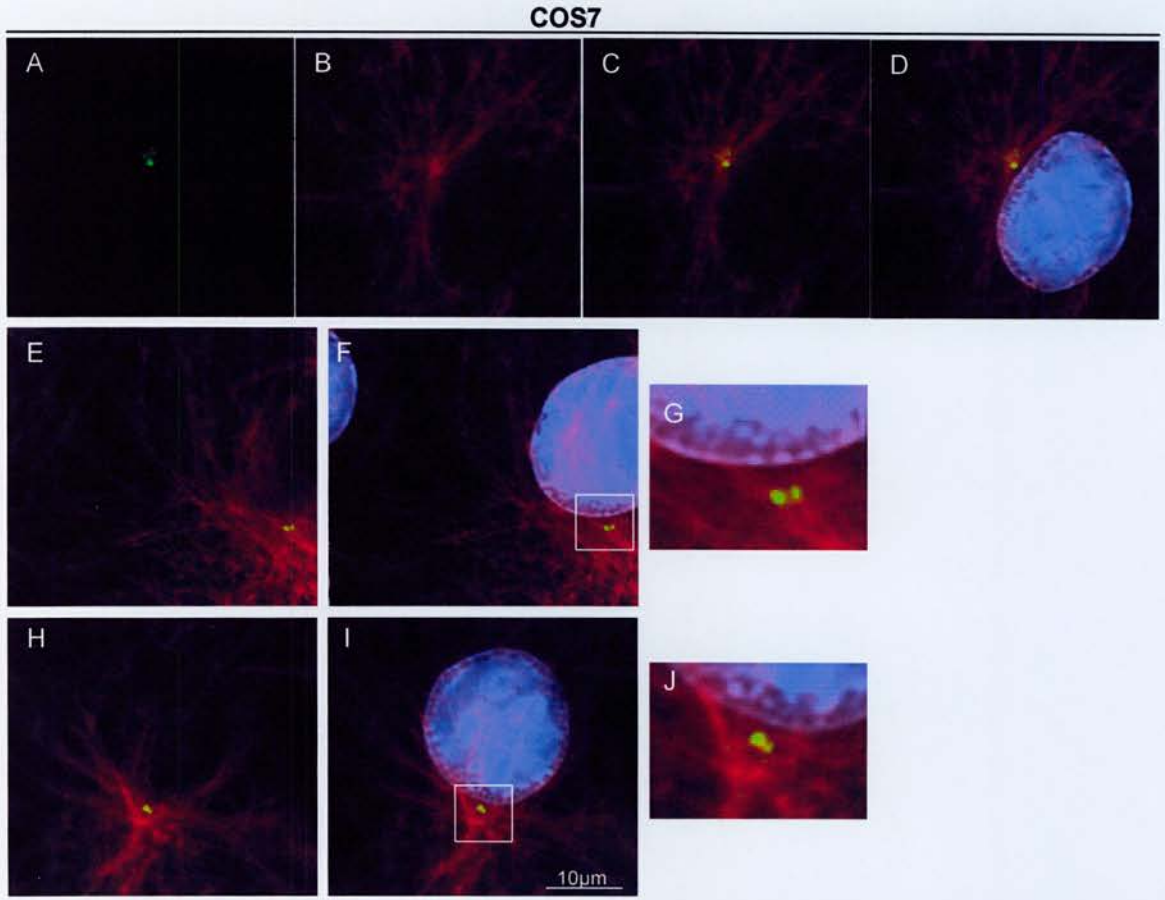

Figure 4.4.A. COS 7 cells were processed for immunofluorescence using α-tubulin (red) and a DISC1 C-terminal antibody (αDISC1 in green). Images A-D represent an interphase stage cell (non-dividing) in which DISC1 co-localises with α-tubulin at the site of microtubule nucleation. Images E-J depict DISC1 asymmetric staining at the centrioles. The centrioles are highlighted within the boxed regions which have been enlarged in images G and J. Nuclei are visualised with DAPI (blue).

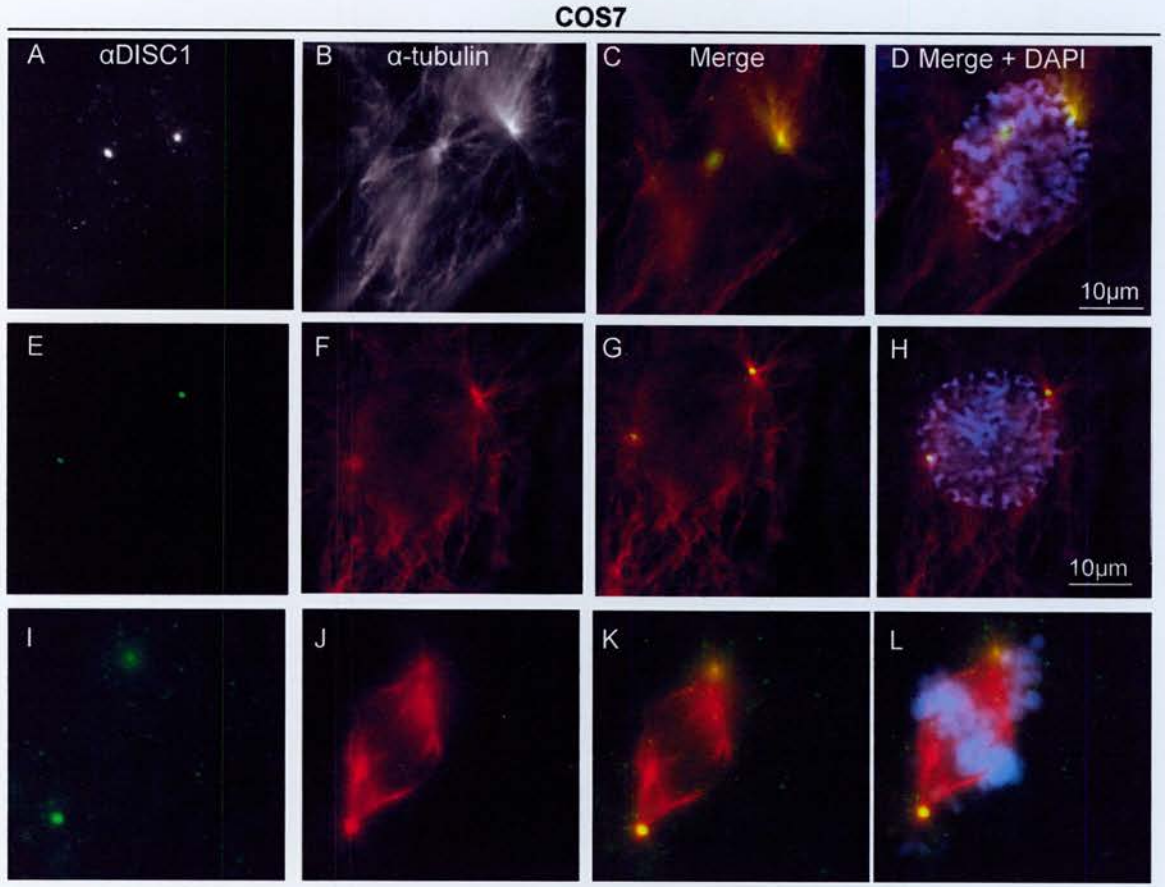

Figure 4.4.B. COS7 cells were processed by immunofluorescence with a DISC1 C-terminal antibody (αDISC1 in green) and α-tubulin (red). Images A-H represent cells in prophase of mitosis and images I-L represent a pro-metaphase cell. DISC1 is clearly localised to the poles of the mitotic spindle at each stage. Nuclei and condensed chromosomes are visualised with DAPI (blue).

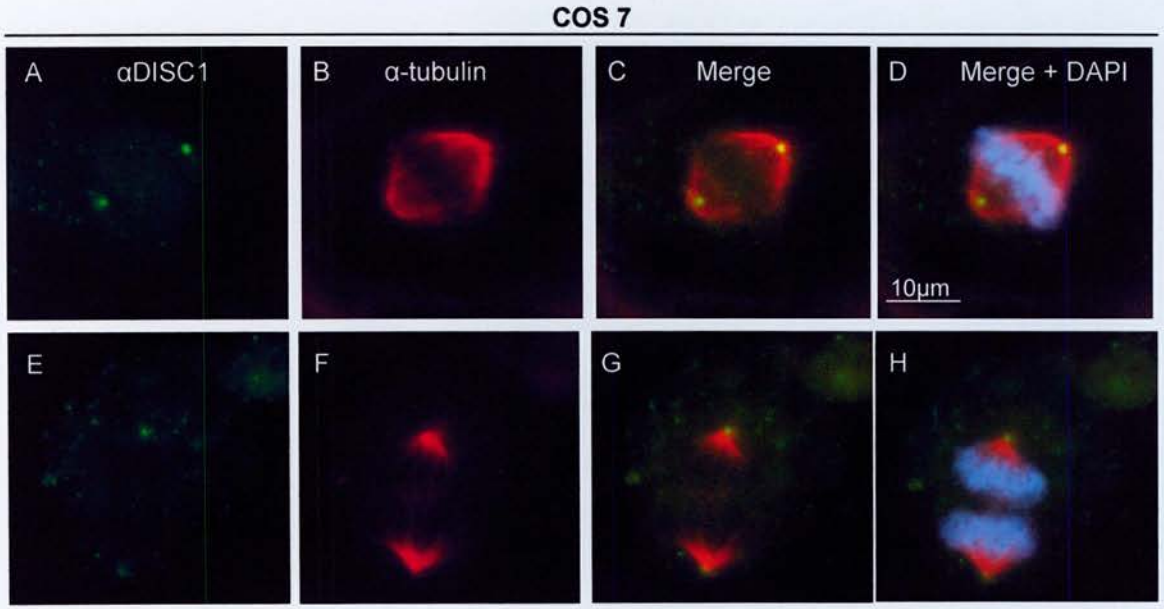

Figure 4.4.C. COS7 cells were processed by immunofluorescence with a DISC1 C-terminal antibody (αDISC1 in green) and α-tubulin (red). DISC1 immunoreactivity is detected at the poles of the mitotic spindle throughout metaphase (images A-D) and anaphase (images E-H) in COS7 cells. Cellular DNA is visualised using DAPI (blue).

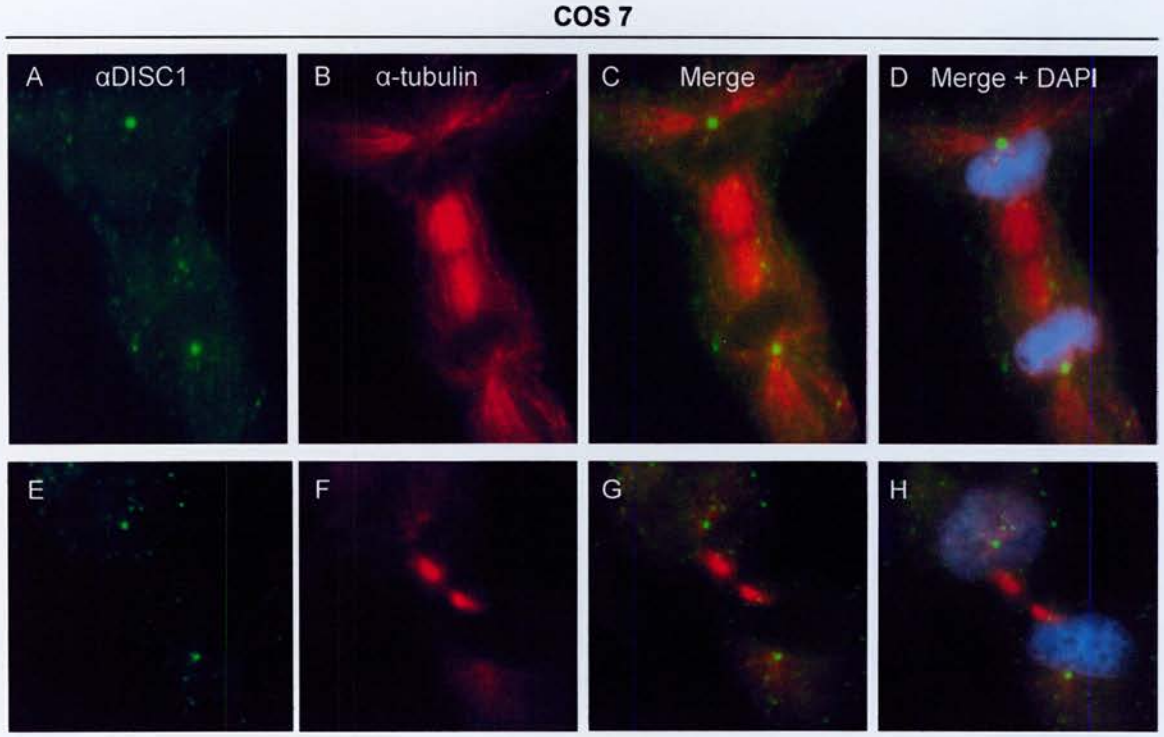

Figure 4.4.D. COS 7 cells were processed by immunofluorescence using a DISC1 C-terminal antibody (αDISC1 in green) and α-tubulin (red). Images A-D and E-H represent cells in early and late telophase respectively. DISC1 remains at the spindle poles even at these late stages of mitosis. Cellular DNA is visualised with DAPI (blue).

4.5 Discussion

The sub-cellular distribution of DISC1 is complex and the subject of much debate within the field. It is clear from many studies that DISC1 assumes multiple locations within the cell and that distinct isoforms occupy different sub-cellular locations. My experiments have confirmed that the 71kDa DISC1 isoform is mitochondrially located as previously published (*James et al. 2004*).

Using immunofluorescence the L (~100kDa) and Lv (~98kDa) DISC1 isoforms are shown to be present as discrete puncta within the cytoplasm and also clearly evident at the centrosome as demonstrated by co-localisation with two centrosomal proteins γ-tubulin and AKAP450. Immunoblotting DISC1 from isolated centrosome fractions further confirms this and suggests that it is most likely the DISC1 L isoform present at this location whilst both the L and Lv are located in the cytoplasm. Additionally these sub-cellular fractionation experiments have demonstrated 75kDa and 80kDa DISC1 isoforms within the centrosome fraction. Unfortunately there are currently no antibodies which specifically detect these isoforms such that this may be confirmed by immunofluorescence.

This data raises the interesting question of whether DISC1 performs isoform specific interactions at distinct sub-cellular locations. As DISC1 has the capacity to interact with multiple proteins it is considered a molecular scaffold protein. Theoretically individual DISC1 isoforms could perform distinct protein-protein interactions and/or traffic specific proteins to their required sub-cellular locations

One example of this has recently been published whereby the 71kDa DISC1 isoform has been shown to interact with Phosphodiesterase type 4B1 (PDE4B1). Both of these protein isoforms are enriched within the mitochondrial fraction indicating that this is where the interaction occurs (*Millar et al. 2005b*). However the ability of DISC1 to bind type 4 phosphodiesterases is not limited to the 4B family although this is the only interaction which has been studied in detail. Indeed DISC1 can also bind to PDE4A, PDE4C and PDE4D isoforms (*Millar et al. 2005b*). Interestingly a

member of the PDE4D family, PDE4D3, has previously been documented to exist at the centrosome and has recently been shown to interact with AKAP450 and PKA (*Tasken et al. 2001, McCahill et al. 2005*). As previously mentioned AKAP450 is a putative DISC1 interactor and these data demonstrate 100kDa DISC1 and AKAP450 co-localisation at the centrosome. This provides further support for a potential DISC1-AKAP450 interaction and highlights the potential for a DISC1-AKAP450-PKA-PDE4D interaction at the centrosome. Confirmation of the DISC1-AKAP450 interaction is needed to substantiate this hypothesis but it is an intriguing hypothesis considering DISC1s already established role in cAMP signal transduction at the mitochondria.

This chapter also examined the localisation of DISC1 at the centrosome in the context of mitosis and cell cycle progression. The centrosome is an important organelle for cell cycle progression and disruption of centrosome function hampers progress through the cell cycle and mitosis (*Doxsey et al. 2005*). Numerous regulatory proteins necessary for cell cycle progression accumulate at the centrosome, including Kendrin/Pericentrin B, which has been reported to be important for DISC1 localisation at the centrosome (*Miyoshi et al. 2004*). DISC1 was seen to be localised at the site of microtubule nucleation in interphase cells as demonstrated by co-localisation with α-tubulin. At early stages of mitosis DISC1 expression was persistent at the centrosome even after centrosome duplication and during centrosome migration. DISC1 remained localised to the poles of the mitotic spindle throughout cell division. This suggests that DISC1 is a core feature of the centrosome which may be necessary for cell cycle progression. The effect of silencing DISC1 expression on cell cycle progression is examined in chapter 6.

Interestingly during interphase DISC1 was present quite often as two bright puncta within the centrosomal region indicating that DISC1 may be a marker of mammalian centrioles. Furthermore DISC1 appeared to be preferentially localised to one of the centrioles although both did possess DISC1 immunoreactivity. It has been reported that certain proteins localise preferentially to the mother (older) centriole in various cell systems and it is possible that DISC1 is preferentially localised to one centriole

in a similar manner. Both centrioles possess the ability to nucleate microtubules; however only the mother centriole possesses a microtubule anchoring capability, with proteins involved in anchoring of microtubules preferentially localising to the mother centriole (*Delgehyr et al. 2005*). Ninein is a mother centriole specific protein that is involved in microtubule nucleation and anchoring (*Delgehyr et al. 2005*). Interestingly NUDEL, a DISC1 interacting protein, has also been shown to co-localise with Ninein specifically at the mother centriole where it contributes to microtubule anchoring (*Guo et al. 2006*). DISC1 may localise preferentially to the mother centriole due to an excess of DISC1 interacting proteins such as NUDEL at the mother centriole. This scenario is depicted in figure 4.5.A below (adapted from *Badano et al. 2005*). It will be interesting to further examine this asymmetry of DISC1 localisation at the centrioles and determine if DISC1 possesses a role in microtubule nucleation and/or anchoring, perhaps via its known interaction with NUDEL (*Morris et al. 2003, Ozeki et al. 2003, Brandon et al. 2004*).

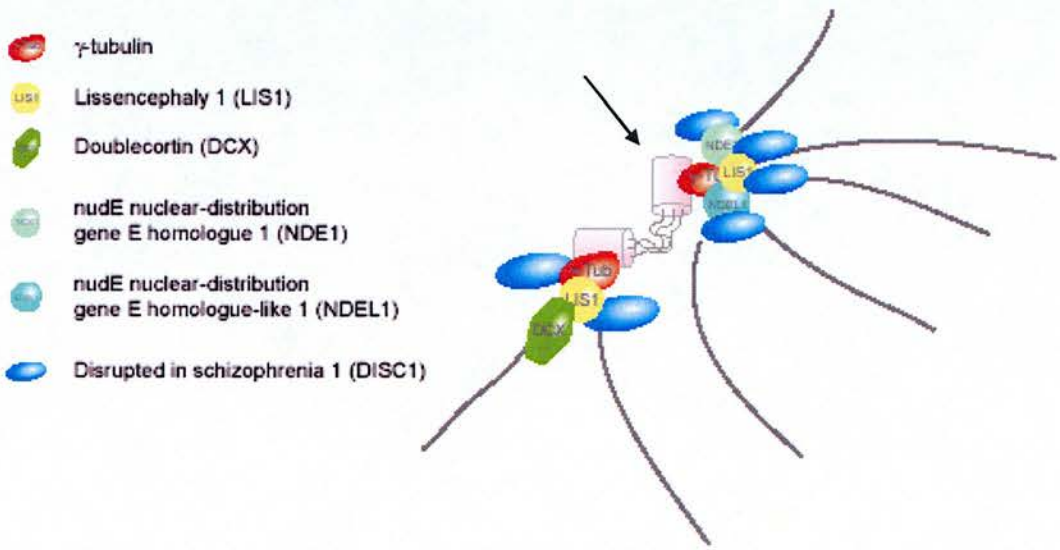

Figure 4.5.A. DISC1 localisation to the mammalian centrioles. DISC1 interacts with many centriolar proteins, some of which preferentially localise to the mother centriole, indicated by the arrow.

In summary, DISC1 was found to exhibit isoform specific localisation, with 100kDa, 75kDa and 80kDa isoforms localising to the centrosome. This 100kDa isoform further appeared to be asymmetrically localised to the centrioles. DISC1 is also shown to be present at the poles of the mitotic spindle where it may perform functions necessary for mitosis and cell cycle progression. See figure 4.5.B below.

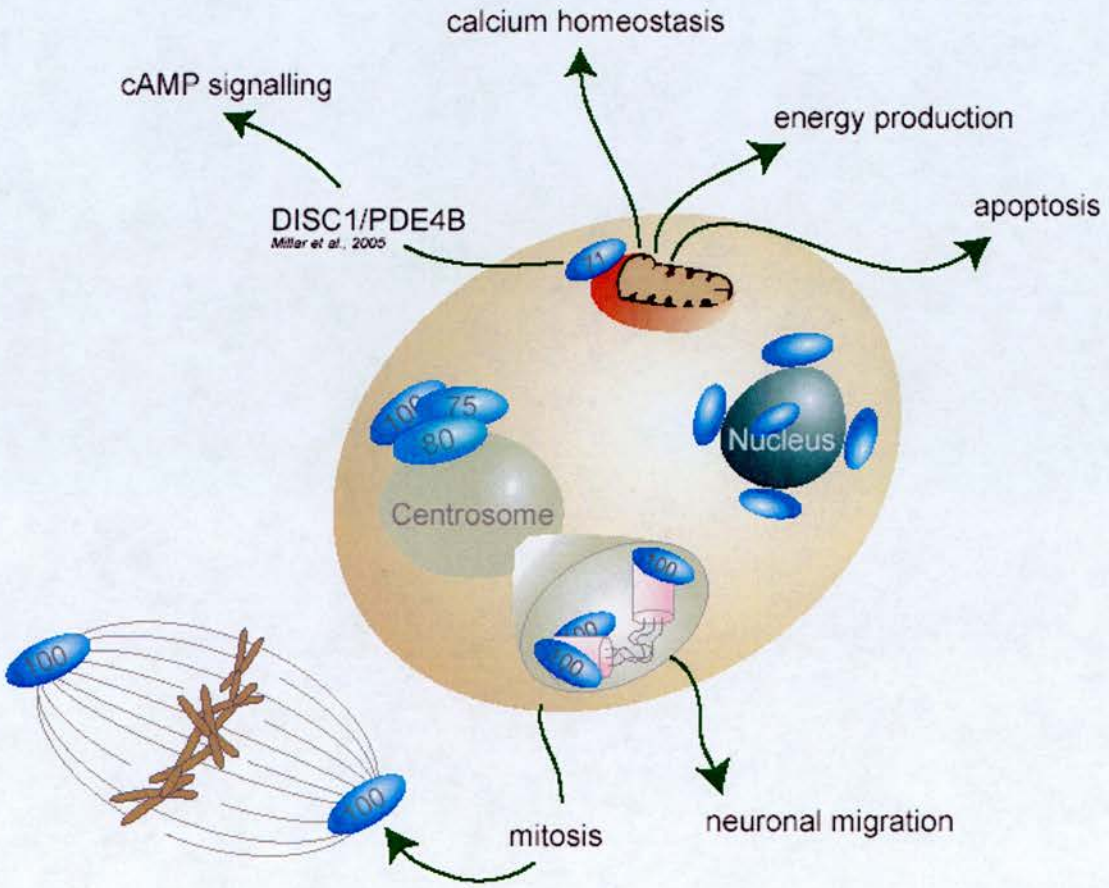

Figure 4.5.B. This figure depicts the isoform specific sub-cellular localisation profile of DISC1. 71kDa DISC1 is predominantly associated with the mitochondrion whereas the 100kDa isoform is mainly localised to the centrosome and can be seen at the poles of the mitotic spindle during cell division. DISC1 isoforms of 80kDa and 75kDa are also localised to the centrosome. Cytoplasmic, perinuclear and nuclear DISC1 isoforms remain to be defined.

Chapter 5

Optimising RNA interference to knock down DISC1

5.1 Preface

The gold standard for elucidating the function of an unknown gene is to create a loss of function mutation and examine the resulting phenotype. To elucidate the functions of *DISC1* at the cellular level, RNA interference has been employed to selectively knock down *DISC1* expression. RNA interference is a powerful technique which can be used to knock down expression of specified genes via double stranded RNA (dsRNA) technology. Short interfering RNAs (siRNAs) are 21 nucleotide dsRNA molecules which elicit gene silencing via the RNA interference pathway in mammals (*Hannon, 2002*). Under normal circumstances gene silencing is triggered by dsRNAs present within the cell. These dsRNA precursors are processed by a ribonuclease (RNase III) enzyme called Dicer to produce siRNAs. These siRNAs are then unwound and one strand is incorporated into an RNA-inducing silencing complex (RISC) which targets homologous transcripts for degradation (*Hannon, 2002*). To date the enzyme responsible for cleaving the homologous mRNA transcripts, termed 'slicer', remains unidentified (*Ketting and Plasterk, 2004*). By using chemically synthesised siRNAs we can take advantage of the RNAi pathway and artificially induce gene knock down.

As the predicted disease model operating within the t(1;11) family is one of haploinsufficiency for DISC1, RNAi will enable us to mimic the effects of the translocation by artificially knocking down DISC1 expression. Hopefully this will not only give insights into the mechanism of disease pathogenesis in the t(1;11) family but will also provide crucial clues to the normal functions of this novel protein at the cellular level.

5.2 DISC1 siRNA oligonucleotides knock down exogenous DISC1 protein

5.2.1 DISC1 siRNA oligonucleotides

The success of RNA interference depends on the choice of siRNA oligonucleotides used to target the required gene. Although siRNAs may be designed by eye there are various algorithms which can be employed to aid their design thus giving the optimal chance of achieving gene knockdown. SiRNA oligonucleotides targeting the 5' region of the target gene have been found to be effective in many cases. It is suggested that 5' and 3' UTR regions are best avoided to evade interference by regulatory proteins in these regions however there is no firm evidence that such proteins hinder siRNA binding (*Tuschl et al.* siRNA user guide, 2004). In fact this can be a useful region to target as resulting RNAi phenotypes can be rescued by transfection of the target gene with an alternative 3'UTR sequence that will not be targeted for knockdown (*McManus and Sharp, 2002*).

For my experiments I chose *silencer* pre-designed siRNA oligonucleotides which were synthesised commercially by Ambion. These oligonucleotides were chosen because the company guarantee silencing effects of greater than 70%. The oligonucleotides were supplied pre-annealed and HPLC purified.

SiRNA oligonucleotides were chosen to target multiple regions along the *DISC1* gene. Figure 5.2.A depicts the position of the oligonucleotides chosen for these experiments. In brief, oligonucleotides were designed to target exons 2, 5, 6, 8 and the 3'UTR region of *DISC1*. The oligonucleotides were given numerical identities as detailed in figure 5.2.A.

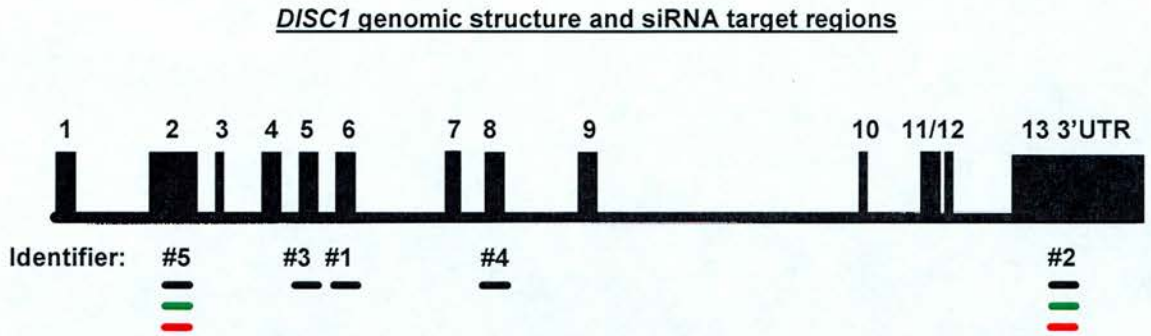

Figure 5.2.A This figure depicts the exonic structure of the *DISC1* gene and the location of siRNAs designed to target the gene. Oligonucleotides were given numerical identifiers. Unlabelled oligonucleotides are shown in black, FAM labelled oligonucleotides are shown in green and Cy3 labelled oligonucleotides are shown in red. Fluorescently labelled oligonucleotides were used to asses RNAi phenotypes by fluorescent microscopy.

5.2.2 DISC1 siRNA oligonucleotides induce efficient knockdown of exogenous FLAG-DISC1 protein

In addition to siRNA oligonucleotide sequence, RNAi induced knockdown is dependent on efficient delivery (transfection) of the siRNA oligonucleotides into the target cell. To assess the efficacy of these oligonucleotides for knocking down *DISC1*, human embryonic kidney cells (HEK 293) and African green monkey kidney cells (COS7) were used initially as established protocols exist for transfection of these cell lines. Despite this it was necessary to determine the optimal transfection reagent and the optimal concentration of siRNA oligonucleotides needed to knock down gene expression. The siRNA oligonucleotides used here are guaranteed to knockdown gene expression to the level of 70% or greater when used at a concentration of 100nM, with target gene expression analysed after 48 hours. However excess siRNA can have non-specific toxic effects on the cell, therefore *DISC1* siRNA oligonucleotides were initially tested at concentrations of 10nM and 50nM. Gene expression was analysed at 24 hours post transfection. Two chemical transfection reagents were chosen to deliver the oligonucleotides, siPORT Amine

and Lipofectamine 2000. Transfections were performed in 12 well tissue culture plates, details of which can be found in chapter 2.

FLAG-DISC1 and *DISC1* siRNAs were co-transfected into COS7 and HEK293 cells. FLAG-DISC1 expression was analysed by SDS-PAGE followed by western blotting. A FLAG antibody and a DISC1 (N-terminal R47) antibody were used to detect DISC1 protein expression levels post transfection. Using siPORT and Lipofectamine, siRNA oligonucleotides for *DISC1* dramatically knocked down protein expression at both 10nM and 50nM concentrations. Figure 5.2.B shows knockdown of exogenous FLAG-DISC1 induced by a 50nM concentration of oligonucleotides #1, #2 and #3 at 24 hours post transfection using siPORT in HEK293 and COS7 cell lines.

This figure suggests that when delivered using siPORT oligonucleotides #1, #2 and #3 knock down exogenous DISC1 with the same efficacy. However, delivery of these oligonucleotides into HEK293 cells using lipofectamine suggests that oligonucleotide #2 knocks down FLAG-DISC1 expression to the greatest extent and also that pooling individual siRNAs may have a synergistic effect on knockdown of DISC1 (figure 5.2.C).

These oligonucleotides were subsequently tested for knock down of endogenous *DISC1*. Two additional oligonucleotides (#4 and #5) were also acquired at a later date, due to an improvement in algorithm design at this point. Oligonucleotides #4 and #5 were not tested for knockdown at the level of exogenous DISC1 but directly tested for knockdown of endogenous *DISC1*.

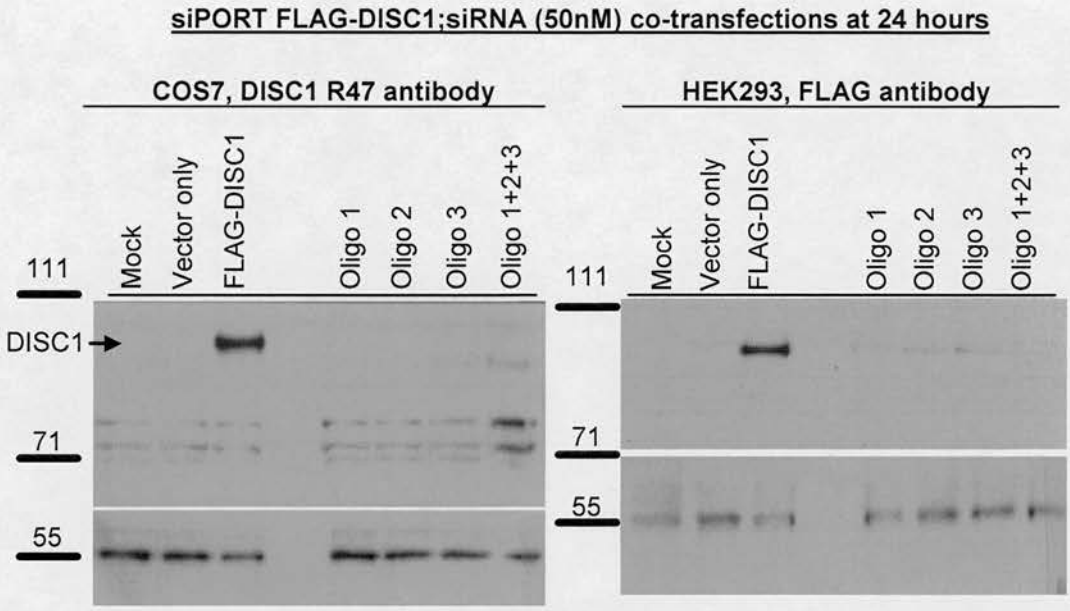

Figure 5.2.B. This figure shows SDS-PAGE followed by western blotting to analyse siRNA induced DISC1 knock down 24 hours post transfection using a 50nM concentration of siRNA oligonucleotides. COS-7 cells were probed with DISC1 N-terminal antibody (R47-15) and HEK293 cells were probed using a FLAG antibody. Loadings were controlled by probing with alpha tubulin.

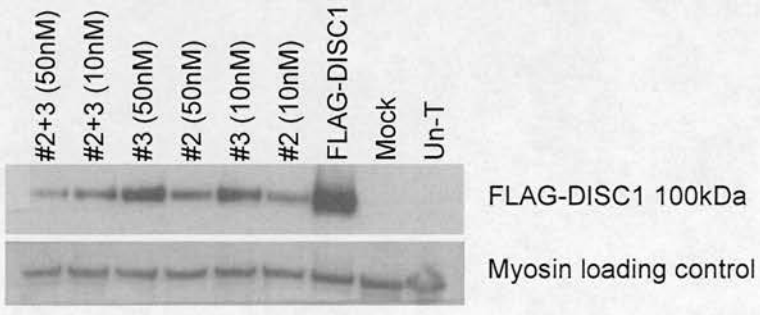

Figure 5.2.C. This figure shows western blot analysis of FLAG-DISC1 expression 24 hours post transfection using lipofectamine. All oligonucleotides show good knockdown of expression with the #2 + #3 oligonucleotide pool producing the most prominent knockdown.

5.3 *DISC1* siRNA oligonucleotides knock down endogenous *DISC1* at the level of mRNA and protein

5.3.1 Real-Time PCR demonstrates RNAi induced knockdown of DISC1 mRNA

To analyse endogenous *DISC1* knockdown siPORT was initially chosen to deliver the siRNA oligonucleotides into HEK293 cells. RNA levels were analysed at 48 and 72 hours post transfection. Transfections were carried out in 12 well tissue culture plates. Cells were harvested, RNA extracted and cDNA prepared as described in chapter 2. Quantitative Real-Time SYBR green PCR (qRT-PCR) was used to determine *DISC1* relative expression between treatment groups. *DISC1* primers for qRT-PCR were designed to exon 2 of *DISC1*. Oligonucleotides #1, #2, #3, #4 and #5 were tested for their ability to knock down *DISC1* by qRT-PCR. *DISC1* expression levels are graphed as relative values compared to a mock or scrambled siRNA control group. When compared to mock transfected cells, oligonucleotides #1 and #2 induced *DISC1* knockdown at 48 hours using a 50nM siRNA concentration. Oligonucleotide #3 demonstrated inconsistent knockdown and was excluded from further testing (Figure 5.3.A). Of the remaining two oligonucleotides #2 showed the most pronounced levels of *DISC1* knockdown. This oligonucleotide was further tested at concentrations of 50 and 100nM at 48 and 72 hour time points. A 100nM concentration of oligonucleotide #2 did not produce further knockdown in comparison to a 50nM concentration of this oligonucleotide and knockdown at 72 hours did not appear more pronounced in comparison to knockdown at 48 hours, although DISC1 mRNA levels are still reduced at this time point (figure 5.3.B).

Oligonucleotide #2 was then tested alongside two new oligonucleotides (#4 and #5) for knockdown in comparison to mock treated controls. Oligonucleotide #2 again consistently knocked down *DISC1* expression. Oligonucleotide #4 did not appear to induce *DISC1* knockdown whereas oligonucleotide #5 was seen to induce knockdown consistently and to a greater extent than oligonucleotide #2 (figure 5.3.C).

At this point non-targeting negative control siRNA oligonucleotides were employed to control for non-specific knock down of gene expression. Negative control siRNA oligonucleotides were provided by Ambion and consisted of a 21bp scrambled sequences that should not target any human gene. *DISC1* oligonucleotides #2 and #5 were taken forward for further testing.

5.3.2 DISC1 oligonucleotides #2 and #5 demonstrate RNAi induced knockdown of both RNA and Protein

Oligonucleotides #2 and #5 were transfected into HEK293 cells using siPORT. Transfections were carried out in 6 well plates and upon harvesting cells were split into two groups to allow for analysis of knockdown at the RNA and protein level. SiRNA oligonucleotides (*DISC1* oligonucleotides #2 and #5 and non-targeting negative control oligonucleotide) were transfected to achieve a final concentration of 50nM. *DISC1* mRNA levels were examined by qRT-PCR using primers designed to exon 2 of *DISC1*. QRT-PCR samples were normalised using *Glyceraldehyde -6-phosphate dehydrogenase (GAPDH)* and *Phosphofructokinase (hPFK)*. DISC1 protein levels were analysed by SDS-PAGE followed by western blotting using DISC1 R47 N-terminal antibody. Relative protein levels were determined using the Image J densitometry software package. Protein values were normalised using α-tubulin or β-actin. This experiment was performed three times independently.

Non-targeting negative control oligonucleotides were not seen to reduce *DISC1* expression levels in comparison to mock treated controls. Using oligonucleotides #2 and #5 these transfection conditions produced the most pronounced *DISC1* mRNA knockdown at 72 hours post transfection in comparison to a non-targeting siRNA control group (figure 5.3.D.). Although these oligonucleotides continually produced *DISC1* knockdown it did not seem as consistent as previous experiments. It may be possible that oligonucleotide delivery was compromised due to reagent instability or oligonucleotide degradation although this was not formally tested.

Only one of the three experiments showed good correlation between mRNA levels and protein levels. For experiment one, RNA and protein levels correlated well at

both 48 hours and 72 hours, showing knockdown at both time points. Experiment two produced RNA knockdown only at 72 hours and protein knockdown was not apparent. Experiment three produced more prominent protein knockdown than RNA knockdown at 48 hours whereas at 72 hours RNA knockdown was very prominent but protein knock down was not. These discrepancies may be due to difficulties in normalising the data. Also it is unknown how stable the DISC1 protein is and therefore at what point post RNA knockdown protein levels will diminish. For future experiments protein turnover could be estimated by combining the use of translation inhibitors and immunoblotting for DISC1 to give an estimation of when RNAi induced knockdown may be seen.

In summary, the negative control non-targeting siRNA oligonucleotide did not knock down *DISC1* expression. *DISC1* siRNA #2 and #5 produced knockdown of *DISC1* RNA and protein at either 48 or 72 hour time points. Unfortunately the levels of mRNA and protein did not correlate well in all experiments. This could potentially be a result of difficulties in normalisation and reliability of software used to determine the relative expression levels; however it has been shown retrospectively that the aliquot of N-terminal R47 DISC1 antibody used in these experiments has lost its affinity for endogenous DISC1 and this is likely to be a major contributing factor.

The most critical test for these oligonucleotides is the observation of knockdown of DISC1 protein post transfection. As the protein knockdown in these experiments was seen to be variable it is also possible that the siRNA oligonucleotides have been partially degraded or oligonucleotide delivery has been compromised resulting in low transfection efficiency. Under these circumstances optimal knock down would not be attainable. To continue analysing protein knockdown using these oligonucleotides new batches were purchased of *DISC1* siRNA #2 and #5 and also of the non-targeting negative control siRNA. These oligonucleotides were purchased conjugated to a fluorescent FAM or Cy3 label to allow analysis of transfection efficiency and protein knockdown by immunofluorescence microscopy. A further DISC1 antibody (α-DISC1) designed to the C-terminus of DISC1 was also employed to analyse protein knockdown.

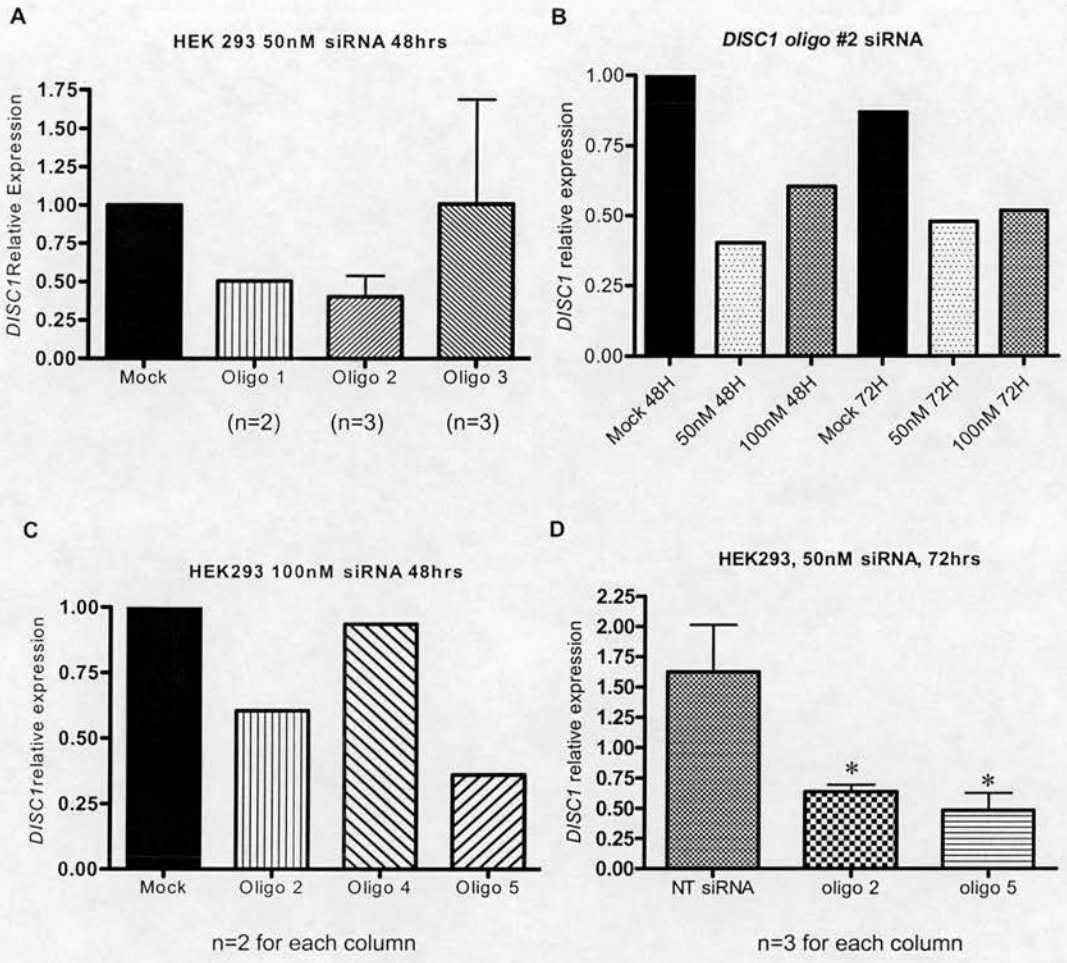

Figure 5.3.A-D. These graphs show data representative of RNAi induced *DISC1 mRNA* knockdown in HEK293 cells. Using 50nM siRNA, 48 hours post transfection, *DISC1* siRNAs #1 and #2 produced approximately 50% reduction in *DISC1* mRNA levels whereas siRNA #3 inconsistently knocked down *DISC1* expression **(A)**. 100nM of siRNA oligo #2 did not produce more pronounced knockdown than 50nM siRNA **(B)**. *DISC1* siRNA #4 failed to induce *DISC1* knockdown however siRNA #5 knocked down *DISC1* levels efficiently **(C)**. *DISC1* siRNAs #2 and #5 were further shown to induce *DISC1* mRNA knockdown in comparison to a non-targeting (NT) negative control siRNA **(D)**. This knockdown was statistically significant as determined by Anova with post hoc Newman-keuls test, *$p<0.05$ (GraphPad prism).

5.4 Fluorescently labelled *DISC1* siRNA oligonucleotides knock down endogenous DISC1 protein

5.4.1 FAM and Cy3 labelled DISC1 oligonucleotides knock down endogenous DISC1 *protein*

Oligonucleotides #2 and #5 were conjugated to FAM (green) or Cy3 (red) fluorescent tags to allow visualisation of oligonucleotides in transfected cells. Using this method it is possible to track transfected cells and examine individual cellular phenotypes in addition to examining whole cell populations. The lipofectamine 2000 reagent was used to deliver the oligonucleotides to HEK293 cells. It was decided to change from the siPORT transfection reagent as oligonucleotides were more visible by fluorescent microscopy after transfection using the lipofectamine reagent. This is most likely due to the mechanism of delivery of the oligonucleotides into the cell (see section 5.4.2).

Before immunofluorescent analysis was carried out, SDS-PAGE followed by western blotting was used to analyse the ability of the labelled oligonucleotides to induce protein knockdown following transfection with lipofectamine. It was shown previously that the oligonucleotide #2 (unlabelled) was capable of inducing exogenous FLAG-DISC1 knockdown using lipofectamine, however this oligonucleotide had not been tested for endogenous DISC1 knockdown using this reagent and oligonucleotide #5 had not previously been tested using lipofectamine for delivery.

Transfections were carried out in 12 well plates as previously described. Cells were transfected with an siRNA pool consisting of *DISC1* oligonucleotides #2 and #5 but a 50nM final transfection concentration was maintained. A DISC1 C-terminal antibody (α-DISC1) was used to determine knock down of the endogenous protein. This antibody was chosen as existing aliquots of the N-terminal antibody (R47) had lost affinity for the endogenous DISC1 protein. This C-terminal antibody detects full length DISC1 and long variant DISC1 at approximately 90-100kDa (*Ogawa et al. 2005*).

Cy3 labelled *DISC1* oligonucleotides #2 and #5 clearly induced DISC1 protein knockdown at 24, 48 and 72 hour time points. At 48 hours post transfection, FAM labelled oligonucleotides also showed clear knock down of DISC1 (Figures 5.4.A and B).

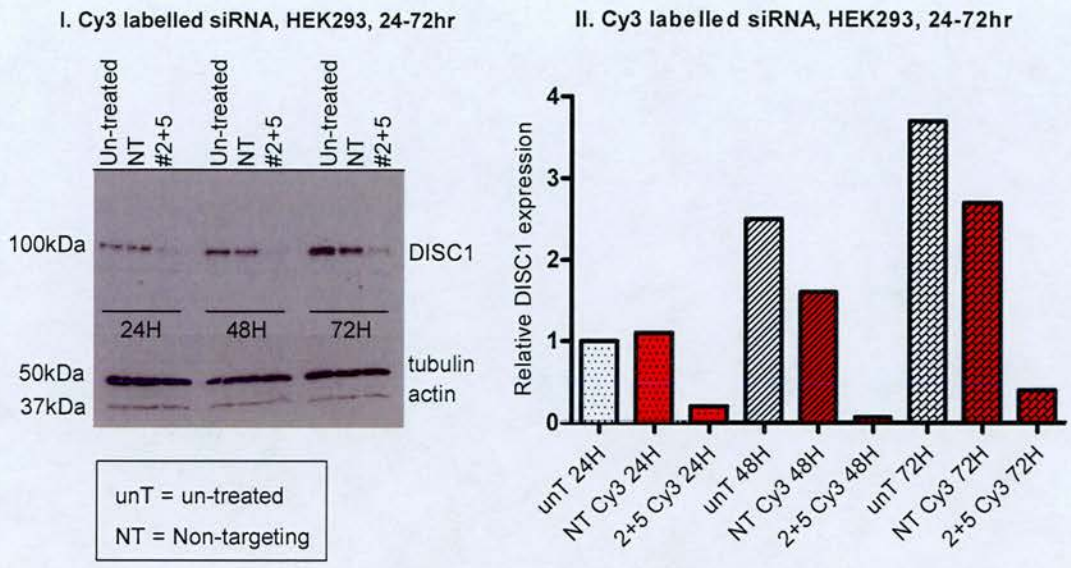

Figure 5.4.A *DISC1* siRNAs labelled with Cy3 fluorescent dye retain their ability to induce DISC1 protein knockdown when delivered using lipofectamine **(I)**. This protein expression data is represented graphically using the Image J densitometry program. Samples are normalised using α-tubulin and β-actin and are scaled relative to the un-transfected control lysate at 24 hours **(II)**.

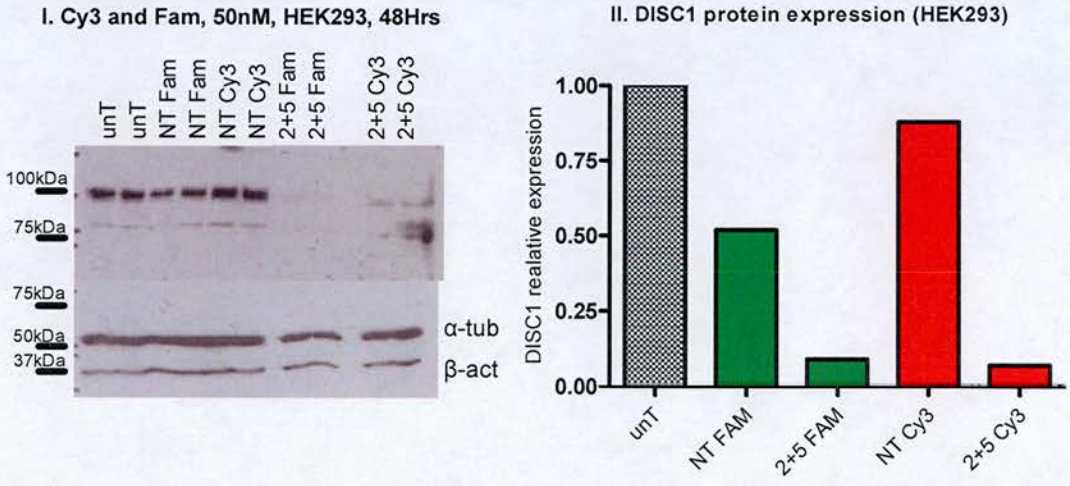

Figure 5.4.B FAM labelled and Cy3 labelled *DISC1* siRNAs reduce DISC1 expression at 48 hours post transfection using lipofectamine **(I)**. Protein expression values were quantified with the Image J densitometry program using α-tubulin and β-actin to normalise **(II)**. This graph shows the average of two replicates in each column scaled relative to the un-transfected control lysates.

5.4.2 Fluorescent microscopy optimisation for analysis of siRNA oligonucleotide delivery into HEK293 cells

To determine successful siRNA oligonucleotide delivery, cells were analysed by fluorescent microscopy 24-48 hours post transfection. Cells were fixed using 4% paraformaldehyde (PFA) and a FITC filter was used to excite the FAM label. Using *GAPDH* FAM labelled control oligonucleotides, siPORT and lipofectamine demonstrated the ability to deliver siRNA oligonucleotides successfully into HEK293 cells at 24 hours post transfection. The oligonucleotides showed a very different pattern of distribution depending on the transfection reagent used. Figure 5.4.C shows FAM labelled oligonucleotides within HEK293 cells 24 hours post transfection using both transfection reagents. Lipofectamine results in a bright punctate pattern of oligonucleotides within the transfected cells whereas siPORT results in a more diffuse pattern of oligonucleotides within the cytoplasm. Although both reagents resulted in successful delivery further analysis revealed that the oligonucleotides were more clearly visible when delivered using lipofectamine. This reagent also resulted in more consistent DISC1 protein knockdown as determined by SDS-PAGE and western blotting. Therefore, analysis of cellular RNAi phenotypes using HEK293 cells was initially carried out by transfecting oligonucleotides with lipofectamine at a concentration of 50nM for 48 hours. Fixation using PFA generally resulted in better visualisation of the oligonucleotides as methanol quenches the FAM signal. A cell number of 0.5 x 10^5 was determined as the optimal plating conditions for a 12 well plate to allow analysis of individual cell phenotypes 48 hours post transfection.

Non-targeting control oligonucleotides were transfected in parallel to control for non-specific phenotypes as a result of siRNA transfection. Unfortunately upon microscopic analysis there was slight toxicity resulting from the transfection procedure. Transfection reagent and siRNA concentrations were titrated further to avoid non-specific phenotypes as a result of toxicity. A concentration of 10nM *DISC1* siRNA was subsequently tested and deemed to be sufficient to induce DISC1

protein knockdown (Figure 5.4.D.). This siRNA concentration was used for subsequent transfections.

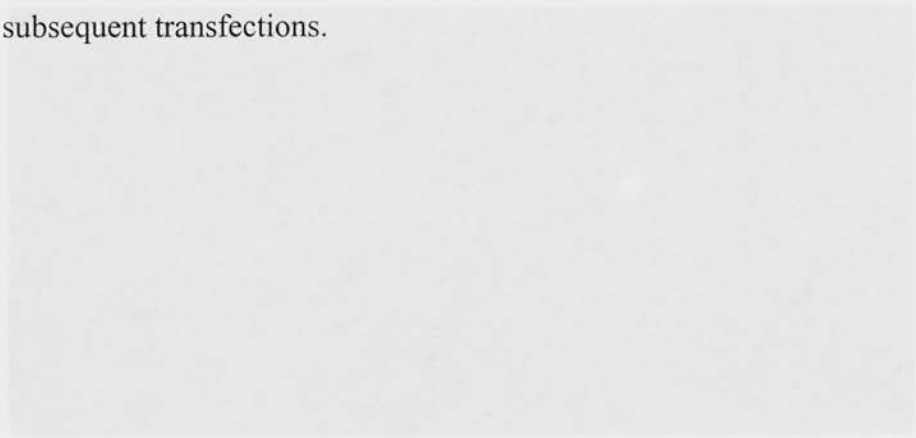

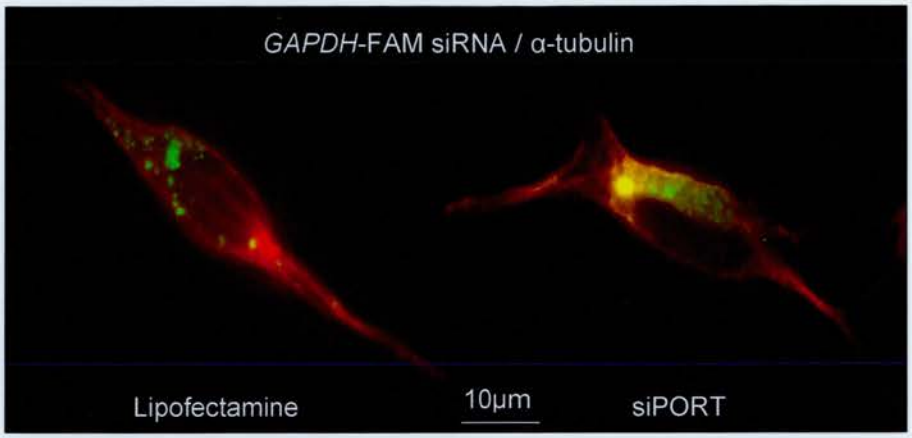

Figure 5.4.C. This figure shows imunofluorescent anaysis of siRNA delivery into HEK293 cells. FAM labelled *Gapdh* siRNA is visualised using a FITC filter (green) and cells were co-stained for Alpha Tubulin (red). Both lipofectamine and siPORT are shown to deliver *Gapdh* siRNA into HEK293 cells. Images are at 100 times magnification.

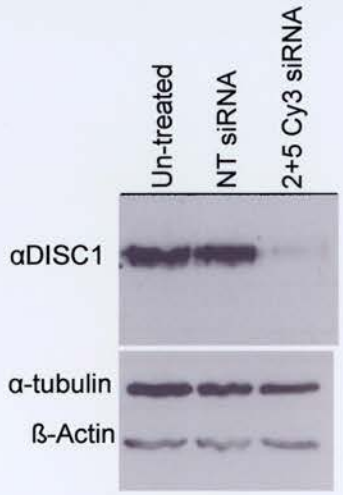

Figure 5.4.D. 10nM *DISC1* siRNA is sufficient to induce protein knockdown 48 hours post transfecting using lipofectamine.

5.5 Discussion

This chapter describes the experimental procedures used to achieve optimal *DISC1* knockdown via siRNA induced RNA interference. Five siRNA oligonucleotides were designed along the length of the *DISC1* gene. Two of these oligonucleotides successfully and consistently knocked down *DISC1* expression. Oligonucleotide #2 was designed to the 3'UTR of *DISC1* and oligonucleotide #5 was designed to exon 2, the largest exon of the *DISC1* gene. These oligonucleotides demonstrated successful knock down of exogenous FLAG-DISC1 protein and endogenous *DISC1* at the level of mRNA and protein. These oligonucleotides produced prominent protein knock down at 48-72 hours post transfection using concentrations of 10-50nM. These experiments were controlled using a non-targeting scrambled siRNA oligonucleotide which should not target any mammalian gene. This oligonucleotide did not show reduction in *DISC1* gene expression below the levels of mock treated cells.

Classical RNAi results in reduced gene expression detectable at the mRNA and protein level. Some siRNAs may also induce gene silencing by translational repression only. Both *DISC1* siRNA oligonucleotides #2 and #5 possessed the ability to knock down *DISC1* mRNA and protein levels and therefore the response elicited by these oligonucleotides is a classical RNAi response.

One caveat to these experiments is that there were low levels of correlation between mRNA and protein levels in some cases, with protein levels appearing to diminish before mRNA levels in one case. This was however not a consistent finding and therefore these discrepancies are considered to be due to difficulties in comparing gene expression data that has been collected in different ways and also due a loss of affinity of the R47 N-terminal DISC1 antibody for endogenous DISC1.

The amount of siRNA used in RNAi interference experiments can vary greatly depending on the gene being targeted. The oligonucleotides used in these experiments were commercially available and came with a guarantee to knock down gene expression greater than 70% if 100nM concentrations were used and gene expression was analysed at 48 hours post transfection. This is a huge

oversimplification of the RNAi process because it is possible to saturate the siRNA RISC complex (*Hutvagner et al. 2004*). Using a higher concentration of oligonucleotides than is actually needed will not result in further reductions in gene expression. Furthermore RNAi is a normal physiological process and 'hijacking' the RNAi machinery using siRNAs may prevent normal cellular functioning thus resulting in aberrant cellular phenotypes. Excess siRNA has been shown to have many adverse effects such as off-target gene silencing, induction of the interferon response and stimulation of non-specific RNA degradation (*Barik, 2006*). Moreover over-saturation of the RNAi pathway has been shown to be lethal in adult mice (*Grimm et al. 2006*). It is therefore desirable to titrate siRNA concentrations as much as possible to reduce the likelihood of undesirable side-effects. Indeed *DISC1* siRNA oligonucleotides were seen to produce good levels of knockdown when used at half to one tenth the recommended concentration and using higher siRNA concentrations did not increase the levels of DISC1 knockdown. The phenotypic outcomes of *DISC1* RNAi in mammalian cells are presented and discussed in chapter 6.

Chapter 6

RNA interference for the DISC1 gene

6.1 Preface

This chapter describes pilot experiments analysing the effects of DISC1 knockdown in HEK cells using RNA interference. I have shown using quantitative Real-Time PCR and polyacrylamide gel electrophoresis techniques that the most likely mechanism of disease pathogenesis operating within the t(1;11) family is one of haploinsufficiency for *DISC1*. To test the hypothesis that reductions in *DISC1* expression may lead to cellular defects, I have utilised RNA interference technology to artificially induce knockdown of *DISC1* gene expression. The optimisation protocols for these experiments are detailed in chapter 5. Knocking down *DISC1* gene expression by 50% should suffice to mimic the effect of the t(1;11) translocation in the t(1;11) family. This RNA interference protocol knocks down DISC1 protein expression by 50% or more and hopefully will give essential clues as to the normal functions of DISC1 at the cellular level.

During the course of these experiments there have been two published studies of RNA interference for *DISC1*. *Kamiya et al. 2005* used *in utero* electroporation to deliver short hairpin RNAs into the developing mouse brain. The authors analysed phenotypes of migrating neurons and found that knocking down *DISC1* expression 'virtually inhibited' neuronal migration. They also used an *in vitro* system in which they over-expressed the hypothetical 'mutant' DISC1 protein, that is predicted to arise from *DISC1* truncation by the t(1;11) translocation. From these experiments they drew the conclusion that the 'mutant' DISC1 protein inhibits the interaction of full length DISC1 with NUDEL, LIS1 and $p150^{glued}$. These proteins are components of a conserved nuclear migration pathway which is an important feature of neuronal migration. The authors make the link between the effects of RNAi on neuronal migration and the effects of the 'mutant' DISC1 protein on the LIS1/NUDEL/$p150^{glued}$ interaction, postulating that inhibition of neuronal migration is a result of perturbations in this nuclear migration pathway. It is possible that these

neuronal migration phenotypes do arise in this manner however, this study did not analyse directly the effects of RNAi on these protein interactions but rather the effects of the 'mutant' DISC1 protein. As my experimental data have shown that this 'mutant' protein is undetectable in cells of t(1;11) patients it is still necessary to demonstrate these defects using an RNA interference approach.

Hashimoto et al. 2006 examined the effects of reduced DISC1 (by siRNA) in primary rat neuronal cultures on ERK (Extracellular signal-related kinase) and Akt (Protein kinase B) signalling as part of a study looking at DISC1 in major depression. The authors demonstrated a reduced abundance of the active phosphorylated form of ERK and Akt in *DISC1* siRNA treated rodent neuronal cultures (*Hashimoto et al. 2006*). This is an interesting finding as DISC1 has recently been reported to be involved in cAMP mediated signal transduction through direct interaction with the Phosphodiesterase 4B and PDE4 activity is modulated by ERK signalling (*Millar et al. 2005b, Houslay and Baillie 2003*).

Confirmation of the existence of DISC1 at the centrosome in chapter 4 opens up many additional possibilities for the functional consequences of knocking down DISC1. The centrosome has already been discussed in the context of neuronal migration but it also has many other vital roles. The centrosome is the microtubule organising centre of the cell and functions to generate and organise the α/β-tubulin microtubule network (*Doxsey 2001*). The centrosome and microtubules are essential for many aspects of cell survival including intracellular transport (of organelles and molecules) and cell proliferation (*Doxsey 2001, Doxsey et al. 2005*). In addition to localising to the centrosome DISC1 has also been shown to be associated with microtubules via either a direct or indirect interaction with α-tubulin, a component of microtubules (*Morris et al. 2003*, *Brandon et al. 2004*). Therefore RNA interference for DISC1 may have cellular consequences through the inhibition of DISC1 function at the centrosome or through interfering with interactions between DISC1 and microtubules.

DISC1 is also localised to the mitochondria; however as discussed in chapter 4, the specific isoforms of DISC1 localised at the centrosome and the mitochondria appear to differ. The mitochondrion is an important organelle as it drives cellular energy production. The mitochondrion is an especially important organelle for brain function as this organ has very high energy demands and mitochondrial dysfunction has been implicated in many brain disorders (*Wallace 1999, Schon 2000*). The mitochondrion is also critical for regulation of intracellular calcium levels and some interesting interactions between DISC1 and cAMP signalling molecules at the mitochondria have been published recently (*Babcock and Hille 1998, Millar et al. 2005b*). One additional important function carried out by the mitochondria is induction of apoptosis as a result of cellular insult (*Green et al. 1998*).

In this chapter I have examined the effects of reduced *DISC1* expression on cell proliferation, cell cycle progression and microtubule network organisation which may be hampered as a result of depletion of centrosomal DISC1. I have also examined the effects of reduced *DISC1* expression on mitochondrial morphology, apoptosis and cellular cAMP signalling. The functions of centrosomal DISC1 and mitochondrial DISC1 are however not mutually exclusive and depletion of either may impact on cAMP signalling and cell survival.

6.2 Analysis of DISC1 knockdown on cell cycle progression, cell proliferation and apoptosis

6.2.1 Reduced DISC1 expression does not affect cell proliferation as measured by BrdU incorporation

The percentage of dividing cells in a population was quantified by analysing the incorporation of 5-bromo-2'-deoxyuridine (BrdU). BrdU is a thymidine analog that can incorporate into the replicating DNA of actively dividing cells. This is then coupled with immunodetection using a monoclonal anti-BrdU antibody for detection of cells with labelled DNA. By pulsing cell populations for a short period of time (typically 30 minutes to 1 hour) only cells that are within S phase of the cell cycle will be labelled. I used a commercially available BrdU labelling kit which uses a

fluorescein conjugated BrdU antibody for detection. After immunodetection of BrdU the cell population was analysed by flow cytometry. The BrdU conjugated fluorescein is excited at a wavelength of 488nm and this identifies the percentage of actively dividing cells in the population. I used this technique to analyse both lymphoblastoid cell lines derived from members of the t(1;11) translocation family and cells with artificially induced DISC1 knockdown. Protocol details can be found in chapter 2.

6.2.1.1 Lymphoblastoid cell lines derived from t(1;11) family members do not show reduced proliferation as a result of translocation

Lymphoblastoid cell lines were fed daily for three days before labelling with BrdU. The cells were pulse labelled with BrdU for 40 minutes at 37°C using a final concentration of 10μM BrdU. After 40 minutes the cells were spun down and washed in fresh cell culture medium prior to the immunodetection procedure. After immunodetection (detailed in chapter 2) cells were resuspended in PBS and analysed by flow cytometry.

Two cell lines possessing a normal karyotype were analysed and three cells lines possessing the t(1;11) translocation were analysed. This experiment was performed twice independently. 10,000 cells were analysed for each cell line as depicted in the sample dot plots shown in figure 6.2.A (A). This figure presents the flow cytometry generated dot plots representing normal and translocation carrying cell lines. Non-proliferating cells are coloured black and proliferating cells are coloured green.

Although there were differences in the percentage of dividing cells between the two independent experiments there was no difference in the percentage of dividing cells between translocation carrying cell lines and normal karyotype controls within each experiment (Table 6.2.A (B)). The upper panel of table 6.2.A (B) shows representative values of the number of dividing cells (S phase) in translocation and non-translocation populations. The presence of the translocation does not appear to alter the rate of proliferation of these cells.

6.2.1.2 Artificially inducing DISC1 knockdown using RNA interference does not reduce cell proliferation in HEK293 cells

HEK293 cells were transfected with a 50nM concentration of siRNA to knock down the expression of *DISC1* (pooled oligonucleotides #2+#5). Each treatment group (i.e. non-transfected, non-targeting siRNA transfected and *DISC1* siRNA transfected) was performed 6 times in replicate. After 72 hours cells were pulse labelled with 10 μM BrdU. Labelled cell populations were then pooled for each treatment group and analysed by flow cytometry as described above. 10,000 cells in each treatment group were counted and the proportion of BrdU positive cells deduced from this. Table 6.2.A (B) (bottom panel) shows the proportion of dividing cells in the non-targeting (NT) siRNA transfected population and *DISC1* siRNA transfected population. The reduction in DISC1 expression was analysed by western blotting using α-tubulin and β-actin to normalise protein loading. Figure 6.2.A (C) depicts the level of DISC1 knockdown achieved in this experiment. From this experiment we can deduce that a high level of transfection efficiency was obtained and knockdown of DISC1 at the protein level is substantial but this does not lead to gross changes in the proportion of proliferating cells. Although 6 replicates of each treatment group were used in this experiment the protocol requires a high number of cells and therefore the replicates were pooled for analysis. In order to perform statistical analyses this experiment should be repeated. Furthermore it was noted that a high level of background was present in the antibody only control group which did not receive BrdU and this may have implications for the results of this experiment. For these reasons additional experiments which analysed cell cycle progression following siRNA transfection were carried out.

A

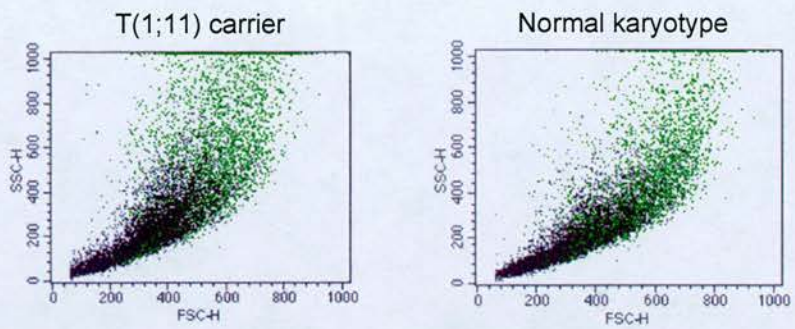

Green = BrdU positive cells

B

% BrdU incorporating lymphoblastoid cells			
Translocation Carriers		Normal karyotype controls	
T1	32.84 %	N1	31.15 %
T2	22.17 %	N2	22.65 %
T3	22.84 %		
% BrdU incorporating cells post siRNA treatment			
NT	23.64 %	DISC1	24.91 %

C

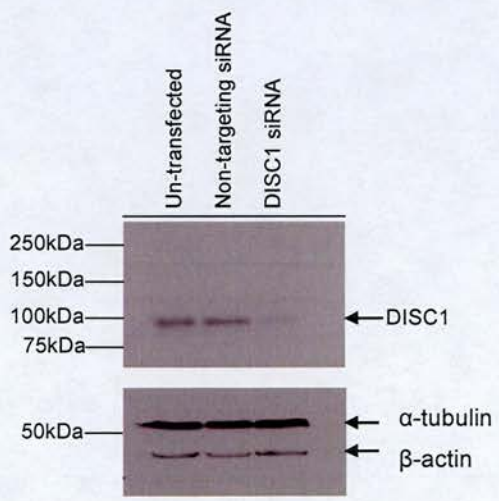

Figure 6.2.A. Analysis of BrdU incorporation by t(1;11) family member cell lines demonstrated no significant difference between the rate of proliferation in translocation carrying cell lines and normal karyotype controls (A + B). Furthermore artificially inducing DISC1 knockdown does not produce gross abnormalities in cellular proliferation (B + C).

6.2.2 Analysis of cell cycle progression following siRNA induced DISC1 knockdown

Analysis of DNA content per cell is an established method for determining cell cycle stage in a cycling population. This method uses fluorescent DNA intercalating agents which when incorporated into DNA can give a measure of the total DNA content per cell. In these experiments I used propidium iodide (P.I.), an analog of ethidium bromide, which can intercalate with double stranded RNA and DNA. Detailed protocols and references are documented in chapter 2. These experiments use flow cytometry to analyse the amount of P.I. staining which is a direct reflection of the amount of DNA per cell. Prior to mitosis cells in G_1 phase are diploid (2N). Once these cells enter S phase they replicate their DNA eventually possessing twice the amount of DNA per cell (4N) before entering mitosis to produce two daughter cells (2 x 2N). These properties of DNA content are used to determine the cycle stage of each cell.

Using this method there is expected to be some overlap in the P.I. staining between distinct phases. For example cells that have just begun S phase will be difficult to distinguish from G_1 phase cells as their DNA content will differ only slightly. Similarly cells nearing completion of S phase will have almost the same DNA content as cells in G_2 phase and therefore some overlap occurs here also. MultiCycle advanced DNA cell cycle analysis software was used to analyse the DNA histogram plots produced by the flow cytometric measuring of P.I. staining and separate out the distinct cycling populations.

HEK293 cells were transfected with 50nM of a non-targeting siRNA oligo or 50nM *DISC1* siRNA (pooled oligos #2 + #5). Within one pilot experiment conducted each treatment was carried out in duplicate and cells were harvested 48 hours post siRNA transfection. After harvesting these cells were incubated in a hypotonic solution with P.I. to stain total cellular DNA. This protocol incorporates a Ribonuclease A step which removes dsRNA from the population being stained so we can be sure that only the DNA is being measured. P.I. was measured by flow cytometry using the FL3 detector and histogram distributions representing DNA content per cell were

generated. 10,000 cells were measured for each treatment group. This histogram plot was exported to the DNA analysis software to determine the percentage of cells within each phase of the cell cycle. Figure 6.2.B (A) depicts the histogram plot generated by the flow cytometry program and (B) represents this same plot following analysis to separate out each population. This histogram plot is from un-transfected HEK293 cells which were processed alongside the experimental samples. The cell cycle stages corresponding to the distribution peaks and troughs are marked on histogram A.

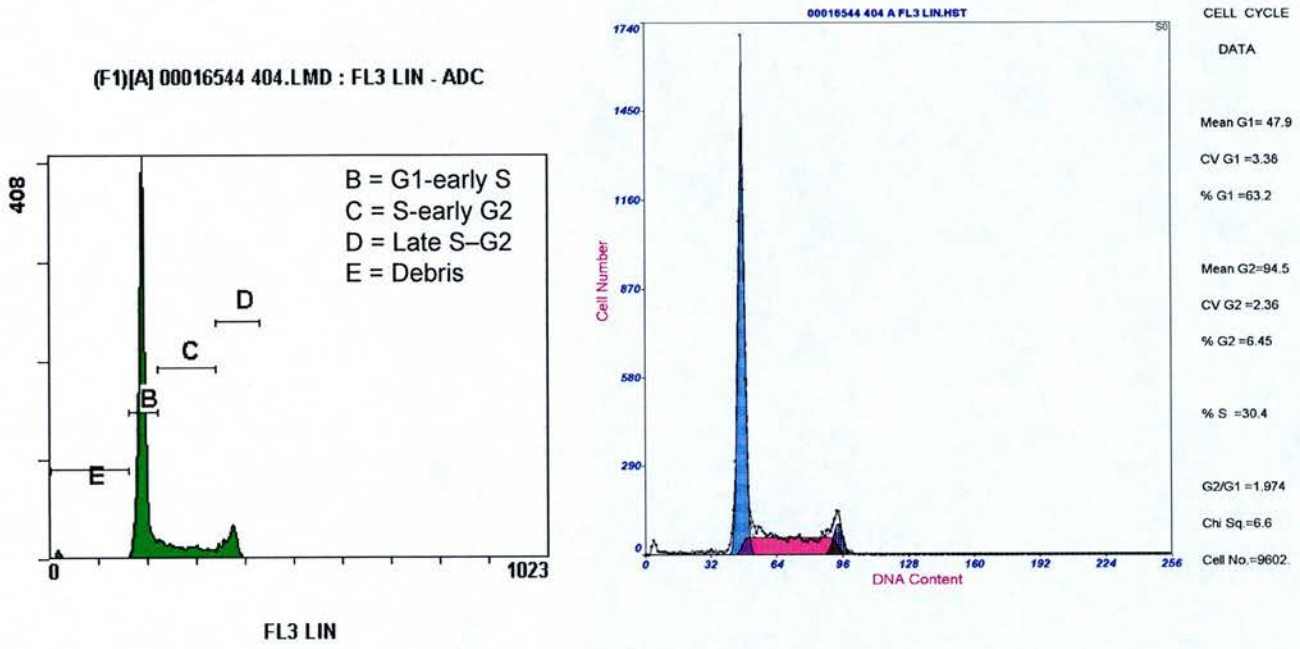

A. Histogram plot of PI staining

B. MultiCycle Analysis of cell cycle

Figure 6.2.B. This figure shows DNA content histogram plots from un-transfected HEK293 cells. Histogram A is generated by the flow cytometry program. Following analysis using the MultiCycle DNA analysis software a histogram plot as seen in B is generated and the percentage of cells within each phase of the cell cycle is calculated.

Western blots carried out on replicate samples demonstrated substantial reductions in DISC1 protein levels between non-targeting siRNA transfected groups (NT siRNA) and *DISC1* siRNA transfected groups (Figure 6.2.C (A)). Values obtained from cell cycle analysis of each sample are graphed in figure 6.2.C (B). Graphs are shown for G_1, S and G_2 stages of the cell cycle. Apoptosis was not measured in this analysis as this experiment was performed separately. There were no substantial differences between the un-transfected (unT) groups and NT siRNA or DISC1 siRNA transfected groups in any of the cell cycle phases. There does however appear to be a small increase in the number of cells within the G_1 phase in the DISC1 siRNA treated group in comparison to the NT siRNA transfected group. Although each treatment was carried out in duplicate these values are from one pilot experiment, thus not permitting statistical analysis. The number of *DISC1* siRNA transfected cells within the S phase also appears to be slightly decreased in comparison to the NT siRNA treated group which would be in concordance with an increased number of cells stalled within the G_1 phase. Although these findings are potentially interesting indicating that DISC1 may play a role in regulation of the cell cycle independent replication is required.

As western blotting from these lysates demonstrated a substantial reduction of DISC1 protein within the *DISC1* siRNA treatment groups differences in the cell cycle profiles of these populations are likely to be a result of reduced levels of the DISC1 protein. The observed differences are however small and need to be replicated in two additional independent experiments to confirm these results. Furthermore, it is important to note that these cell populations are not synchronised and have been analysed at 48 hours post transfection only. Analysis at longer time-points and using synchronised cultures may lead to more apparent differences in the cycling profiles and should be considered for future experiments.

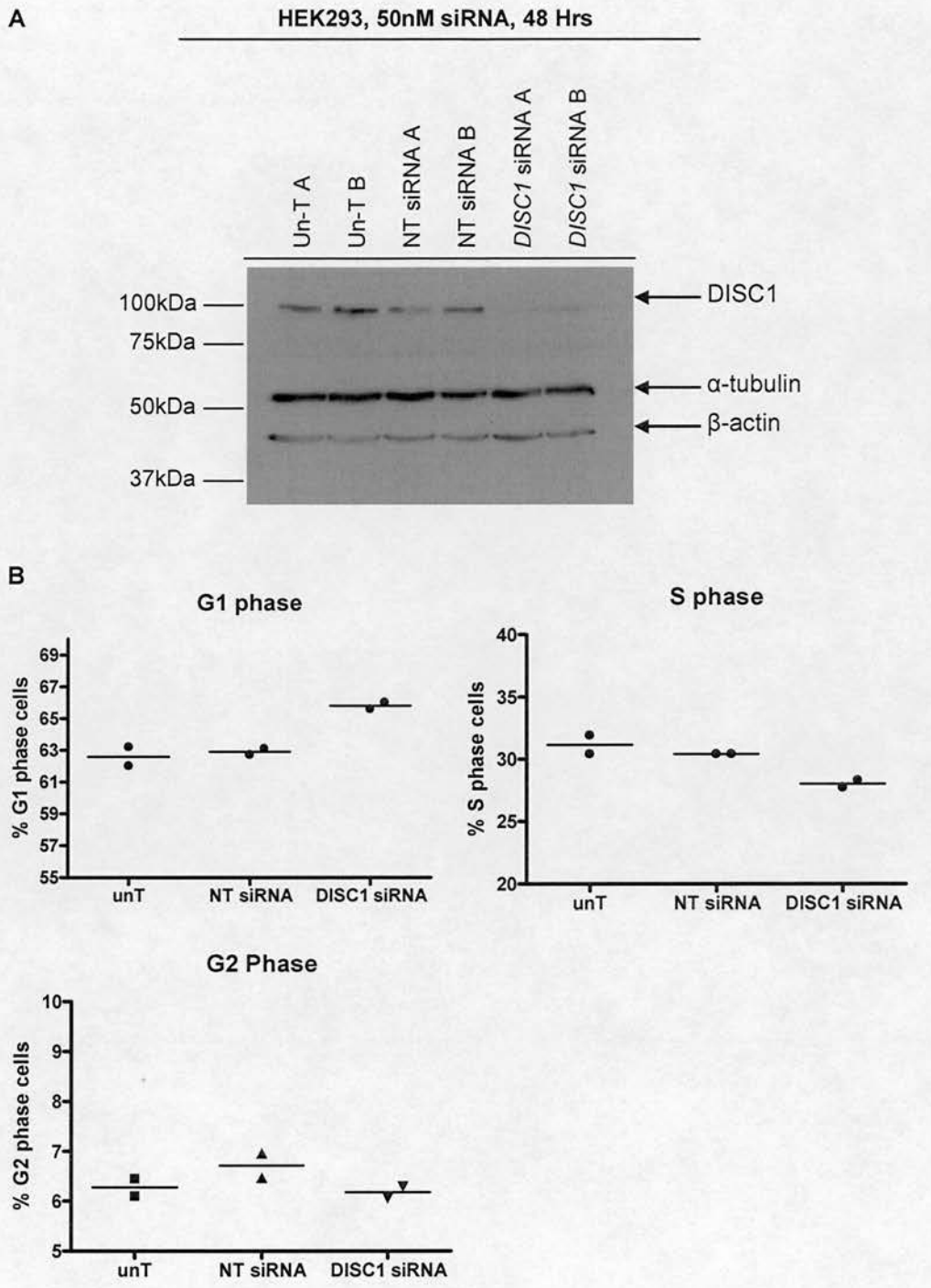

Figure 6.2.C. Data from one pilot experiment examining the cell cycle profile post siRNA treatment. Western blotting of two replicate samples from each treatment group determined substantial knockdown of DISC1 protein levels in comparison to un-transfected cells and non-targeting siRNA transfected cells (NT siRNA) **(A)**. This knockdown of DISC1 resulted in small changes in the cell cycle profile of these treatment groups **(B)**. However these values are only from one representative experiment and need to be repeated to confirm any changes that might occur.

6.2.3 Analysis of apoptosis following DISC1 knockdown

Apoptosis is an essential physiological process required for development and to eliminate abnormal cells from an otherwise healthy population. As the mitochondrion is an important organelle for inducing apoptosis I was interested to see if apoptosis was affected in *DISC1* siRNA treated cell populations. During apoptotic cell death dying cells translocate the membrane phospholipid phosphatidylserine (PS) to the outer leaflet of the cell membrane. Techniques which analyse apoptosis generally take advantage of this by using the phospholipid binding protein Annexin V that binds to PS on the membrane surface of apoptotic cells. I used a commercially available kit that uses Annexin V conjugated to a FITC fluorophore. Annexin V staining is usually combined with P.I. staining to identify cells with a disrupted cell membrane i.e. late stage apoptotic or necrotic cells. P.I. will not permeate early apoptotic cells. Therefore this technique allows the identification of early apoptotic cells with Annexin V bound to PS on the outer membrane, late stage apoptotic cells with Annexin V bound to PS that will also take up the vital dye P.I., and necrotic or dead cells which will only take up P.I.

Three treatment groups were analysed, mock transfected, non-targeting siRNA transfected (NT siRNA) and *DISC1* siRNA transfected, each of which was performed in triplicate, within one pilot experiment. By this stage further optimisation of the siRNA transfection process had demonstrated that 10nM siRNA is sufficient to induce DISC1 knockdown. For this experiment HEK293 cells were treated with siRNA at a final concentration of 10nM and analysed 48 hours post transfection. After harvesting cells were incubated with Annexin V-FITC and P.I. as described in chapter 2 and were analysed by flow cytometry. Figure 6.2.D (A+B) shows dot plots generated from the flow cytometry procedure. Un-stained HEK293 cells were used to set detectors for the FL1 (Annexin V-FITC) and FL3 (propidium iodide) channels. The dot plot in figure 6.2.D (A) shows these un-stained cells. All cells sit within the bottom left quadrant (A3) and represent healthy cells. The dot plot in figure 6.2.D (B) depicts a mock transfected cell population stained with Annexin V-FITC and propidium iodide. Quadrant A1 detects red stained cells only (i.e. necrotic or dead cells), quadrant A4 detects green cells only (i.e. early apoptotic

cells) and quadrant A2 detects cells which are both green and red (i.e. late apoptotic cells). Green or red detection is indicated by either red or green shapes surrounding the cell populations in each quadrant.

20,000 cells were counted by flow cytometry for Annexin V-FITC and P.I. staining in each group and the quadrant statistics were analysed to determine whether there were any differences in the number of dying cells, or indeed the progress of apoptosis between the treatment groups. The first thing that was apparent from this experiment was that a lot of cell death had occurred in the mock transfected cell population indicating either an unhealthy cell population to begin with or a highly toxic transfection procedure. For the purposes of further experimentation the amount of transfect agent used was titrated further to avoid possible toxicity. The data from the individual quadrants was used to create graphs representing the number of viable cells, early apoptotic cells and late apoptotic cells. These graphs are shown in figure 6.2.D (C, D and E). Within this pilot experiment there were no significant differences between the replicate values (n=3) for the mock transfected group and the NT siRNA transfected group in either the percentage of viable, early apoptotic or late apoptotic cells. However there were significant differences in all three categories between the replicate values from the NT siRNA transfected cells and *DISC1* siRNA transfected cells. Within the *DISC1* siRNA transfected cell populations there were significantly more viable cells in addition to significantly reduced numbers of early and late apoptotic cells in comparison to the NT siRNA cell populations (two-tailed t-test, $*p < 0.05$). The extent of DISC1 protein knockdown was determined by western blotting and densitometry analysis (Figure 6.2.E (A+B)). Although there was variability in the DISC1 levels within triplicates of a given treatment group, the mean value of DISC1 in the *DISC1* siRNA transfection group is far reduced in comparison to the NT siRNA transfected controls. All three *DISC1* siRNA treated replicates had a higher percentage of viable cells and a lower percentage of both early apoptotic and late apoptotic cells. However, these are within experiment replicates and independent replications of this experiment need to be conducted. These results suggest that DISC1 may have a role in apoptotic signalling and that knock down of DISC1 may result in a block in apoptosis under stressful or toxic conditions.

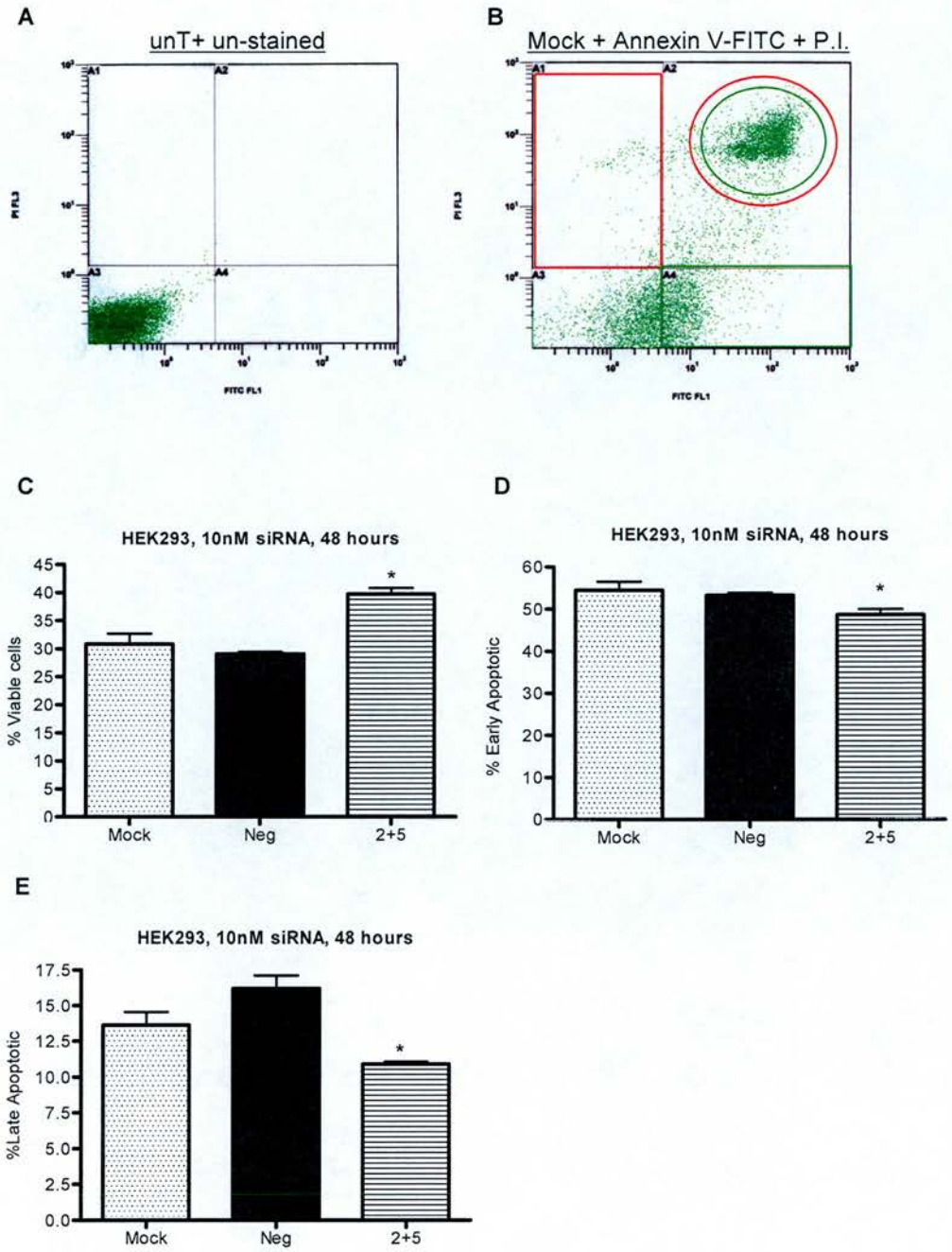

Figure 6.2.D. This figure shows data from one pilot experiment (N=1) analysing apoptosis post DISC1 siRNA treatment (n=3 per treatment group). Un-stained cells were used to set the baseline FL1 and FL3 levels **(A)**. Mock transfected cells are shown as an example of a positively stained population **(B)**. The percentage of cells within each quadrant is graphed in figures **C-E**. Graphs show the mean and SEM of three replicates. *DISC1* siRNA transfection resulted in an increase in the number of viable cells **(C)** and a decrease in the number of both early and late stage apoptotic cells **(D and E)**. These differences were deemed to be statistically significant in comparison to the negative (neg) control (non-targeting siRNA) treated group (two-tailed t-test, *$p<0.05$). These values represent statistical analysis within one pilot experiment only and need to be replicated independently.

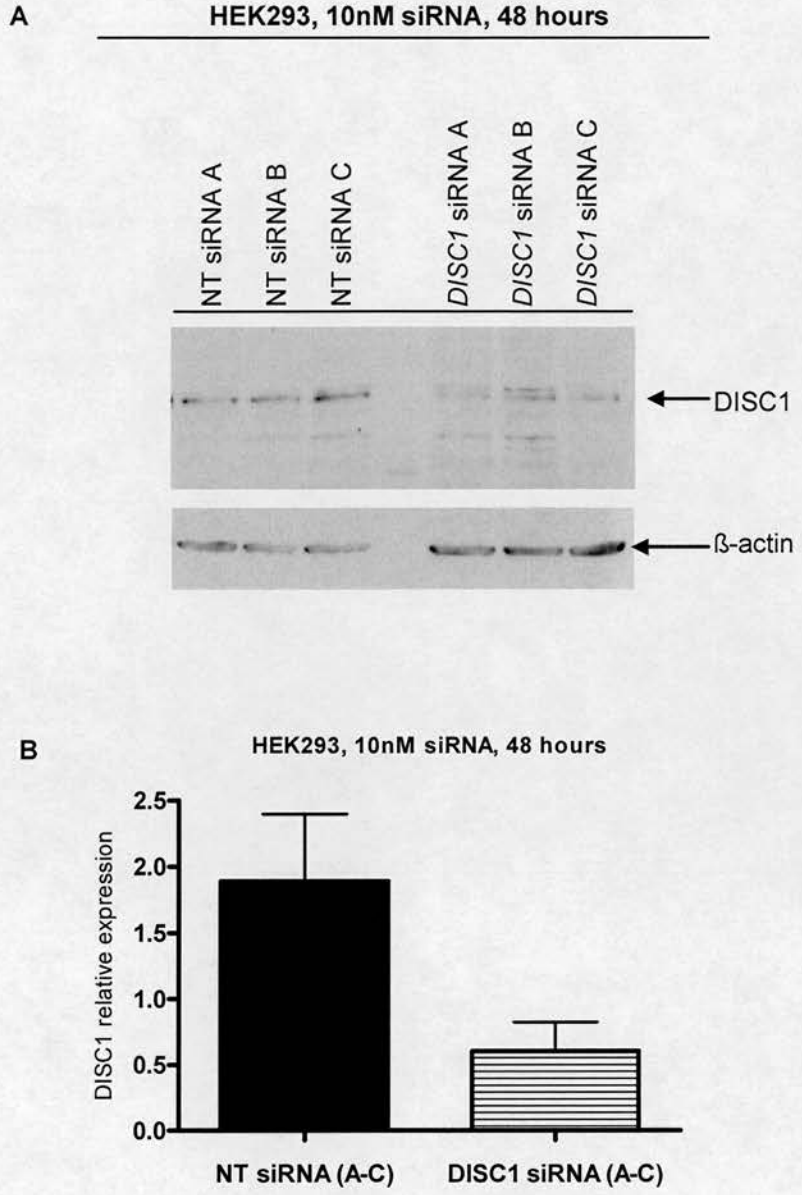

Figure 6.2.E. A decrease in the levels of DISC1 protein is apparent by western blotting of NT siRNA and *DISC1* siRNA lysates **(A)**. Protein loading was not equal between the individual lysates so densitometry analysis was performed to determine DISC1 protein levels. The mean and SEM values for the two groups are graphed **(B,** n=3 for each column). There is a large reduction in the mean value of DISC1 protein present within the *DISC1* siRNA treated samples. However there is variation between the replicates and this reduction does not reach statistical significance.

6.3 Reduction of DISC1 levels via RNAi has implications for cellular cAMP signalling

It has recently been published that DISC1 interacts with Phosphodiesterase type 4B (*Millar et al. 2005b*). Phosphodiesterases (PDEs) are the only means of quenching cAMP signalling within the cell (*Houslay and Adams 2003*). DISC1 is hypothesised to bind a low-activity un-phosphorylated form of PDE4B, which is then released upon phosphorylation by Protein Kinase A in response to elevated cAMP production (*Millar et al. 2005b*). As such I was interested to examine whether reductions in the levels of the DISC1 protein induced by *DISC1* siRNA would alter PDE4 specific hydrolysis of cAMP. To examine this I induced DISC1 knockdown in HEK293 cells using 10nM siRNA (pooled siRNAs #2 and #5) and measured the ability of PDE4 to hydrolyse cAMP 48 hours post transfection.

To do this I used tritium labelled cAMP (H^3-cAMP) which was incubated with fresh cell lysates containing endogenous phosphodiesterase activity. Active phosphodiesterases will hydrolyse the H^3-cAMP substrate to produce H^3-5'AMP, which is subsequently de-phosphorylated. The non-hydrolysed H^3-cAMP is then removed using a Dowex ion exchange resin by virtue of its negative charge so that only the hydrolysed H^3-AMP remains in the lysate. The level of hydrolysed H^3-AMP is then measured using a scintillation counter. For details of the assay protocol refer to chapter 2.

For this pilot experiment each treatment group was performed three times in replicate. Cells were plated in a 6 well tissue culture plate at a density of 1×10^5 and transfected 36 hours after plating. Cells were transfected using either 10nM of a non-targeting siRNA (NT siRNA) or 10nM of *DISC1* siRNA. 48 hours post transfection cells were harvested. Replicates for each group were pooled and the protein concentration was determined by taking the average of three optical density readings. 10μg of protein was used to assay the levels of cAMP hydrolysis in each experimental group. 10-20μg of protein was determined as the optimum lysate concentration from a PDE4 activity standard curve (data not shown) carried out on this cell type. The assay was performed in triplicate for each experimental group. A

control group which contained no lysate was included to estimate the background readings from the assay. For each experimental group and the control group cAMP hydrolysis was measured in both the presence and absence of rolipram (a specific PDE4 inhibitor). This enables us to determine the amount of cAMP hydrolysis resulting from PDE4 activity in comparison to total PDE activity within the cell.

The RNAi for DISC1 in the *DISC1* siRNA treatments groups was deemed successful by SDS-PAGE followed by immunoblotting (Figure 6.3.A (A)). Using this hydrolysis assay it was determined firstly that most of the phosphodiesterase activity in this cell type was due to members of the PDE4 family as rolipram reduced PDE activity to background levels (Figure 6.3.A (B)). Secondly transfection of *DISC1* siRNA resulted in dowregulation of PDE4 activity in comparison to non-targeting siRNA oligos (Figure 6.3.A (C)). This reduction was such that the levels of hydrolysis were comparable to the control groups. Figure 6.3.A, graph (D) shows PDE4 activity expressed as a percentage of activity seen in the NT siRNA treatment groups, using the highest value as 100%. PDE4 activity is reduced in the DISC1 siRNA treated group. It is noted that these analyses use only two values from the NT siRNA group as the PDE4 assay was not successfully completed for one sample. It is necessary to repeat this experiment to confirm these results.

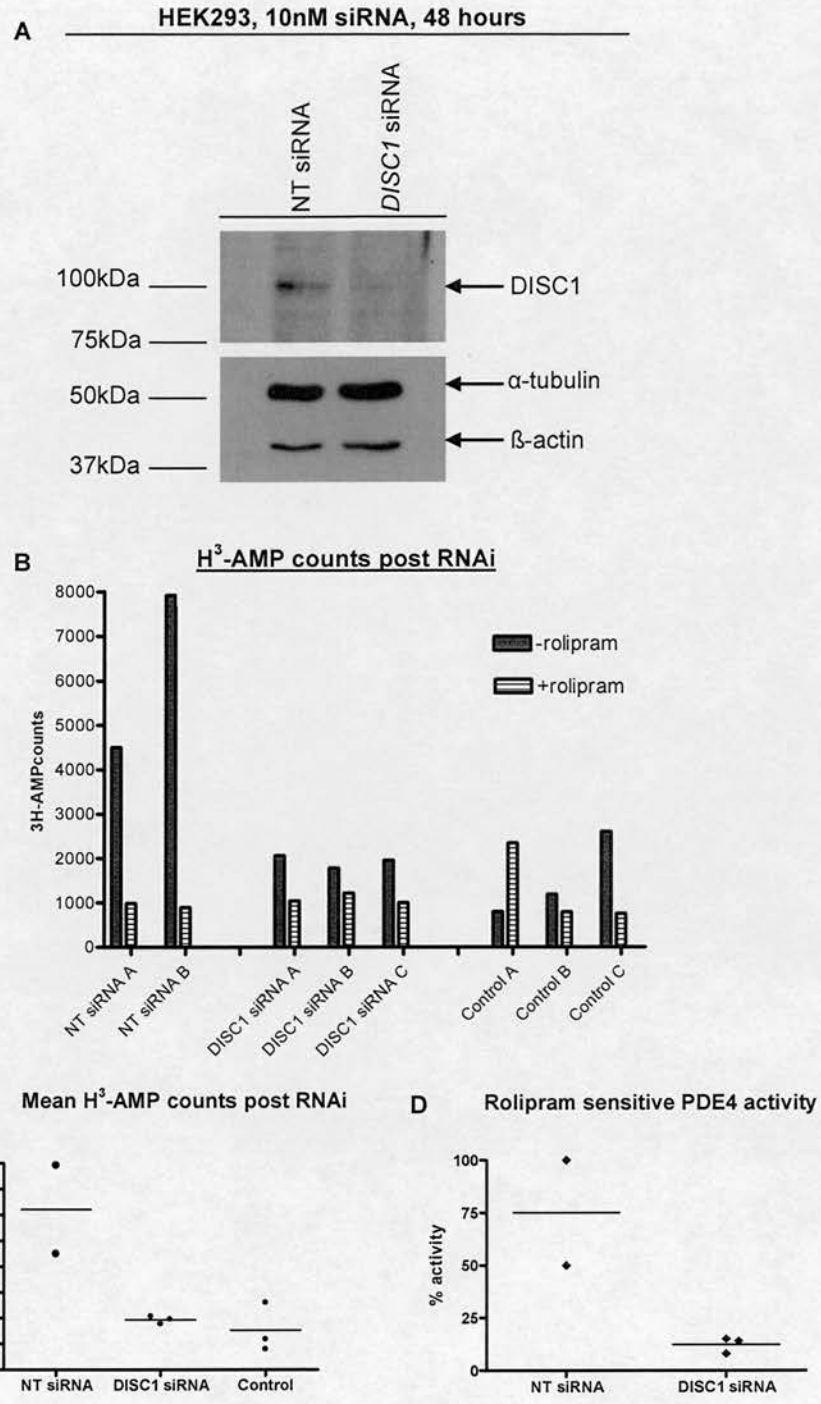

Figure 6.3.A. This figure represents data from one pilot experiment analysing PDE4 activity levels post DISC1 siRNA treatment. DISC1 protein levels are reduced 48 hours post RNAi **(A)**. PDE4 hydrolysis assays performed on these lysates demonstrate that PDE4 is the main phosphodiesterase activity present in HEK293 cells **(B)**. The mean level of cAMP hydrolysis is far lower in the DISC1 siRNA treated assay samples (n=3) compared to NT siRNA treated samples (n=2) **(C).** This reduction appears to be a result of decreased PDE4B activity **(D)**. Graphs show the mean or average of replicates for each group.

6.4 Examination of cellular phenotypes by fluorescence microscopy following DISC1 RNA interference

Studies of DISC1 knockdown by RNA interference have reported defects in localisation of various interacting proteins suggesting that DISC1 may have a role in anchoring or trafficking of certain cellular proteins. In particular *Kamiya et al. 2005* reported that reducing DISC1 expression by RNA interference resulted in defective neuronal migration and imply that this is a result of disruption of LIS1 and NUDEL and $p150^{glued}$ localisation at the centrosome. This implication is made on the basis that RNAi for DISC1 hampers neuronal migration and that over-expression of the 'mutant' DISC1 protein results in failure of LIS1, NUDEL and $p150^{glued}$ to accumulate at the centrosome and hinders neuronal migration (*Kamiya et al. 2005, Ozeki et al. 2003*). The authors did not however examine directly the localisation of these proteins in cells treated with shRNA for DISC1. This mutant protein was also shown to disrupt the β-tubulin microtubule network which may have further implications for cell morphology and neuronal migration. The effect of DISC1 on localisation of proteins important for neuronal migration is a particularly important aspect of DISC1 function considering the developmental hypotheses surrounding schizophrenia that involve hampered neuronal migration and aborization (*Harrison and Weingerber 2005*). For these reasons I have revisited some of these areas to assess the effects of reduced DISC1 on cell morphology of the microtubule network and centrosome structure.

As introduced previously mitochondrial dysfunction is also a feature of schizophrenia and considering DISC1's localisation to the mitochondrion I wished to examine the morphology and distribution of mitochondria in cells with reduced DISC1 protein. Furthermore the morphology of mitochondria has been shown to be altered in cells over-expressing DISC1 suggesting that DISC1 may play a role in mitochondrial fission and fusion (*Millar et al. 2005a*).

Except where stated all siRNA transfections were carried out using a final concentration of 10nM of either a non-targeting siRNA control oligonucleotide or pooled *DISC1* siRNA oligonucleotides #2 and #5.

6.4.1 Detection of DISC1 by fluorescence microscopy in RNAi treated cells

FLAG-DISC1 localises to a perinuclear location likely to correspond to the centrosome when over-expressed in SH-SY5Y cells. Localisation of exogenous FLAG-DISC1 was examined in SH-SY5Y cells transfected with FLAG-DISC1 alone or cells co-transfected with FLAG-DISC1 and *DISC1* siRNA #2 or #5. 72 hours post transfection cells were fixed and processed by immunofluorescence for FLAG-DISC1. Cells were examined by fluorescence microscopy. Four or five randomly chosen regions from each coverslip were counted for FLAG-DISC1 immunoreactivity at the centrosome. Of the cells transfected there was approximately 50% less cells possessing FLAG-DISC1 immunoreactivity at the centrosome in cells co-transfected with FLAG-DISC1 and siRNA for *DISC1* (Figure 6.4.A). As co-transfected cells that received FLAG-DISC1 should also have received the siRNA for *DISC1* it can be inferred that these siRNA oligonucleotides reduce exogenous DISC1 accumulation at the centrosome.

Further to this it is necessary to determine whether reductions in endogenous DISC1 are also apparent following siRNA transfection and that this is specific to *DISC1* siRNA and due not to siRNA or transfection in general. These experiments were carried out in HEK293 cells as these are the cells for which protein knockdown has been optimised (see chapter 5). In order to examine DISC1 knockdown in transfected cells it was first necessary to determine which cells have been transfected with the siRNA oligos. Most research of this type is carried out by co-transfection with GFP to detect transfected cells however it is possible that GFP itself may produce effects post transfection. Therefore I chose FAM labelled siRNA oligos which can be visualised by fluorescent microscopy to track transfected cells. These labelled oligonucleotides function just as efficiently as the unlabelled siRNA oligonucleotides and are visualised as bright green spots within the cytoplasm or at a perinuclear location (see chapter 5). 48 hours post siRNA transfection cells were processed for immunofluorescence using the αDISC1 C-terminal antibody as this successfully

detected DISC1 knockdown at the protein level by immunoblotting. Initially it was decidedly difficult to detect knockdown of DISC1 by immunofluorescence as a high number of cells were transfected and the amount of siRNA oligonucleotide was such that it was difficult to find non-transfected cells which could be used for comparison of DISC1 expression levels. In order to overcome this problem I used a lower volume of lipofectamine/siRNA complexes to transfect the cells. This produced a much lower transfection level and allowed examination of positively transfected cells and non-transfected cells on the same coverslip.

With this lower transfection efficiency it was possible to detect DISC1 knockdown in cells that received *DISC1* siRNA in comparison to adjacent cells that had not been transfected (Figures 6.4.B and C). In some cells this reduction was seen as a less intense or absent perinuclear dense spot likely to correspond to DISC1 centrosomal staining (Figure 6.4.B); in other cells a general reduction in expression was seen (Figure 6.4.C). There were however some cells which received siRNA but which did not apparently have reduced DISC1 levels therefore any phenotypic abnormalities observed as a result of siRNA transfection will have to be subject to cell counting and statistical analysis to determine the relationship between transfection of siRNA and the observed phenotype. DISC1 knockdown was also detectable using the DISC1 R47 N-terminal antibody. Figure 6.4.D depicts HEK293 cells transfected with 50nM *DISC1* siRNA 72 hours post transfection. The two cells containing *DISC1* siRNA clearly have negligible DISC1 staining in comparison to the non-transfected cells.

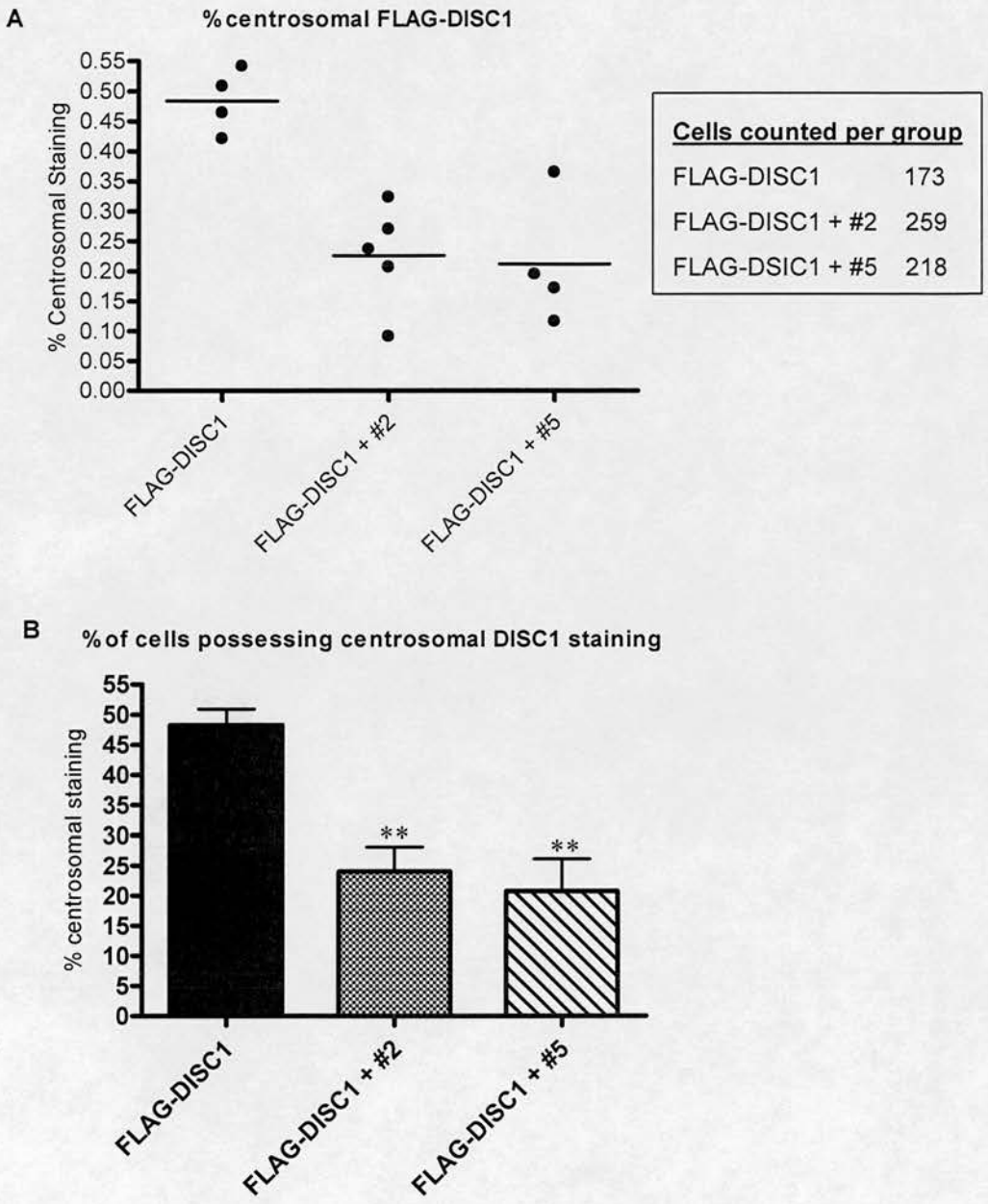

Figure 6.4.A. This figure shows a pilot experiment demonstrating exogenous DISC1 knockdown by immunofluorescent staining post siRNA treatment with DISC1 siRNAs #2 and #5. The percentage of cells possessing exogenous FLAG-DISC1 staining at the centrosome was determined by counting 4-5 fields of view on each coverslip. These values are depicted as a dot plot **(A)**. Using these values a significant reduction in the number of cells containing FLAG-DISC1 at the centrosome was observed in *DISC1* siRNA co-transfected populations (one-tailed t-test, **p<0.01, n>3 for each column) **(B).** Graph B shows the mean and SEM of each group (n>3) from this one experiment (N=1).

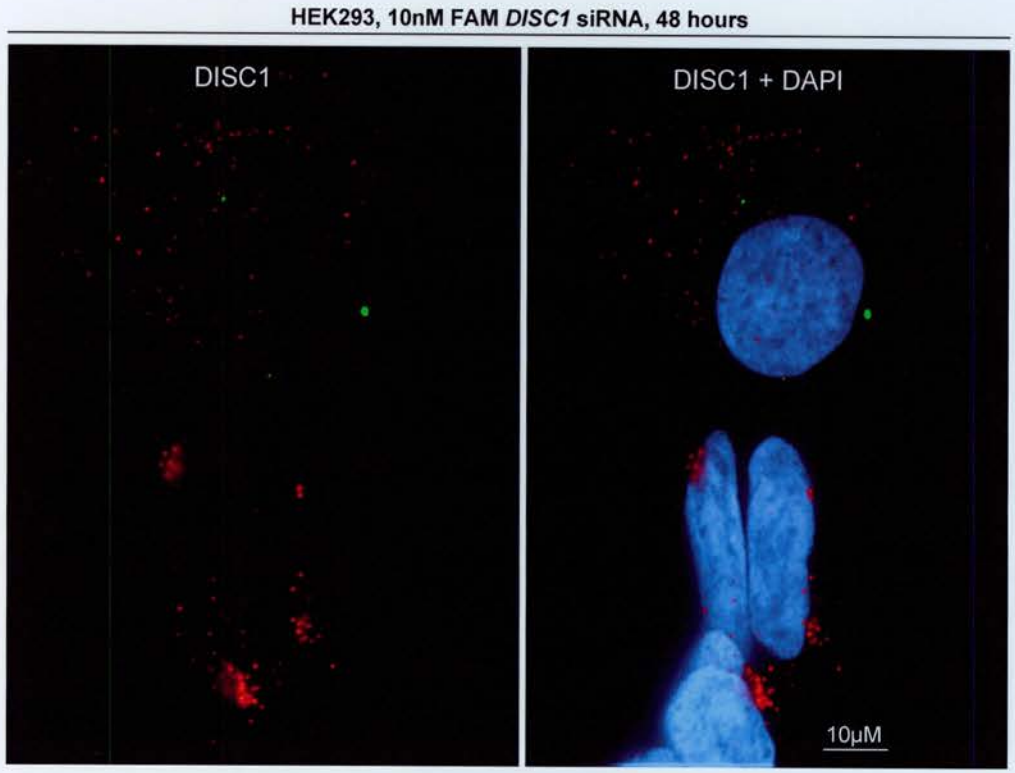

Figure 6.4.B Representative image of DISC1 knockdown post siRNA transfection. *DISC1* siRNA is visualised in green, DISC1 is visualised in red using the αDISC1 C-terminal antibody and nuclei are visualised using DAPI (blue). Of the four clearly visible cells in this image the uppermost cell contains *DISC1* siRNA and appears to have reduced DISC1 in comparison to the non-transfected cells lower down.

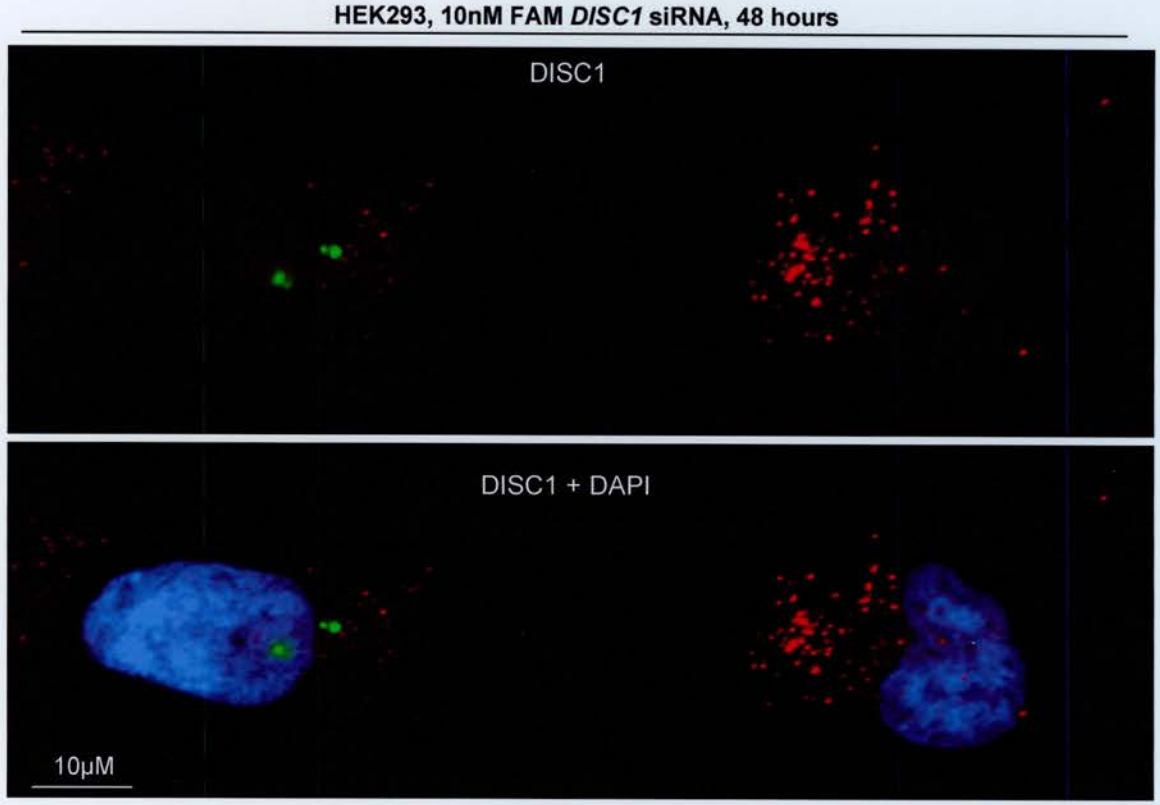

Figure 6.4.C. Representative image of DISC1 knockdown post siRNA transfection. *DISC1* siRNA is visualised in green, DISC1 is visualised in red using the αDISC1 C-terminal antibody and nuclei are DAPI stained (blue). Of the two cells shown in this image the leftmost cell contains *DISC1* siRNA and appears to have reduced DISC1 in comparison to the non-transfected cell on the right.

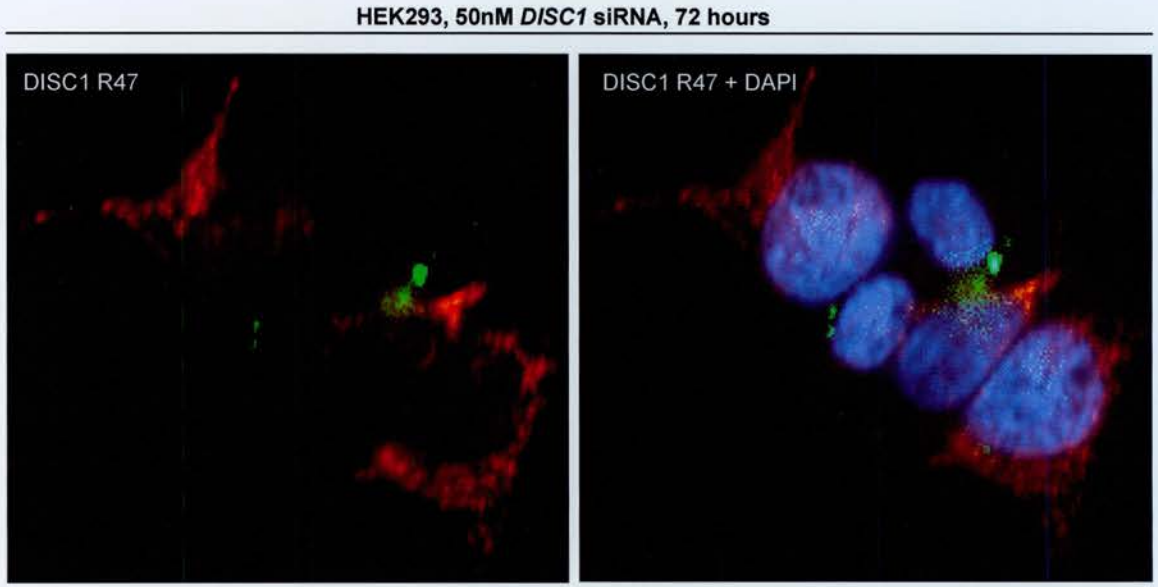

Figure 6.4.D. Representative image of DISC1 knockdown post siRNA transfection. *DISC1* siRNA is visualised in green, DISC1 is visualised in red using the DISC1 R47 N-terminal antibody and nuclei are visualised in blue using DAPI. Of the cells shown in this image two clearly contain *DISC1* siRNA and appear to have reduced DISC1 in comparison to the non-transfected cells. Images were taken at 40X.

6.4.2. DISC1 siRNA is not associated with disruption of the α/β-tubulin microtubule network

48 hours post transfection of *DISC1* siRNA, cells were processed by immunofluorescence with an antibody against α-tubulin to detect the microtubule network of the cell. DISC1 has been reportedly associated directly and indirectly with α-tubulin (*Morris et al. 2003, Brandon et al. 2004*) therefore we might expect to see some abnormalities in the microtubule network. Again transfected and non-transfected cells from the same coverslip were examined simultaneously for alterations in the microtubule structure that may be associated with siRNA transfection. No gross changes in the α-tubulin microtubule network were seen to be associated with *DISC1* siRNA in comparison to non-targeting siRNA controls (Figure 6.4.E). Furthermore the microtubule nucleating centre is still clearly visible in the *DISC1* siRNA transfected cells as indicated by an arrow in figure 6.4.E. Similar results were obtained using β-tubulin to detect the microtubule network. From these experiments it is clear that reduction of DISC1 does not grossly alter the microtubule network.

6.4.3 DISC1 siRNA is not associated with abnormalities in mitochondrial morphology

As in previous experiments cells were processed by immunofluorescence 48 hours post transfection. An antibody to mitochondrial cytochrome oxidase subunit II (MTCO2) was used to examine the morphology of mitochondria in transfected versus non-transfected cells from the same coverslip. Examination of MTCO2 revealed no apparent abnormalities in the morphology of the mitochondria in transfected versus non-transfected cells (Figure 6.4.F). Although the number of mitochondria per cell was not formally counted there were no obvious differences in the distribution or intensity of MTCO2 staining between transfected and non-transfected cells suggesting that these factors remained unchanged.

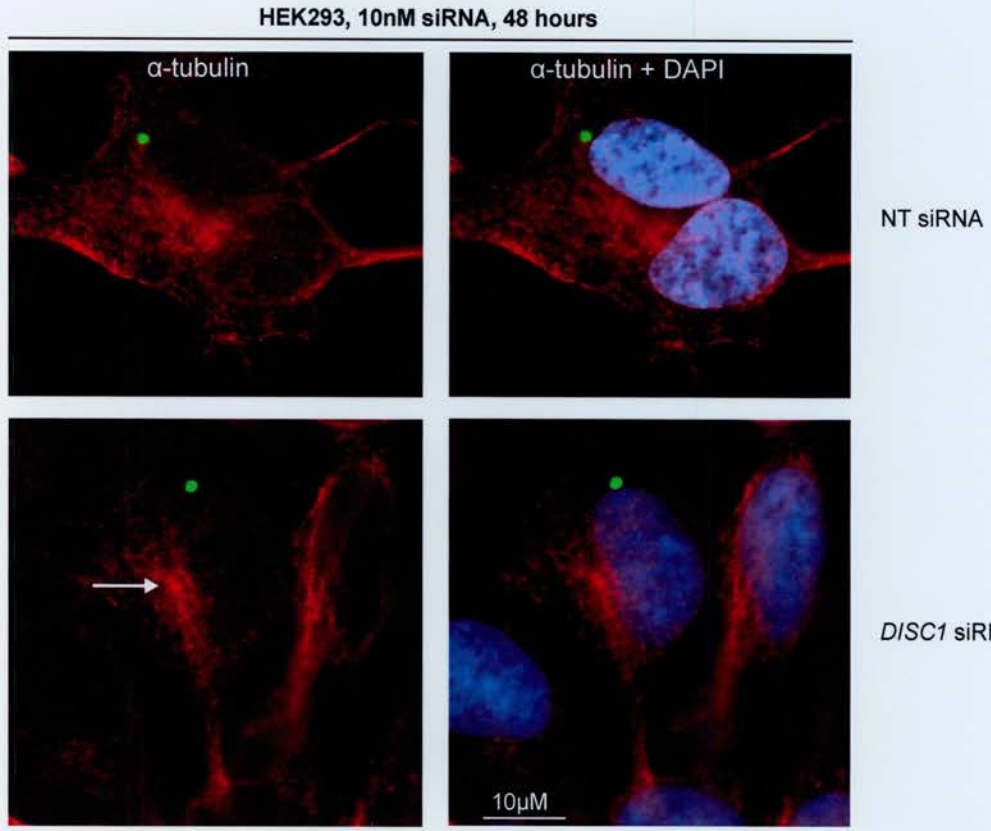

Figure 6.4.E. This figure is a representative image of the α-tubulin microtubule network (red) in transfected and non-transfected cells. SiRNA is visualised as green perinuclear spots and nuclei are DAPI stained (blue). The upper panel of images shows cells transfected with a non-targeting siRNA and the lower panel shows *DISC1* targeting siRNA transfected cells. There is no apparent change in the structure of the microtubule network between NT and *DISC1* siRNA transfected cells. The microtubule organising centre is still clearly visible as indicated with an arrowhead.

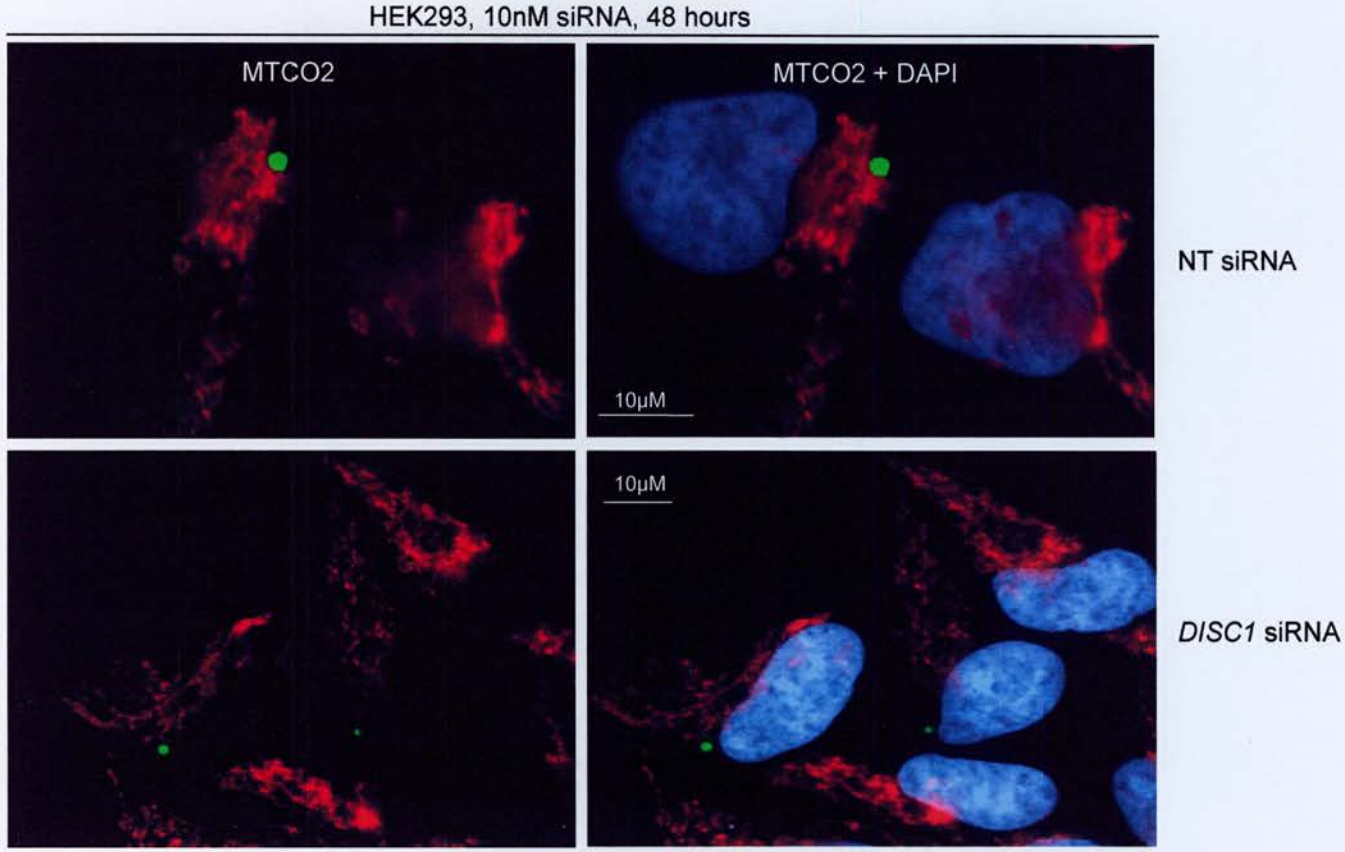

Figure 6.4.F. This figure shows representative images of the mitochondrial morphology using MTCO2 (red) in siRNA transfected cells. Nuclei are DAPI stained (blue). The upper images have been transfected with a non-targeting siRNA and the lower have been transfected with a *DISC1* siRNA. There is no difference in the mitochondrial morphology between transfected and non-transfected cells in either group.

6.5 Discussion

This chapter details pilot RNA interference experiments for the *DISC1* gene and serves as a taster for the different phenotypes that may arise as a result of depletion of DISC1. In all experiments DISC1 protein levels were substantially reduced and this correlated with a number of phenotypes. An altered cell cycle profile was observed in *DISC1* siRNA transfected populations, producing a small increase in the number of cells within G_1 phase and a small decrease in the number of cells within S phase. This alteration may arise as a result of reduced DISC1 at the centrosome. Exogenous FLAG-DISC1 immunoreactivity was shown to be reduced at the centrosome in cells co-transfected with *DISC1* siRNA and endogenous DISC1 staining was also seen to be reduced using two DISC1 antisera (αDISC1 and DISC-R47). The centrosome is important for cell cycle regulation and has been shown to be important for the G_1 to S phase transition (*Hinchcliffe et al. 2001, Doxsey et al. 2005*). This is in concordance with the differences observed in these experiments. However, the data form these experiments comprises one pilot experiment with replicates. Furthermore, these experiments did not use synchronised cultures and only examined one time-point of 48 hours. Additional independent experiments including synchronisation studies at extended time-points are required to confirm the differences in the cycling profiles of *DISC1* siRNA treated populations.

Another caveat to these experiments is that the BrdU incorporation experiment to measure actively dividing cells did not find differences in the levels of proliferation in *DISC1* siRNA transfected and non-targeting siRNA transfected populations. This protocol was complex; it required a high cell number such that 6 replicates of each treatment group were pooled for analysis. Furthermore the protocol required multiple rounds of centrifugation and resuspension of cell pellets resulting in a high number of cells being lost, hence the high starting number. The monoclonal BrdU antibody also produced a very high level of background staining compared to un-stained populations. Therefore, for reasons of high cell loss and high background staining the results from this experiment may not be entirely accurate, although attempts were made to exclude background as much as possible. It is my opinion that the DNA content analysis is a more reliable procedure as it requires a smaller number of cells

and the cells are only spun down once at the time of harvesting so no cells are lost during the procedure. Furthermore the analysis of DNA content and conversion into cell cycle data is carried out using computer analysis software which accounts for overlap between stages and is likely to be more accurate than manually setting thresholds in the presence of high background staining.

Interestingly, LIS1, a DISC1 interactor has also been shown to be actively involved in mitosis. Over-expression of LIS1 and RNAi mediated depletion of LIS1 results in an increase in the mitotic index of transfected cell populations. Various mitotic defects were reported in these populations including delayed chromosomal alignment resulting in delayed onset of anaphase, loss of chromosomes from the metaphase plate and misorientation of the spindle axis (*Faulkner et al. 2000*). There was some indication from my preliminary siRNA experiments that reduced DISC1 may result in additional cell cycle defects, including chromosome alignment and cytokinesis defects. Future work will incorporate an in depth analysis to try and confirm this. Some examples are shown in figure 6.5.A. Figure 6.5.A images A and B-C show two cells from the same coverslip one of which has been successfully transfected with *DISC1* siRNA. The positively transfected cell appears to have either a lagging chromosome or a chromosome that has been lost from the metaphase plate (image C is the same as B but with more intense DAPI staining). This is in contrast to the non-transfected cell in which all chromosomes have aligned at the metaphase plate. Images D-F in this figure depict cells at anaphase/cytokinesis. The mitotic spindle has been detected using α-tubulin. Images D, E and F depict a cell which has received *DISC1* siRNA and images G and H depict an un-transfected cell (not from the same coverslip). Again in the cell that has received *DISC1* siRNA there may be some DNA lagging behind after midbody formation in preparation for cytokinesis (image F is the same as image E but with more intense DAPI staining). The un-transfected cell is shown for comparison however this cell is at a slightly later stage of mitosis. These figures are merely examples and synchronisation of cultures will be necessary to determine the nature of any abnormalities that may arise. Time-lapse imaging will also prove useful in determining cell cycle phenotypes.

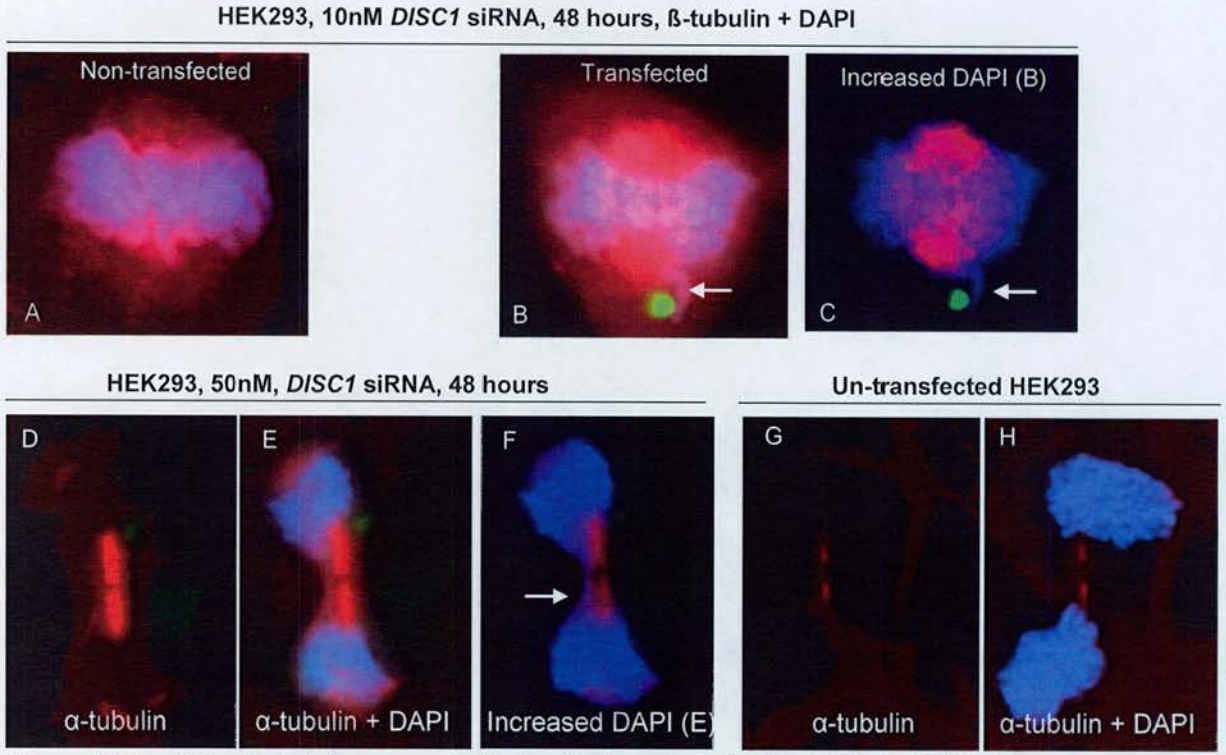

Figure 6.5.A. This pilot data suggests that cells transfected with *DISC1* siRNA (green) may exhibit chromosomal alignment abnormalities during cell cycle progression (A and B-C). Cell cycle stages were determined by α or β-tubulin (red) staining. In images B+C a lost or lagg ng chromosome (seen using DAPI in blue) is indicated with an arrow in the cell that has received *DISC1* siRNA. Images D to F depict a *DISC1* siRNA transfected cell which may also have lagging DNA (indicated by an arrow) after midbody formation prior to cytokinesis. Figure F is a higher exposure of figure E. Images G and H are from an un-transfected cell and are shown for comparison however this cell is at a slightly later stage of mitosis.

Given the large amount of mitochondrially localised DISC1 and the role of the mitochondrion in apoptosis I decided to measure the levels of cell death in siRNA treated populations. Unfortunately Annexin-V FITC and propidium iodide staining revealed that either the transfection procedure was highly toxic or the cell population used in this experiment was unhealthy prior to transfection. The latter is considered more likely as cell death of this magnitude was not apparent in other independent experiments. Although this was a disappointing finding it serendipitously revealed that cell populations transfected with *DISC1* siRNA had a higher number of viable cells and lower number of apoptotic cells in comparison to mock transfected and NT siRNA transfected populations. These differences were again small, percentage wise and require independent replication. These findings suggest that reduced DISC1 may have a protective effect against apoptosis under toxic or stressful conditions. DISC1 has been implicated in the cellular stress response via interactions with the eukaryotic translation initiation factor 3 (eIF3) (*Ogawa et al. 2005*). *Ogawa et al.* demonstrated that over-expression of DISC1 resulted in accumulation of eIF3 and DISC1 within stress granules in human neuroblastoma cells (*Ogawa et al. 2005*). The specific role of DISC1 at the mitochondrion or how DISC1 participates in the cellular stress response is not currently known. Previous studies have shown that mitochondrially associated DISC1 is resistant to trypsin digestion suggesting that DISC1 is localised within the mitochondrion or the mitochondrial membrane and work to define its exact location in ongoing within the lab (*James et al. 2004*). At this point in time we can only speculate about what role DISC1 may have in facilitating apoptosis induction and hypothesise that it may be as a result of altered DISC1 protein levels at/in the mitochondrion. Induction of apoptosis is an intrinsically complex process involving alterations in mitochondrial membrane potential, cytochrome c release and caspase activation (*Smith et al. 2005, Hill et al. 2003*). It is possible that DISC1 may facilitate these signalling events in some manner. Interestingly it has recently been reported that high levels of PDE4B2 limits apoptosis in B lymphocytes (*Smith et al. 2005*). High levels of PDE4B in this cell type appear to quench the effects of cAMP induced apoptosis via inhibition of the AKT pathway. These events are independent of PKA, the normal cellular cAMP effector kinase (*Smith et al. 2005*). This in an intriguing finding considering the

recent report of DISC1-PDE4B interaction at the mitochondria (*Millar et al. 2005b*). The main difference between these studies is the isoform of PDE4B implicated. 71kDa DISC1, the mitochondrially localised isoform, has been shown to bind PDE4B1 and is hypothesised to regulate its cAMP hydrolysing activity in a negative manner. It is possible therefore that the absence of DISC1 (via siRNA depletion) may alter the activity of PDE4B1 affecting cAMP signalling and hence the induction of apoptosis in HEK293 cells under stressful conditions. One other crucial difference between these two studies is that that the DISC1-PDE4B interaction is PKA sensitive and up-regulation of PKA culminates in release of DISC1 from PDE4B1 (*Millar et al. 2005b*), whilst *Smith et al. 2005* reports a PKA independent mechanism for cAMP induction of apoptosis in B lymphocytes. Together these two studies in combination with data generated from these siRNA experiments suggest a role for DISC1 and PDE4B and most likely DISC1-PDE4B interactions in mediating cAMP induced apoptosis via the mitochondrial apoptosome, however the underlying mechanism in HEK293 cells is unclear and likely to differ from that of B lymphocytes. Intriguingly mitochondrial associated apoptosis is a critical feature of normal brain development (*Roth and D'Sa, 2001*).

One piece of convergent evidence is provided by a recent study by *Hashimoto et al. 2006* which reported that siRNA mediated depletion of DISC1 in rodent neuronal cultures results in a decrease in the phosphorylation of AKT. The authors did not examine any phenotypic abnormalities associated with cell death, however these data suggest that DISC1 may be involved in both PKA and AKT mediation of cAMP signalling.

Continuing along the signalling theme, I also examined the effect of *DISC1* siRNA on levels of cAMP hydrolysis by the type 4 phosphodiesterases. This follows on from the recent work demonstrating an interaction between PDE4B and DISC1 with implications for cAMP signalling (*Millar et al. 2005b*). This work demonstrated that DISC1 was associated with PDE4B1 in its non-phosphorylated form. This is a dynamic interaction which appears to be disrupted by up-regulation of PKA signalling and cAMP production. This previous work hypothesised that DISC1 may

inhibit the hydrolysis of cAMP by PDE4B1 until such time as cAMP levels are increased and PDE4B1 activity is needed. My pilot experiment demonstrated that reduction in DISC1 by siRNA actually decreased the level of hydrolysis of cAMP by PDE4s (in comparison to NT siRNA) which seems counterintuitive to the current hypothesis. This is perplexing finding, if replicable, as it suggests that the presence of DISC1 is so vital that in its absence virtually no cAMP hydrolysis occurs. In order for this to happen, DISC1 must either have a direct effect on expression of PDE4s or must have a far greater role in cAMP signalling than originally thought.

Modification of PKA signalling has been shown to be important for progress from G_1 into S phase of the cell cycle in thyroid cells (*Feliciello et al. 2000*). Depression of the cAMP pathway and cellular translocation of PKA is required for progress into S phase in this cell type. Activation of cAMP signalling (and PKA) via addition of 8-Br-cAMP and phosphodiesterase inhibitor (IBMX) resulted in failure to progress from G_1 to S phase (*Feliciello et al. 2000*). From my siRNA experiment cAMP hydrolysis is dramatically reduced following DISC1 depletion comparable to that of phosphodiesterase inhibition which may account for the previously discussed delay in G_1 to S phase progression in these cells.

Knockdown of DISC1 was also examined by fluorescence microscopy in transfected cells. FAM labelled siRNA was utilised to allow individual transfected cells to be identified. Transfection efficiencies were purposely low to allow examination of positively transfected and negatively transfected cells within the same experiment. *DISC1* siRNA successfully knocked down expression of both the exogenous and endogenous DISC1 protein.

The β-tubulin network has previously been reportedly disrupted by over-expression of the 'mutant' DISC1 protein (*Kamiya et al. 2005*). The authors demonstrate that over-expression of 'mutant' DISC1 disrupts the normal cellular distribution of full length DISC1 and imply that this is the root cause of these abnormalities. It follows therefore that analysis of the tubulin network following siRNA mediated depletion of DISC1 may produce similar defects. In the case of these experiments analysis of the

α/β-tubulin microtubule network did not yield any gross abnormalities in comparison to non-targeting siRNA controls. It may be the case that knockdown is not sufficient to induce defects; however the levels of DISC1 knockdown observed by SDS-PAGE and immunoblotting were such that I would expect to see a defect if DISC1 is involved in microtubule nucleation or stabilisation. It is possible that these methods are not sensitive enough to detect very minor abnormalities however it is also possible that in the *Kamiya et al. 2005* study the 'mutant' DISC1 protein is altering the microtubule network by having additional effects and is not directly related to disruption of full length DISC1. Furthermore work from this laboratory does not support the finding that over-expression of 'mutant' DISC1 disrupts the microtubule network (unpublished observation) and *Ogawa et al. 2005* has shown that over-expression of DISC1 results in the formation of stress granules in transfected cells. Therefore aberrant expression of DISC1 or 'mutant' DISC1 may result in cellular stress that could cause alterations in the tubulin network as seen by *Kamiya et al. 2005*

It was also demonstrated by *Kamiya et al. 2005* that 'mutant' DISC1 causes re-distribution of LIS1, NUDEL and $p150^{glued}$ from their normal centrosomal location. Unfortunately at the time of these experiments antibodies suitable for immunodetection of these proteins were not available to me and these experiments will be carried out in the future.

Examination of mitochondrial morphology was also carried out as previous work has demonstrated altered mitochondrial morphology following DISC1 over-expression (*Millar et al. 2005a*). In this study a mitochondrial ring phenotype was observed following DISC1 over-expression suggesting that DISC1 may play a role in mitochondrial fission and fusion. However using mitochondrial cytochrome oxidase subunit II there were no obvious defects associated with the mitochondria in *DISC1* siRNA transfected cells. Although no physical abnormalities are observed upon DISC1 knockdown there may be underlying defects in mitochondrial respiration or signalling, which is possible considering the apoptosis defects seen in these studies. Future plans will aim to study and characterise any defects in mitochondrial

respiration in terms of ATP production post RNAi and any signalling defects that may be associated with the apoptotic RNAi phenotype.

In summary, pilot experiments of DISC1 depletion using siRNA have resulted in various abnormalities in cell cycle progression, apoptosis and cAMP signalling (see figure 6.5.B). Multiple independent experiments failed to detect abnormalities associated with mitochondrial morphology or the microtubule network although defects in these have previously been reported following DISC1 over-expression and 'mutant' DISC1 over-expression respectively (*Millar et al. 2005a, Kamiya et al. 2005*). The siRNA pilot experiments performed in this chapter serve as a taster for some of the effects reduced DISC1 might have in affected cells. Repeat experiments including rescue experiments are yet to be performed to confirm the specificity of these findings. Furthermore, these experiments are restricted to one cell type and it is conceivable that DISC1 may function differently in different cell types and also at different times during development as DISC1 has been shown to be developmentally regulated (*Schurov et al. 2004, Brandon et al. 2004*). Considering its potential roles in apoptosis and cell cycle progression reductions in DISC1 expression as a result of the t(1;11) translocation may have implications for cell division during the early stages of brain development and also for selective apoptosis during later developmental stages (*Morilak et al. 2000, Roth and D'Sa 2001*). This may help to explain the high incidence of psychosis in individuals possessing this translocation.

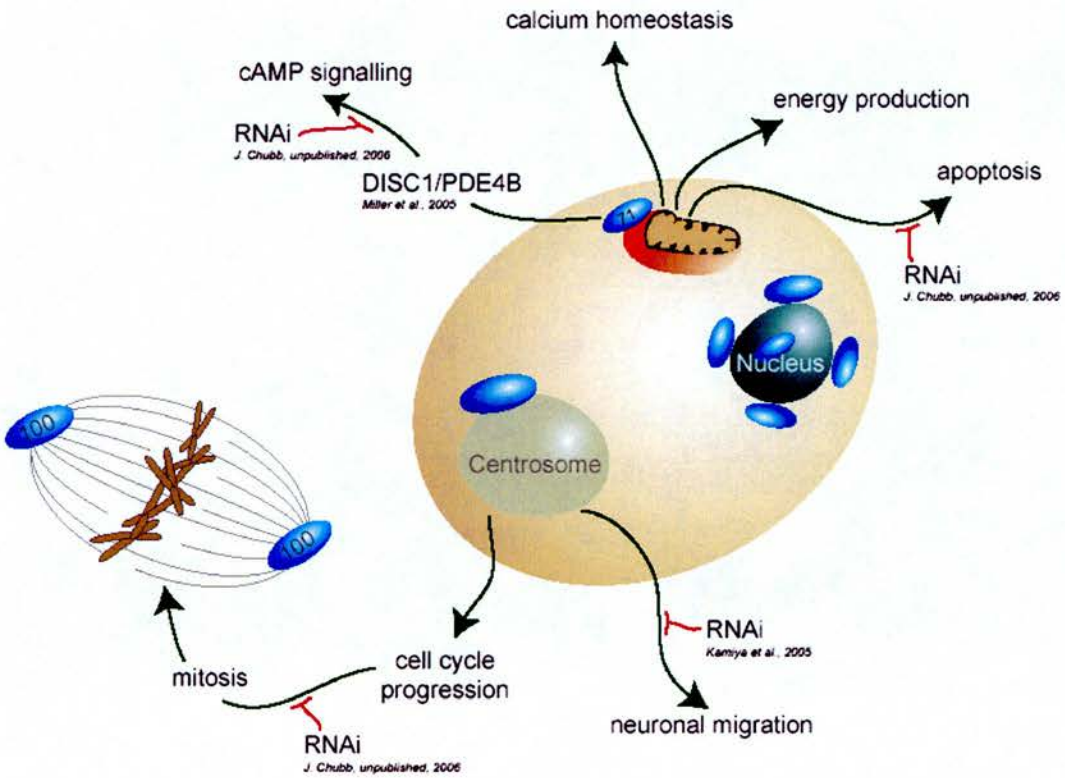

Figure 6.5.B. DISC1 knockdown using RNAi may result in disruption of diverse cellular functions including cAMP signalling, apoptosis, cell cycle progression and neuronal migration.

Chapter 7

DISC1 expression is dynamically regulated in human embryonic stem cell neuronal progenitors

7.1 Preface

Stem cells derived from isolated human embryos or foetal tissues possess the ability to regenerate all the various cell types in the human body. The study of mouse and human embryonic stem (ES) cells is an invaluable resource for uncovering the intricacies of neuronal differentiation. Using current technologies it is possible to generate specific neuronal populations which will be valuable for examining the specificities of gene transcription and regulation that culminate in neuronal differentiation of a particular subset of neurons. Neurons generated in this manner exhibit functionality *in vitro* possessing the capacity to produce GABA, glutamate and dopamine neurotransmitters (*Li et al. 1998, Perrier et al. 2004, Park et al. 2005*).

There is particular interest in studying human ES cells with the aim of utilising derived neurons in cell replacement therapy for neurodegenerative diseases. Unfortunately although it is possible to generate specific neuronal populations, for example midbrain dopaminergic neurons which are destroyed in Parkinson's disease, there have been no successful attempts to re-integrate these neurons such that they exhibit functionality *in vivo* (*Park et al. 2005*). With respect to schizophrenia, cell replacement therapy is not currently a viable research area as there is no cell type specific neuronal loss associated with schizophrenia; however the use of neural stem cells for investigating the mechanisms of neuronal specification and differentiation is important considering the likely neurodevelopmental nature of this disorder.

A number of functional studies have implicated DISC1 in neuronal migration and neurite outgrowth (*Ozeki et al. 2003, Miyoshi et al. 2003*). Of particular importance, DISC1 has been shown to perform developmentally regulated protein interactions that may be important for neuronal migration (*Brandon et al. 2004*) and shRNA

mediated depletion of DISC1 results in aberrant neuronal migration in the developing mouse cortex (*Kamiya et al. 2005*). For these reasons I have undertaken a pilot study of *DISC1* expression in hES cell neuronal progenitors. *DISC1* levels were measured by quantitative Real-Time PCR in hES cells at various stages of neuronal differentiation, however none of the hES cells in this study have reached a stage of terminal differentiation and remain capable of differentiation into multiple neuronal lineages. This study therefore indicates whether *DISC1* may be dynamically regulated during neuronal differentiation but does not specify a role for DISC1 in terminal differentiation of particular subtypes of neurons.

7.2 *DISC1* is dynamically regulated during neuronal differentiation

Human embryonic stem cell RNA for this study was provided by Dr. Wei Cui (Roslin Institute, Edinburgh, UK). RNA was extracted in the laboratory of Dr. Cui from three hES cell lines that had been differentiated down a neuronal lineage. This RNA was extracted at various stages of the neuronal differentiation process. Three hES cell lines were used in this study, H1 (male), H7 (female) and T5 (derived from the H1 line). This RNA was reverse transcribed to produce cDNA which was used for analysis of *DISC1* expression by quantitative Real-Time PCR. Two housekeeping genes, *Glyceraldehyde-3-phosphate dehydrogenase* (*GAPDH*) and *Glucose-6-phosphate dehydrogenase* (*G6PD*) were used to normalise *DISC1* expression. *DISC1* expression was measured using primers spanning exons 4-6 of the *DISC1* gene. All primer pairs amplified specific products from the hES cell cDNAs and produced primer efficiencies within the recommended 90-110% range (Figure 7.2.A and 7.2.B). *DISC1* expression was normalised using each of the housekeeping genes individually to examine the expression profile during neuronal differentiation.

Normalisation using either of these housekeeping genes indicated a dynamic regulation of *DISC1* expression during neuronal differentiation (Figures 7.2.C, D and E). *DISC1* expression varied over time in all three hES cell lines with statistically significant differences between some neuronally differentiated groups compared to the un-differentiated samples (*$p<0.05$, ANOVA with post hoc Newman-Keuls test,

see graphs in figures 7.2.C-E). Statistical analysis was performed using the GraphPad Prism software.

These expression analyses were carried out on actively differentiating cell lines, therefore it is possible that housekeeping gene expression may be altered throughout the differentiation process. If changes in *DISC1* expression were as a result of changing reference gene expression we would expect to see inverse correlations in the expression patterns of *DISC1* and the reference gene. For example, increasing expression of a reference gene will affect the normalisation of *DISC1* gene expression such that the expression would appear lower. To rule out an effect of alterations in reference gene expression, I compared the gene expression patterns of *GAPDH* and *DISC1* throughout the differentiation process. The expression of each gene was normalised using the second reference gene *G6PD*. For each cell line expression is graphed as the relative fold change in expression relative to day 0 (un-differentiated), see figures 7.2.F,G and H. From these graphs it is clear that *GAPDH* expression fluctuates slightly throughout the differentiation procedure. However, these changes in *GAPDH* cannot account for the changes in *DISC1* gene expression as the patterns are not identical and the fold changes in *DISC1* expression are much more pronounced than those for *GAPDH*.

Unfortunately the quantities of RNA received to carry out these experiments meant that three independent amplifications were carried out for the *DISC1* normalised to *GAPDH* only. *DISC1* normalised to *G6PD* was carried out in duplicate however only on one occasion were both reference genes included in the same experiment. Therefore the graphs comparing the expression profiles of *DISC1* and *GAPDH* normalised to *G6PD* contain only one *GAPDH* expression value for each sample. Further replicates therefore may be needed to further validate the reference genes; however the fact that a similar *DISC1* expression profile is generated using both genes independently suggests that these genes are reliable in this instance.

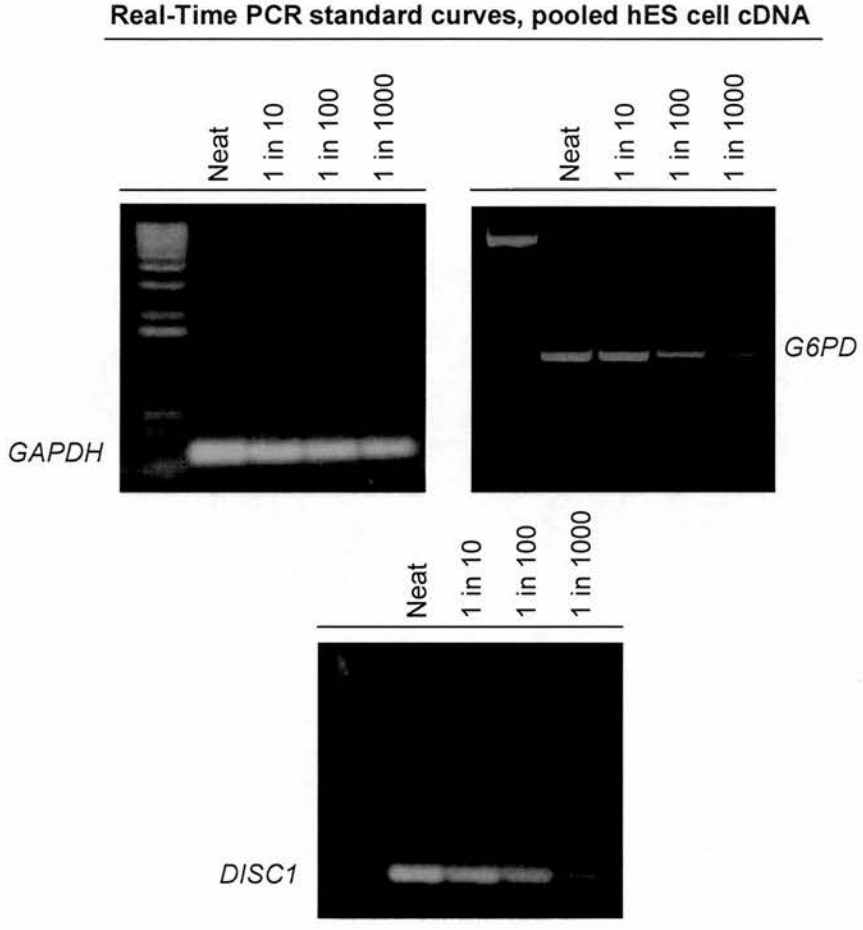

Figure 7.2.A. Standard curves for each housekeeping gene and *DISC1* primers were carried out on pooled hES cell cDNA. Four point dilution curves were constructed using neat, 1-10, 1-100 and 1-1000 dilutions of cDNA. This figure shows the product specificity of each primer pair by running end point PCR products on a 1% TAE agarose gel.

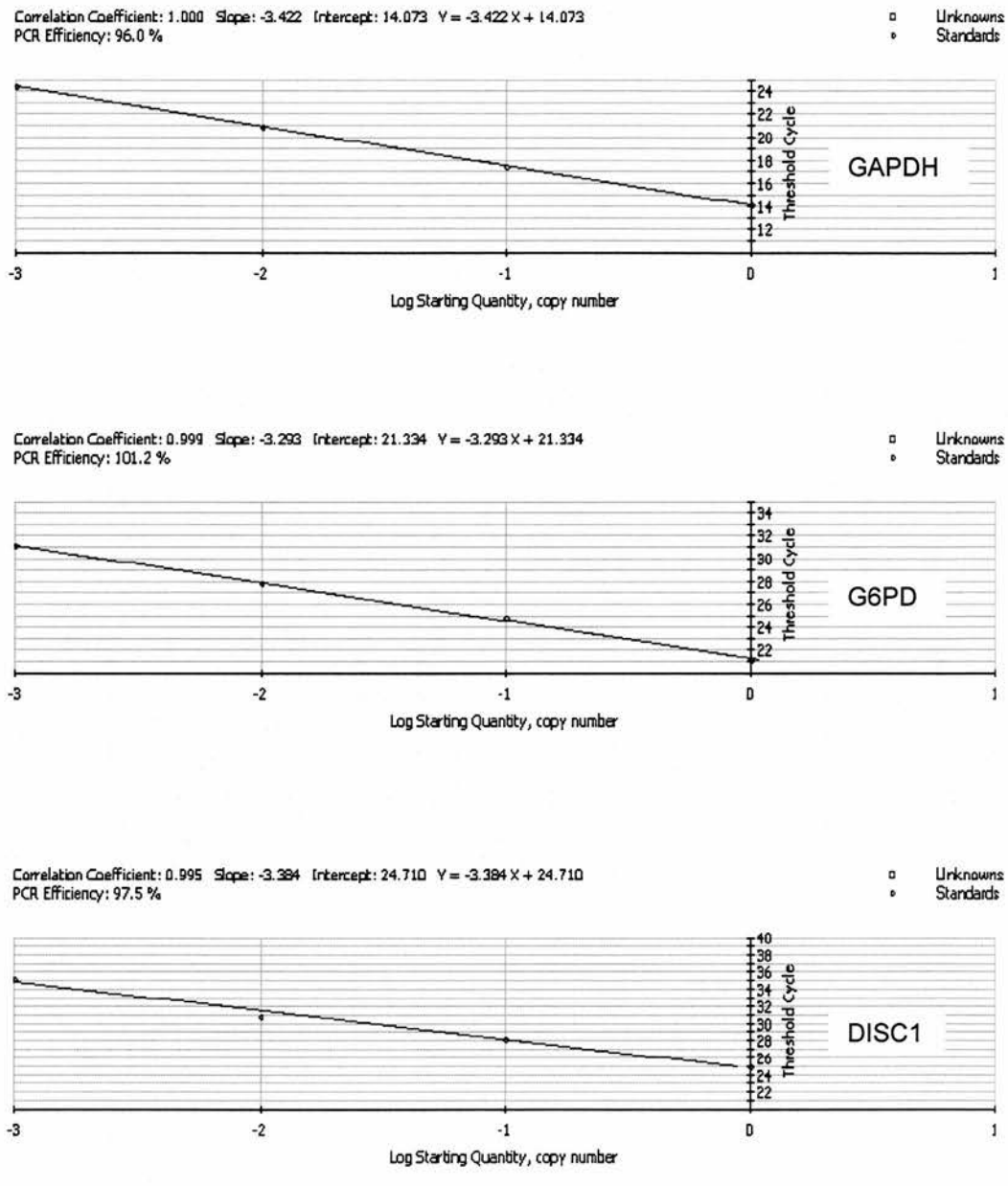

Figure 7.2.B. This figure shows representative standard curves to determine primer efficiencies on hES cell cDNA. All primer efficiencies should ideally fall between 90% and 110% with correlation coefficients greater than 0.995

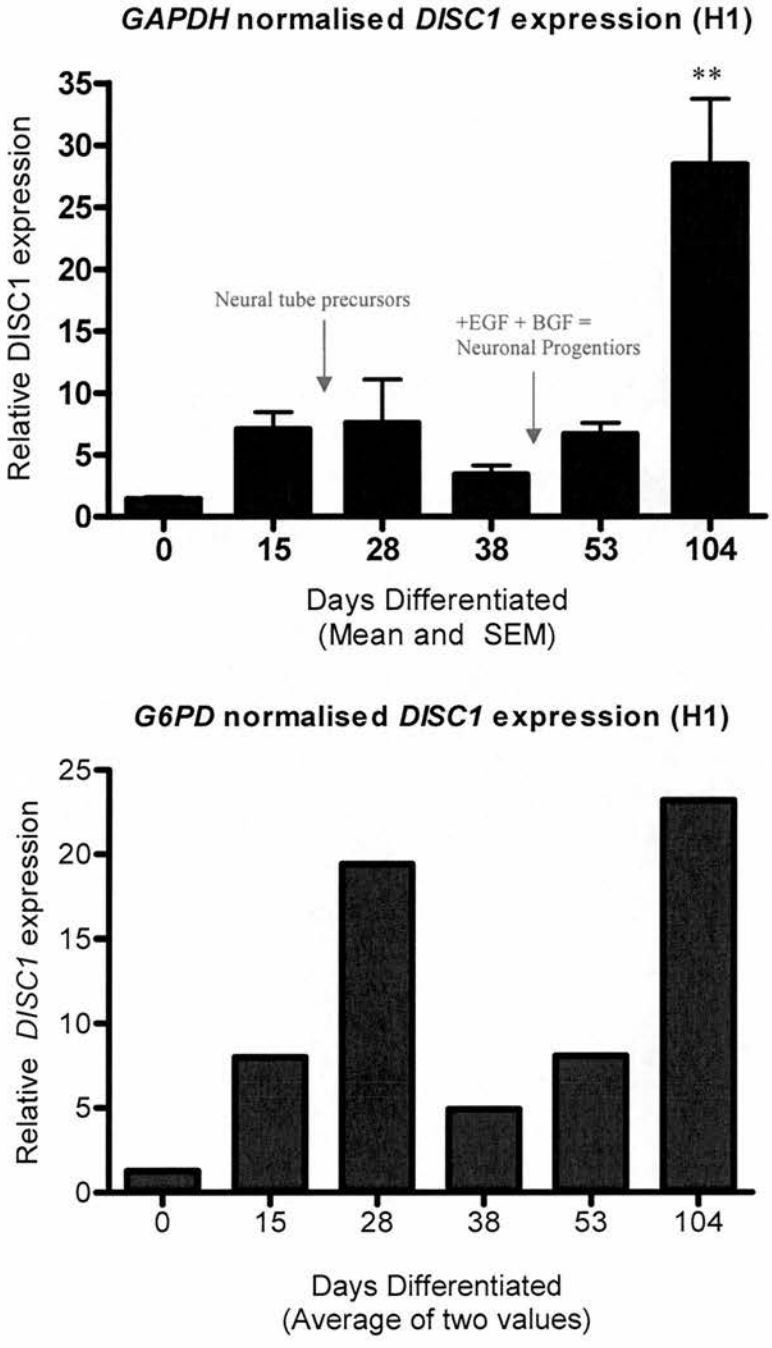

Figure 7.2.C. This figure graphically represents pilot *DISC1* expression data from the H1 hES cell line. *DISC1* is seen to be dynamically regulated throughout neuronal differentiation. Normalisation using *GAPDH* and *G6PD* produce similar patterns of *DISC1* expression. *DISC1* normalised to *GAPDH* was shown to be significantly altered at day 104 of the differentiation process compared to day 0 (ANOVA with post hoc Newman-keuls test **$p<0.01$, $n = 3$ for each column). *G6PD* normalised data was from only 2 independent experiments thus the average values are shown and statistical analysis not carried out.

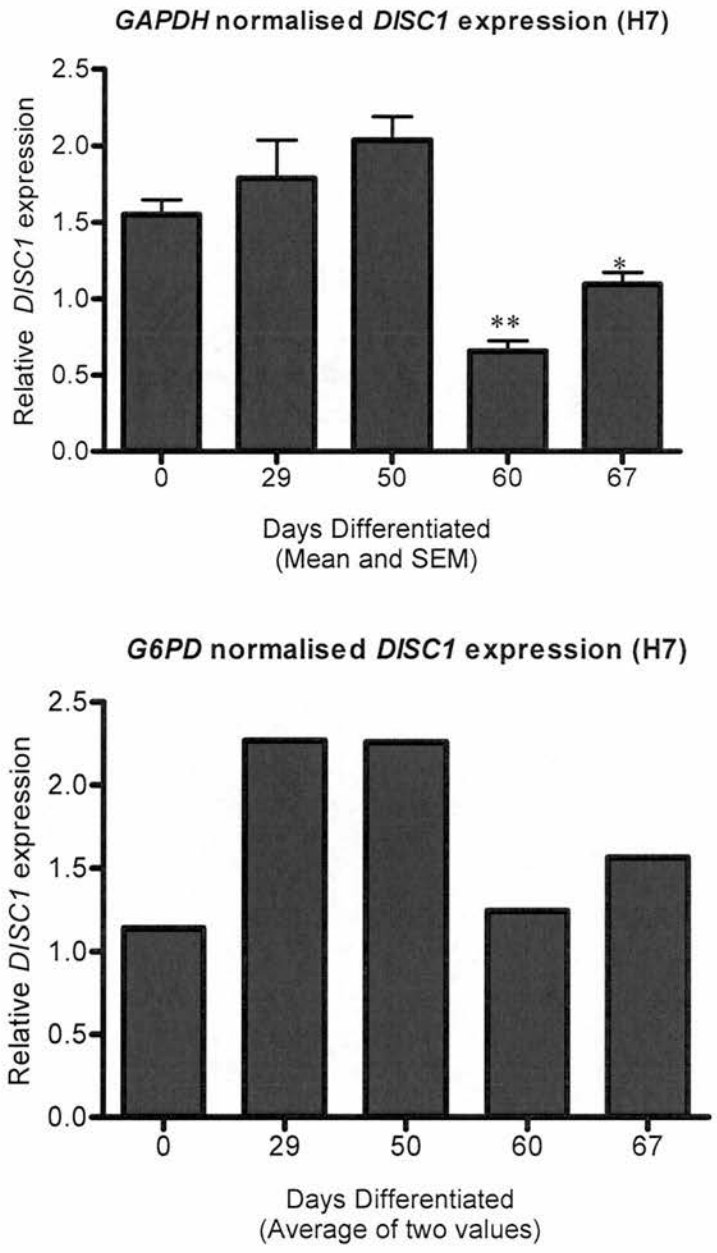

Figure 7.2.D. This figure graphically represents pilot *DISC1* expression data from the H7 hES cell line. *DISC1* is seen to be dynamically regulated throughout neuronal differentiation. Normalisation using *GAPDH* and *G6PD* produce similar patterns of *DISC1* expression. *DISC1* normalised to *GAPDH* was shown to be significantly altered at days 60 and 67 of the differentiation process compared to day 0 (ANOVA with post hoc Newman-Keuls test, Day 60 **$p<0.01$, Day 67 *$p<0.05$, n = 3 for each column). *G6PD* normalised data was from only 2 independent experiments thus the average values are shown and statistical analysis not carried out.

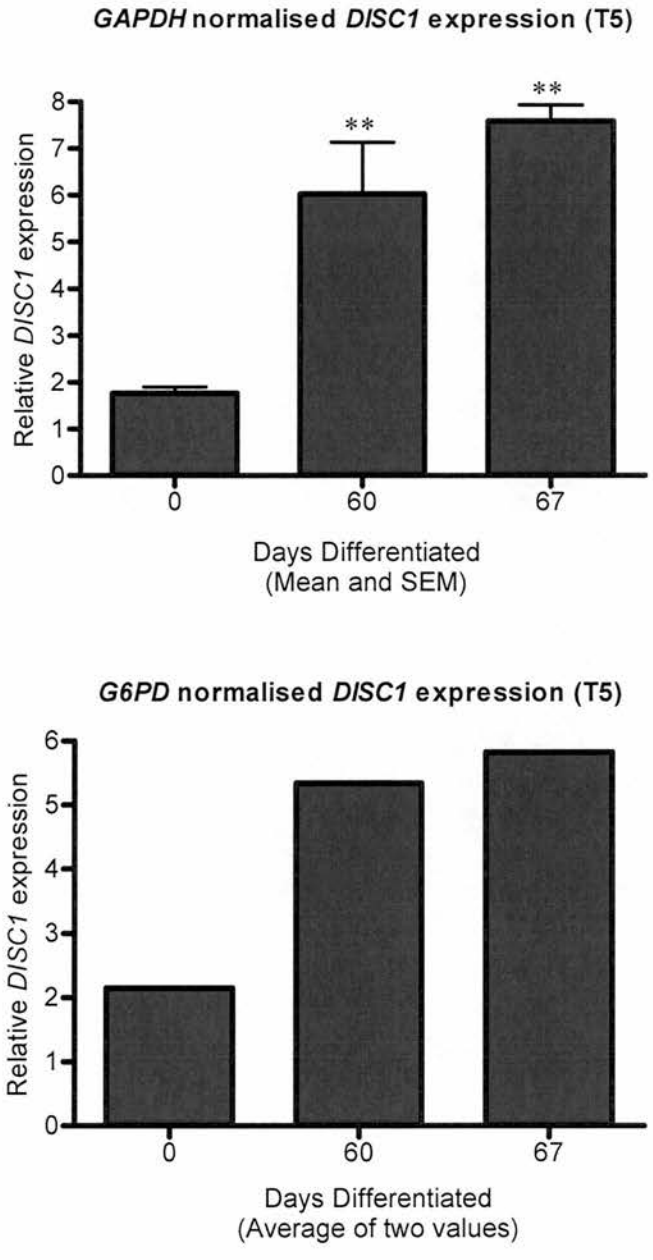

Figure 7.2.E. This figure graphically represents *DISC1* pilot expression data from the T5 hES cell line. *DISC1* expression is seen to be dynamically regulated throughout neuronal differentiation. The pattern of *DISC1* expression is similar using both *GAPDH* and *G6PD* housekeeping genes. *DISC1* expression normalised to *GAPDH* was significantly different at days 60 and 67 of the differentiation process in comparison to day 0 (ANOVA with post hoc Newman-Keuls test **$p<0.01$, $n = 3$ for each column). *G6PD* normalised data was from only 2 independent experiments thus the average values are shown and statistical analysis not carried out.

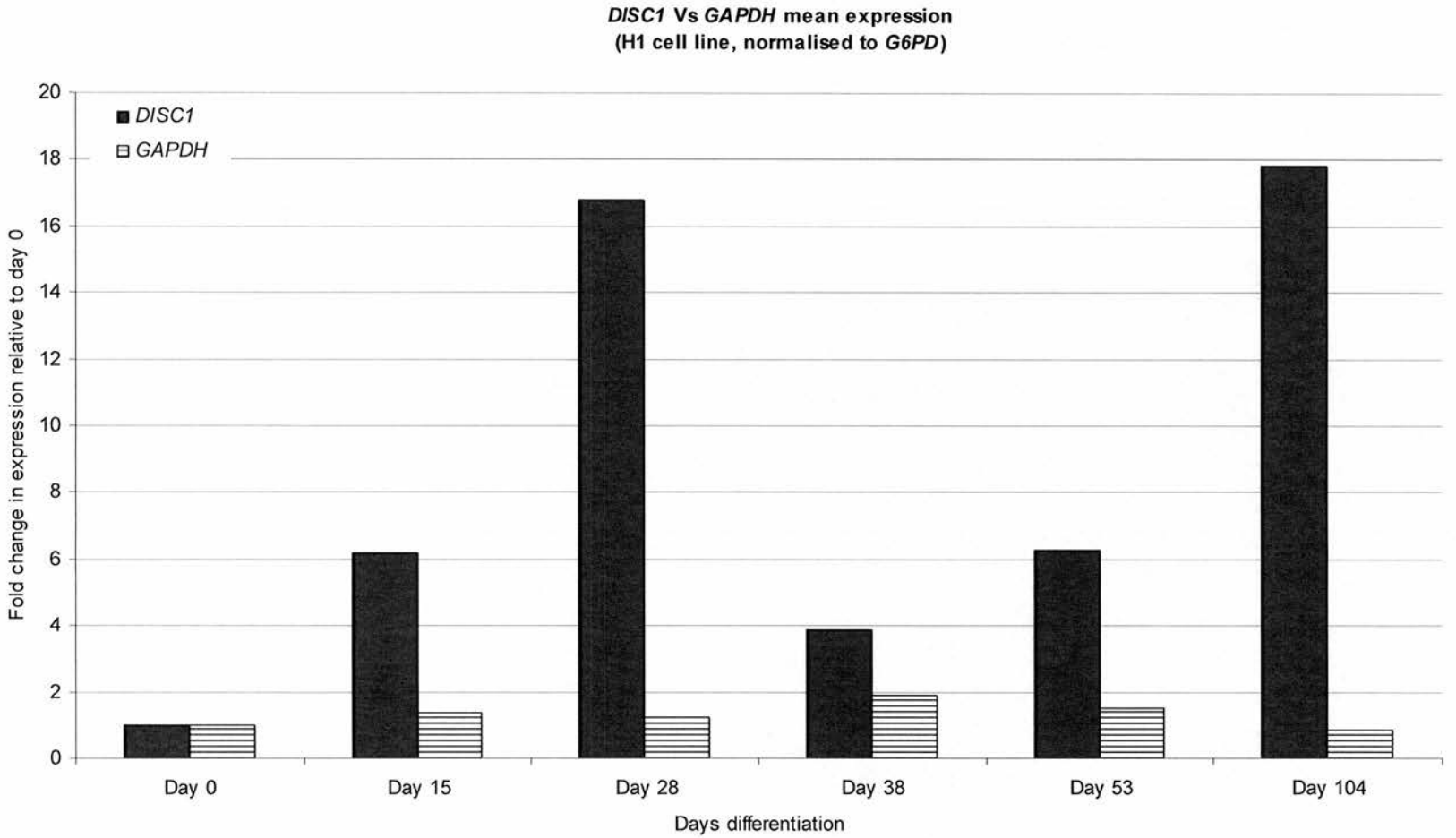

Figure 7.2.F. This graph depicts the fold change in gene expression of *DISC1* and *GAPDH* (normalised to *G6PD*) throughout neuronal differentiation of the H1 cell line. Fold change is relative to undifferentiated (Day 0) gene expression. *DISC1* fold change was calculated using the average of two independent data points. *GAPDH* data is from one experiment.

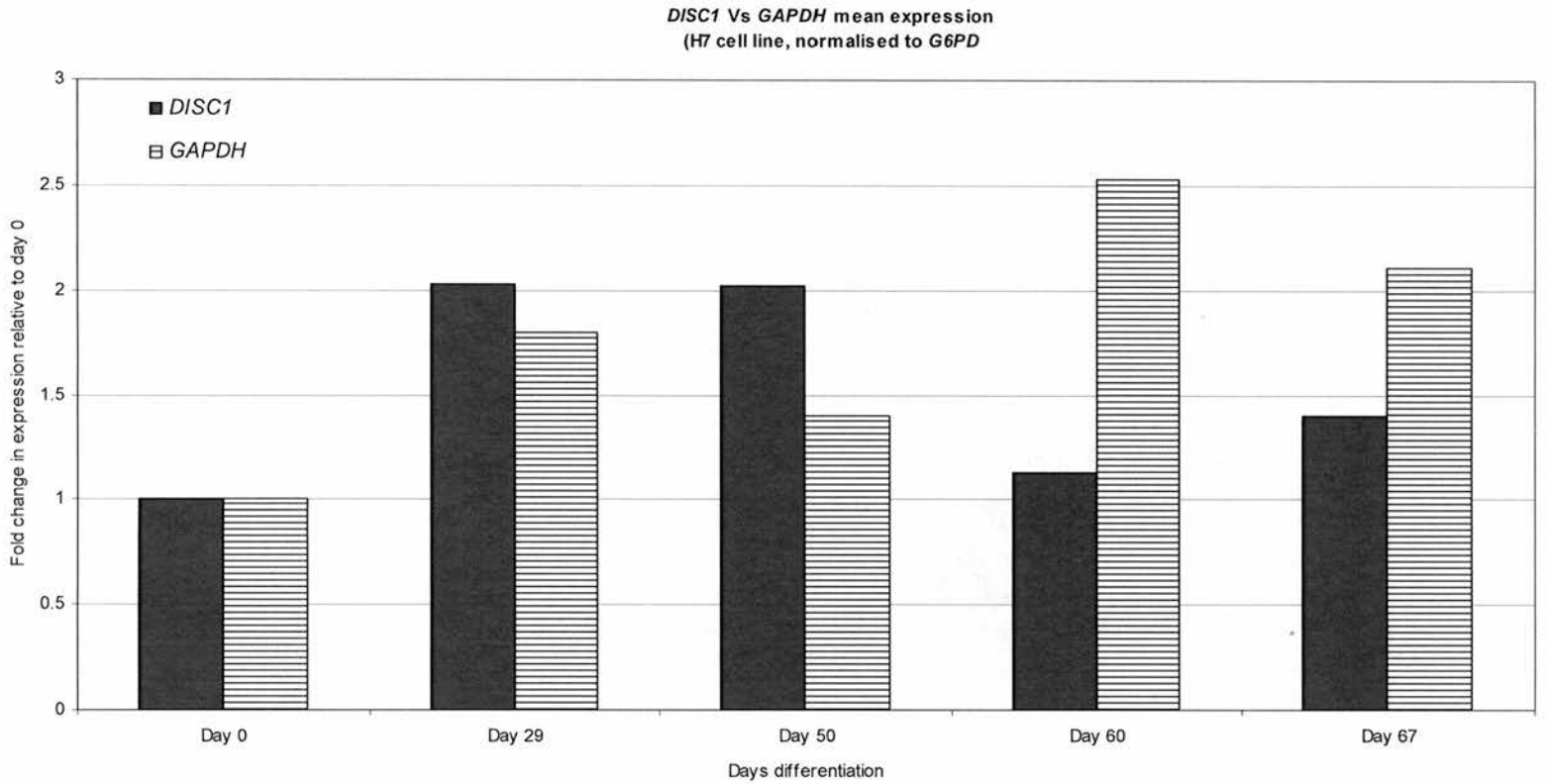

Figure 7.2.G. This graph depicts the fold change in gene expression of *DISC1* and *GAPDH* (normalised to G6PD) throughout neuronal differentiation of the H7 cell line. For *DISC1* the average of two independent data points was used to compute the fold change. GAPDH data is from a single experiment. Fold change is relative to undifferentiated (Day 0) gene expression.

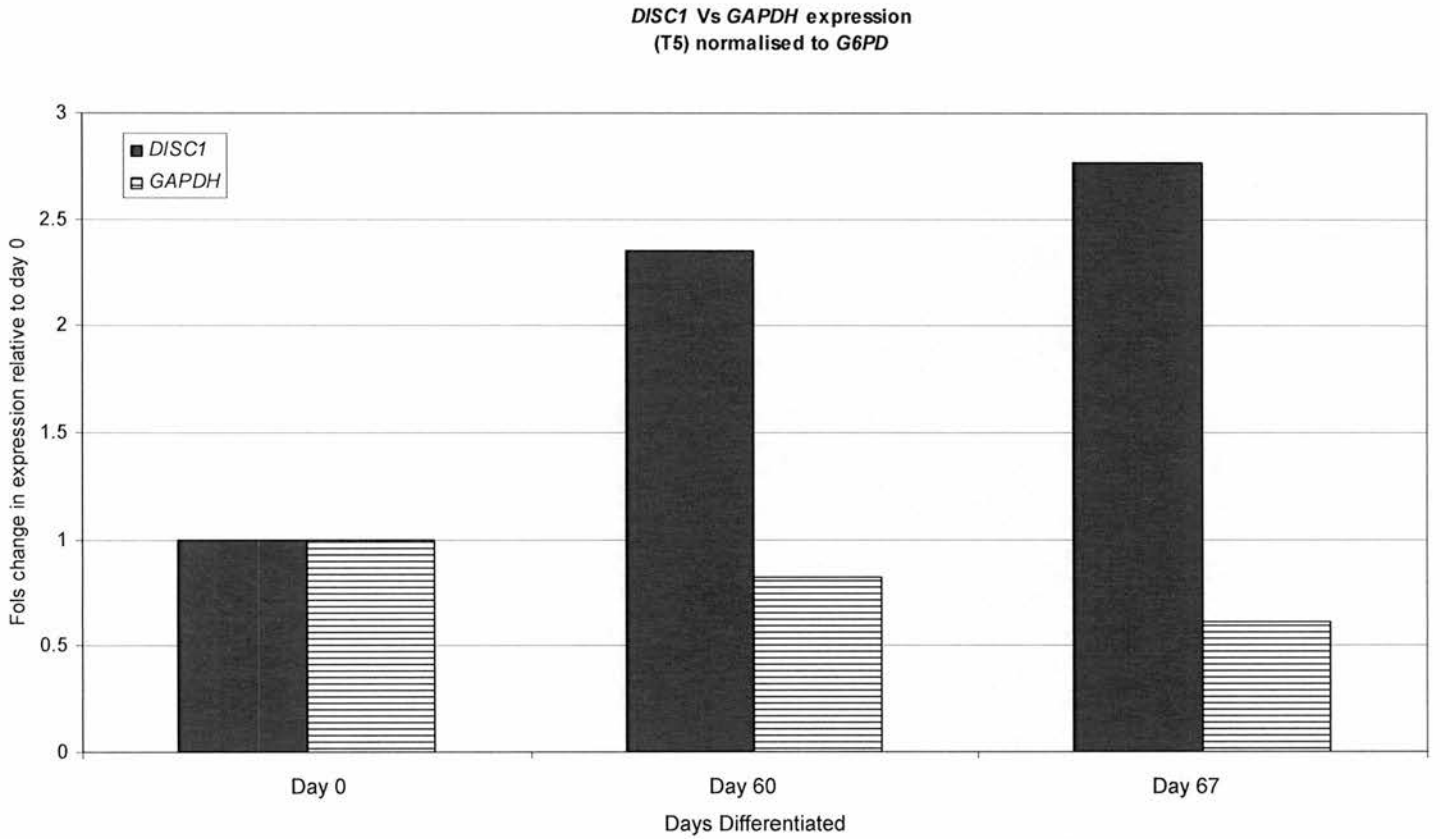

Figure 7.2.H. This graph depicts the fold change in gene expression of *DISC1* and *GAPDH* (normalised to *G6PD*) throughout neuronal differentiation of the T5 cell line. For *DISC1* an average of two independent data points was used to compute the fold change in expression. For *GAPDH* data is from a single experiment. Fold change is relative to undifferentiated (Day 0) gene expression.

7.3 Discussion

This chapter has examined the expression profile of *DISC1* at the RNA level in three hES cells lines at various stages of differentiation along a neuronal pathway. In the H1 and T5 cells lines *DISC1* expression appeared to be up-regulated in hES cells that had reached a neuronal progenitor state in comparison to undifferentiated cells of the same line. For the T5 cell line there are only three time-points of differentiation, time 0 (undifferentiated) and time-points 60 and 67 days post-differentiation by which time cells have been treated to acquire a neuronal progenitor fate. As this T5 cell line was originally derived from the H1 line it is interesting to examine similar time-points during differentiation of the H1 line. The nearest time-points in the H1 cell line are day 0 (undifferentiated) and day 53 post-differentiation. The relative *DISC1* expression values at these time points are in concordance with each other in both cell lines with *DISC1* being approximately 3-4 times more abundant at days 60-67 in the T5 line and day 53 in the H1 line relative to day 0 in either cell line. Despite the limited number of time-points from the T5 line, it appears that *DISC1* is up-regulated following neuronal differentiation, however examination of intermediate and later time-points in the H1 line reveal that *DISC1* levels oscillate and exhibit a more complex expression pattern than would have been deduced from the T5 line.

Examination of *DISC1* levels in the same manner in the H7 line reveals smaller oscillations in *DISC1* levels during differentiation. *DISC1* expression appears to drop between day 50 and day 60 following neuronal differentiation however by day 67 *DISC1* levels are on the increase again. It would be interesting to examine further time-points to deduce whether expression levels continue to rise in this cell line as in the H1 line.

It must be noted that the *DISC1* expression values in these experiments are 'relative' to other time-points from the same cell line and are not comparable between cell lines. These are not a measure of actual *DISC1* levels. For example, even though there is a less apparent increase in *DISC1* in the H7 cell line than in the H1 cell line it does not mean that the H1 cell line possesses more *DISC1* than the H7 cell line. It may be the case that the H7 line naturally expresses *DISC1* at a higher level and

therefore a less dramatic increase in expression levels is seen following neuronal differentiation, although this is purely speculative. Furthermore, the T5 subclone of H1 is suspected to carry a duplication of the 1q region of chromosome 1 harbouring the *DISC* locus and therefore may already have augmented *DISC1* expression in comparison to the other cell lines examined. Despite this, there still appears to be a dynamic change in *DISC1* expression throughout the differentiation procedure.

From these experiments it appears that *DISC1* is a dynamic factor involved in (or in response to) neuronal differentiation. To confirm or refute this hypothesis it is necessary to examine *DISC1* expression in more detail using additional cells lines and later time-points. In particular it would be interesting to examine *DISC1* expression during differentiation of particular neuronal populations e.g. dopaminergic neurons. It would be desirable also to examine the cell morphology at each stage of differentiation and compare the *DISC1* expression levels such that specific stages of development may be correlated with increasing or decreasing *DISC1* levels. It will also be interesting to examine if changes in the levels of *DISC1* expression are isoform specific.

Chapter 8

DISC2

8.1 Preface

The *DISC2* gene is directly disrupted by the t(1;11) translocation and was identified from expressed sequence tags (ESTs) surrounding the chromosome 1 breakpoint region (*Millar et. al* 2000). *DISC2* represents a large polyadenylated transcript of unknown size that is transcribed in the reverse orientation to *DISC1*. RACE PCR (Rapid Amplification of cDNA ends) successfully identified 15kb of *DISC2* sequence and located the 3' end of *DISC2* within intron 8 of the *DISC1* gene (*Millar et. al* 2000). The 5' end of *DISC2* remained to be identified; however it was hypothesised to lie within intron 9 of the *DISC1* gene. Interestingly this intron 9 region is very large encompassing approximately 150kb of genomic DNA in humans, 50kb in mouse and 4kb in pufferfish (*Fugu rubipes*) (*Millar et al. 2001, Ma et al. 2002, Taylor et al., 2003*). Similar to the human and mouse *DISC1* genes, intron 9 is the largest intron of pufferfish *DISC1* suggesting that some functional importance may be attributable to this intron.

Analysis of the known *DISC2* sequence demonstrated the absence of significant open reading frames (ORF) (*Taylor, M. unpublished, 2001*). As a result of this *DISC2* is hypothesised to represent a non-coding RNA gene partially anti-sense to *DISC1*. However, the remaining gene sequence must be identified in order to substantiate this hypothesis.

With an ever expanding body of evidence suggesting a role for non-coding RNAs in the regulation of sense gene expression it is plausible that *DISC2* may regulate the expression of *DISC1*. This chapter describes my efforts to identify the 5' end of the *DISC2* gene and to establish the transcriptional activity of this gene in cell lines derived from t(1;11) family members. The normal functions of this gene may be affected by the translocation. For this reason I was also interested to determine

whether *DISC2* was expressed from both the non-translocated and derived *DISC2* alleles in translocation carrying cell lines.

8.2 *DISC2* is transcribed in cell lines derived from t(1;11) family members

8.2.1. DISC2 is a low abundance transcript expressed in lymphoblastoid cell lines from t(1;11) family members

In order to assess the effects of the translocation on *DISC2* it was necessary to determine whether this antisense gene is expressed in cell lines derived from the t(1;11) family. Reverse transcriptase PCR (RT-PCR) was carried out using primers designed within the region of known *DISC2* sequence (AF222981). This sequence encompasses *DISC1* exon 9 and some *DISC1* intronic sequence flanking this exon. *DISC2* primers were designed within the intronic region to avoid amplification of *DISC1* cDNA sequences. Moreover expression analysis was carried out using cDNA produced from polyadenylated RNA to avoid contamination with heterogeneous nuclear RNA (hnRNA) which may contain unprocessed or partially processed *DISC1* mRNAs.

Analysis of t(1;11) cell lines demonstrated that *DISC2* was indeed transcribed however, it is a low abundance transcript as nested PCR was required to detect a product by non-quantitative PCR (Figure 8.2.A).

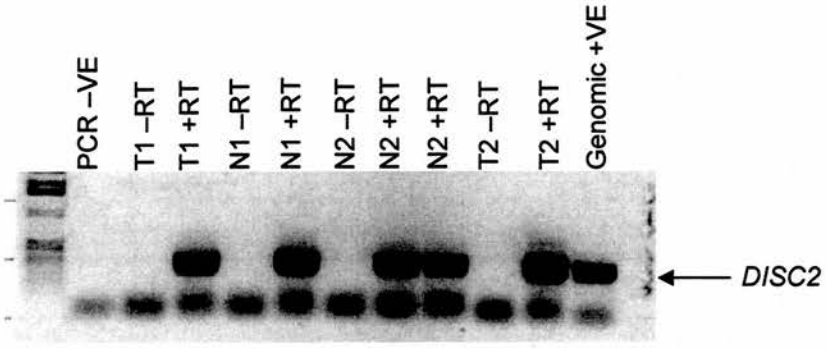

Figure 8.2.A. *DISC2* expression is detected by nested PCR in t(1;11) cell lines possessing the translocation (T) and in normal karyotype controls (N).

8.2.2 DISC2 transcripts are produced from the translocated DISC2 allele

I next assessed t(1;11) cell lines for evidence of *DISC2* transcription occurring from the normal and derived chromosome 11 *DISC2* allele. To do this it was necessary to identify a single nucleotide polymorphism (SNP) which could discriminate between transcription from the two alleles. An intronic SNP rs1535530, within the *DISC2* known sequence, was chosen and genotyped in t(1;11) cell lines in the same manner as for *DISC1* (chapter 3). This SNP is located distal to the translocation breakpoint located just outside of exon 9 region (within intron 9) of *DISC1* (SNP rs1535530 position chr1 228989432). The translocated *DISC2* allele was found to be represented by the A allele of SNP rs1535530 and the normal allele is represented by the G allele of this SNP.

Transcription from the normal and derived *DISC2* alleles was determined using nested allele specific PCR. Allele specific PCR primers were designed and optimised using gradient PCR to ensure specificity for the individual alleles of SNP rs1535530 (Figure 8.2.B (I)). This specificity was further confirmed using allele specific PCR on genomic DNA controls (where the genotype of this SNP was known) performed alongside allele specific RT-PCR on t(1;11) cell line cDNAs (Figure 8.2.B(II)). As can be seen in figure 8.2.B (II) transcripts appear to be produced from both the non-translocated and translocated *DISC2* alleles. This is not necessarily surprising as the translocated *DISC2* allele should retain its 5' end. This data suggests that the region of chromosome 11 harbouring the translocated *DISC2* allele can support transcription of this gene.

In figure 8.2.B (II) expression from the translocated (A) allele appears to be weaker in the normal karyotype controls compared to translocation carriers. Although this is a potentially interesting finding this allele-specific PCR is non-quantitative and no definitive conclusions can be drawn from this.

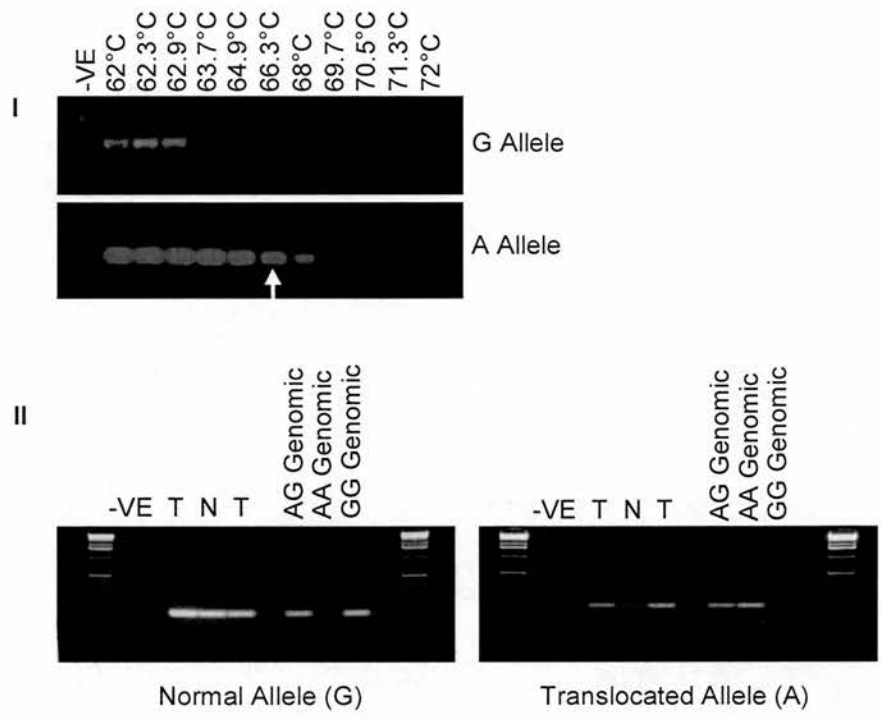

Figure 8.2.B. PCR primers specific for the A allele of SNP rs1535530 were optimised by gradient PCR **(I)**. A working temperature of 66°C (indicated by arrow) was chosen as the optimum temperature as primers amplify the A allele specifically at this temperature, with no non-specific amplification of the G allele. G allele specific primes were optimized in a similar manner. Known genomic controls were used to ensure primer specificity. Allele specific PCR on t(1;11) cell lines demonstrated that both alleles produce a transcript in translocation carriers (T) and normal karyotype controls (N) **(II)**.-VE reactions indicate no DNA controls.

8.3 Identification of the *DISC2* 5' end

It is hypothesised that *DISC2* represents a non-coding antisense transcript that may regulate *DISC1*. To explore this hypothesis further I sought to identify the 5' end of the *DISC2* gene. To do this I initially employed a bioinformatics approach and used a variety of transcription factor search engines and promoter prediction programs to search for the 5' end within intron 9 of *DISC1*. To search for transcription factors I used the TRANSFAC database and to search for promoters I utilised both GRAIL and Genscan promoter prediction programs (see chapter 2 for program details). All of these programs were designed with the intention of identifying protein coding genes and their potential to find promoters for non-coding genes is unknown. As the *DISC2* 5' end is thought to reside within *DISC1* intron 9, a very large intron of approximately 150kb in size, it was initially decided to focus on predictions located within conserved regions of the intron. Conservation was determined using the UCSC genome browser; at this time only mouse and rat conservations were available. Mouse syntenic regions were also examined independently for regulatory elements. One caveat to this approach is that there is no evidence for *DISC2* transcripts in mouse or rat however absence of evidence is not evidence of absence and this seemed a sensible approach to identify potentially important regions within the intron.

I initially searched for clusters of transcription factors which might point to the transcriptional start site of *DISC2*. A large number of transcription factor binding sites were identified; however there was no apparent clustering or conservation of transcription factor binding sites. This approach therefore did not narrow down the region likely to harbour the *DISC2* 5' end. The situation was similar for the promoter prediction programs. Of the few good predictions, most did not reside within conserved sequence and all other predictions were marginal. With the bioinformatics approach not proving fruitful it was decided to proceed down a more direct experimental route. Moreover any positive predictions acquired using bioinformatics would also need to be confirmed experimentally. I therefore decided to attempt 5' RACE to identify the 5' end of *DISC2*.

8.3.1 Identifying the 5' end of the DISC2 gene using Rapid Amplification of cDNA Ends

RACE uses cDNA populations that have been ligated to 3' or 5' adaptor sequences to identify full length cDNAs. Primers specific for these adaptor sequences in combination with gene specific primers are used to extend the known sequence of a transcript. *DISC2* was originally extended to the 3' end using RACE. The 5' end was not successfully identified using this method (*Millar et al. 2000*). This is likely due to the fact that *DISC2* is a large transcript. Currently 15kb of *DISC2* sequence has been defined.

8.3.1.1 Narrowing down the *DISC2* 5' region using PCR

Before performing the RACE experiments it was decided to attempt to narrow down the region that is likely to harbour the *DISC2* 5' end before continuing. To do this I used a human heart cDNA population. PCR primers were designed throughout the intron 9 region and used to amplify *DISC2* by PCR (Figure 8.3.A). *DISC2* transcripts were only amplified using the first primer pair designed within intron 9 (Figure 8.3.A.). This sequence was confirmed as being *DISC2* by amplification with two additional sets of *DISC2* primers. Contamination of *DISC1* sequence was ruled out using an intronic primer pair located outside the region of *DISC2* (Figure 8.3.B.).

Unlike the t(1;11) cell lines, *DISC2* amplified well within 36 PCR cycles indicating its much higher expression level in heart. This suggests also that the RACE procedure should successfully amplify *DISC2* from a human heart cDNA library and further indicates that the 5' end of *DISC2* may be close to exon 9 of *DISC1*.

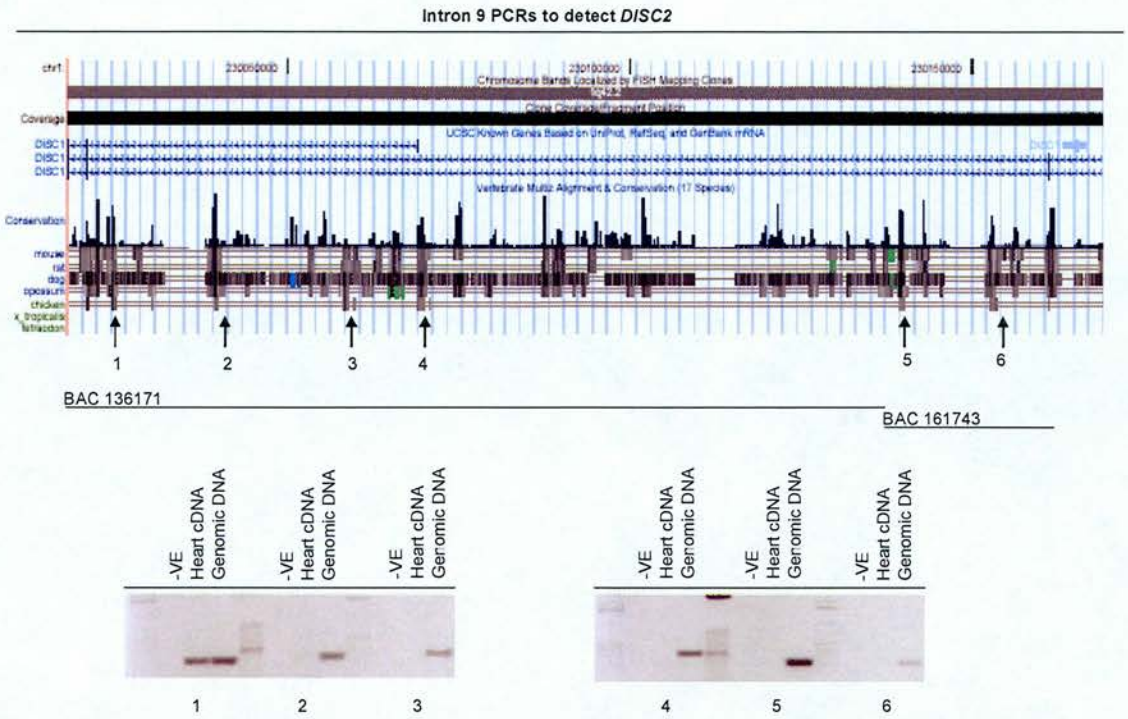

Figure 8.3.A. This figure depicts the intron 9 region of *DISC1* using the UCSC genome browser. Intronic primers were designed adjacent to conserved sequences throughout the intron as indicated by arrows 1-6. Primer pairs were used to amplify *DISC2* from human heart cDNA. Only primer pair 1, located closest to exon 9 of *DISC1*, detected *DISC2* transcription. –VE reactions correspond to no DNA controls.

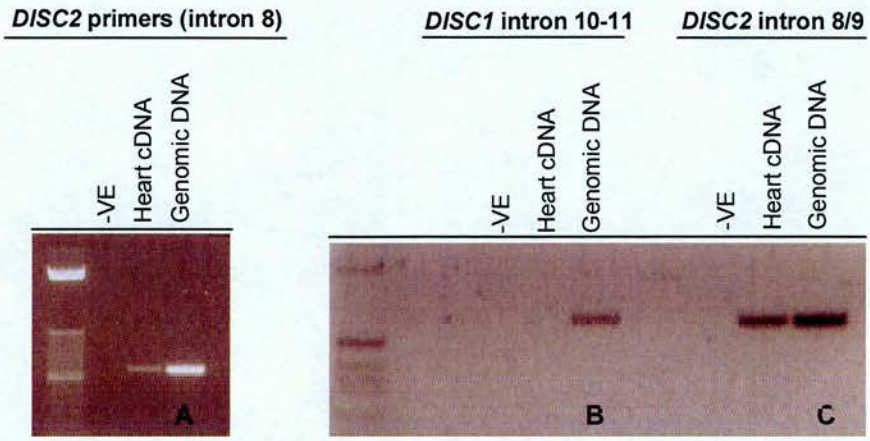

Figure 8.3.B. This figure confirms that *DISC2* sequence is transcribed from the intron 8 and intron 9 region of *DISC1* **(A and C)**. It further rules out the possibility that these transcripts represent un-processed *DISC1* using an intronic primer pair located outside of the *DISC2* known region **(B)**.

8.3.1.2 Amplification of the *DISC2* 5' end using RACE

RACE can be a frustrating procedure because cDNA libraries often contain truncated transcripts especially if transcripts are long, like *DISC2*, or contain a high level of secondary structure. Furthermore as RACE is a PCR-based technique, truncated (smaller) cDNAs will be more efficiently amplified than full length transcripts (if they exist) further reducing the chance of identifying the 5' end. However, since the original study by *Millar et al. 2000* there have been significant advances in the available RACE technologies. For these experiments an RNA-ligase mediated RACE system from Ambion was used. This particular RACE system is specifically designed to identify 5' gene ends. This technique used a human heart cDNA library, also from Ambion, which should only contain full length transcripts. Full length mRNAs contain a cap structure at their 5' end. Prior to the RACE procedure the cDNA library was treated using a calf intestinal phosphatase to remove the un-capped 5' phosphate group from truncated mRNAs in addition to rRNA, tRNA and DNA which are subsequently degraded. Following this the cap structure is removed from full length mRNAs and these are ligated to a specific 5' adapter sequence. Primers for this adapter are then used in conjunction with gene specific primers to amplify the gene (and hence locate the 5' end). A heart cDNA population was chosen as *DISC2* was seen to be highly expressed in heart by northern blotting (*Millar et al. 2000*).

Considering that the 5' end of *DISC2* is thought to lie somewhere within a 150kb intronic region it has the potential to produce a very large transcript. The processivity of the polymerase used to amplify the RACE products would be important if this technique were to be successful. I therefore chose a highly processive enzyme for use in these experiments (details can be obtained in chapter 2).

The 5' RACE protocol uses nested PCR; an outer 5' adapter primer is combined with an outer gene specific primer and used to amplify the cDNA library; the resulting PCR products are subsequently re-amplified using a second (inner) 5' adapter primer and a second (inner) gene specific primer. For these RACE experiments I used the

outer primer of primer pair 1 (see figure 8.3.A), which successfully amplified *DISC2* from human heart cDNA and designed a new inner gene specific primer for the nested PCR reaction.

The RACE was carried out twice and produced 3 RACE products each time, a doublet at approximately 600bp and a single product at approximately 500bp (Figure 8.3.C (A1 and A2)). These products were gel purified and re-run to determine the DNA concentration subsequent to sequencing (Figure 8.3.C (B)). The doublet at approximately 600bp was run on a 3% TAE gel to try and separate the products (figure 8.3.C (C)). These two products were again gel-purified followed by sequencing. Both products from the upper doublet and the lower product were sequenced twice. Sequences were subjected to blast searching and were found to align to *DISC2* and intronic *DISC1* sequence on chromosome 1 (Figure 8.3.D).

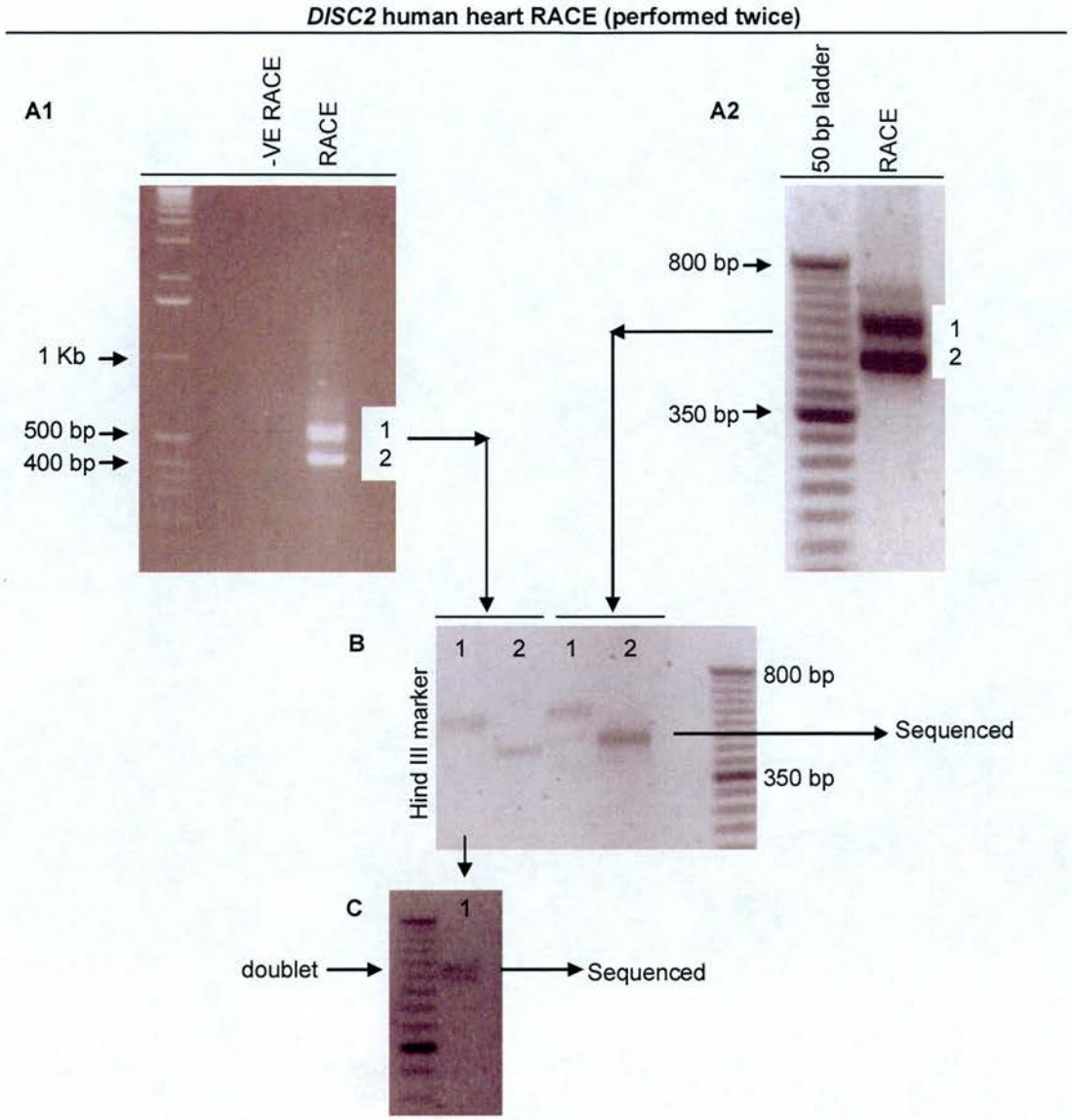

Figure 8.3.C. This figure depicts two repeats of the RACE procedure for *DISC2* using human heart cDNA **(A1 and A2)**. Products labelled 1 and 2 were gel-purified and re-run and the lower band excised for sequencing **(B)**. Product 1 was re-run to resolve the doublet and both bands were excised for sequencing **(C)**. The –VE reactions correspond to no DNA controls.

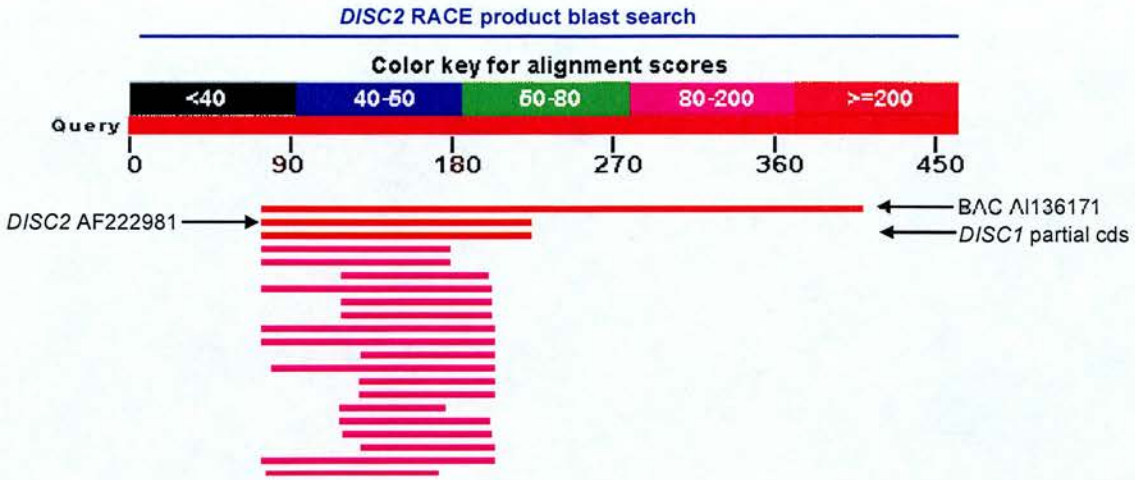

Sequences producing significant alignments:	Score (Bits)	E Value
gi|10944139|emb|AL136171.17| Human DNA sequence from clone RP...	367	2e-98
gi|8163870|gb|AF222981.1|AF222981 Homo sapiens 1 DISC2 gene, com	244	2e-61
gi|8163844|gb|AF222987.1|AF222987 Homo sapiens DISC1 protein ...	244	2e-61
gi|29788794|gb|AC090842.3| Homo sapiens chromosome 3 clone RP...	107	3e-20
gi|24942866|gb|AC090940.2| Homo sapiens chromosome 3 clone RP...	107	3e-20
gi|16972866|emb|AL355877.25| Human DNA sequence from clone RP...	105	1e-19
gi|21629068|gb|AC119038.4| Homo sapiens 3 BAC RP11-508018 (Ro...	103	5e-19
gi|19774304|gb|AC112916.3| Homo sapiens X BAC RP11-765I9 (Ros...	101	2e-18
gi|18921245|gb|AC097348.5| Homo sapiens X BAC RP11-489K4 (Ros...	101	2e-18

Figure 8.3.D. This figure depicts blast search results from representative *DISC2* RACE product sequence. This sequence aligns to the human BAC AL136171 which overlaps intron 9 of *DISC1*. It also aligns to *DISC2* and *DISC1* sequence within intron 9.

8.4 Analysis of RACE products

Blast searching reveals that the RACE products align to sequence within human BAC AL136171, which overlaps the intron 9 region of *DISC1*. However these alignments are not all from one region of this BAC. Alignments of all RACE products revealed similar matches to two different regions of AL136171 separated by almost 25Kb of sequence (Figure 8.4.A). It is possible that these RACE products represent spliced *DISC2* transcripts therefore the boundaries between the two regions of alignment were analysed for splice site consensus sequences. A 5' splice site contains the consensus sequence GT at the exon/intron boundary and the 3' splice site contains AG at the intron/exon boundary with some conservation of sequence surrounding these sites (Figure 8.4.B). The exon/intron boundaries of the *DISC2* RACE products were compared to these consensus sequences. These comparisons are shown in figure 8.4.B. Both 5' and 3' splice sites conform to the consensus with only one base pair difference indicating that these are functional splice sites. Therefore it appears that a new splice variant of *DISC2*, consisting of two novel exons, has been identified using this RACE procedure.

On further examination of the *DISC2* region using the UCSC genome browser newly added spliced EST sequences were identified (DA536261, DA566884, DA562083, figure 8.4.C). I examined these EST sequences and compared them to my RACE products. The genomic structure and sequence of these ESTs was compared to known *DISC2* and the novel *DISC2* RACE sequence (Figure 8.4.D). The most 5' RACE exon matched the 5' exon of all three ESTs, and the second RACE exon matched two of the ESTs; the third EST sequence lacked an exon at this position (Figure 8.4.D). Furthermore all three spliced ESTs contained a third exon which was within the known *DISC2* sequence (AF222981). This exon was not detected using my RACE primers as this exon is located further towards the 3' end of *DISC2*. These EST sequences were derived from 5' oligo capped human heart cDNA and were cross referenced to *Kimura et al. 2006*. This paper was involved in examination of 5' gene ends to identify alternative promoters for human genes. Considering the authors particular effort to examine only 5' gene ends it is very likely that the 5' exon of these ESTs and the *DISC2* RACE product represents the true 5' end of *DISC2*.

Although this 5' exon is likely to represent the 5' end, the genomic structure of full length *DISC2* remains unknown. Some potential *DISC2* transcripts are depicted in figure 8.4.E but more experimental work is needed to elucidate the full genomic potential of *DISC2*. My attempts to define the promoter region of *DISC2* are discussed in the subsequent section.

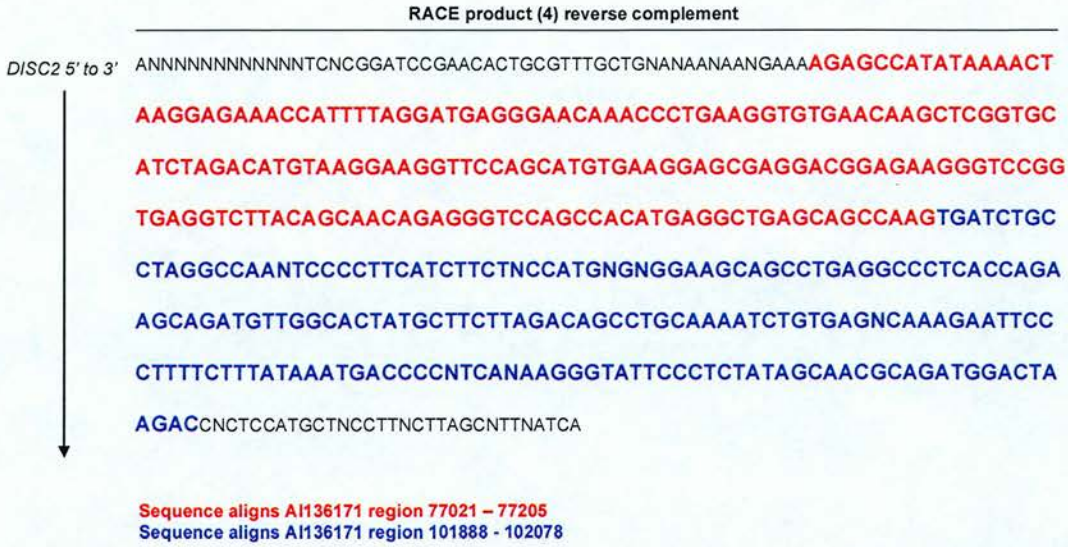

Figure 8.4.A. This figure depicts representative *DISC2* RACE sequence and the region of alignment to BAC AL136171. This RACE sequence aligns in two pieces separated by ~25Kb of sequence.

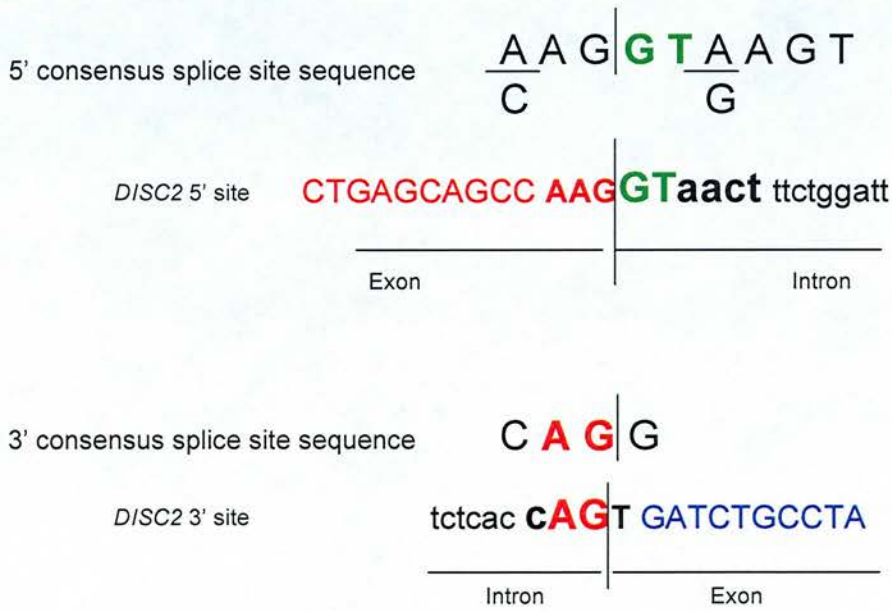

Figure 8.4.B. This figure depicts consensus 5' and 3' splice site sequences and the corresponding *DISC2* splice sites. The *DISC2* RACE splice site sequences are good matches to both 5' and 3' consensus sequence.

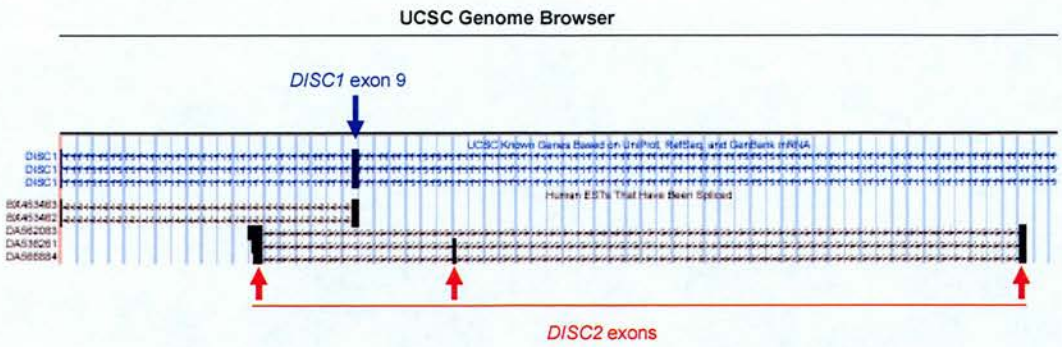

Figure 8.4.C. 3 new spliced EST sequences were identified within the *DISC2* region using the UCSC genome browser. *DISC1* exon 9 is indicated with a blue arrow and novel *DISC2* exons are indicated with red arrows.

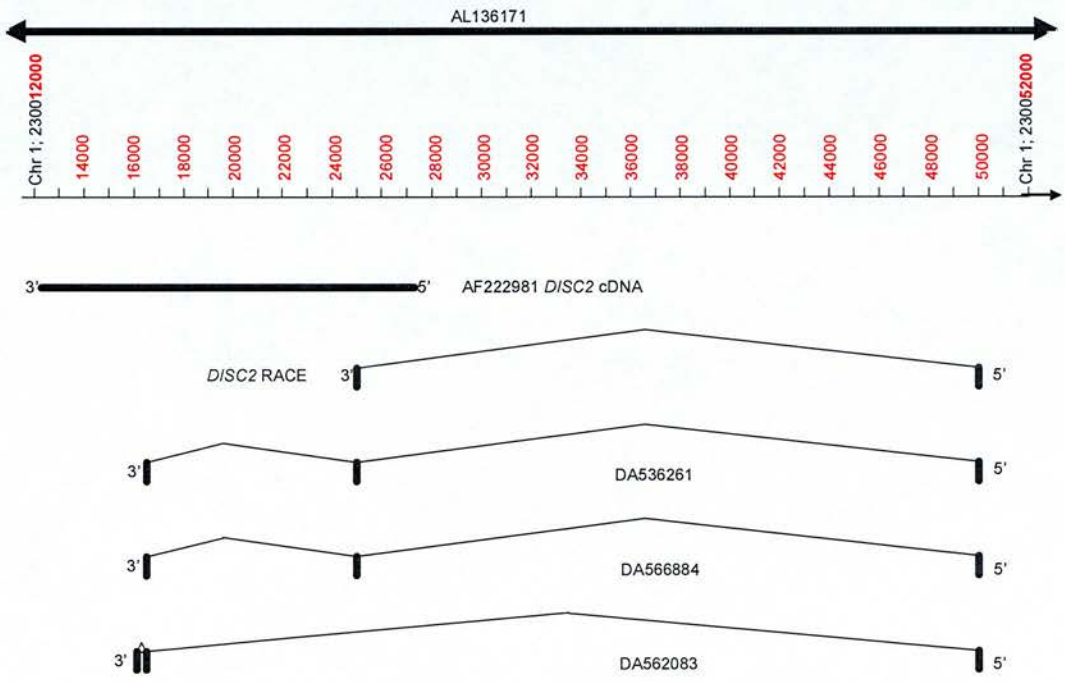

Figure 8.4.D. *DISC2* RACE sequence was compared to ESTs from the UCSC genome browser. The most 5' exon of *DISC2* aligns with all of the spliced EST sequences. *RACE* exon 2 also aligns to two of the ESTs however the third EST lacks this exon. Furthermore all three ESTs contain a novel exon within the known *DISC2* sequence.

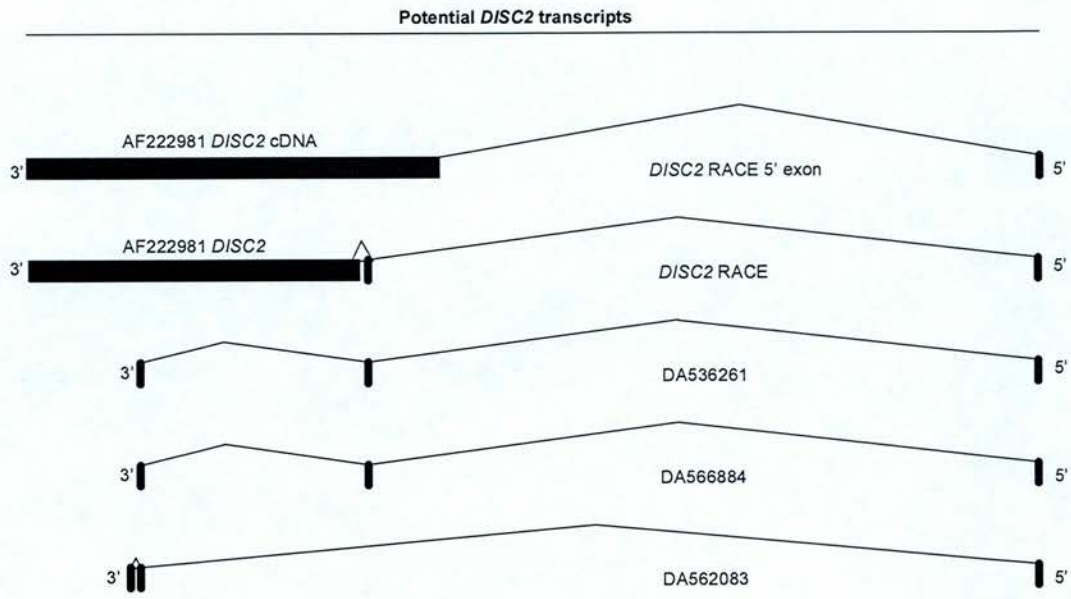

Figure 8.4.E. Some potential *DISC2* transcripts are shown, in addition to the three novel ESTs which possibly represent true *DISC2* splice variants.

8.5 Searching for the *DISC2* promoter

As the RACE procedure appears to have successfully located the 5' end of *DISC2,* promoter searching began again to try and define the *DISC2* promoter. Eukaryotic promoters have many characteristic features including a TATA box (TATAAA), Initiator sequence (PyPyAN(T/A)PyPy, see abbreviations), CAAT box (CCAAT), GC box (GGGCGG) and E box (CACGTG). These elements can be distributed at various positions throughout the promoter region and only a selection of these elements are likely be present within any given promoter.

Using the FPROM and TSSG mammalian promoter prediction programs (www.softberry.com) a putative promoter was identified overlapping the 5' RACE region. This sequence consisted of a putative TATA box at start of the 5' exon of *DISC2* and an initiator sequence approximately 11 bases downstream (Promoter 1 figure 8.5.A). It is puzzling that the promoter elements in this case appear to be within the cDNA sequence therefore this may not represent the real promoter region. Alternatively the TATA box at the 5' end of the RACE sequence is also a good consensus initiator sequence and therefore *DISC2* could have a TATA-less promoter and consist of an initiator sequence in addition to upstream transcription factor binding sites (Promoter 2 figure 8.5.A).

This promoter prediction program also identified 3 additional putative promoters within approximately 700bp of the 5' RACE sequence. Some of these promoter predictions are likely to be false positives and therefore any prediction requires experimental confirmation. Furthermore as *DISC2* is a novel non-coding RNA gene, for which the promoter characteristics are not well understood, it is possible that these prediction programs are not applicable in this situation.

Figure 8.5.A. This figure depicts promoter predictions for the *DISC2* cDNA sequence. Promoter prediction 1 was identified using the FPROM and TSSG mammalian promoter prediction programs. However it was noted that the TATA box sequence of this promoter is also a good initiator sequence (promoter prediction 2) and as such *DISC2* could potentially possess a TATA-less promoter.

8.6 Discussion

Only 1.4% of the human genome consists of protein coding genes, of which we possess approximately 20,000-25,000 (*Szymanski and Barciszewski 2002, International Human Genome Sequencing consortium 2004*). This is far reduced in comparison to that of lower eukaryotes and demonstrates that the complexity of a human cannot be clearly linked to the number of protein coding genes we possess (*Szymanski and Barciszewski 2002*). This further suggests that an additional layer of complexity may be present. Additional complexity is indeed provided by the non-coding transcriptome and also by multifaceted use of protein-coding genes. It has been estimated that more than 50% of all protein coding genes use alternative splicing to produce multiple transcripts from the same genomic locus (*Lander et al. 2001 International Human Genome Sequencing Consortium*). This is in addition to approximately 52% of known genes which use alternative promoters to diversify the range of transcripts produced by a single gene (*Kimura et al. 2006*). By considering that many protein coding genes employ alternative splicing, alternative promoters or both, we can begin to understand how a complex organism such as a human being can be generated from a mere 25,000 protein coding genes. Add to this the additional complexity of non-coding genes that can either regulate protein coding genes or perform independent functions and we can begin to embrace the complex nature of the human genome. These non-coding genes can be housekeeping genes such as ribosomal RNA or transfer RNA but they may also be regulatory and impact on the expression of their cognate sense gene products.

This chapter attempted to further characterise such a non-coding gene, *DISC2*, which is disrupted by the t(1;11) translocation. If *DISC2* has a role in regulating expression of its sense gene partner *DISC1*, then disruption by the t(1;11) translocation may have effects on transcription from the *DISC1* gene. This is in addition to the independent effects of the translocation on *DISC1*. *DISC2* has been relatively uncharacterised to date with one large exon identified by RACE sequencing but the 5' end remaining uncharacterised (*Millar et al. 2000*).

The experiments in this chapter have shown that *DISC2* is a low abundance transcript within lymphoblastoid cell lines derived from t(1;11) family members. Furthermore translocation results in the production of abnormal transcripts in these cell lines with preliminary evidence supporting potential up-regulation of *DISC2* in translocation carriers (Figure 8.2.B and exon 9 qRT-PCR data, chapter 3). However as the function of *DISC2* is unknown we can only speculate that this may affect *DISC1* expression in some manner.

I set out to attempt to identify the 5' end of this gene. As an initial bioinformatics approach proved unfruitful a more direct experimental route was chosen. PCR was used initially to narrow down the *DISC2* gene region followed by RACE PCR to identify the 5' end. The RACE procedure identified novel splicing of the *DISC2* gene with this new splice variant encompassing two novel exons. These novel exons are separated by almost 25kb of genomic sequence. On examination of this genomic region using the UCSC genome browser, three new EST sequences were identified (DA536261, DA566884, DA562083). These EST sequences were in the same orientation as *DISC2* and on comparison of RACE and EST sequences it was noted that the 5' exon of the RACE products corresponded to the 5' exon of all three ESTs. The RACE products and the ESTs were all generated from heart cDNA libraries enriched for 5' gene ends and therefore this 5' exon is likely to represent the true 5' end of *DISC2*. These newly incorporated EST data also identified a third novel *DISC2* exon within the current known sequence.

Promoter prediction programs were employed to search for the promoter within the 5' region of the RACE sequence. These programs identified multiple promoters in this region, highlighting the likely high false positive rate of promoter prediction programs. The prediction nearest the 5' end suggested that a TATA box element is present followed by an initiator sequence however these elements were present within the cDNA sequence of the 5' exon and are unlikely to represent the real promoter. It was noted that a good initiator sequence is present at the start of the 5' exon and therefore it is possible that *DISC2* possesses a TATA-less promoter which is a common phenomenon. However these predictions need to be validated by experimental data. It is important to note also that *DISC2* is a putative non-coding

gene and promoter elements for these genes are not well characterised. The prediction programs used here search for promoter elements present within protein coding genes and therefore they may not be applicable in this situation.

In summary, these data have presented evidence for the existence of the *DISC2* 5' end some 22kb from the known sequence, making this gene approximately 37kb in length. The majority of this novel sequence comprises a large intron, however the RACE procedure identified two novel *DISC2* exons and examination of new EST data also identified a further novel exon within the known *DISC2* sequence. Attempts can now be made to characterise the genomic structure, coding potential and function of this novel gene, *DISC2*.

Chapter 9

Concluding Remarks

9.1 Preface

DISC1 and *DISC2* were originally identified as candidate genes for schizophrenia and related affective disorders in a large multi-generation Scottish family. This family possesses a balanced 1;11 translocation disrupting the *DISC* locus, which segregates in a statistically significant manner with major psychiatric illness (*Blackwood et al. 2001, Millar et al. 2000*). There now exists a large body of independent genetic evidence implicating the *DISC* locus in psychiatric illness.

In recent years *DISC1* has come into the limelight as an important and functionally relevant gene implicated in brain structure and function. The *DISC2* gene however has remained uncharacterised. Despite insights into the function of the DISC1 protein the disease mechanism operating within the t(1;11) family has been the subject of much debate, with differing hypotheses regarding haploinsufficiency and the presence of a 'mutant' DISC1 protein. This PhD thesis aimed to shed light on the pathogenesis of illness within this family by investigating the effects of the t(1;11) translocation on the expression and function of the *DISC* locus.

9.2 Discussion and future work

From the mRNA and protein expression experiments in chapter 3 it is relatively clear that there is no truncated DISC1 protein produced as a result of the t(1;11) translocation. Therefore the most likely disease mechanism operating within this family is one of haploinsufficiency. There are still some grey areas however surrounding the effects of the t(1;11) translocation on transcription from the *DISC1* and *DISC2* genes. In particular Real-Time PCR using primers within the exon 9 region of *DISC1* appeared to show a less dramatic reduction or even increased expression in some cell lines carrying the translocation. Whilst it is clear that this is not due to an increase in *DISC1* expression, this region of chromosome 1 also harbours the *DISC2* gene. It is possible therefore that this apparent upregulation may

be due to transcription of *DISC2* from the derived chromosome 11 allele. In support of this it has been shown that *DISC2* is apparently transcribed from this derived allele. It remains therefore to examine the expression levels of *DISC2* in t(1;11) cell lines carrying the translocation compared to karyotypically normal controls. If the derived *DISC2* allele is transcribed in cells of t(1;11) individuals it may have a significant impact if, in concordance with the current hypothesis, *DISC2* represents a bone-fide functional non-coding RNA gene.

Experiments described in chapter 8 have successfully identified the 5' end of this novel *DISC2* gene providing a platform on which to take forward the functional characterisation of this gene and to test the current hypothesis. The genomic structure of *DISC2* has not yet been fully defined, however it appears to be more complex than originally thought with multiple different splice variants. Further RACE experiments may help to define the genomic structure and northern blotting is now possible to define the number and sizes of transcripts produced from this gene. Hopefully expression of *DISC2* constructs will shed light on whether this antisense non-coding RNA gene acts as a riboregulator of *DISC1*. It will be interesting also to examine the expression profiles of *DISC1* and *DISC2* in high expressing tissue such as heart and brain, however as *DISC2* appears to be a human specific gene the availability of appropriate tissue may prove a hindrance. Real-Time PCR data presented in chapter 7 provided evidence for a dynamic regulation of *DISC1* expression in human embryonic stem cells during neuronal differentiation. These cells lines may also be used to analyse *DISC2* expression and determine a possible developmentally correlated expression profile for this gene.

This work has provided support for the somewhat controversial localisation of DISC1 at the centrosome. It can be concluded from data presented in chapter 4 that in fact specific DISC1 isoforms are prominently associated with the centrosome, and the centrioles in particular. DISC1 also localises to the poles of the mitotic spindle, a previously unknown location. The centrosome is a multifunctional organelle with roles in nuclear migration, mitosis and protein degradation (*Badano et al. 2005, Doxsey et al. 2005*). Considering the potential cell cycle defects reported following

siRNA induced knockdown of DISC1, it will be interesting to examine the centrosomal localisation of DISC1 further. It has been shown that some proteins involved in centrosome function to do not remain associated with this organelle throughout the cell cycle. For example *Chen et al.* have reported that ninein, a mother centriole protein, appears at the centrosome in interphase but disappears during the mitotic phase and re-appears at telophase (*Chen et al. 2003*). From the experiments thus far DISC1 appears to remain associated with the centrosome throughout the cell cycle. Time-lapse microscopy in combination with cell cycle markers will be useful in clarifying this localisation of DISC1 throughout mitosis. Furthermore, DISC1 centrosomal interactors, including NUDEL (Ndel1), LIS1, dynein and dynactin, have been shown to be localised to centrosomes, spindle microtubules and kinetochores during mitosis and play an important role in spindle formation, chromosome alignment and checkpoint control (*Faulkner et al. 2000, Siller et al. 2005, Yan et al. 2003*). It will be interesting therefore to examine whether DISC1 occupies similar additional locations or participates in similar functions during mitosis.

As haploinsufficiency is the most likely disease model operating with the t(1;11) family much of the future work will focus on the phenotypic abnormalities arising as a result of DISC1 knockdown using an RNAi interference approach. Phenotypes assessed so far have shown that reduced DISC1 may cause delays in progression from G_1 into S phase of the cell cycle. This would be consistent with localisation of DISC1 to the centrosome. Initially it will be necessary to carry out independent repetitions of this experiment. Furthermore cell cultures should be synchronised to allow exact comparisons of cell cycle stages between experimental populations. In addition to using DNA content as a measure of cell cycle stage, additional strategies should also be employed to define cell cycle progression. As the cell cycle is basically a complex signalling cascade, it is possible to look at protein markers of cell cycle progression. Moreover time-lapse microscopy of synchronised cultures should be carried out to examine more specifically the delays in cell cycle progression and the reasons for this. Using time-lapse microscopy it will be possible to examine the formation of the bipolar spindle, chromosome segregation and

chromosome alignment, the timing of the onset of anaphase and also cytokinesis which will hopefully yield important information regarding the reasons for cell cycling defects that may result from DISC1 knockdown.

Apoptosis is also an interesting area which will be explored in more detail. To further analyse the apoptotic phenotype it will be necessary to first determine if this defect is due to effects on mitochondrial DISC1 and thus represents mitochondria elicited apoptotic defects or defects in an alternative apoptotic signalling cascade. To do this it is possible to examine mitochondrial membrane potential and protein markers of apoptosis that are specifically associated with mitochondrial signalling. It is also possible to specifically induce the apoptotic response via the mitochondrial apoptosome. These experiments will hopefully shed light on the apoptotic defects that are occurring as a result of DISC1 knockdown. These experiments may also give insights into the normal function of DISC1 at the mitochondria. Additional experiments to define this should include examination of mitochondrial respiration, via ATP production, following DISC1 knockdown as defects in mitochondrial respiration have been implicated in schizophrenia (*Ben-Shachar 2002*).

DISC1 already has a defined role in cAMP signalling via interactions with phosphodiesterase type 4B (*Millar et al. 2005b*). The RNAi experiments presented here demonstrate further that the hydrolysing activity of PDE4 enzymes is dramatically reduced when DISC1 levels are reduced. This was not expected as the *Millar et al. 2005* study presented data showing DISC1 to have an inhibitory effect on PDE4B hydrolysing activity, which suggests that reduced DISC1 levels should result in increased PDE4 activity. The results from these experiments imply that DISC1 has a wider role in cAMP signalling and that this pathway is dramatically affected by reductions in DISC1. It seems unlikely that this effect is occurring within cells of t(1;11) patients as a complete block in hydrolysing cAMP would have extremely deleterious effects. In this respect it is possible therefore that reducing DISC1 expression by RNAi is more useful in determining the normal functions of DISC1 rather than elucidating the exact effects of the t(1;11) translocation. It is necessary to examine PDE4B activity directly in t(1;11) cell lines to deduce further the effect of the translocation on cAMP signalling.

The possibility that DISC1 has a wider role in cAMP signalling than previously appreciated is however becoming an exciting possibility considering its prominent localisation to the centrosome. I have shown that DISC1 co-localises with AKAP450 at the centrosome. This AKAP protein is involved in centrosomal targeting of PKA and also in binding to phosphodiesterase type 4D, which also binds PKA at the centrosome (*McCahill et al. 2005, Tasken et al. 2001*). AKAP450 is also a putative DISC1 interactor and therefore there is the possibility of an AKAP450/PKA/PDE4D/DISC1 complex at the centrosome. It is also possible that this may be extended to mitochondrial cAMP signalling where DISC1 binds PDE4B and that DISC1 may be a general component of AKAP/PKA/PDE signalling complexes. To substantiate this hypothesis it is necessary to examine the interaction between DISC1 and AKAP450 further and also to examine interactions between DISC1 and mitochondrial AKAP proteins.

Lastly it remains to be said that with much of the future work plans employing RNAi mediated knockdown of DISC1 it will be necessary to implement good controls to minimise identification of non-specific phenotypic abnormalities as potentially important. Despite the implementation of controls there is still some controversy surrounding the use of siRNAs and their resulting off target effects, therefore DISC1 rescue experiments should be performed whilst bearing in mind that overexpression experiments raise additional problems of their own. The phenotypes observed thus far from RNAi mediated DISC1 knockdown seem to correlate well with expected phenotypes and with the localisation of DISC1 within the cell and its suspected role as a protein scaffold protein. Therefore although RNA interference is not a foolproof science, *"as with everything else in life, good planning and moderation are keys to success"* (*Barik, 2006*).

9.3 Final conclusions

DISC1 haploinsufficiency is the most likely disease mechanism operating within the t(1;11) family. Resulting decreases in DISC1 may have wide implications for cell biology including cell cycle progression, apoptosis and cAMP signalling. These are

crucial processes which are integral to brain development and function. Perturbation of DISC1 at the centrosome may have implications for cell division or neuronal differentiation during early stages of brain development and for selective apoptosis to define the brain circuitry during later developmental stages. These defects in combination with additional neuronal migratory abnormalities may contribute to aberrant neuronal positioning and connectivity within the schizophrenic brain. Perturbations in cAMP signalling may have implications for neurotransmission and information processing within the brain and this in combination with subtle neuroanatomical defects may be the underlying cause of psychiatric illness in the t(1;11) family.

References

Aoki, K., R. Ishida, et al. (1997). "Isolation and characterization of a cDNA encoding a Translin-like protein, TRAX." FEBS Lett **401**(2-3): 109-12.

Altar, C. A., Jurata, L.W., Charles, V., Lemire, A., Liu, P., Bukhman, Y., Young, T.A., Bullard, J., Yokoe, H., Webster, M.J., Knable, M.B., Brockman, J.A. (2005). "Deficient hippocampal neuron expression of proteasome, ubiquitin, and mitochondrial genes in multiple schizophrenia cohorts." Biol Psychiatry **58**(2): 85-96.

Attardi, G. and G. Schatz (1988). "Biogenesis of mitochondria." Annu Rev Cell Biol **4**: 289-333.

Attwell, D. and A. Gibb (2005). "Neuroenergetics and the kinetic design of excitatory synapses." Nat Rev Neurosci **6**(11): 841-9.

Austin, C. P., B. Ky, et al. (2004). "Expression of Disrupted-In-Schizophrenia-1, a schizophrenia-associated gene, is prominent in the mouse hippocampus throughout brain development." Neuroscience **124**(1): 3-10.

Austin, C. P., L. Ma, et al. (2003). "DISC1 (Disrupted in Schizophrenia-1) is expressed in limbic regions of the primate brain." Neuroreport **14**(7): 951-4.

Babcock, D. F. and B. Hille (1998). "Mitochondrial oversight of cellular Ca^{2+} signaling." Curr Opin Neurobiol **8**(3): 398-404.

Bachevalier, J., M. C. Alvarado, et al. (1999). "Memory and socioemotional behavior in monkeys after hippocampal damage incurred in infancy or in adulthood." Biol Psychiatry **46**(3): 329-39.

Badano, J. L., T. M. Teslovich, et al. (2005). "The centrosome in human genetic disease." Nat Rev Genet **6**(3): 194-205.

Barik, S. (2006). "RNAi in moderation." Nat Biotechnol **24**(7): 796-7.

Bartel, D. P. (2004). "MicroRNAs: genomics, biogenesis, mechanism, and function." Cell **116**(2): 281-97.

Bauman, A. L., A. S. Goehring, et al. (2004). "Orchestration of synaptic plasticity through AKAP signaling complexes." Neuropharmacology **46**(3): 299-310.

Beavo, J. A. and L. L. Brunton (2002). "Cyclic nucleotide research -- still expanding after half a century." Nat Rev Mol Cell Biol **3**(9): 710-8.

Ben-Shachar, D. (2002). "Mitochondrial dysfunction in schizophrenia: a possible linkage to dopamine." J Neurochem **83**(6): 1241-51.

Ben-Shachar, D., Zuk, R., Gazawi, H., Ljubuncic, P. (2004). "Dopamine toxicity involves mitochondria complex I inhibition: implications to dopamine-related neuropsychiatric disorders." Biochem Pharmacol **67**(10): 1965-1974.

Benson, M. A., S. E. Newey, et al. (2001). "Dysbindin, a novel coiled-coil-containing protein that interacts with the dystrobrevins in muscle and brain." J Biol Chem **276**(26): 24232-41.

Berridge, K. C. and T. E. Robinson (1998). "What is the role of dopamine in reward: hedonic impact, reward learning, or incentive salience?" Brain Res Rev **28**(3): 309-69.

Bharath, S., B. N. Gangadhar, et al. (2000). "P300 in family studies of schizophrenia: review and critique." Int J Psychophysiol **38**(1): 43-54.

Blackwood, D. H., A. Fordyce, et al. (2001). "Schizophrenia and affective disorders--cosegregation with a translocation at chromosome 1q42 that directly disrupts

brain-expressed genes: clinical and P300 findings in a family." Am J Hum Genet **69**(2): 428-33.

Boada, J., Cutillas, B., Roig, T., Bermudez, J., Ambrosio, S. (2000). "MPP+ induced mitochondrial dysfunction is potentiated by dopamine." Biochem Biophys Res Commun **268**(3): 916-920.

Brandon, N. J., E. J. Handford, et al. (2004). "Disrupted in Schizophrenia 1 and Nudel form a neurodevelopmentally regulated protein complex: implications for schizophrenia and other major neurological disorders." Mol Cell Neurosci **25**(1): 42-55.

Brandon, N. J., I. Schurov, et al. (2005). "Subcellular targeting of DISC1 is dependent on a domain independent from the Nudel binding site." Mol Cell Neurosci **28**(4): 613-24.

Brzustowicz, L. M., K. A. Hodgkinson, et al. (2000). "Location of a major susceptibility locus for familial schizophrenia on chromosome 1q21-q22." Science **288**(5466): 678-82.

Callicott, J. H., R. E. Straub, et al. (2005). "Variation in DISC1 affects hippocampal structure and function and increases risk for schizophrenia." Proc Natl Acad Sci U S A **102**(24): 8627-32.

Camargo, L. M., V. Collura, et al. (2007). "Disrupted in Schizophrenia 1 Interactome: evidence for the close connectivity of risk genes and a potential synaptic basis for schizophrenia." Mol Psychiatry **12**(1): 74-86.

Cannon, T. D., W. Hennah, et al. (2005). "Association of DISC1/TRAX haplotypes with schizophrenia, reduced prefrontal gray matter, and impaired short- and long-term memory." Arch Gen Psychiatry **62**(11): 1205-13.

Cardno, A., McGuffin, P. (2002). Quantitative Genetics. Psychiatric Genetics and Genomics. P. McGuffin, Owen M.J., Gottesman I.I. New York, Oxford**:** 31-54.

Chen, C. H., S. L. Howng, et al. (2003). "Molecular characterization of human ninein protein: two distinct subdomains required for centrosomal targeting and regulating signals in cell cycle." Biochem Biophys Res Commun **308**(4): 975-83.

Chen, C. N., S. Denome, et al. (1986). "Molecular analysis of cDNA clones and the corresponding genomic coding sequences of the Drosophila dunce+ gene, the structural gene for cAMP phosphodiesterase." Proc Natl Acad Sci U S A **83**(24): 9313-7.

Chen, Q. Y., Q. Chen, et al. (2006). "Case-control association study of Disrupted-in-Schizophrenia-1 (DISC1) gene and schizophrenia in the Chinese population." J Psychiatr Res **41**(5): 428-34

Chumakov, I., M. Blumenfeld, et al. (2002). "Genetic and physiological data implicating the new human gene G72 and the gene for D-amino acid oxidase in schizophrenia." Proc Natl Acad Sci U S A **99**(21): 13675-80.

Colledge, M. and J. D. Scott (1999). "AKAPs: from structure to function." Trends Cell Biol **9**(6): 216-21.

Collier, D. A. and T. Li (2003). "The genetics of schizophrenia: glutamate not dopamine?" Eur J Pharmacol **480**(1-3): 177-84.

Costa, F. F. (2005). "Non-coding RNAs: new players in eukaryotic biology." Gene **357**(2): 83-94.

Curtis, D., G. Kalsi, et al. (2003). "Genome scan of pedigrees multiply affected with bipolar disorder provides further support for the presence of a susceptibility locus on chromosome 12q23-q24, and suggests the presence of additional loci on 1p and 1q." Psychiatr Genet **13**(2): 77-84.

Davenport, N. D., S. R. Sponheim, et al. (2006). "Neural anomalies during visual search in schizophrenia patients and unaffected siblings of schizophrenia patients." Schizophr Res **82**(1): 15-26.

de Leon, J. and F. J. Diaz (2005). "A meta-analysis of worldwide studies demonstrates an association between schizophrenia and tobacco smoking behaviors." Schizophr Res **76**(2-3): 135-57.

Delgehyr, N., J. Sillibourne, et al. (2005). "Microtubule nucleation and anchoring at the centrosome are independent processes linked by ninein function." J Cell Sci **118**(Pt 8): 1565-75.

Derosse, P., C. A. Hodgkinson, et al. (2006). "Disrupted in Schizophrenia 1 Genotype and Positive Symptoms in Schizophrenia." Biol Psychiatry, Epub PMID 17054920

Devon, R. S., S. Anderson, et al. (2001). "Identification of polymorphisms within Disrupted in Schizophrenia 1 and Disrupted in Schizophrenia 2, and an investigation of their association with schizophrenia and bipolar affective disorder." Psychiatr Genet **11**(2): 71-8.

Devon, R. S., S. Anderson, et al. (2001). "The genomic organisation of the metabotropic glutamate receptor subtype 5 gene, and its association with schizophrenia." Mol Psychiatry **6**(3): 311-4.

Devon, R. S., K. L. Evans, et al. (1997). "Novel transcribed sequences neighbouring a translocation breakpoint associated with schizophrenia." Am J Med Genet **74**(1): 82-90.

Devon, R. S. and D. J. Porteous (1997). "Physical mapping of a glutamate receptor gene in relation to a balanced translocation associated with schizophrenia in a large Scottish family." Psychiatr Genet **7**(4): 165-9.

Diviani, D. and J. D. Scott (2001). "AKAP signaling complexes at the cytoskeleton." J Cell Sci **114**(Pt 8): 1431-7.

Dobyns, W. B., O. Reiner, et al. (1993). "Lissencephaly. A human brain malformation associated with deletion of the LIS1 gene located at chromosome 17p13." Jama **270**(23): 2838-42.

Doxsey, S. (2001). "Re-evaluating centrosome function." Nat Rev Mol Cell Biol **2**(9): 688-98.

Doxsey, S., D. McCollum, et al. (2005). "Centrosomes in cellular regulation." Annu Rev Cell Dev Biol **21**: 411-34.

Drubach, D. (2000). The Brain Explained. New Jersey, Pentice Hall.

Dudai, Y., Y. N. Jan, et al. (1976). "dunce, a mutant of Drosophila deficient in learning." Proc Natl Acad Sci U S A **73**(5): 1684-8.

Eddy, S. R. (1999). "Noncoding RNA genes." Curr Opin Genet Dev **9**(6): 695-9.

Eddy, S. R. (2001). "Non-coding RNA genes and the modern RNA world." Nat Rev Genet **2**(12): 919-29.

Efimov, V. P. and N. R. Morris (2000). "The LIS1-related NUDF protein of Aspergillus nidulans interacts with the coiled-coil domain of the NUDE/RO11 protein." J Cell Biol **150**(3): 681-8.

Egan, M. F., R. E. Straub, et al. (2004). "Variation in GRM3 affects cognition, prefrontal glutamate, and risk for schizophrenia." Proc Natl Acad Sci U S A **101**(34): 12604-9.

Ekelund, J., W. Hennah, et al. (2004). "Replication of 1q42 linkage in Finnish schizophrenia pedigrees." Mol Psychiatry **9**(11): 1037-41.

Ekelund, J., I. Hovatta, et al. (2001). "Chromosome 1 loci in Finnish schizophrenia families." Hum Mol Genet **10**(15): 1611-7.

Faulkner, N. E., D. L. Dujardin, et al. (2000). "A role for the lissencephaly gene LIS1 in mitosis and cytoplasmic dynein function." Nat Cell Biol **2**(11): 784-91.

Feliciello, A., Gallo, A., Mele, E., Procellini, A., Troncone, G., Garbi, C., Gottesman, M.E., Avvedimento, E.V. (2000). "The localisation and activity of cAMP-dependent Protein kinase affects cell cycle progression in Thyroid cells." J Biol Chem **275**(1): 303-311.

Feliciello, A., M. E. Gottesman, et al. (2001). "The biological functions of A-kinase anchor proteins." J Mol Biol **308**(2): 99-114.

Flory, M. R., M. J. Moser, et al. (2000). "Identification of a human centrosomal calmodulin-binding protein that shares homology with pericentrin." Proc Natl Acad Sci U S A **97**(11): 5919-23.

Frith, C., Johnstone, E. (2003). Schizophrenia; A very short introduction, Oxford University press.

Gambello, M. J., D. L. Darling, et al. (2003). "Multiple dose-dependent effects of Lis1 on cerebral cortical development." J Neurosci **23**(5): 1719-29.

geNorm geNorm website, http://medgen.ugent.be/~jvdesomp/genorm.

Ghose, S., C. S. Weickert, et al. (2004). "Glutamate carboxypeptidase II gene expression in the human frontal and temporal lobe in schizophrenia." Neuropsychopharmacology **29**(1): 117-25.

Gillingham, A. K. and S. Munro (2000). "The PACT domain, a conserved centrosomal targeting motif in the coiled-coil proteins AKAP450 and pericentrin." EMBO Rep **1**(6): 524-9.

Gluck, M. R., Zeevalk, G.D. (2004). "Inhibiton of brain mitochondrial respiration by dopamine and its metabolites: implications for Parkinson's disease and catecholamine-associated diseases." J Neurochem **91**(4): 788-795.

Gogos, J. A., M. Santha, et al. (1999). "The gene encoding proline dehydrogenase modulates sensorimotor gating in mice." Nat Genet **21**(4): 434-9.

Gordon, D., C. Abajian, et al. (1998). "Consed: a graphical tool for sequence finishing." Genome Res **8**(3): 195-202.

Green, D. R., Reed, J.C. (1998). "Mitochondria and Apoptosis." Science **281**(5381): 1309-1312.

Green, E. K., N. Norton, et al. (2006). "Evidence that a DISC1 frame-shift deletion associated with psychosis in a single family may not be a pathogenic mutation." Mol Psychiatry **11**(9): 798-9.

Grimm, D., K. L. Streetz, et al. (2006). "Fatality in mice due to oversaturation of cellular microRNA/short hairpin RNA pathways." Nature **441**(7092): 537-41.

Gu, Z., Q. Jiang, et al. (2005). "Regulation of NMDA receptors by neuregulin signaling in prefrontal cortex." J Neurosci **25**(20): 4974-84.

Guo, J., Z. Yang, et al. (2006). "Nudel contributes to microtubule anchoring at the mother centriole and is involved in both dynein-dependent and -independent centrosomal protein assembly." Mol Biol Cell **17**(2): 680-9.

Gurling, H. M., G. Kalsi, et al. (2001). "Genomewide genetic linkage analysis confirms the presence of susceptibility loci for schizophrenia, on chromosomes 1q32.2, 5q33.2, and 8p21-22 and provides support for linkage to schizophrenia, on chromosomes 11q23.3-24 and 20q12.1-11.23." Am J Hum Genet **68**(3): 661-73.

Hajos, M. (2006). "Targeting information-processing deficit in schizophrenia: a novel approach to psychotherapeutic drug discovery." Trends Pharmacol Sci **27**(7): 391-398.

Hall, J., J. Chubb, et al. (2005). Workshop on Schizophrenia and Related disorders (meeting report) URL: www.mrc.ac.uk

Hall, J., H. C. Whalley, et al. (2006). "A neuregulin 1 variant associated with abnormal cortical function and psychotic symptoms." Nat Neurosci **9**(12): 1477-8

Hamshere, M. L., P. Bennett, et al. (2005). "Genomewide linkage scan in schizoaffective disorder: significant evidence for linkage at 1q42 close to DISC1, and suggestive evidence at 22q11 and 19p13." Arch Gen Psychiatry **62**(10): 1081-8.

Hannon, G. J. (2002). "RNA interference." Nature **418**(6894): 244-51.

Harrison, P. (1999). "The neuropathology of schizophrenia; A critical review of the data and their interpretation." Brain **122**(Pt 4): 593-624.

Harrison, P., Weinberger, D.R. (2005). "Schizophrenia genes, gene expression, and neuropathology: on the matter of their convergence." Mol Psychiatry **10**(1): 40-68.

Harrison, P. J. and M. J. Owen (2003). "Genes for schizophrenia? Recent findings and their pathophysiological implications." Lancet **361**(9355): 417-9.

Hashimoto, R., T. Numakawa, et al. (2006). "Impact of the DISC1 Ser704Cys polymorphism on risk for major depression, brain morphology and ERK signaling." Hum Mol Genet **15**(20): 3024-33.

Hashimoto, R., R. E. Straub, et al. (2004). "Expression analysis of neuregulin-1 in the dorsolateral prefrontal cortex in schizophrenia." Mol Psychiatry **9**(3): 299-307.

Hashimoto, T., Volk, D.W., Eggan, S.M., Mirnics, K., Pierri, J.N., Sun, Z., Sampson, A.R., Lewis, D.A. (2003). "Gene expression deficits in a subclass of GABA neurons in the prefrontal cortex of subjects with schizophrenia." J Neurosci **23**(15): 6315-6326.

Heckers, S. (2001). "Neuroimaging studies of the hippocamus in schizophrenia." Hippocampus **11**(5): 520-528.

Hennah, W., A. Tuulio-Henriksson, et al. (2005). "A haplotype within the DISC1 gene is associated with visual memory functions in families with a high density of schizophrenia." Mol Psychiatry **10**(12): 1097-103.

Hennah, W., T. Varilo, et al. (2003). "Haplotype transmission analysis provides evidence of association for DISC1 to schizophrenia and suggests sex-dependent effects." Hum Mol Genet **12**(23): 3151-9.

Higashi, Y., M. Asanuma, et al. (2000). "Inhibition of tyrosinase reduces cell viability in catecholaminergic neuronal cells." J Neurochem **75**(4): 1771-4.

Hill, M. M., Adrain, C., Martin, S.J. (2003). "Portrait of a killer: The mitochondrial apoptosome emerging from the shadows." Mol Interv **3**(1): 19-24.

Hinchcliffe, E. H., F. J. Miller, et al. (2001). "Requirement of a centrosomal activity for cell cycle progression through G1 into S phase." Science **291**(5508): 1547-50.

Hirota, T., N. Kunitoku, et al. (2003). "Aurora-A and an interacting activator, the LIM protein Ajuba, are required for mitotic commitment in human cells." Cell **114**(5): 585-98.

Hodgkinson, C. A., D. Goldman, et al. (2004). "Disrupted in schizophrenia 1 (DISC1): association with schizophrenia, schizoaffective disorder, and bipolar disorder." Am J Hum Genet **75**(5): 862-72.

Houslay, M. D. and D. R. Adams (2003). "PDE4 cAMP phosphodiesterases: modular enzymes that orchestrate signalling cross-talk, desensitization and compartmentalization." Biochem J **370**(Pt 1): 1-18.

Houslay, M. D. and G. S. Baillie (2003). "The role of ERK2 docking and phosphorylation of PDE4 cAMP phosphodiesterase isoforms in mediating cross-talk between the cAMP and ERK signalling pathways." Biochem Soc Trans **31**(Pt 6): 1186-90.

Hovatta, I., T. Varilo, et al. (1999). "A genomewide screen for schizophrenia genes in an isolated Finnish subpopulation, suggesting multiple susceptibility loci." Am J Hum Genet **65**(4): 1114-24.

Hutvagner, G., M. J. Simard, et al. (2004). "Sequence-specific inhibition of small RNA function." PLoS Biol **2**(4): E98.

Hwu, H. G., C. M. Liu, et al. (2003). "Linkage of schizophrenia with chromosome 1q loci in Taiwanese families." Mol Psychiatry **8**(4): 445-52.

Inouye, M. (1988). "Antisense RNA: its functions and applications in gene regulation--a review." Gene **72**(1-2): 25-34.

International Human Genome sequencing consortium, I. H. G. C. (2004). "Finishing the euchromatic sequence of the human genome." Nature **431**(7011): 931-45.

Iwamoto, K., M. Bundo, et al. (2005). "Altered expression of mitochondria-related genes in postmortem brains of patients with bipolar disorder or schizophrenia, as revealed by large-scale DNA microarray analysis." Hum Mol Genet **14**(2): 241-53.

Jacobs, P. A., Frackiewicz, A., Newton, M., Cook, P.J.L., Robson, E.B. (1970). "Studies on a family with three cytogenetic markers." Ann Hum Gen (Lond) **33**: 325-336.

James, R., R. R. Adams, et al. (2004). "Disrupted in Schizophrenia 1 (DISC1) is a multicompartmentalized protein that predominantly localizes to mitochondria." Mol Cell Neurosci **26**(1): 112-22.

Kamiya, A., K. Kubo, et al. (2005). "A schizophrenia-associated mutation of DISC1 perturbs cerebral cortex development." Nat Cell Biol **7**(12): 1167-78.

Kapur, S. (2004). "How antipsychotics become anti-'psychotic' - from dopamine to salience to psychosis." Trends Pharmacol Sci **25**(8): 402-406.

Karry, R., Klein, E., Ben-Shachar, D. (2004). "Mitochondrial Complex I subunits expression is altered in schizophrenia: a postmortem study." Biol Psychiatry **55**(7): 676-684.

Katsel, P., David, K.L., Haroutunian, V. (2005). "Variations in myelin and oligodendrocyte-related gene expression across multiple brain regions in schizophrenia: a gene ontology study." Schizophr Res **79**(2-3): 157-173.

Keryer, G., O. Witczak, et al. (2003). "Dissociating the centrosomal matrix protein AKAP450 from centrioles impairs centriole duplication and cell cycle progression." Mol Biol Cell **14**(6): 2436-46.

Ketting, R. F. and R. H. Plasterk (2004). "What's new about RNAi? Meeting on siRNAs and miRNAs." EMBO Rep **5**(8): 762-5.

Khodjakov, A. and C. L. Rieder (2001). "Centrosomes enhance the fidelity of cytokinesis in vertebrates and are required for cell cycle progression." J Cell Biol **153**(1): 237-42.

Kimura, K., A. Wakamatsu, et al. (2006). "Diversification of transcriptional modulation: large-scale identification and characterization of putative alternative promoters of human genes." Genome Res **16**(1): 55-65.

Kinney, G. G., M. Burno, et al. (2003). "Metabotropic glutamate subtype 5 receptors modulate locomotor activity and sensorimotor gating in rodents." J Pharmacol Exp Ther **306**(1): 116-23.

Kockelkorn, T. T., M. Arai, et al. (2004). "Association study of polymorphisms in the 5' upstream region of human DISC1 gene with schizophrenia." Neurosci Lett **368**(1): 41-5.

Koike, H., P. A. Arguello, et al. (2006). "Disc1 is mutated in the 129S6/SvEv strain and modulates working memory in mice." Proc Natl Acad Sci U S A **103**(10): 3693-7.

Kramer, A., N. Mailand, et al. (2004). "Centrosome-associated Chk1 prevents premature activation of cyclin-B-Cdk1 kinase." Nat Cell Biol **6**(9): 884-91.

Kuhn, D. M., R. E. Arthur, Jr., et al. (1999). "Tyrosine hydroxylase is inactivated by catechol-quinones and converted to a redox-cycling quinoprotein: possible relevance to Parkinson's disease." J Neurochem **73**(3): 1309-17.

Kumar, M. and G. G. Carmichael (1998). "Antisense RNA: function and fate of duplex RNA in cells of higher eukaryotes." Microbiol Mol Biol Rev **62**(4): 1415-34.

Lachman, H. M., D. F. Papolos, et al. (1996). "Human catechol-O-methyltransferase pharmacogenetics: description of a functional polymorphism and its potential application to neuropsychiatric disorders." Pharmacogenetics **6**(3): 243-50.

Lander, E. S., L. M. Linton, et al. (2001). "Initial sequencing and analysis of the human genome." Nature **409**(6822): 860-921.

Law, A. J., B. K. Lipska, et al. (2006). "Neuregulin 1 transcripts are differentially expressed in schizophrenia and regulated by 5' SNPs associated with the disease." Proc Natl Acad Sci U S A **103**(17): 6747-52.

Lee, K. S., T. Z. Grenfell, et al. (1998). "Mutation of the polo-box disrupts localization and mitotic functions of the mammalian polo kinase Plk." Proc Natl Acad Sci U S A **95**(16): 9301-6.

Levinson, D. F., P. A. Holmans, et al. (2002). "No major schizophrenia locus detected on chromosome 1q in a large multicenter sample." Science **296**(5568): 739-41.

Li, D., D. A. Collier, et al. (2006). "Meta-analysis shows strong positive association of the neuregulin 1 (NRG1) gene with schizophrenia." Hum Mol Genet **15**(12): 1995-2002.

Li, J., W. L. Lee, et al. (2005). "NudEL targets dynein to microtubule ends through LIS1." Nat Cell Biol **7**(7): 686-90.

Li, J. Z., M.P. Vawter, et al. (2004). "Systematic changes in gene expression in postmortem human brains associated with tissue pH and terminal medical conditions." Hum Mol Genet **13**(6): 609-616.

Li, M., L. Pevny, et al. (1998). "Generation of purified neural precursors from embryonic stem cells by lineage selection." Curr Biol **8**(17): 971-4.

Lin, J. W., M. Wyszynski, et al. (1998). "Yotiao, a novel protein of neuromuscular junction and brain that interacts with specific splice variants of NMDA receptor subunit NR1." J Neurosci **18**(6): 2017-27.

Linden, D. E. (2005). "The p300: where in the brain is it produced and what does it tell us?" Neuroscientist **11**(6): 563-76.

Lipska, B. K. (2004). "Using animal models to test a neurodevelopmental hypothesis of schizophrenia." J Psychiatry Neurosci **29**(4): 282-6.

Liu, Y., B. Ford, et al. (2001). "Neuregulins increase alpha7 nicotinic acetylcholine receptors and enhance excitatory synaptic transmission in GABAergic interneurons of the hippocampus." J Neurosci **21**(15): 5660-9.

Liu, Y. L., C. S. Fann, et al. (2006). "A single nucleotide polymorphism fine mapping study of chromosome 1q42.1 reveals the vulnerability genes for schizophrenia, GNPAT and DISC1: Association with impairment of sustained attention." Biol Psychiatry **60**(6): 554-62.

Livak, K. J. and T. D. Schmittgen (2001). "Analysis of relative gene expression data using real-time quantitative PCR and the 2(-Delta Delta C(T)) Method." Methods **25**(4): 402-8.

Lo Nigro, C., C. S. Chong, et al. (1997). "Point mutations and an intragenic deletion in LIS1, the lissencephaly causative gene in isolated lissencephaly sequence and Miller-Dieker syndrome." Hum Mol Genet **6**(2): 157-64.

Lotta, T., J. Vidgren, et al. (1995). "Kinetics of human soluble and membrane-bound catechol O-methyltransferase: a revised mechanism and description of the thermolabile variant of the enzyme." Biochemistry **34**(13): 4202-10.

Ma, L., Y. Liu, et al. (2002). "Cloning and characterization of Disc1, the mouse ortholog of DISC1 (Disrupted-in-Schizophrenia 1)." Genomics **80**(6): 662-72.

Macgregor, S., P. M. Visscher, et al. (2002). "Is schizophrenia linked to chromosome 1q?" Science **298**(5602): 2277.

Macgregor, S., P. M. Visscher, et al. (2004). "A genome scan and follow-up study identify a bipolar disorder susceptibility locus on chromosome 1q42." Mol Psychiatry **9**(12): 1083-90.

Malhotra, A. K., Szeszko, P., Hodgkinson, C., Lencz, T., DeRosse, P., Burdick, K., Kane, J., Goldman, D. (2006). Structural and functional implications of DISC1 genotype in schizophrenia. Am J Hum Genet **141B**(7): 704

Marchbanks, R. M., Ryan, M., Day, I.N.M., Owen, M., McGuffin, P., Whatley, S.A. (2003). "A mitochondrial DNA sequence variant associated with schizophrenia and oxidative stress." Schizophr Res **65**(1): 33-38.

Marquis, J. P., S. Goulet, et al. (2006). "Neonatal lesions of the ventral hippocampus in rats lead to prefrontal cognitive deficits at two maturational stages." Neuroscience **140**(3): 759-67.

Martorell, L., Segues, T., Folch, G., Valero, J., Joven, J., Labad, A., Velella, E. (2006). "New variants in the mitochondrial genomes of schizophrenic patients." Eur J Hum Gen **14**(5): 520-528.

Marumoto, T., S. Honda, et al. (2003). "Aurora-A kinase maintains the fidelity of early and late mitotic events in HeLa cells." J Biol Chem **278**(51): 51786-95.

McCahill, A., T. McSorley, et al. (2005). "In resting COS1 cells a dominant negative approach shows that specific, anchored PDE4 cAMP phosphodiesterase isoforms gate the activation, by basal cyclic AMP production, of AKAP-tethered protein kinase A type II located in the centrosomal region." Cell Signal **17**(9): 1158-73.

McCarthy, C. (1996). Chromas version 1.45. web link: http://www.technelysium.com.au/chromas.html

McManus, M. T. and P. A. Sharp (2002). "Gene silencing in mammals by small interfering RNAs." Nat Rev Genet **3**(10): 737-47.

Mesngon, M. T., C. Tarricone, et al. (2006). "Regulation of cytoplasmic dynein ATPase by Lis1." J Neurosci **26**(7): 2132-9.

Michailov, G. V., M. W. Sereda, et al. (2004). "Axonal neuregulin-1 regulates myelin sheath thickness." Science **304**(5671): 700-3.

Millar, J. K., S. Christie, et al. (2001). "Genomic structure and localisation within a linkage hotspot of Disrupted In Schizophrenia 1, a gene disrupted by a translocation segregating with schizophrenia." Mol Psychiatry **6**(2): 173-8.

Millar, J. K., S. Christie, et al. (2003). "Yeast two-hybrid screens implicate DISC1 in brain development and function." Biochem Biophys Res Commun **311**(4): 1019-25.

Millar, J. K., R. James, et al. (2005a). "Disrupted in schizophrenia 1 (DISC1): subcellular targeting and induction of ring mitochondria." Mol Cell Neurosci **30**(4): 477-84.

Millar, J. K., B. S. Pickard, et al. (2005b). "DISC1 and PDE4B are interacting genetic factors in schizophrenia that regulate cAMP signaling." Science **310**(5751): 1187-91.

Millar, J. K., J. C. Wilson-Annan, et al. (2000). "Disruption of two novel genes by a translocation co-segregating with schizophrenia." Hum Mol Genet **9**(9): 1415-23.

Mirnics, K., F. A. Middleton, et al. (2001b). "Disease-specific changes in regulator of G-protein signaling 4 (RGS4) expression in schizophrenia." Mol Psychiatry **6**(3): 293-301.

Mirnics, K., Middleton, F.A., Lewis, D.A., Levitt, O. (2001a). "Analysis of complex brain disorders with gene expression microarrays: schizophrenia as a disorder of the synapse". Trends Neurosci **24**(8): 479-486.

Mirnics, K., Middleton, F.A., Marquez, A., Lewis, D.A., Levitt, P. (2000). "Molecular characterisation of schizophrenia viewed by microarray analysis of gene expression in prefrontal cortex." Neuron **28**(1): 53-57.

Miyazaki, I., M. Asanuma, et al. (2006). "Methamphetamine-induced dopaminergic neurotoxicity is regulated by quinone-formation-related molecules." Faseb J **20**(3): 571-3.

Miyoshi, K., M. Asanuma, et al. (2004). "DISC1 localizes to the centrosome by binding to kendrin." Biochem Biophys Res Commun **317**(4): 1195-9.

Miyoshi, K., A. Honda, et al. (2003). "Disrupted-In-Schizophrenia 1, a candidate gene for schizophrenia, participates in neurite outgrowth." Mol Psychiatry **8**(7): 685-94.

Moghaddam, B. (2003). "Bringing order to the glutamate chaos in schizophrenia." Neuron **40**(5): 881-4.

Morilak, D. A., Porteus, M.H., Ciaranello, R.D. (2000) "Molecular and Cellular Mechanisms of Brain Development."
DOI: http://www.acnp.org/G4/GN401000065/CH065.html

Morris, J. A., G. Kandpal, et al. (2003). "DISC1 (Disrupted-In-Schizophrenia 1) is a centrosome-associated protein that interacts with MAP1A, MIPT3, ATF4/5 and NUDEL: regulation and loss of interaction with mutation." Hum Mol Genet **12**(13): 1591-608.

Morris, N. R. (2000). "Nuclear migration. From fungi to the mammalian brain." J Cell Biol **148**(6): 1097-101.

Morrison, T. B., J. J. Weis, et al. (1998). "Quantification of low-copy transcripts by continuous SYBR Green I monitoring during amplification." Biotechniques **24**(6): 954-8, 960, 962.

Mosharov, E. V., Gong, L.W., Khanna, B., Sulzer, D., Lindau, M. (2003). "Intracellular patch electrochemistry: regulation of cytosolic catecholamines in chromaffin cells." J Neurosci **23**(13): 5835-5845.

Moudjou, M., N. Bordes, et al. (1996). "gamma-Tubulin in mammalian cells: the centrosomal and the cytosolic forms." J Cell Sci **109**(Pt 4): 875-87.

Moudjou, M., Bornens, M. (1998). Method of Centrosome Isolation from Cultured Animal Cells, Academic Press.

Moy, L. Y., Zeevalk, G.D., Sonsalla, P.K. (2000). "Role for dopamine in malonate-induced damage in vivo in striatum and invitro in mesencephalic cultures." J Neurochem **74**(4): 1656-1665.

Munroe, S. H. and J. Zhu (2006). "Overlapping transcripts, double-stranded RNA and antisense regulation: A genomic perspective." Cell Mol Life Sci **63**(18): 2102-18.

Muramatsu, T., A. Ohmae, et al. (1998). "BC1 RNA protein particles in mouse brain contain two y-,h-element-binding proteins, translin and a 37 kDa protein." Biochem Biophys Res Commun **247**(1): 7-11.

Murphy, K. C. (2002). "Schizophrenia and velo-cardio-facial syndrome." Lancet **359**(9304): 426-30.

N.I.M.H. (1972). Schizophrenia, Is there an answer? Health, National Institute for Mental Health, Rockville MD, DHEW publication no (HSM) 73-9086.

Neale, J. H., T. Bzdega, et al. (2000). "N-Acetylaspartylglutamate: the most abundant peptide neurotransmitter in the mammalian central nervous system." J Neurochem **75**(2): 443-52.

Nemes, J. P., K. A. Benzow, et al. (2000). "The SCA8 transcript is an antisense RNA to a brain-specific transcript encoding a novel actin-binding protein (KLHL1)." Hum Mol Genet **9**(10): 1543-51.

Niethammer, M., D. S. Smith, et al. (2000). "NUDEL is a novel Cdk5 substrate that associates with LIS1 and cytoplasmic dynein." Neuron **28**(3): 697-711.

Numakawa, T., Y. Yagasaki, et al. (2004). "Evidence of novel neuronal functions of dysbindin, a susceptibility gene for schizophrenia." Hum Mol Genet **13**(21): 2699-708.

Nussbaum, R. L. and C. E. Ellis (2003). "Alzheimer's disease and Parkinson's disease." N Engl J Med **348**(14): 1356-64.

Ogawa, F., M. Kasai, et al. (2005). "A functional link between Disrupted-In-Schizophrenia 1 and the eukaryotic translation initiation factor 3." Biochem Biophys Res Commun **338**(2): 771-6.

Owen, M. J., O'Donovan, M. (2002). Schizophrenia. Psychiatric Genetics and Genomics. P. McGuffin, Owen M.J., Gottesman I.I., Oxford University Press: 247-266.

Ozeki, Y., T. Tomoda, et al. (2003). "Disrupted-in-Schizophrenia-1 (DISC-1): mutant truncation prevents binding to NudE-like (NUDEL) and inhibits neurite outgrowth." Proc Natl Acad Sci U S A **100**(1): 289-94.

Park, C. H., Y. K. Minn, et al. (2005). "In vitro and in vivo analyses of human embryonic stem cell-derived dopamine neurons." J Neurochem **92**(5): 1265-76.

Passani, L. A., J. P. Vonsattel, et al. (1997). "Distribution of N-acetylaspartylglutamate immunoreactivity in human brain and its alteration in neurodegenerative disease." Brain Res **772**(1-2): 9-22.

Patel, S. H. and P. N. Azzam (2005). "Characterization of N200 and P300: selected studies of the Event-Related Potential." Int J Med Sci **2**(4): 147-54.

Pericak-Vance, M. A. (1998). LOD score analysis. Approaches to gene mapping in complex human diseases. J. L. Haines, Pericak-Vance, M.A., Wiley-Liss: 253-273.

Perrier, A. L., V. Tabar, et al. (2004). "Derivation of midbrain dopamine neurons from human embryonic stem cells." Proc Natl Acad Sci U S A **101**(34): 12543-8.

Petit, J., P. Boisseau, et al. (1999). "A YAC contig encompassing the 11q14.3 breakpoint of a translocation associated with schizophrenia, and including the tyrosinase gene." Mamm Genome **10**(6): 649-52.

Petronis, A. (2004). "The origin of schizophrenia: genetic thesis, epigenetic antithesis, and resolving synthesis." Biol Psychiatry **55**(10): 965-70.

Pfaffl, M. W. (2001). "A new mathematical model for relative quantification in real-time RT-PCR." Nucleic Acids Res **29**(9): e45.

Pfeiffer, B. E. and K. M. Huber (2006). "Current advances in local protein synthesis and synaptic plasticity." J Neurosci **26**(27): 7147-50.

Pietraszek, M., J. Nagel, et al. (2006). "The role of group I metabotropic glutamate receptors in schizophrenia." Amino Acids **32**(2): 173-8.

Polster, B. M., C. L. Robertson, et al. (2003). "Postnatal brain development and neural cell differentiation modulate mitochondrial Bax and BH3 peptide-induced cytochrome c release." Cell Death Differ **10**(3): 365-70.

Porteous, D. J. and J. K. Millar (2006). "Disrupted in schizophrenia 1: building brains and memories." Trends Mol Med **12**(6): 255-61.

Prigozhina, N. L., C. E. Oakley, et al. (2004). "gamma-tubulin plays an essential role in the coordination of mitotic events." Mol Biol Cell **15**(3): 1374-86.

Reiner, O., R. Carrozzo, et al. (1993). "Isolation of a Miller-Dieker lissencephaly gene containing G protein beta-subunit-like repeats." Nature **364**(6439): 717-21.

Robinson, M. B., R. D. Blakely, et al. (1987). "Hydrolysis of the brain dipeptide N-acetyl-L-aspartyl-L-glutamate. Identification and characterization of a novel N-acetylated alpha-linked acidic dipeptidase activity from rat brain." J Biol Chem **262**(30): 14498-506.

Roth, K. A. and C. D'Sa (2001). "Apoptosis and brain development." Ment Retard Dev Disabil Res Rev **7**(4): 261-6.

Sachs, N. A., A. Sawa, et al. (2005). "A frameshift mutation in Disrupted in Schizophrenia 1 in an American family with schizophrenia and schizoaffective disorder." Mol Psychiatry **10**(8): 758-64.

Sambrook, J., Fritsch, E.F., Maniatis, T. (1989). Moleclular Cloning; A laboratory manual, Cold Spring Harbor Laboratory Press.

Sasaki, S., A. Shionoya, et al. (2000). "A LIS1/NUDEL/cytoplasmic dynein heavy chain complex in the developing and adult nervous system." Neuron **28**(3): 681-96.

Schmidt, P. H., D. T. Dransfield, et al. (1999). "AKAP350, a multiply spliced protein kinase A-anchoring protein associated with centrosomes." J Biol Chem **274**(5): 3055-66.

Schon, E. A. (2000). "Mitochondrial genetics and disease." Trends Biochem Sci **25**(11): 555-60.

Schurov, I. L., E. J. Handford, et al. (2004). "Expression of disrupted in schizophrenia 1 (DISC1) protein in the adult and developing mouse brain indicates its role in neurodevelopment." Mol Psychiatry **9**(12): 1100-10.

Semple, C. A., R. S. Devon, et al. (2001). "Identification of genes from a schizophrenia-linked translocation breakpoint region." Genomics **73**(1): 123-6.

Shu, T., R. Ayala, et al. (2004). "Ndel1 operates in a common pathway with LIS1 and cytoplasmic dynein to regulate cortical neuronal positioning." Neuron **44**(2): 263-77.

Silhavey, T., Berman, M., Enquist, L. (1984). Experiments with gene fusions, Cold Spring Harbor Press.

Siller, K. H., M. Serr, et al. (2005). "Live imaging of Drosophila brain neuroblasts reveals a role for Lis1/dynactin in spindle assembly and mitotic checkpoint control." Mol Biol Cell **16**(11): 5127-40.

Slusher, B. S., M. B. Robinson, et al. (1990). "Rat brain N-acetylated alpha-linked acidic dipeptidase activity. Purification and immunologic characterization." J Biol Chem **265**(34): 21297-301.

Smith, D. S., M. Niethammer, et al. (2000). "Regulation of cytoplasmic dynein behaviour and microtubule organization by mammalian Lis1." Nat Cell Biol **2**(11): 767-75.

Smith, P. G., Wang, F., Wilkinson, K.N., Savage, K.J., Klein, U., Neuberg, D.S., Bollag, G., Shipp, M.A., Aguiar, R.C.T. (2005). "The Phosphodiesterase PDE4B limits cAMP-associated PI3K/AKT-dependent apoptosis in diffuse large B-cell lymphoma." Blood **105**(1): 308-316.

St Clair, D., D. Blackwood, et al. (1990). "Association within a family of a balanced autosomal translocation with major mental illness." Lancet **336**(8706): 13-6.

Stefansson, H., E. Sigurdsson, et al. (2002). "Neuregulin 1 and susceptibility to schizophrenia." Am J Hum Genet **71**(4): 877-92.

Sullivan, J. (2006). "www.cellsalive.com."

Swerdlow, N. R., N. Halim, et al. (2001). "Lesion size and amphetamine hyperlocomotion after neonatal ventral hippocampal lesions: more is less." Brain Res Bull **55**(1): 71-7.

Szymanski, M. and J. Barciszewski (2002). "Beyond the proteome: non-coding regulatory RNAs." Genome Biol **3**(5): reviews0005.1-reviews0005.8.

Szymanski, M. and J. Barciszewski (2006). "RNA regulation in mammals." Ann N Y Acad Sci **1067**: 461-8.

Takahashi, M., H. Shibata, et al. (1999). "Characterization of a novel giant scaffolding protein, CG-NAP, that anchors multiple signaling enzymes to centrosome and the golgi apparatus." J Biol Chem **274**(24): 17267-74.

Takahashi, M., A. Yamagiwa, et al. (2002). "Centrosomal proteins CG-NAP and kendrin provide microtubule nucleation sites by anchoring gamma-tubulin ring complex." Mol Biol Cell **13**(9): 3235-45.

Talbot, K., W. L. Eidem, et al. (2004). "Dysbindin-1 is reduced in intrinsic, glutamatergic terminals of the hippocampal formation in schizophrenia." J Clin Invest **113**(9): 1353-63.

Tasken, K. A., P. Collas, et al. (2001). "Phosphodiesterase 4D and protein kinase a type II constitute a signaling unit in the centrosomal area." J Biol Chem **276**(25): 21999-2002.

Taylor, M. (2001). Comparative and molecular characterisation of a schizophrenia susceptibility locus. Medical Genetics. Edinburgh, University of Edinburgh. PhD Thesis.

Taylor, M. S., R. S. Devon, et al. (2003). "Evolutionary constraints on the Disrupted in Schizophrenia locus." Genomics **81**(1): 67-77.

Thompson, P. M., C. Vidal, et al. (2001). "Mapping adolescent brain change reveals dynamic wave of accelerated gray matter loss in very early-onset schizophrenia." Proc Natl Acad Sci U S A **98**(20): 11650-5.

Thomson, P. A., S. E. Harris, et al. (2005a). "Association between genotype at an exonic SNP in DISC1 and normal cognitive aging." Neurosci Lett **389**(1): 41-5.

Thomson, P. A., N. R. Wray, et al. (2005b). "Association between the TRAX/DISC locus and both bipolar disorder and schizophrenia in the Scottish population." Mol Psychiatry **10**(7): 657-68, 616.

Tsai, G., L. A. Passani, et al. (1995). "Abnormal excitatory neurotransmitter metabolism in schizophrenic brains." Arch Gen Psychiatry **52**(10): 829-36.

Tsai, L. H. and J. G. Gleeson (2005). "Nucleokinesis in neuronal migration." Neuron **46**(3): 383-8.

Turetsky, B. I., Cannon, T.D., Gur, R.E. (2000). "P300 subcomponent abnormalities in schizophrenia:III. Deficits in unaffected siblings of schizophrenic probands." Biol Psychiatry **47**(5): 380-390.

Tuschl, T., Elbashir, S., Harborth, J., Weber, K. (2004). "The siRNA user guide." URL: http://www.reckefeller.edu/labheads/tuschl/sirna.html

Vandesompele, J., K. De Preter, et al. (2002). "Accurate normalization of real-time quantitative RT-PCR data by geometric averaging of multiple internal control genes." Genome Biol **3**(7): RESEARCH0034.1-11

Vanhee-Brossollet, C. and C. Vaquero (1998). "Do natural antisense transcripts make sense in eukaryotes?" Gene **211**(1): 1-9.

Vawter, M. P., C. Shannon Weickert, et al. (2004). "Gene expression of metabolic enzymes and a protease inhibitor in the prefrontal cortex are decreased in schizophrenia." Neurochem Res **29**(6): 1245-55.

Velagaleti, G. V., G. A. Bien-Willner, et al. (2005). "Position effects due to chromosome breakpoints that map approximately 900 Kb upstream and approximately 1.3 Mb downstream of SOX9 in two patients with campomelic dysplasia." Am J Hum Genet **76**(4): 652-62.

Vindelov, L. L., I. J. Christensen, et al. (1983). "Limits of detection of nuclear DNA abnormalities by flow cytometric DNA analysis. Results obtained by a set of methods for sample-storage, staining and internal standardization." Cytometry **3**(5): 332-9.

Vindelov, L. L., I. J. Christensen, et al. (1983). "Long-term storage of samples for flow cytometric DNA analysis." Cytometry **3**(5): 317-22.

Vindelov, L. L., I. J. Christensen, et al. (1983). "A detergent-trypsin method for the preparation of nuclei for flow cytometric DNA analysis." Cytometry **3**(5): 323-7.

Vindelov, L. L., I. J. Christensen, et al. (1983). "Standardization of high-resolution flow cytometric DNA analysis by the simultaneous use of chicken and trout red blood cells as internal reference standards." Cytometry **3**(5): 328-31.

Wallace, D. C. (1999). "Mitochondrial diseases in man and mouse." Science **283**(5047): 1482-1488.

Weickert, C. S., R. E. Straub, et al. (2004). "Human dysbindin (DTNBP1) gene expression in normal brain and in schizophrenic prefrontal cortex and midbrain." Arch Gen Psychiatry **61**(6): 544-55.

Weiss, A. P., Zalesak, M., DeWitt, I., Goff, D., Kunkel, L., Heckers, S. (2004). "Impaired hippocampal function during the detection of novel words in schizophrenia." Biol Psychiatry **55**(7): 668-675.

Whitehead, R. E., J. V. Ferrer, et al. (2001). "Reaction of oxidized dopamine with endogenous cysteine residues in the human dopamine transporter." J Neurochem **76**(4): 1242-51.

Wilson-Annan, J. C., D. H. Blackwood, et al. (1997). "An allelic association study of two polymorphic markers in close proximity to a balanced translocation t(1:11) that co-segregates with mental illness." Psychiatr Genet **7**(4): 171-4.

Winterer, G., Egan, M.F., Readler, T., Sanchez, C., Jones, D.W., Coppola, R., Weinberger, D.R. (2003). "P300 and Genetic risk for schizophrenia." Arch Gen Psychiatry **60**(11): 1158-1167.

Winterer, G., Weinberger, D.R. (2004). "Genes, dopamine and cortical signal-to-noise ratio in schizophrenia." Trends Neurosci **27**(11): 683-690.

Witczak, O., B. S. Skalhegg, et al. (1999). "Cloning and characterization of a cDNA encoding an A-kinase anchoring protein located in the centrosome, AKAP450." Embo J **18**(7): 1858-68.

Wright, I., Rabe-Hesketh, S., Woodruff, P., David, A., Murray, R., Bullmore, E. (2000). "Meta-Analysis of regional brain volumes in Schizophrenia." Am J Psychiatry **157**(1): 16-25.

Xiang, X., A. H. Osmani, et al. (1995). "NudF, a nuclear migration gene in Aspergillus nidulans, is similar to the human LIS-1 gene required for neuronal migration." Mol Biol Cell **6**(3): 297-310.

Yan, X., F. Li, et al. (2003). "Human Nudel and NudE as regulators of cytoplasmic dynein in poleward protein transport along the mitotic spindle." Mol Cell Biol **23**(4): 1239-50.

Yang, X. L., Y. Z. Huang, et al. (2005). "Neuregulin-induced expression of the acetylcholine receptor requires endocytosis of ErbB receptors." Mol Cell Neurosci **28**(2): 335-46.

Yelin, R., D. Dahary, et al. (2003). "Widespread occurrence of antisense transcription in the human genome." Nat Biotechnol **21**(4): 379-86.

Zhang, X., M. Tochigi, et al. (2005). "Association study of the DISC1/TRAX locus with schizophrenia in a Japanese population." Schizophr Res **79**(2-3): 175-80.

Zimmerman, W. C., J. Sillibourne, et al. (2004). "Mitosis-specific anchoring of gamma tubulin complexes by pericentrin controls spindle organization and mitotic entry." Mol Biol Cell **15**(8): 3642-57.

Appendices

Appendix I

Relevant publications

together with growth retardation and neurological abnormalities. This is consistent with the expression pattern of *Gtf2ird1* in the developing brain and craniofacial areas (*23*) and its ability to regulate expression of *goosecoid* (*Gsc*) and *Hoxc8*, genes that control craniofacial and skeletal development (*3*, *4*). *Gsc*-null mice die soon after birth with craniofacial defects, rib fusions, and sternum abnormalities (*24*); *Hoxc8* $EE^{-/-}$ mice, where temporal regulation of *Hoxc8* is altered but not abolished, have skeletal pathologies and signs of neurological dysfunction (*25*). We used a short interfering RNA (siRNA) that knocks down levels of endogenous GTF2IRD1 by ~60% to show regulation of *GSC* by GTF2IRD1 in human embryonic kidney (HEK) 293T cells. In cotransfection experiments, the GTF2IRD1 siRNA reduced expression of a pGL3-*GSC*prom luciferase reporter construct (Fig. 4), suggesting that GTF2IRD1 influences gene transcription at endogenous levels. To date, few upstream regulators of *Gsc* have been defined in vivo, even though its developmental importance in *Drosophila* and humans is well established. Misregulation of *GSC* expression due to absence or lower levels of GTF2IRD1 probably contributes to the craniofacial pathologies seen in WBS and *Gtf2ird1*-null mice.

Of the other genes deleted in HR, *CYLN2* probably contributes to, but is not solely responsible for, the neurological phenotype in WBS. Although no human case of isolated haploinsufficiency for *CYLN2* has been reported, $Cyln2^{-/-}$ and $Cyln2^{+/-}$ mice present with mild structural brain abnormalities, hippocampal dysfunction, and deficits in motor coordination, alongside mild growth deficiency but no craniofacial defects (*26*). However, haploinsufficiency for *CYLN2* and *GTF2IRD1* alone cannot explain all the clinical features of WBS, because HR displays a milder clinical profile. The more pronounced facial and cognitive/behavioral phenotypes associated with the larger deletion implicate other telomeric genes in these features, specifically *GTF2I*, which lies distal to *GTF2IRD1* and is deleted in classic WBS cases. GTF2I and GTF2IRD1 share many structural properties and are likely to have overlapping functions; indeed, both have been shown to regulate gene activity through a common DNA element, DICE (*27*). This work introduces members of the *TFII-I* gene family as critical regulators of craniofacial and neurological development.

Our findings allow us to compile a picture of the molecular pathology of WBS, a classical human microdeletion syndrome. No single gene is responsible for the craniofacial or cognitive features of WBS. We suggest that cumulative dosage of *TFII-I*–family genes explains the main phenotypes. *Gtf2ird1*-null mice and classic WBS individuals have two functioning copies (in trans and cis, respectively), whereas HR has three functioning genes of the *GTF2IRD1*/*GTF2I* cluster and shows milder WBS phenotypes. Whether one gene has more effect than the other or whether the effects are additive or multiplicative remains to be determined. Haploinsufficiency for other genes in the WBS critical region explains the vascular features and may contribute to the full syndrome, but it is not the main cause. Because adjacent duplicated but diverged genes are common in the human genome, such cumulative dosage effects may underlie the pathology of other chromosomal syndromes where members of different gene families are deleted or duplicated.

References and Notes

1. S. Alappat, Z. Y. Zhang, Y. P. Chen, *Cell Res.* **13**, 429 (2003).
2. T. A. Hinsley, P. Cunliffe, H. J. Tipney, A. Brass, M. Tassabehji, *Protein Sci.* **13**, 2588 (2004).
3. C. Ring *et al.*, *Genes Dev.* **16**, 820 (2002).
4. D. Bayarsaihan, F. H. Ruddle, *Proc. Natl. Acad. Sci. U.S.A.* **97**, 7342 (2000).
5. A. L. Roy *et al.*, *EMBO J.* **16**, 7091 (1997).
6. M. Tassabehji *et al.*, *Eur. J. Hum. Genet.* **7**, 737 (1999).
7. J. V. O'Mahoney *et al.*, *Mol. Cell. Biol.* **18**, 6641 (1998).
8. H. J. Tipney, T. A. Hinsley, A. Brass, D. Donnai, M. Tassabehji, *Eur. J. Hum. Genet.* **12**, 551 (2004).
9. A. K. Ewart *et al.*, *Nat. Genet.* **5**, 11 (1993).
10. C. A. Morris, S. A. Demsey, C. O. Leonard, C. Dilts, B. L. Blackburn, *J. Pediatr.* **113**, 318 (1988).
11. D. Donnai, A. Karmiloff-Smith, *Am. J. Med. Genet.* **97**, 164 (2000).
12. A. Reiss, S. Eliez, S. J. E. Schmitt, *J. Cogn. Neurosci.* **12** (suppl.), 65 (2000).
13. M. Tassabehji, *Hum. Mol. Genet.* **15**, 229 (2003).
14. M. Bayes, L. F. Magano, N. Rivera, R. Flores, L. A. Perez Jurado, *Am. J. Hum. Genet.* **73**, 131 (2003).
15. J. M. Frangiskakis *et al.*, *Cell* **86**, 59 (1996).
16. M. Tassabehji *et al.*, *Am. J. Hum. Genet.* **64**, 118 (1999).
17. A. Botta *et al.*, *J. Med. Genet.* **36**, 478 (1999).
18. R. Heller, A. Rauch, S. Luttgen, B. Schroder, A. Winterpacht, *J. Med. Genet.* **40**, E99 (2003).
19. A. Karmiloff-Smith *et al.*, data not shown.
20. P. Hammond *et al.*, *Am. J. Med. Genet. A* **126**, 339 (2004).
21. P. Hammond *et al.*, *Am. J. Hum. Genet.*, in press.
22. M. E. Durkin, C. L. Keck-Waggoner, N. C. Popescu, S. S. Thorgeirsson, *Genomics* **73**, 20 (2001).
23. J. A. Rivera-Pérez, M. Mallo, M. Gendron-Maguire, T. Gridley, R. R. Behringer, *Development* **121**, 3005 (1995).
24. A. H. Juan, F. H. Ruddle, *Development* **130**, 4823 (2003).
25. D. Bayarsaihan *et al.*, *Gene Expr. Patterns* **3**, 579 (2003).
26. C. C. Hoogenraad *et al.*, *Nat. Genet.* **32**, 116 (2002).
27. D. Tantin, M. I. Tussie-Luna, A. L. Roy, P. A. Sharp, *J. Biol. Chem.* **279**, 5460 (2004).

28. Supported by Wellcome Trust grant 061183 (M.T.). Scanners were funded by BDF NewLife (P.H.). Surfim loaned specialist scanning equipment. We thank the families and W. Fergusson, M. J. Carrette, and W. Beckett for their assistance.

Supporting Online Material

www.sciencemag.org/cgi/content/full/1116142/DC1
Materials and Methods
Figs. S1 to S4
References

15 June 2005; accepted 5 October 2005
Published online 3 November 2005;
10.1126/science.1116142
Include this information when citing this paper.

DISC1 and PDE4B Are Interacting Genetic Factors in Schizophrenia That Regulate cAMP Signaling

J. Kirsty Millar,[1]*† Benjamin S. Pickard,[1]* Shaun Mackie,[1] Rachel James,[1] Sheila Christie,[1] Sebastienne R. Buchanan,[1] M. Pat Malloy,[1] Jennifer E. Chubb,[1] Elaine Huston,[2] George S. Baillie,[2] Pippa A. Thomson,[1] Elaine V. Hill,[2] Nicholas J. Brandon,[3] Jean-Christophe Rain,[4] L. Miguel Camargo,[3] Paul J. Whiting,[3] Miles D. Houslay,[2] Douglas H. R. Blackwood,[1,5] Walter J. Muir,[1,5] David J. Porteous[1]

The *disrupted in schizophrenia 1* (*DISC1*) gene is a candidate susceptibility factor for schizophrenia, but its mechanistic role in the disorder is unknown. Here we report that the gene encoding phosphodiesterase 4B (*PDE4B*) is disrupted by a balanced translocation in a subject diagnosed with schizophrenia and a relative with chronic psychiatric illness. The PDEs inactivate adenosine 3′,5′-monophosphate (cAMP), a second messenger implicated in learning, memory, and mood. We show that DISC1 interacts with the UCR2 domain of PDE4B and that elevation of cellular cAMP leads to dissociation of PDE4B from DISC1 and an increase in PDE4B activity. We propose a mechanistic model whereby DISC1 sequesters PDE4B in resting cells and releases it in an activated state in response to elevated cAMP.

Schizophrenia and bipolar affective disorder are common, debilitating conditions that are determined in part by genetic factors. The *DISC1* gene (for *disrupted in schizophrenia 1*) is a candidate susceptibility factor for psychiatric illness with both genetic and biological plausibility (*1*). *DISC1* is disrupted by a balanced chromosomal translocation t(1;11)(q42;q14) cosegregating with schizophrenia (7 cases), bipolar affective disorder (1 case), and related affective disorders (10 cases) in a large Scottish family [maximum logarithm of the odds ratio for linkage (lod score) = 7.1] (*2*, *3*). Translocation carriers, even without a major

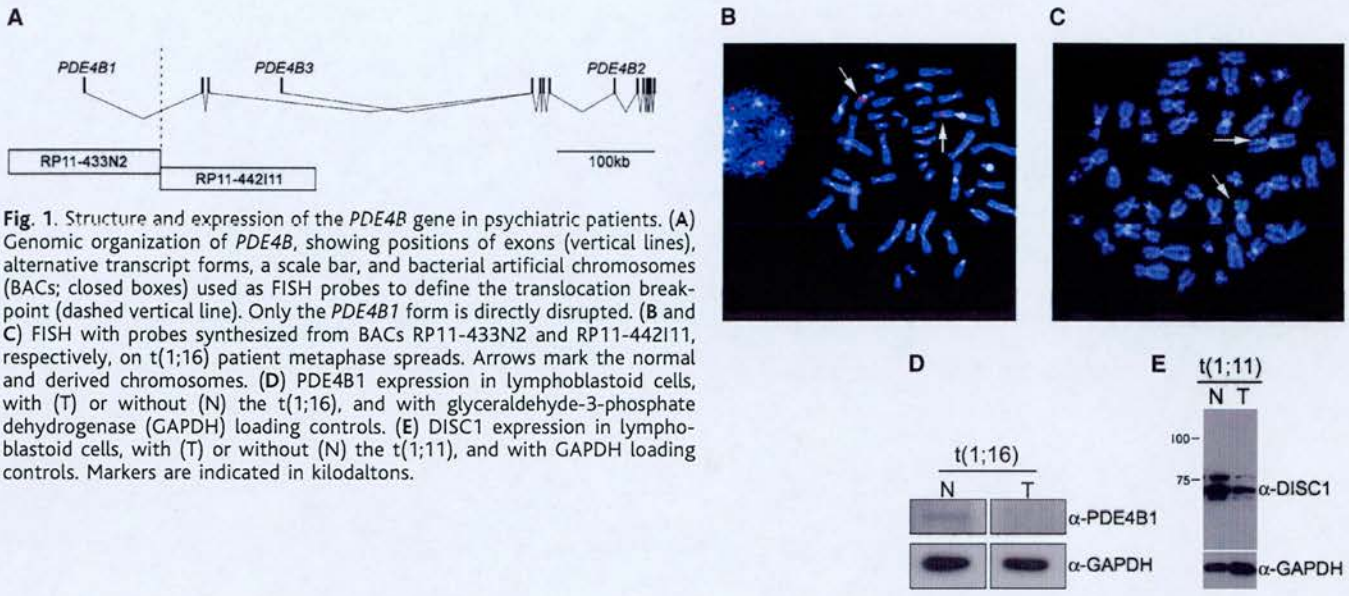

Fig. 1. Structure and expression of the *PDE4B* gene in psychiatric patients. (**A**) Genomic organization of *PDE4B*, showing positions of exons (vertical lines), alternative transcript forms, a scale bar, and bacterial artificial chromosomes (BACs; closed boxes) used as FISH probes to define the translocation breakpoint (dashed vertical line). Only the *PDE4B1* form is directly disrupted. (**B** and **C**) FISH with probes synthesized from BACs RP11-433N2 and RP11-442I11, respectively, on t(1;16) patient metaphase spreads. Arrows mark the normal and derived chromosomes. (**D**) PDE4B1 expression in lymphoblastoid cells, with (T) or without (N) the t(1;16), and with glyceraldehyde-3-phosphate dehydrogenase (GAPDH) loading controls. (**E**) DISC1 expression in lymphoblastoid cells, with (T) or without (N) the t(1;11), and with GAPDH loading controls. Markers are indicated in kilodaltons.

psychiatric diagnosis, have reduced amplitudes of the P300 event-related potential, consistent with an underlying cognitive defect (*3*). A number of independent genetic linkage and association studies provide confirmatory evidence for involvement of the *DISC1* locus in schizophrenia, schizoaffective disorder, and bipolar affective disorder (*1*–*4*). DISC1 is expressed in regions of the brain implicated in the genesis of psychiatric symptoms (*5*–*7*) and binds diverse proteins in the central nervous system, including the neurodevelopmental proteins FEZ1 (*8*) and NUDEL (*9*, *10*).

In ongoing studies of psychiatric patients with chromosomal abnormalities, we identified a proband with schizophrenia who carried a balanced t(1;16)(p31.2;q21) translocation. The subject had a history of repeated psychotic episodes with auditory hallucinations and delusions and was treated with standard antipsychotic medications. A cousin of the proband who also carried the translocation had a psychotic illness with prolonged hospital admission but was not available for interview (*11*). Using fluorescence in situ hybridization (FISH) (*11*), we showed that the translocation breakpoint on chromosome 16 lies within an intron of the

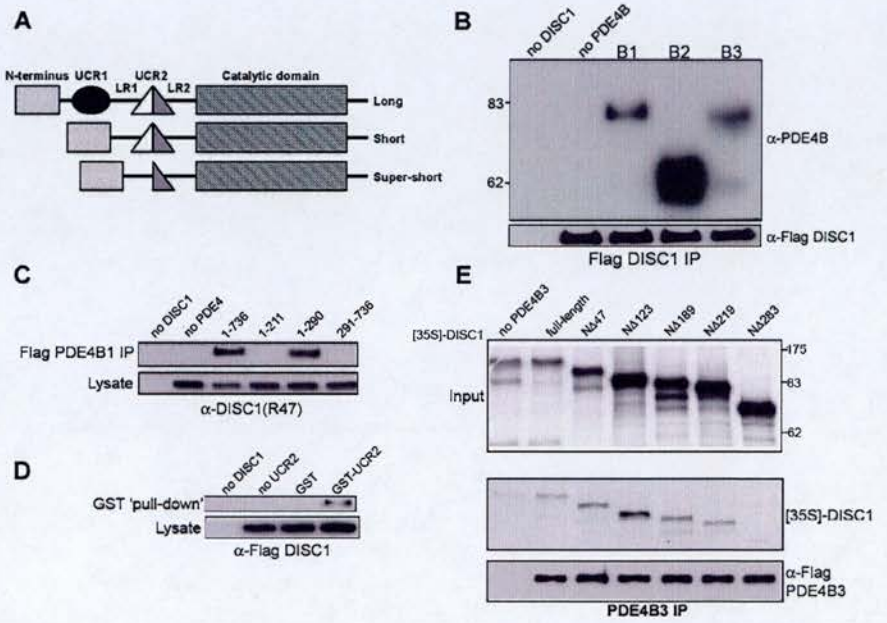

Fig. 2. Human DISC1 binds the PDE4B UCR2 domain in transfected cells. (**A**) Domain organization of type 4 phosphodiesterases. The common structure of core regions forming the UCR1/UCR2 module and the catalytic domain are indicated. Each PDE4 isoform contains a unique N terminus. (**B**) HEK293 cells were cotransfected with DISC1 and PDE4 expression vectors. FLAG epitope–tagged immunoprecipitates from lysates prepared from HEK293 cells cotransfected with either empty vector or FLAG-DISC1 and PDE4B1-B3 plasmids, probed by Western blot analysis with antibodies against FLAG and pan-PDE4B. Markers are indicated in kilodaltons. (**C**) FLAG-tagged immunoprecipitates from HEK293 cells cotransfected with DISC1 and the indicated FLAG-PDE4B1 constructs (top) probed by Western analysis with the R47 antibody to detect total DISC1 and PDE4B1-associated DISC1. For a schematic representation of PDE4B1 constructs and expression of the corresponding FLAG-tagged PDE4B1 proteins, see fig. S6. (**D**) Glutathione *S*-transferase (GST) pull-downs from lysates of HEK293 cells cotransfected with empty FLAG vector or FLAG-DISC1 and GST or GST-UCR2 plasmids, probed with antibody against FLAG to detect total DISC1 and DISC1 that specifically interacts with the UCR2 domain. (**E**) Mapping the PDE4B binding site on DISC1. ^{35}S-labeled NΔ DISC1 fragments (depicted in fig. S8) and FLAG-tagged, unlabeled PDE4B3 were synthesized by in vitro transcription-translation, mixed, and incubated for 3 hours in a binding reaction before immunoprecipitation with antibody against FLAG. Input DISC1 and PDE4B3-bound DISC1 were detected by SDS–polyacrylamide gel electrophoresis (SDS-PAGE) followed by autoradiography. Equal capture of FLAG-tagged PDE4B3 was determined by Western analysis with antibody against FLAG (lower). Input signal represents 1/50 of total binding reaction. Markers are indicated in kilodaltons.

[1]Medical Genetics Section, Molecular Medicine Centre, University of Edinburgh, Edinburgh EH4 2XU, UK. [2]Molecular Pharmacology Group, Division of Biochemistry and Molecular Biology, Institute of Biomedical and Life Sciences, Wolfson Building, University of Glasgow, Glasgow G12 8QQ, UK. [3]The Neuroscience Research Centre, Merck Sharp and Dohme, Ltd. (MSD), Terlings Park, Harlow, Essex, CM20 2QR, UK. [4]Hybrigenics S.A., 3-5 Impasse Reille–75014 Paris, France. [5]Division of Psychiatry, University of Edinburgh, Royal Edinburgh Hospital, Edinburgh EH10 5HF, UK.

*These authors contributed equally to this work.
†To whom correspondence should be addressed. E-mail: Kirsty.Millar@ed.ac.uk

Cadherin 8 (*CDH8*) gene (fig. S1) and that the 1p31.2 translocation breakpoint disrupts the B1 isoform of the phosphodiesterase 4B (*PDE4B*) gene (Fig. 1, A to C). CDH8 is a cell adhesion molecule that potentially has a neuronal function (*11*), but we focused on PDE4B for the following reasons: (i) PDE action is the sole means of inactivating intracellular adenosine 3′,5′-monophosphate (cAMP), a key second messenger involved in learning, memory, and mood (*12–14*). (ii) Mutations in the fruit fly *Drosophila dunce* gene, which encodes an ortholog of mammalian PDE4, cause learning and memory deficits (*13*). (iii) Mice deficient in PDE4D behave as if they are taking antidepressants (*15*). (iv) Rolipram, an antidepressant, is a selective inhibitor of PDE4 (*16*). And (v), most intriguingly, we found PDE4B (but not CDH8) to interact robustly with DISC1 in a large-scale yeast two-hybrid screen using full-length DISC1 as bait (*9*).

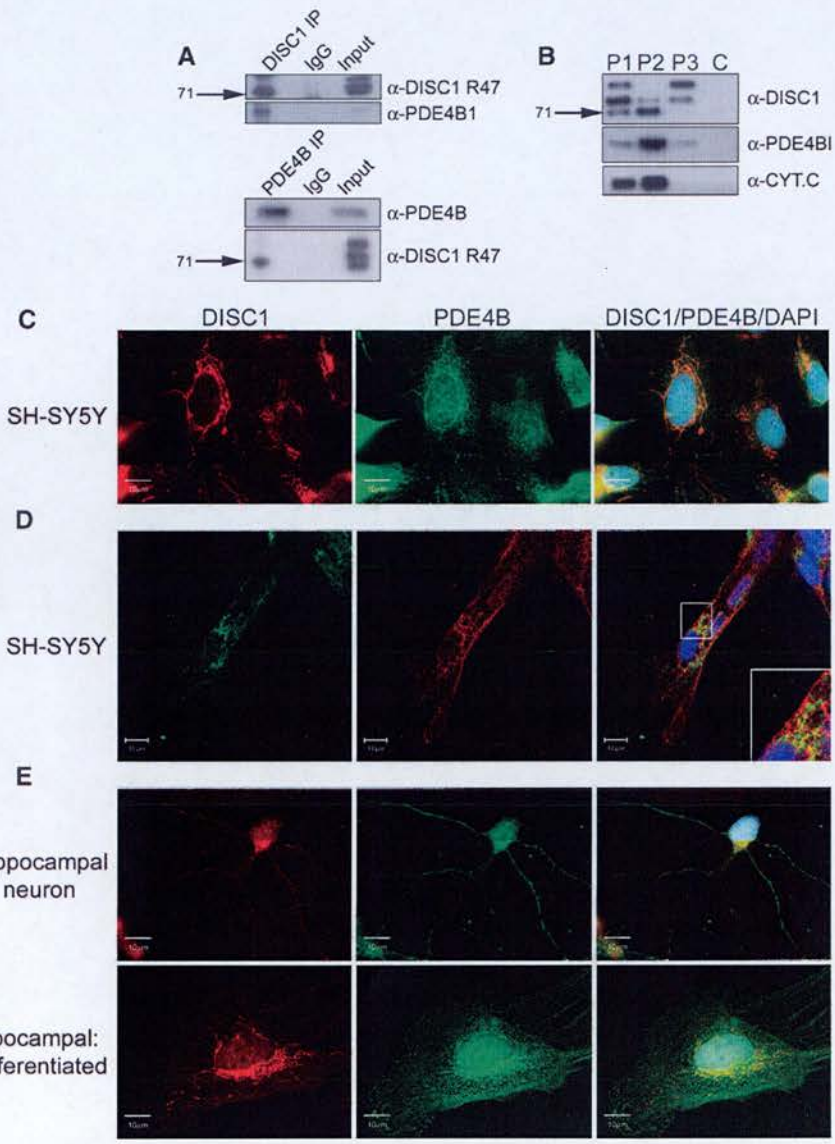

Fig. 3. Interaction of endogenous DISC1 and PDE4B in human SH-SY5Y cells. (**A**) Control immunoglobulin IgG and DISC1 immunoprecipitates (R47) from lysates of SH-SY5Y cell were probed by Western blot analysis to detect DISC1 (R47) and PDE4B1 (top), and PDE4B immunoprecipitates (pan-PDE4B) from SH-SY5Y cell extracts were probed for PDE4B (pan-PDE4B) and DISC1 (bottom). The DISC1 71-kD isoform is indicated with an arrow. (**B**) Protein extracts from SH-SY5Y subcellular fractions were probed by Western analysis with antibodies against DISC1, PDE4B1, and cytochrome c (as labeled). P1, nuclear fraction plus whole-cell debris; P2, predominantly mitochondrial; P3, other membrane elements; C, cytosolic. The DISC1 71-kD isoform is indicated with an arrow. (**C**) Immunofluorescence in SH-SY5Y human neuroblastoma cells. (Left) DISC1 (R47 antibody); middle, PDE4B (antibody against pan-PDE4B); (right) merged signal plus DAPI (nuclear DNA) stain (See also fig. S11). (**D**) Confocal immunofluorescence in differentiated SH-SY5Y human neuroblastoma cells, left to right as in (C). (Inset) Highlighted region enlarged 2.5 times. (**E**) Immunofluorescence in hippocampal primary cells, neuron and undifferentiated cell, left to right as in (C), except (left), DISC1 (C2 antibody) (See also fig. S11). Neurons were identified by using an antibody against NeuN.

To determine the effect of the t(1;16) and t(1;11) translocations on PDE4B and DISC1 expression respectively, we analyzed patient-derived lymphoblastoid cell lines. Cell lines derived from family members with or without the t(1;16) translocation revealed that PDE4B1 protein expression was reduced by ~50% in the presence of the t(1;16) translocation (Fig. 1D; fig. S2). In the case of the t(1;11) translocation, we demonstrated transcription of DISC1 from the derived chromosome 1 (fig. S3A). However, DISC1 transcript levels are reduced overall, and when we used antibody R47, which is specific for an epitope within the N terminus of DISC1 (*7*), we found no evidence [fig. S3, B to D, and (*11*)] for a putative C-terminally truncated protein (*8*, *9*). Expression of all DISC1 species was consistently reduced to about half normal levels in each of five t(1;11) cell lines from different individuals (Fig. 1E; fig. S2). These are the same DISC1 species that are detectable in human brain tissue (*7*), which indicates that proportionate reduction of DISC1 expression in brain is the most likely consequence of inheriting the translocation. The reduction in DISC1 is specific, as we see no change in the relative level of TRAX, which maps immediately 5′ of DISC1 (fig. S4, A and B). Haploinsufficiency for DISC1 in the t(1;11) translocation cases and for PDE4B in the t(1;16) translocation cases is therefore the most likely mechanistic explanation for susceptibility to schizophrenia in these individuals.

PDE4 isoforms are classified as long, short, or supershort (*17*), depending on the presence of conserved regulatory regions (UCR1 and UCR2) linked to the catalytic unit (Fig. 2A). Long isoforms uniquely express UCR1, whose phosphorylation by protein kinase A (PKA) triggers a conformational change in the UCR1 and 2 module, leading to increased catalytic activity (*17*). To determine which of the many known PDE4 isoforms could interact with DISC1, we transfected expression constructs into HEK293 cells (*11*). We analyzed the long PDE4B1 and PDE4B3 isoforms, which each contain UCR1, as well as the short PDE4B2 isoform, which does not. All three of these human isoforms co-immunoprecipitate with DISC1 (Fig. 2B), which shows that binding is not specific to one particular isoform. Indeed, DISC1 binds representative long isoforms from all four PDE4 genes (fig. S5). Removal of UCR2 abolished PDE4B1 binding to DISC1 (Fig. 2C; fig. S6). Moreover, the UCR2 domain alone was capable of binding DISC1 (Fig. 2D), which suggests that UCR2 is a specific DISC1 interaction domain.

To identify the site of PDE4 binding on DISC1, we performed binding assays after expression of DISC1 and PDE4B by in vitro transcription-translation. Full-length DISC1 (1 to 854), a C-terminal truncated DISC1 (1 to

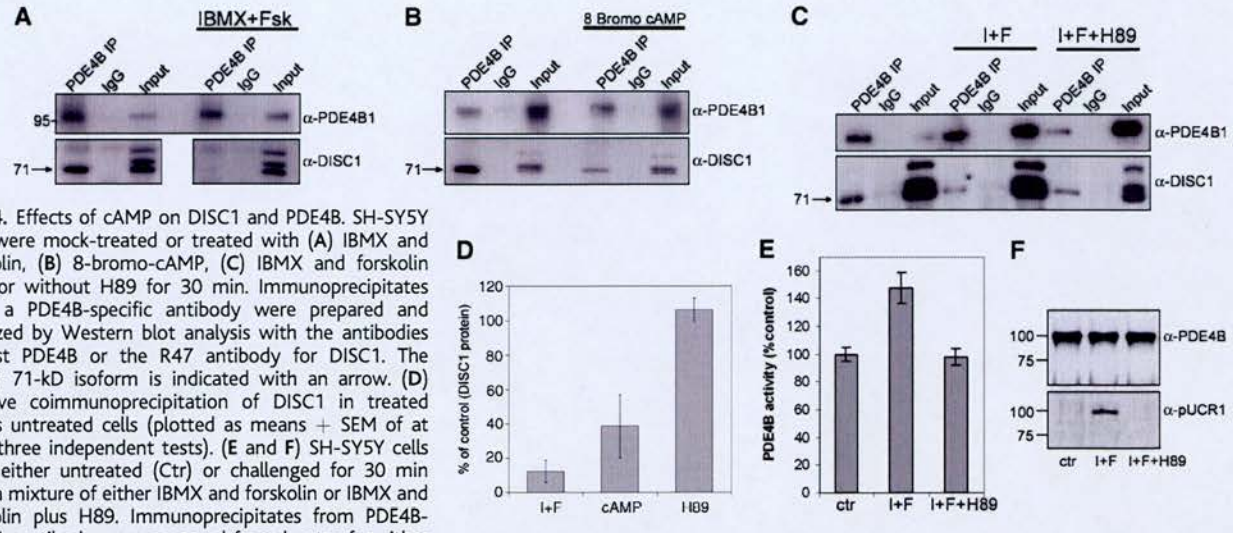

Fig. 4. Effects of cAMP on DISC1 and PDE4B. SH-SY5Y cells were mock-treated or treated with (**A**) IBMX and forskolin, (**B**) 8-bromo-cAMP, (**C**) IBMX and forskolin with or without H89 for 30 min. Immunoprecipitates from a PDE4B-specific antibody were prepared and analyzed by Western blot analysis with the antibodies against PDE4B or the R47 antibody for DISC1. The DISC1 71-kD isoform is indicated with an arrow. (**D**) Relative coimmunoprecipitation of DISC1 in treated versus untreated cells (plotted as means + SEM of at least three independent tests). (**E** and **F**) SH-SY5Y cells were either untreated (Ctr) or challenged for 30 min with a mixture of either IBMX and forskolin or IBMX and forskolin plus H89. Immunoprecipitates from PDE4B-specific antibody were prepared from lysates for either (E) PDE4 activity assays by measurement of cAMP hydrolyzing activity, or (F) Western blot analysis with a PDE4B-specific antibody or with an antiserum specific for the single PKA phosphorylation site in UCR1. Methods for obtaining these data are available online [refs. S8, S9, S13, S14, and S21 in (*11*)].

597), and the N-terminal "head" domain of DISC1 (1 to 358) were tested for their ability to bind ^{35}S-labeled PDE4B3 in vitro. All three V5-tagged DISC1 protein fragments efficiently coimmunoprecipitated PDE4B3 (fig. S7), which indicated that PDE4B binding to DISC1 is direct and that the DISC1 N-terminal domain is required for the interaction. We next generated a series of constructs that progressively delete amino acids from the N terminus of DISC1 (Fig. 2E; fig. S8) and showed that amino acids 219 to 283 are required for binding to PDE4B. DISC1 binding was restored by amino acids 180 to 250 (fig. S9).

To determine whether and where endogenous DISC1 and PDE4B interact, we performed coimmunoprecipitation and colocalization studies using conventional and confocal microscopy in the human neuroblastoma–derived cell lines SH-SY5Y and LAN5 and in primary rat hippocampal cells. DISC1 antiserum (R47) coprecipitates PDE4B1 from SH-SY5Y extracts (Fig. 3A, top), whereas pan-PDE4B, an antibody that recognizes all PDE4B isoforms, specifically coimmunoprecipitates the 71-kD DISC1 isoform (Fig. 3A, bottom). Thus, isoform PDE4B1 associates with the 71-kD isoform of DISC1. In cell fractionation studies, the PDE4B1 isoform was most abundant in the mitochondria-enriched fraction P2 (Fig. 3B), as was the 71-kD isoform of DISC1, which is also predominantly mitochondrial (*7*). PDE4B partially colocalizes with DISC1 in the mitochondria of SH-SY5Y (Fig. 3, C and D; fig. S10 and S11) and LAN5 (fig. S10) cells. In rat hippocampal primary cultures, DISC1 and PDE4B expression overlap substantially in both neurons and proliferating nonneuronal cells (Fig. 3E; fig. S10 and S11).

To further investigate DISC1-PDE4 binding, we determined the effect of elevated cAMP. Overexpression studies show that long PDE4 isoforms are activated by PKA in response to increased intracellular cAMP and, thereby, provide part of the cellular desensitization system for cAMP signaling (*18*, *19*). PKA phosphorylation of UCR1 induces conformational changes that concomitantly affect enzymatic activity and the interaction between UCR1 and UCR2 (*20*). To increase cAMP production and simultaneously to block its hydrolysis, SH-SY5Y cells were treated with forskolin plus the nonspecific phosphodiesterase inhibitor 3-isobutyl-1-methylxanthine (IBMX). This dramatically decreased the amount of DISC1 coprecipitating with PDE4B (Fig. 4, A and D). When cAMP levels were raised by using the cell permeable cAMP analog 8-bromo-cAMP, we similarly observed a reduction in PDE4B-DISC1 binding (Fig. 4, B and D). The action of forskolin plus IBMX was ablated when we added the PKA-specific inhibitor H89 (Fig. 4, C and D). These data indicate that the interaction between PDE4B and DISC1 is dynamic and directly influenced by altered cAMP levels through the action of PKA. Our data also indicate that DISC1 binds predominantly to the dephosphorylated, low-activity form of PDE4B, consistent with a model whereby PKA phosphorylation leads to release, from DISC1, of an activated population of PDE4B in response to elevated cAMP levels (fig. S12). To test this, we measured PDE4B cAMP hydrolyzing activity in SII-SY5Y cells and observed a 48% increase over controls, in the presence of IBMX and forskolin, that was inhibited by H89, consistent with PKA mediation of this increase (Fig. 4E). This increase in PDE4B activity is due to activation of UCR1-containing long PDE4B isoforms, because the short isoform PDE4B2 was not immunoprecipitated from SH-SY5Y cells (Fig. 4F). Using an antibody specific for the PKA-phosphorylated forms of PDE4 (*18*, *21*), we identified a 104-kD PDE4B immunoreactive species in PDE4B immunoprecipitates from cells treated with IBMX and forskolin (Fig. 4F) that is not seen in control cells, consistent with PKA phosphorylation of UCR1 as the mechanism of PDE4B activation.

Our study provides primary evidence for PDE4B as a genetic susceptibility factor for schizophrenia. We show that DISC1, an established candidate, interacts with PDE4B in a compartmentalized fashion. This interaction is dynamic and is cAMP- and PKA-dependent. We speculate that functional variation in DISC1 and/or PDE4 will modulate their interaction and affect mitochondrial cAMP catabolism with a concomitant physiological and psychiatric outcome. A unifying link between schizophrenia and bipolar affective disorder, and between DISC1 and PDE4, may occur at the cognitive level of learning and memory and at the molecular level of cAMP signaling.

References and Notes

1. P. J. Harrison, D. R. Weinberger, *Mol. Psychiatry* **10**, 40 (2005).
2. J. K. Millar *et al.*, *Hum. Mol. Genet.* **9**, 1415 (2000).
3. D. H. Blackwood *et al.*, *Am. J. Hum. Genet.* **69**, 428 (2001).
4. P. A. Thomson *et al.*, *Mol. Psychiatry* **10**, 616 (2005).
5. L. Ma *et al.*, *Genomics* **80**, 662 (2002).
6. C. P. Austin, L. Ma, B. Ky, J. A. Morris, P. J. Shugrue, *Neuroreport* **14**, 951 (2003).
7. R. James *et al.*, *Mol. Cell. Neurosci.* **26**, 112 (2004).
8. K. Miyoshi *et al.*, *Mol. Psychiatry* **8**, 685 (2003).
9. N. J. Brandon *et al.*, *Mol. Cell. Neurosci.* **25**, 42 (2004).
10. M. A. Hayashi *et al.*, *Proc. Natl. Acad. Sci. U.S.A.* **102**, 3828 (2005).
11. Materials and methods are available as supporting material on *Science* Online.
12. A. L. Bauman, A. S. Goehring, J. D. Scott, *Neuropharmacology* **46**, 299 (2004).
13. R. L. Davis, J. Cherry, B. Dauwalder, P. L. Han, E. Skoulakis, *Mol. Cell. Biochem.* **149**, 271 (1995).
14. R. Lamprecht, *Cell. Mol. Life Sci.* **55**, 554 (1999).
15. H. T. Zhang *et al.*, *Neuropsychopharmacology* **27**, 587 (2002).
16. J. M. O'Donnell, H. T. Zhang, *Trends Pharmacol. Sci.* **25**, 158 (2004).
17. M. D. Houslay, D. R. Adams, *Biochem. J.* **370**, 1 (2003).
18. S. J. MacKenzie *et al.*, *Br. J. Pharmacol.* **136**, 421 (2002).
19. C. Sette, M. Conti, *J. Biol. Chem.* **271**, 16526 (1996).

20. M. B. Beard *et al.*, *J. Biol. Chem.* **275**, 10349 (2000).
21. A. McCahill *et al.*, *Cell. Signal.* **17**, 1158 (2005).
22. This study was approved by the appropriate local research ethics committee. We thank M. Lai for help with the primary neuronal cultures and S. Cooper for assistance with figure production. Supported by a collaborative research agreement between Merck and Co. and the University of Edinburgh (D.J.P., D.H.R.B, W.J.M., J.K.M., B.S.P.), the Medical Research Council UK (G0100266 to D.J.P., D.H.R.B, W.J.M., G8604010 to M.D.H.) the Stanley Medical Research Institute (01-093 to J.K.M), the Scottish Hospital Endowment Research Trust (RG45/01 to B.S.P. and RG51/01 to J.K.M.), the Wellcome Trust (069300/Z/02/A to J.E.C., J.K.M. and 066717 to D.J.P., D.H.R.B., W.J.M., and others), the Chief Scientist Office of the Scottish Executive (K/MRS/50/C2789 to D.H.R.B, W.J.M., D.J.P.). W.J.M. was an MRC Clinician Scientist for part of this work.

Supporting Online Material
www.sciencemag.org/cgi/content/full/310/5751/1187/DC1
Materials and Methods
Figs. S1 to S12
References and Notes

29 March 2005; accepted 3 October 2005
10.1126/science.1112915

Altered TCR Signaling from Geometrically Repatterned Immunological Synapses

Kaspar D. Mossman,[1,2,3] Gabriele Campi,[4] Jay T. Groves,[1,2,3]* Michael L. Dustin[4]*

The immunological synapse is a specialized cell-cell junction that is defined by large-scale spatial patterns of receptors and signaling molecules yet remains largely enigmatic in terms of formation and function. We used supported bilayer membranes and nanometer-scale structures fabricated onto the underlying substrate to impose geometric constraints on immunological synapse formation. Analysis of the resulting alternatively patterned synapses revealed a causal relation between the radial position of T cell receptors (TCRs) and signaling activity, with prolonged signaling from TCR microclusters that had been mechanically trapped in the peripheral regions of the synapse. These results are consistent with a model of the synapse in which spatial translocation of TCRs represents a direct mechanism of signal regulation.

Antigen recognition by T cells requires interactions between TCRs and antigenic peptides bound to major histocompatibility complex molecules (pMHCs) on antigen-presenting cells (APCs) (*1*). A coordinated recognition process ensues in which surface proteins on the T cell, along with their respective ligands, become organized into micron-scale, spatially patterned motifs known as immunological synapses (ISs) (*2*, *3*). TCRs and pMHCs occupy a region designated the central supramolecular activation cluster (c-SMAC). This is surrounded by a ring of interactions between leukocyte function-associated antigen–1 (LFA-1) on the T cell and intercellular adhesion molecule-1 (ICAM-1) on the APC, termed the peripheral supramolecular activation cluster (p-SMAC). Ultimately, an elaborate collage of adhesion, costimulatory, and signaling molecules, along with cytoskeletal attachments (*4*, *5*) and lipid rafts (*6*–*8*), organizes to sustain signaling over the hours required for full T cell activation. Although previous observations have suggested that the spatial organization of the c-SMAC is directly involved both in increasing and extinguishing TCR signaling (*9*, *10*), a direct causal relation between changes in the synaptic pattern and signaling remains to be established.

We have developed an experimental platform that enables direct manipulation of IS patterns in living T cells. A supported membrane, consisting of a continuous and fluid lipid bilayer coating a silica substrate (*11*), is used to create an artificial APC surface (*12*). Inclusion of glycosylphosphatidylinositol (GPI)–linked pMHC and ICAM-1 into the supported membrane is sufficient to enable IS formation between a T cell and the synthetic surface (*13*). This hybrid live cell–synthetic bilayer IS is illustrated schematically in Fig. 1. Fluidity is a characteristic property of supported bilayers and distinguishes them from solid and polymeric substrates. Movement within the bilayer, however, can be manipulated by fabricating geometrically defined patterns of solid-state structures on the substrate (Fig. 1) (*14*). We posited that such substrate-imposed constraints might be used to guide molecular motion in the supported bilayer and linked cell-surface receptors to generate alternatively patterned synapses.

Silica substrates displaying various configurations of chromium lines (100 nm wide and 5 nm high) were fabricated using electron-beam lithography (*15*). Supported proteolipid membranes were assembled on these substrates by vesicle fusion. As receptors on the T cell surface engage their respective ligands in the bilayer, they become subject to the geometrical restrictions on mobility imposed by the chromium lines. T cell blasts expressing the cloned AND TCR, specific for moth cytochrome c (MCC) 88-103 peptide bound to I-E^k (pMHC), were used in all IS formation experiments. In control experiments with nonactivating peptide, T cells failed to form IS patterns on substrates with chromium lines, confirming specificity of the system (fig. S1). Under conditions of specific antigen recognition, a series of IS patterns, formed under different geometries of constraint patterns, were compared with the unrestricted IS patterns (Fig. 2A). Arrays of parallel lines were found to restrict protein mobility in one dimension and skew the synaptic pattern from a circular to a rectangular shape in which a central band of TCR-pMHC is flanked by two bands of LFA-1–ICAM-1 (Fig. 2B). Multifocal ISs were observed to form in response to grid constraint

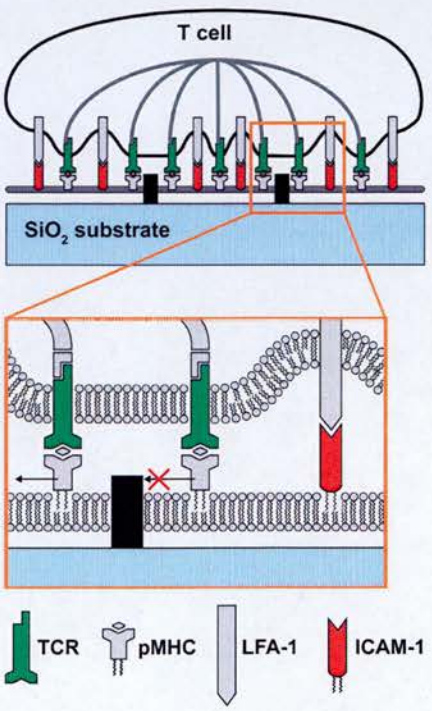

Fig. 1. Diagram of a hybrid live T cell–supported membrane junction. Receptors on the cell surface engage cognate ligands in the supported membrane and become subject to constraints on mobility imposed by physical barriers. The cytoskeleton is represented schematically to reflect the active source of central organization observed in our experiments.

[1]Biophysics Graduate Group and [2]Department of Chemistry, University of California, Berkeley, CA 94720, USA. [3]Physical Biosciences and Materials Sciences Divisions, Lawrence Berkeley National Laboratory, Berkeley, CA 94720, USA. [4]Department of Pathology, New York University School of Medicine, and the Program in Molecular Pathogenesis, Skirball Institute of Biomolecular Medicine, 540 First Avenue, New York, NY 10016, USA.

*To whom correspondence should be addressed. E-mail: JTGroves@lbl.gov (J.T.G.); Dustin@saturn.med.nyu.edu (M.L.D.)

www.sciencemag.org/cgi/content/full/310/5751/1187/DC1

Supporting Online Material for

DISC1 and PDE4B Are Interacting Genetic Factors in Schizophrenia That Regulate cAMP Signaling

J. Kirsty Millar,* Benjamin S. Pickard, Shaun Mackie, Rachel James, Sheila Christie, Sebastienne R. Buchanan, M. Pat Malloy, Jennifer E. Chubb, Elaine Huston, George S. Baillie, Pippa A. Thomson, Elaine V. Hill, Nicholas J. Brandon, Jean-Christophe Rain, L. Miguel Camargo, Paul J. Whiting, Miles D. Houslay, Douglas H.R. Blackwood, Walter J. Muir, David J. Porteous

*To whom correspondence should be addressed. Medical Genetics Section, Molecular Medicine Centre, University of Edinburgh, Edinburgh EH4 2XU, UK. E-mail: Kirsty.Millar@ed.ac.uk.

Published 18 November 2005, *Science* **310**, 1187 (2005)
DOI: 10.1126/science.1112915

This PDF file includes

Supporting Online Material
SOM Text
Materials and Methods
Figs S1 to S12.
References

SOM Text Notes

Investigation of the existence of a theoretical C-terminally truncated DISC1 protein species in lymphoblastoid cells carrying the t(1;11)

To look for biallelic transcription of *DISC1* in translocation-carrying cell lines, polyadenylated RNA was prepared from a cell line heterozygous for exonic SNP rs2492367. RT-PCR products were sequenced and both SNP alleles were detected (fig. S3A), demonstrating that *DISC1* is transcribed from both the normal and the translocated alleles in this cell line. To quantify *DISC1* transcript levels, primers specific for exon 2 (the same as those used to amplify rs2492367, above) were used in quantitative RT-PCR experiments. *DISC1* transcripts were found to be present at reduced levels in cells carrying the translocation (fig. S3B). Because exon 2 is located proximal to the translocation breakpoint, the primers used for quantitative RT-PCR should amplify truncated transcripts as well as normal transcripts. Detection of similar transcript levels between normal and translocation cell lines using these primers would therefore have indicated that truncated transcripts are present at normal levels. Detection of reduced transcript levels however, most likely indicates a reduction in truncated transcript abundance.

DISC1-specific antibody R47 was raised to an epitope within the N-terminus (*S1*). To confirm the ability of this antibody to detect C-terminally truncated forms of DISC1, COS7 cells were transfected with plasmids designed to express DISC1 amino acids 1-358 (essentially the head domain only) or 1-597 (up to the position of the translocation breakpoint) with a C-terminal V5 peptide tag. Two forms of C-terminal truncation were used since the extent of any putative truncated protein will depend upon the utilisation of an unknown cryptic transcription stop site, polyadenylation site and translation stop codon. These may occur within either chromosome 1 or 11 sequence, and it is therefore not possible to predict how large a theoretical truncated protein produced from the derived chromosome 1 would be. Expression of these proteins was confirmed using antiserum specific for the V5 peptide tag (fig. S3C) and antibody R47 clearly detected each exogenous protein against the background endogenous bands (fig. S3C). The larger of the two exogenous proteins migrates at a size similar to, but distinguishable from, that of the endogenous protein (fig. S3C). Thus using this antibody there is no positive evidence for a hypothetical truncated protein in t(1;11) cells and certainly no evidence for overexpression of such a protein. There is a theoretical possibility that a low level of truncated protein may be present in lymphoblastoid cell lines, but undetectable due to masking by the endogenous protein.

In overexpression experiments artificial C-terminally truncated forms of DISC1 adopt a quantitatively different subcellular localization than the full-length protein in many cells, with full-length DISC1 appearing mainly punctate in association with mitochondria in HeLa cells while truncated DISC1 is mainly diffuse within the cytoplasm (*S2*, *S3*). In COS7 mitochondrial localization is maintained regardless of C-terminal truncation, but truncated DISC1 occupies additional diffuse cytoplasmic and

strong nuclear localizations (*S4*) and displays an altered fractionation profile (*S5*). We therefore examined subcellular fractions of t(1;11) lymphoblastoid cells to look for evidence of an aberrant C-terminally truncated DISC1 species. Fractionation profiles of normal cells and cells carrying the t(1;11) were found to be indistinguishable (fig. S3D), providing further evidence against the presence of a truncated DISC1 species.

Finally, it is worth noting that linkage and association studies point to a general effect of DISC1 variation on vulnerability to psychiatric illness. There is no evidence to suggest that these variants produce truncated proteins of dominant-negative effect. The weight of evidence from the t(1;11) family is for haploinsufficiency. This and other mechanisms, including qualitative or quantitative effects on protein-protein interactions, may explain these generalized effects.

t(1;16) disruption of the *CDH8* gene

The t(1;16) translocation results in the formation of two fusion genes. On the der(16), the *PDE4B* promoter and exon 1a are juxtaposed to exon 2 of the *CDH8* gene. The translocation breaks before the *PDE4B* translation start site, so no productive protein is expected. On the der(1), the fusion of *CDH8* with *PDE4* is out of frame, introduces multiple stop codons immediately after the translocation break and thus is not expected to produce active *PDE4B*. In support of this, we have found no evidence from t(1;16) proband Western blots for a truncated or fusion *PDE4B* peptide.

We have not investigated *CDH8* further, but for completeness, we note that it is a member of the Type II, or atypical, cadherins, cell adhesion molecules which are defined by the lack of an extracellular tripeptide motif, HAV, possibly involved in the binding specificity of Type I cadherins (*S6*). The cytoplasmic tail is thought to signal the presence of interactions to the intracellular compartment by mediating receptor clustering through interaction with the proteins such as α-catenin, β-catenin and, eventually, the cytoskeletal proteins, actin and α-actinin. In this way, adhesion to adjacent cells can affect the cytoarchitecture of the cell and may even play a role in cell motility. The two principal roles of neuronal cadherins are thought to be in the mediation of certain developmental pathways in the brain and the regulation of synaptic function. CDH8 proteins preferentially bind to each other prompting the hypothesis that cadherins are responsible for the aggregation or interconnection of similar cells within an organ. In the brain, CDH8 expression is restricted to particular sub-regions and neuronal patches (*S7*).

Materials and Methods

The t(1;16) proband

The proband carrying the t(1;16) had onset of mental illness in his mid twenties, and index admission three years after first presentation. There was clear evidence for development of a schizophrenic illness with persistent second person auditory hallucinations and persecutory delusions. Treatment was with routine phenothiazines with evidence for remission of symptoms. However, over the next 20 years, there were a series of relapses again with clear auditory hallucinations and persecutory delusion requiring inpatient treatment. DSM-IV criteria for chronic schizophrenia were fully met using evidence gathered by a structured SADS-L interview of the proband and case-note review. A cousin of the proband who also carried the translocation was found on review

of hospital notes to have had a psychotic illness with prolonged hospital admission, but was not accessible for the present study.

Plasmids

Plasmids encoding untagged or FLAG-DISC1 in pcDNA3.1, PDE4 isoforms PDE4B1, B2, B3, PDE4A10, PDE4C2, PDE4D5 and pEBG plasmids expressing GST or a GST-UCR2 domain of PDE4D have been described previously (*S1*, *S2*, *S8–S11*). PDE4B1 and PDE4B3 open reading frames (ORFs) were amplified by PCR and cloned into pCMV4A (Invitrogen, Paisley, UK) to generate carboxyl-terminal FLAG-tagged proteins. The DISC1 ORF and progressive amino-terminal deletions were generated by nested PCR amplification and cloning into pcDNA6 (Invitrogen). The DISC1 ORF and specific deletion fragments were amplified by PCR and cloned into pcDNA-DEST40 (V5 tag) or pcDNA6 (both Invitrogen). DISC1 ORF fragments spanning amino acids 1-180, 1-250 and 1-300 were generated by PCR using DISC1 specific 3' primers and a primer 5' to the T7 promoter in pcDNA DISC1 and used directly as a DNA template for IVTT. All plasmid inserts were confirmed by DNA sequencing.

Preparation of rat hippocampal primary cultures

Hippocampi were isolated from day 18 rat embryos, and cells dissociated in trypsin then plated on poly L-Lysine (Sigma, Gillingham, UK) coated glass coverslips at a density of 1×10^5 cells/ml in neurobasal medium/10% fetal bovine serum/0.5 mM L-glutamine. After 24 hours, the medium was removed and replaced with neurobasal medium/1% B27/penicillin-streptomycin. All media were supplied by Invitrogen. Cells were grown for 5 days prior to fixation.

Antibodies

DISC1-specific antibodies R47, R1443/1, pan-PDE4B and a PDE4B1-specific antibody (PDE4B-228), as well as sera specific for PDE4A, C & D have been described previously (*S1*, *S12–S14*). DISC1-specific antibody C2 (*S15*) was provided by Akira Sawa (The Johns Hopkin University). Anti-V5 antibody was obtained from Invitrogen, anti-FLAG M2 from Sigma and anti-cytochrome *c* from Clontech, Basingstoke, UK. Mitochondria were detected using antibody ab3298 (Abcam, Cambridge, UK) or an antibody specific for mitochondrial Hsp70 (Abcam). Neuronal cell types in primary cultures were identified using an antibody to NeuN (Abcam).

Yeast two-hybrid screening

DISC1 full-length bait sequence in a Gal4-based N-terminal plasmid (pB23) was screened against an adult human brain library as previously described (*S2*). In total, 64 proteins of interest were identified, 16 of which are considered high confidence interactions based upon a method (*S16*, *S17*) that takes account of whether the clone matches known ORFs, the number of clones identified for a given gene, and whether a protein is promiscuous, that is, identified in several independent yeast-two hybrid screens. From this screen we have previously reported the interaction of DISC1 with NUDE and Nudel (*S2*). Amongst the high confidence interactors, three independent PDE4B clones were identified all corresponding to approximately the same portion of PDE4B (amino acids 187-361 of isoform PDE4B1, accession number Q07343).

Fluorescence In Situ Hybridization mapping of the t(1:16) breakpoint
Fluorescence in situ hybridization was conducted as previously described using labelled YAC and BAC clones (*S18*). Breakpoint-spanning YACs were identified by fluorescence *in situ* hybridization (FISH), and BAC clones corresponding to positive YAC regions were arranged into contigs by consulting Washington University FPC (*S19*) and the UCSC Human Genome Browser (*S20*). BAC positions at breakpoints were determined using FISH. The mapping of the chromosome 1 breakpoint to PDE4B with bacterial artificial chromosome clones RP11-433N2 and RP11-442I11 is shown in Fig. 1. For completeness, we show in fig. S1 that on the derived chromosome 16, BACs RP11-875E12 and RP11-685M21 flank the other breakpoint. This lies within a second gene, Cadherin 8 (*CDH8*), demonstrating that this gene is also disrupted.

Fluorescence Imaging
Images were captured on a Zeiss Axioskop 2 MOT epifluorescence microsocope, using SmartCapture 2 version 2.3.1 (Digital Scientific Ltd, Cambridge UK).

Immunofluorescence
Cells on glass coverslips were probed with antibodies using standard methods. Primary antibodies were detected using AlexaFluor 488 or 594-conjugated secondary antibodies (Molecular Probes, Paisley, UK).

Confocal microscopy
Human SH-SY5Y cells were probed with a pan4B antibody and DISC1 antibody R47, labeled with alexa 594 and alexa 488 respectively and observed
using a Zeiss Pascal laser scanning microscope. The images shown are of a slice through the centre of the cell.

Cell fractionation
Cells were fractionated as described previously (*S1*). The fractions correspond to: P1; nuclei, plus whole-cell debris, P2; predominantly mitochondrial, P3; other membrane elements, and C; cytosolic.

Transfection
HEK293 cells were maintained at 37°C with 5% CO_2 in DMEM (Sigma) with 10% FBS and transfected with lipofectamine 2000 (Invitrogen) at 90% confluence, 15-24 hours after removal of antibiotics.

Immunoprecipitation
Cells were lysed in ice-cold PBS containing 1% Triton X-100/1 mM DTT/2 mM PMSF/10 mM sodium fluoride/5 mM pyrophosphate/protease inhibitor cocktail (Roche). Lysates were solubilized by incubation for 1 hr at 4°C on a rotary wheel and centrifuged at 13,000 rpm for 30 min. Lysates were pre-cleared by incubation with protein G-Sepharose (Sigma) for 15 min. Indicated antibody was added to the supernatant, incubated for 3 hours or overnight, protein G was added to capture immune complexes and immunoprecipitates washed three times in lysis buffer plus protease inhibitors.

GST pull-downs
Cells were lysed as for immunoprecipitation and GST-protein complexes captured by overnight incubation with glutathione-sepharose. Beads were then washed five times in PBS/1% Triton X-100 with NaCl added to a final concentration of 0.5 M plus protease inhibitors.

Protein synthesis *in vitro*
T7,T3 or SP6-coupled reticulocyte lysate system (TNT, Promega, Southampton, UK) was used to synthesize proteins. For *in vitro* binding assays equivalent amounts of [^{35}S]-labelled and unlabelled lysates were mixed and diluted to a final buffer concentration of 1× PBS/1% Triton X-100 in 600 µl reaction volume. After 3 hours at 4°C protein complexes were isolated by addition of anti-V5 or anti-FLAGM2 antibody plus protein G sepharose. Immune complexes were washed five times in the above buffer.

PDE4B phosphorylation assay
SH-SY5Y cells were either untreated (Ctr) or challenged for 30 min with a mixture of either IBMX + Forskolin (I/F) or IBMX + Forskolin (I/F) + H89 (I/F/H89) at the concentrations used for expts described in Fig 4A. The selective immunoprecipitation of PDE4B from SYH-SY5Y cells was done using a specific antibody targeted to the unique C-terminal region of this sub-family through a procedure performed exactly as described previously (*S13*, *S21*). The immunoprecipitated PDE4B was then analysed as previously described by (i) immunoblotting with a PDE4B specific antiserum (*S8*, *S14*), (ii) immunoblotting with an antiserum specific for the single PKA phosphorylation site in UCR1 (*S2*, *S9*) and (iii) assayed for cAMP hydrolysing PDE4 activity (*S13*, *S21*). Activity measurements are means ± SD for n=3 separate experiments.

Cell culture
Cell lines SH-SY5Y, LAN5, COS7 and HEK293 were cultured in DMEM/10% fetal bovine serum. Lymphoblastoid cell lines established from t(1;11), t(1;16) subject and karyoptypically normal controls were cultured in RPMI/10% fetal bovine serum (all media supplied by Invitrogen). Forskolin, IBMX, H-89 and 8-bromo-cAMP (all Sigma) were added to cultures at 100 µM, 20 µM, 10 µM and 100 µM respectively, and incubated at 37°C for 30 min prior to harvesting of cells. To differentiate SH-SY5Y cells, retinoic acid was added to the medium at a final concentration of 1 µM for 5 days.

Immunoblotting
Proteins separated by SDS-PAGE were transferred to Hybond-P (Amersham Biosciences, Little Chalfont, UK) or Invitrolon (Invitrogen) membranes. Primary antibodies were detected using horseradish peroxidase-conjugated secondary antibodies (Sigma) and proteins visualized using ECL-Plus (Amersham Biosciences).

Densitometry
Densities of protein bands visualised on photographic film were determined using UVIDoc software (UVITech, Cambridge, UK). Immunoreactivity was expressed as the ratio of DISC1:GAPDH or PDE4B:GAPDH. To allow for between-gel comparisons all values from translocation cell lines are given as % of expression in a cell line derived from a karyotypically normal relative measured from the same gel.

Biallelic transcription of DISC1 in t(1;11) cell line

SNP rs2492367 ([tctctctc**G/A**gcccttca] within exon 2, proximal to the translocation breakpoint) was used to distinguish between the normal and translocated alleles of DISC1. A t(1;11) translocation-carrying lymphoblastoid cell line heterozygous for rs2492367 was studied. Previous family genotyping had demonstrated that the A allele is located on the derived (translocated) chromosome. Random-primed cDNA (First Strand cDNA synthesis kit; Roche, Lewes, UK) was prepared from polyA RNA extracted from this cell line (PolyA Pure mRNA purification kit; Ambion, Huntingdon, UK). Oligonucleotides corresponding to the SNP region were designed (Forward Primer:gaacgtggagaagcagaagg, ReversePrimer: cagagaactggaggagccag). Thermostart Taq Polymerase (Abgene, Epsom, UK) was used to amplify this region and the resulting products were directly sequenced (Big Dye version 3.1, Applied Biosytems, Warrington, UK) to determine (nonquantitatively) if both alleles were represented.

Real-Time RT-PCR

RNA was extracted from Lymphoblastoid cell lines using the RNAeasy kit (Qiagen). and treated to ensure no DNA contamination using Turbo DNA-*free* (Ambion). cDNA was made using the First Strand cDNA synthesis Kit (Roche).

Primers for *DISC1* were designed using PRIMER3 software on the Biology Workbench website (http://workbench.sdsc.edu/). Primers were designed in exon 2 of *DISC1* and should detect all known spliced variants. Relative quantification of *DISC1* was determined using the MyiQ Real-Time PCR detection system and associated optical software system version 1.0 (Bio-Rad Laboratories, Ltd). Real-Time PCR was carried out in a final volume of 15 µl, containing 7.5 µl of iQ SYBR Green Supermix (Bio-Rad Laboratories Ltd.), 150 ng primers (Forward and Reverse) and 1 µl of reverse transcribed cDNA. Reference genes, *glyceraldehyde-3-phosphate dehydrogenase* (GAPDH) and *human phosphofructokinase*, muscle (PFKM), were amplified in parallel and used to facilitate normalisation. The thermal profile included 95°C (3 min), then 40 cycles of 95°C (10 s), 66°C (30 s), 72°C (45 s). Double stranded product was measured during the 72°C extension step using fluorescence emitted by incorporation of SYBR green I into the product. Melt curve analysis was performed after PCR amplification to ensure specificity of products. All reactions were carried out in duplicate and standard curves for all primer sets were run in parallel to determine primer efficiencies.

Primers used are as follows;

DISC1	Forward J14 5'-GAACGTGGAGAAGCAGAAGG-3'
	Reverse J15 5'-CAGAGAACTGGAGGAGCCAG-3'
GAPDH	Forward 5'- GGGAGCCAAAAGGGTCATCA-3'
	Reverse 5' - GTGGCAGTGATGGCATGGAC-3'
hPFK	Forward 5'-AGAGCGTTTCGATGATGCTT -3'
	Reverse 5'-GTGTTCCTCCCAGTCGTCAT-3'

S1A

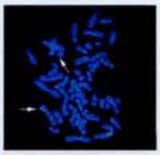

S1B

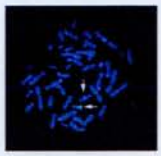

S1C

S2

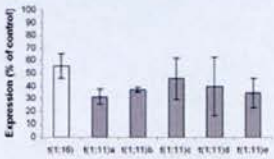

S3A

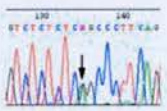

S3B

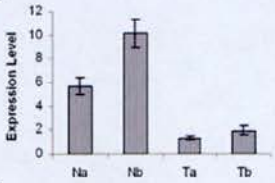

S3C

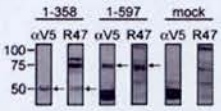

S3D

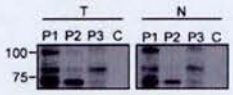

S4A

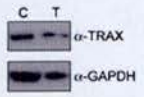

S4B

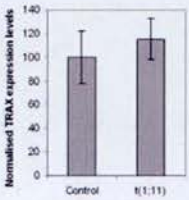

S5

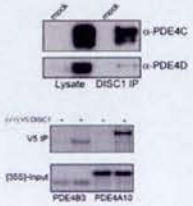

S6

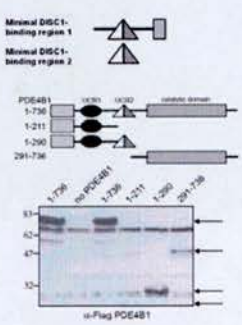

S7

S8

S9

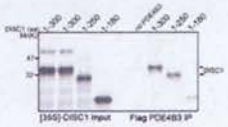

S12A

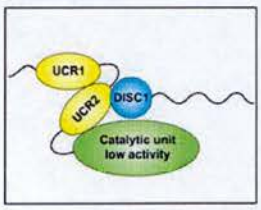

S12B

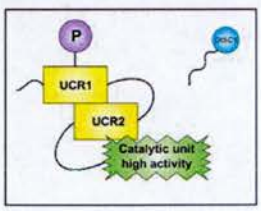

Fig. S1. Fluorescence in situ hybridization mapping of t(1:16): chromosome 16 breakpoint.
(A, B) FISH using BAC clone RP11-875E12 and RP11-685M21 probes, respectively, on t(1;16) patient metaphase spreads. Arrows mark FISH signals on the normal and derived chromosome 16.
(C) CDH8 genomic organisation showing positions of exons (vertical lines) and BAC clones (closed boxes) used as probes to define the translocation breakpoint (dotted line).

Fig. S2. Reduced PDE4B expression in the t(1;16) lymphoblastoid cell line and reduced DISC1 expression in five independent lymphoblastoid cell lines (a-e) carrying the t(1;11), compared to one and four cell lines, respectively, from karyotypically normal relatives, all expressed as a percentage of normal levels and relative to GAPDH. There was no reduction in the levels of TRAX (SOM fig.S4) between t(1;11) carriers and karyotypically normal relatives.

Fig. S3. Detection of truncated DISC1 in lymphoblastoid cell lines.
(A) Biallelic *DISC1* transcription in t(1;11) lymphoblastoid cell lines determined by sequencing across heterozygous SNP rs2492367.
(B) Quantitative RT-PCR using DISC1-specific primers designed from exon 2 sequence (translocation breakpoint proximal) in lymphoblastoid cells with (Ta, Tb) or without (Na, Nb) the t(1;11). Each cell line was assayed four times.
(C) Detection of C-terminally truncated DISC1 species by DISC1-specific antibody R47. COS7 cells were mock-transfected (mock) or transfected with pDEST40 vectors expressing DISC1 amino acids 1-358 or 1-597 with a V5 peptide tag. Due to the variable intensity of the DISC1 endogenous bands it should be noted that the mock transfection was carried out simultaneously with the DISC1 (1-597) transfection and is therefore separate from the DISC1 (1-358) transfection. These constructs were selected as they may mimic the hypothetical truncated DISC1 protein resulting from the translocation. Exogenous DISC1 detected with R47 antiserum or V5-specific antiserum is indicated with arrows, other bands are due to recognition of endogenous DISC1 by R47. Markers are indicated in kiloDaltons.
(D) Subcellular fractionation profile of DISC1 in lymphoblastoid cells with (T) or without (N) the t(1;11). This experiment should be interpreted in the context of the previously reported altered subcellular distribution of C-terminally truncated forms of DISC1. Loadings have been adjusted so that DISC1 levels are comparable between cell lines. P1: nuclear fraction, plus whole-cell debris; P2: predominantly mitochondrial; P3: other membrane elements; C: cytosolic. Markers are in indicated kilodaltons.

Fig. S4. TRAX expression is not perturbed in t(1;11) lymphobastoid cells lines.
(A) Western blots of protein extracts from control and t(1;11) lymphoblastoid cell lines were probed sequentially with α-TRAX and α-GAPDH antibodies.
(B) TRAX protein levels are plotted as the ratio of α-TRAX over α-GAPDH, normalised with respect to the control cell line. The graph shows the mean results of three independent Western blots.

Fig. S5. Co-immunoprecipitation of PDE4A, B, C and D with DISC1.
Representative long PDE4 isoforms containing a UCR2 domain were assayed for binding to DISC1. Anti-FLAG immunoprecipitates from lysates prepared from HEK293 cells co-transfected with empty Flag vector (mock) or Flag-DISC1 and PDE4C2 or PDE4D5 were probed by Western blot analysis with pan-PDE4C or PDE4D antibodies (top). Anti-V5 immunoprecipitates from *in vitro* transcribed/translated [^{35}S]-PDE4B3 or PDE4A10 incubated with either V5 antibody or V5 antibody and V5-DISC1. Immune complexes were separated by SDS-PAGE and visualised by autoradiography (bottom). Signals obtained by Western blot analysis or autoradiography were consistent with the expected MW of the PDE4 isoforms tested.

Fig. S6. Mapping the DISC1 binding site on PDE4B1
Minimal DISC1 binding regions 1 and 2 (top) were identified by yeast two-hybrid screening and binding studies in mammalian cells, respectively. PDE4B1 deletion constructs used to map the DISC1 interaction domain (fig.2C) were generated as in-frame C-terminal Flag tagged fusion proteins and expressed in HEK293 cells. Amino acid residues which comprise the PDE4B1 truncations are indicated (middle). Detection of expressed Flag tagged PDE4B1 protein fragments was carried out by Western blot analysis of total cell lysates and the position of individual fragments at the expected MW are indicated by an arrow (bottom). Markers are indicated in kilodaltons.

Fig. S7. PDE4B binds the DISC1 amino terminus.
Anti-V5 immunoprecipitates from *in vitro* transcribed/translated [^{35}S]-PDE4B3 incubated with V5-DISC1 fragments (DISC1 residues 1-854, 1-597 and 1-358) were separated by SDS-PAGE and visualised by autoradiography (upper). Labelled PDE4B3 input signal represents 1/50 of that present in the binding reaction (bottom).

Fig. S8. Schematic of DISC1 N-terminal deletion constructs.
The indicated amino-terminal DISC1 deletion fragments (NΔ) were constructed in plasmid pcDNA6A to initially identify a PDE4B3 binding site (fig.2E). DNA fragments encoding DISC1 amino acids 1-180, 1-250 and 1-300 were generated to confirm the position of the PDE4B3 interaction site on DISC1 (fig.S9).

Fig. S9. Mapping the PDE4B binding site on DISC1.
[^{35}S]-labeled amino-terminal DISC1 fragments were incubated with unlabelled Flag tagged PDE4B3, immunoprecipitated with anti-Flag antibody and immune complexes were resolved by SDS PAGE and detected by autoradiography. Input DISC1 signal represents 1/50 of the total binding reaction (left). DISC1 fragments which specifically bind to PDE4B3 are indicated by arrows (right). Markers are indicated in kilodaltons.

Fig. S12. A model for dynamic cAMP-responsive binding of PDE4B to DISC1.
(A) When cellular cAMP is low PDE4B activity is low, and PDE4B binds to DISC1 via UCR2.

(B) When cellular cAMP levels are high, UCR1 is phosphorylated by PKA, causing a UCR1-UCR2 conformational change and dissociation of PDE4B from DISC1, with subsequent catalytic unit conformation change and activation.

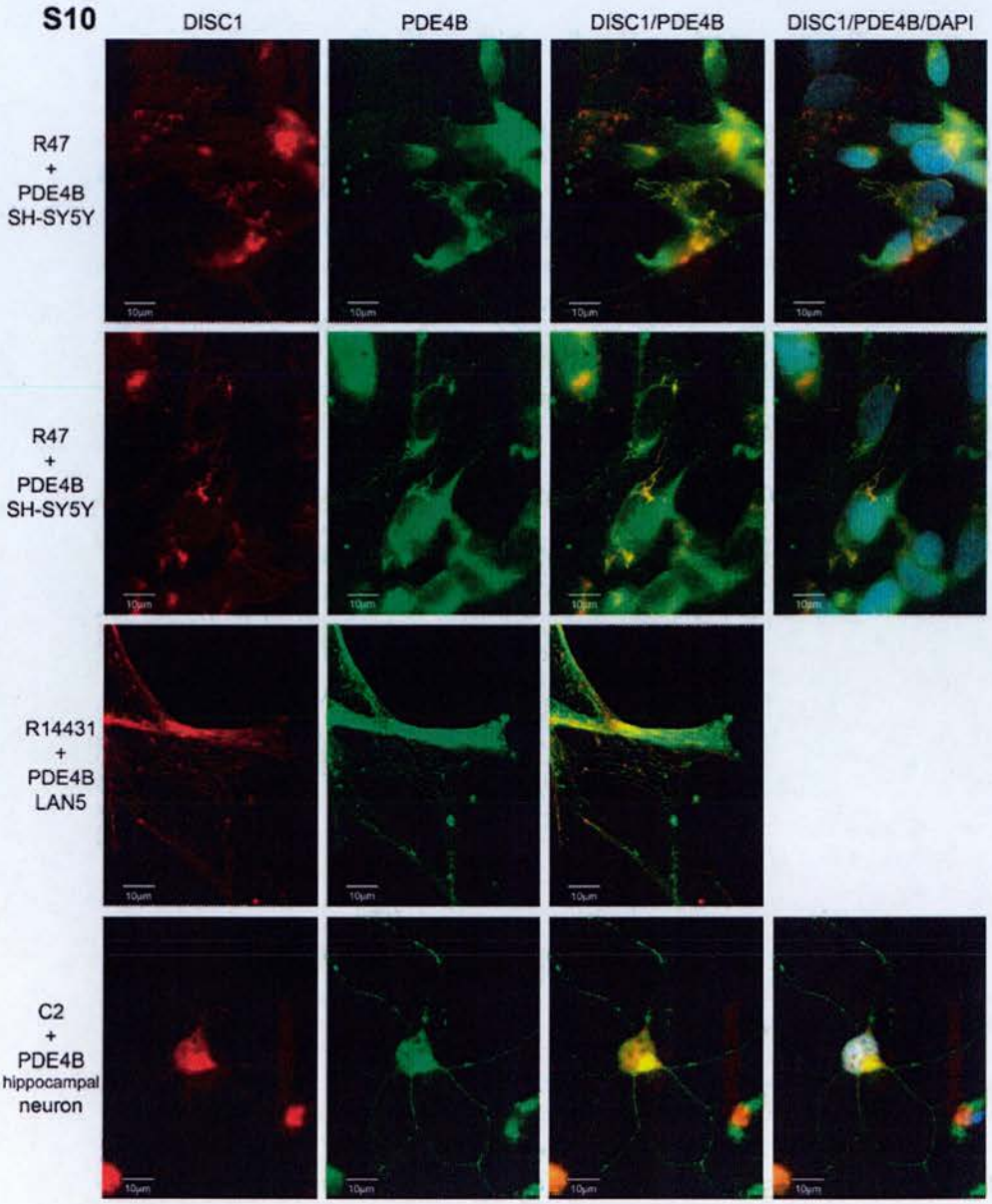

Fig. S10. Additional images of native DISC1 and PDE4B co-expression (see Fig. 3C, D, and E).
Upper, DISC1 (R47 or R1443/1 antibodies) and PDE4B (pan-PDE4B antibody) expression in SH-SY5Y (rows 1 & 2, respectively) and LAN5 human neuroblastoma cells (row 3). Nuclei were visualised with DAPI.
Lower, Hippocampal primary neuron probed with DISC1 (C2) and PDE4B (pan-PDE4B). Neurons were identified using an antibody to NeuN. Nuclei were visualised with DAPI.

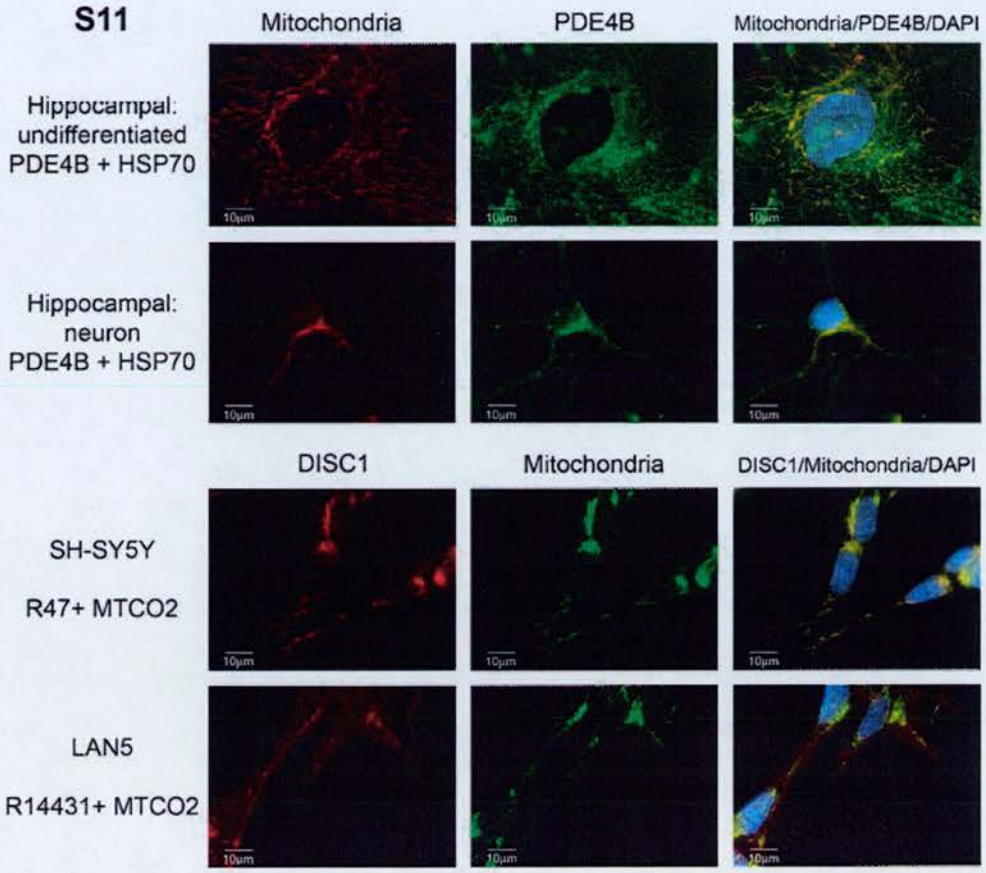

Fig. S11. DISC1 and PDE4B co-localize with mitochondrial markers.
Top, Mitochondria (Hsp70 antibody) and PDE4B (pan-PDE4B antibody) in an undifferentiated hippocampal cell (row 1) and a hippocampal neuron (row 2). Neurons were identified using an antibody to NeuN. Nuclei were visualised with DAPI.
Bottom, DISC1 (R47 or R1443/1 antibodies) and mitochondria (MTCO2 antibody) in SH-SY5Y (row 1) and LAN5 (row 2) neuroblastoma cells. Nuclei were visualized with DAPI.

Supplementary References

S1. R. James *et al.*, *Mol. Cell. Neurosci.* **26**, 112 (2004).
S2. N.J. Brandon *et al.*, *Mol. Cell. Neurosci.* **25**, 42 (2004).
S3. J.A. Morris *et al.*, *Hum. Mol. Genet.* **12**, 1591 (2003).
S4. J.K. Millar *et al.*, *Biochem Biophys Res Commun.* **311**, 1019 (2003)
S5. Y. Ozeki *et al.*, *Proc Natl Acad Sci U S A.* **100**, 289 (2003)
S6. C. Redies, *Prog Neurobiol.* **61**, 611 (2000)
S7. K. Korematsu *et al.*, *Exp Neurol.* **154**, 531 (1998)
S8. S.J. MacKenzie *et al.*, *Br. J. Pharmacology* **136**, 421 (2002).
S9. E. Huston *et al.*, *Biochem. J.* **328**, 549 (1997).
S10. G. Rena *et al.*, *Mol. Pharmacol.* **59**, 996 (2001).
S11. G.B. Bolger *et al.*, *Biochem. J.* **328**, 539 (1997).
S12. C. Sette, M. Conti, *J. Biol. Chem.* **271**, 16526 (1996)
S13. S.J. Mackenzie, M.D.Houslay, *Biochem. J.* 347, 571 (2000)
S14. A. McCahill *et al.*, *Cell. Signal.* **17**, 1158-1173 (2005).
S15. K. Miyoshi *et al.*, *Mol. Pyschiatry* **8**, 685 (2003).
S16. J.C. Rain *et al.*, *Nature*. **409**, 211 (2001).
S17. F. Colland *et al.*, *Genome Res.*, **14**, 1324 (2004).
S18. B.S. Pickard *et al.*, *Am J Med Gen (Neuropsy Gen)* **136**, 26 (2005)
S19. Arizona Genomics Institute, http://www.genome.arizona.edu/fpc/
S20. UCSC Genome Bioinformatics, http://genome.ucsc.edu/
S21. M.C. Shepherd *et al.*, *Br. J. Pharmacol.* **142**, 339 (2004).

Appendix II

Reagents and Solutions

Solutions

This appendix provides details regarding preparation of the solutions indicated in chapter 2. Some of the required reagents are listed along with suppliers in the subsequent reagents section.

H^3-cAMP
2μM (3μCi) cAMP solution is prepared in Tris/Mg^{2+} buffer. Store at -20°C. Caution: radioactive material, add in fume hood wearing double gloves.

Cell freezing medium
RPMI or DMEM depending on cell type
10% Fetal Bovine Serum
10% DMSO
Aliquot and store at -20°C.

Centrosome isolation lysis buffer

HEPES (1M)	200μl
NP-40	1ml
$MgCl_2$	100μl
2-Mercaptoethanol	200μl
Pepstatin A (5mg/ml)	40μl

Make up to 200mls in distilled water, store in 20ml aliquots at -20°C. Add 400μl of 50X protease inhibitors to a 20ml aliquot of lysis buffer before use.

Citrate buffer

Sucrose	85.5g
Trisodium citrate	11.76g
Distilled water	800ml

Once dissolved add 50ml of tissue culture grade DMSO and adjust final volume to 1L. Adjust pH to 7.6. Store at -20°C.

Coomassie Brilliant Blue protein fix/stain

Coomassie stain	0.25g
Methanol;water (1;1 v/v)	90ml
Glacial Acetic acid*[NB]	10ml

Filter solution and store at room temperature (RT).

*NB: Always add acid to water

Coomassie de-stain (Methanol:Acetic acid)

Glacial acetic acid	100ml
Methanol	300ml

Make to 1L with distilled water, store at RT.

Cytochalasin D
Add 5mg vial to 1ml DMSO, store in aliquots at -20°C. Protect from dark.

Dowex slurry
Dowex ion exchange resin is prepared 1:1 in water. Before use mix dowex:ethanol at a ratio of 2:1. Store dowex at 4°C.

Ethanol fixative solution (BrdU incorporation assay)
300mls Glycine solution (50mM, pH 2.0)
700mls 100% Ethanol
Store at RT.

IF blocking buffer
Blocking buffer consists of a 10% solution of animal serum (in PBS/BSA .02% solution) from which the secondary antibody was raised.

Mowiol
Step 1. Mowiol 7.5g
Glycerol 10ml
dH_20 25mls
Make up solution in a 250ml conical flask, cover in parafilm and incubate at RT overnight.
Step 2. Add 50mls of Tris.HCL (0.2M, pH 8.5), mix and heat at 100°C for 20 minutes.
Step 3. Allow to cool and add 1.75g DABCO. Aliquot and store at -20°C long term or 4°C short term.

Mowiol/DAPI
DAPI was added to Mowiol to achieve a final concentration of 250ng/ml.

Nocodazole
Add 10mg vial to 33.3mls DMSO, store in 1ml aliquots at -20°C.

10X Orange G loading buffer
Ficoll 400 3g (15%)
SDS (20% solution) 50µl (0.05%)
EDTA (0.5M) 800µl (20mM)
Orange G 0.125%
Make up to 20mls with distilled water, store at RT.

4% Paraformaldehyde
Dissolve paraformaldehyde powder in 1X PBS (in fume hood, wear face mask) to achieve a final concentration of 4%. Solution may need heating to dissolve. Aliquot and store at minus 20°C.

PBS/BSA (.02%)
0.06g Bovine Serum Albumin in 300mls of PBS

Ponceau stain

Distilled water	100mls
Ponceau S	0.5g
Acetic Acid*	2mls

Store at RT; This stain is re-usable.

PBST blocking buffer (western blotting)

1X PBS, 5% semi-skimmed milk (MAVREL), 0.2% Tween20.

Propidium Iodide solution C

Propidium iodide	208mg
Spermine tetrahydrochloride	500mg

Adjust volume to 500mls with trisodium citrate/spermine stock solution. Adjust pH to 7.6. Store at -20°C.

50X Protease inhibitors (Complete)

1 tablet dissolved in 1ml distilled water, aliquot and store at -20°C.

Protein sample buffer (2X Laemmli)

Tris(hydroxymethyl)-methylamine (1M, pH6.8)	1ml (100mM)
Glycerol	2ml (20%)
SDS (20% solution)	2ml (4%)
Bromophenol Blue	0.2g (.02%)

Adjust volume to 10mls with distilled water and store at RT. Add 100mM DTT before use.

RIPA buffer

Tris(hydroxymethyl)-methylamine(1M, pH7.5)	2.5ml
Sodium Chloride (NaCl, 3M)	2.5ml
Igepal	500µl
Sodium Deoxycholate (10% solution)	2.5ml
Sodium Dodecyl Sulphate (20% solution)	250µl

Make up to 50ml with distilled water and store at 4°C. Add protease inhibitors before use.

Semi-Dry transfer buffer

Tris(hydroxymethyl)-methylamine	(48mM) 5.8g
Glycine	(39mM) 2.9g
20% Sodium Dodecyl Sulphate	(0.04%) 2mls
Methanol	(20%) 200mls

Make up to 1L using distilled water, store at 4°C.

Snake venom

1mg/ml in distilled water, store at -20°C. This is toxic wear double gloves and face mask when adding to reactions.

1X TBST (Tris buffered saline with Tween20)
1M Tris, pH7.5 50ml
Sodium Chloride 8.75g
Make up to 1L with distilled water; add 1ml Tween20 (0.1%).

TBST blocking Buffer (Western blotting)
1X TBST plus 1% Marvel.

1.5M Tris pH 8.8 (for SDS-PAGE gel preparation)
181.5g of Tris(hydroxymethyl)-methylamine in 1L distilled water, pH using Hydrochloric Acid (HCL), store at RT.

0.5M Tris pH 6.8 (for SDS-PAGE gel preparation)
60.5g of Tris(hydroxymethyl)-methylamine in 1L distilled water, pH using HCL, store at RT.

PDE Tris buffer
20mM Tris-HCL buffer (2.42g of Tris.HCL in 1L of distilled water), pH to 7.4 using HCL, store at 4°C.

Tris/Mg^{2+}
20nM PDE Tris buffer plus 10mM $MgCl_2$.

50X Tris-Acetate electrophoresis buffer
Tris(hydroxymethyl)-methylamine 242g
Galcial Acetic Acid 57ml
EDTA (0.5M, pH 8.0) 100ml
Make up to 1L with distilled water, store at RT, dilute to 1X before use.

Trisodium citrate/Spermine stock solution
Trisodium citrate 2g
Tris(hydroxymethyl)-methylamine 121mg
Spermine tetrahydrochloride 1.04g
Igepal (NP-40) 2ml
Make up to 2 litres with distilled water and adjust pH to 7.6.

Trypsin solution A
15mg of trypsin dissolved in 500mls of trisodium citrate/spermine stock solution. Adjust pH to 7.6. Store at -20°C.

Trypsin inhibitor/Ribonuclease A solution B
250mg Trypsin inhibitor
50mg Ribonuclease A (RNase A)
Make up to 500ml using trisodium citrate/spermine stock solution and adjust pH to 7.6. Store at -20°C.

3T3 Lysis buffer
25mM HEPES pH 7.5
2.5mM EDTA
50mM NaCl
50nM NaF
30mM Sodium pyrophosphate
10% Glycerol
1% Triton-X100

Reagents

8-H^3 cAMP	Amersham Biosciences
Cytochalasin D	Sigma
DABCO	Sigma
Dowex ion exchange resin	Sigma
Mowiol	Sigma
Nocodazole	Sigma
Pepstatin A	Sigma
Propidium iodide	Sigma
Sodium Dodecyl Sulphate (20% solution)	Fischer Scientific
Spermine tetrahydrochloride	Sigma
Trisodium citrate	Sigma
Trypsin	Sigma
Trypsin inhibitor	Sigma